

MECHANICAL

TECHNICAL

RECEIVED ON

FACILITY FORM 602

A65-22561 -
178 (PAGES) 1 (CODE)
CR62280 (NASA CR OR T-4X OR AD NUMBER) 15 (CATEGORY)

MECHANICAL TECHNOLOGY INCORPORATED

968 Albany Shaker Road

Latham, New York

MTI-62TR26

**ANALYSIS OF THE HYDROSTATIC JOURNAL
AND THRUST GAS BEARING FOR THE
NASA AB-5 GYRO GIMBAL BEARING**

By

**J. W. Lund
R. J. Wernick
S. B. Malanowski**

Contract No. NAS8-2588

Technical Report

MTI 62TR26
October 23, 1962

ANALYSIS OF THE HYDROSTATIC JOURNAL
AND THRUST GAS BEARING FOR THE
NASA AB-5 GYRO GIMBAL BEARING

By

J. W. Lund
R. J. Wernick
S. B. Malanoski

Prepared under

Contract NAS8-2588
Subcontract 213-03-72120-6244

Supported by

National Aeronautics and Space Administration
Huntsville, Alabama

Administered by

The General Electric Company
Pittsfield, Massachusetts

Reproduction in Whole or in Part is Permitted
for any Purpose of the U.S. Government

MECHANICAL TECHNOLOGY INC.
LATHAM, N.Y.

TABLE OF CONTENTS

| | <u>Page</u> |
|--|-------------|
| LIST OF FIGURES | ii |
| ABSTRACT | 1 |
| INTRODUCTION | 3 |
| RESULTS | 6 |
| 1. Orifice and Millipore Characteristics | 6 |
| 2. Bearing Dimensions and Air Data | 7 |
| 3. Bearing Stiffness and Flow at Eccentricity = 0 | 8 |
| 4. Bearing Load vs. Eccentricity Ratio | 10 |
| 5. Dynamic Bearing Stiffness | 13 |
| 6. Turbine Torque | 15 |
| 7. Summary of Results | 18 |
| DISCUSSION | 20 |
| CONCLUSIONS | 22 |
| RECOMMENDATIONS | 23 |
| ACKNOWLEDGMENT | 24 |
| REFERENCES | ?5 |
| APPENDICES: | |
| Appendix A: General Equations | 26 |
| Appendix B: The Static Load Carrying Capacity of Hydrostatic Bearings with Orifice Restricted Line Feeding | 35 |
| Appendix C: Static Load Carrying Capacity of Hydrostatic Journal Bearing with Orifice Source Feeding | 48 |
| Appendix D: Reformulation of an Infinite Series Encountered in the Analysis Performed in Appendix C | 63 |
| Appendix E: Static Load Carrying Capacity of Hydrostatic Thrust Bearing with Orifice Source Feeding | 66 |
| Appendix F: Effect of Eccentricity Ratio on the Load Carrying Capacity of Hydrostatic Journal Bearing | 76 |
| Appendix G: The Dynamic Load Carrying Capacity of the Hydrostatic Journal Bearing with Orifice Restricted Line Feeding | 78 |
| Appendix H: The Dynamic Load Carrying Capacity of the Hydrostatic Thrust Bearing with Orifice Restricted Line Feeding | 85 |

TABLE OF CONTENTS (Cont.)

| | <u>Page</u> |
|---|-------------|
| FORTRAN LISTINGS OF COMPUTER PROGRAMS: | |
| 1. PN0020: Static Load and Flow for Journal and Thrust Bearing with Line Source Feeding | 93 |
| 2. PN0031: Static Load for Thrust Bearing with Point Source Feeding | 104 |
| 3. PN0040: Static Load for Journal Bearing with Point Source Feeding | 107 |
| 4. PN0045: Static Load for Infinitely Short Journal Bearing with Line Source Feeding | 125 |
| 5. PN0047: Dynamic Load for Journal and Thrust Bearing with Line Source Feeding | 128 |

FIGURES 1 to 33

NOMENCLATURE

LIST OF FIGURES

- Fig. 1 Geometry of Gimbal Air Bearing
2 Vena Contracta Coefficient
3 Journal Bearing - Dimensionless Load vs. A_t
4 Journal Bearing - Dimensionless Flow vs. A_t
5 Thrust Bearing - Dimensionless Load vs. A_t
6 Thrust Bearing - Dimensionless Flow vs. A_t
7 AB-5 Pierced Holes Airbearing. Radial Stiffness vs. Clearance
8 AB-5 Pierced Holes Airbearing. Radial Loading - Sleeve Flow vs. Clearance
9 AB-5 Pierced Holes Airbearing. Axial Stiffness vs. Clearance
10 AB-5 Pierced Holes Airbearing. Axial Loading - Endplate Flow vs. Clearance
11 AB-5 Millipore Airbearing. Radial Stiffness vs. Clearance
12 AB-5 Millipore Airbearing. Radial Loading - Sleeve Flow vs. Clearance
13 AB-5 Millipore Airbearing. Axial Stiffness vs. Clearance
14 AB-5 Millipore Airbearing. Axial Loading - Endplate Flow vs. Clearance
15 Journal Bearing - Load and Flow Optimization
16 Thrust Bearing with Recess. N=12. Downstream Orifice Pressure vs. Source Strength
17 Thrust Bearing with Recess. N=12. Dim. Load vs. Source Strength
18 Thrust Bearing without Recess. N=6,12,18. Downstream Orifice Pressure vs. Source Strength
19 Thrust Bearing without Recess. N=6,12,18. Dim. Load vs. Source Strength
20 Axial Loading - Air Gap vs. Load. $P_a = 14.6 \text{ psia}$, $\Delta P = 12.8 \text{ psi}$
21 Axial Loading - Air Gap vs. Load. $P_a = 14.6 \text{ psia}$, $\Delta P = 1.25 \text{ psi}$
22 Axial Loading - Air Gap vs. Load. $P_a = 7.0 \text{ and } 1.0 \text{ psia}$, $\Delta P = 1.25 \text{ psi}$
23 Radial Loading - Air Gap vs. Load. $P_a = 14.5 \text{ psia}$, $\Delta P = 12.8 \text{ psi}$
24 Radial Loading - Air Gap vs. Load. $P_a = 14.5 \text{ psia}$, $\Delta P = 1.25 \text{ psi}$
25 Radial Loading - Air Gap vs. Load. $P_a = 7.0 \text{ and } 1.0 \text{ psia}$, $\Delta P = 1.25 \text{ psi}$
26 Journal Bearing - Dynamic Load vs. Frequency Number
27 Journal Bearing - Load Phase Angle vs. Frequency Number
28 Journal Bearing - Dynamic Moment vs. Frequency Number
29 Journal Bearing - Moment Phase Angle vs. Frequency Number
30 Thrust Bearing - Dynamic Load vs. Frequency Number
31 Thrust Bearing - Load Phase Angle vs. Frequency Number
32 Thrust Bearing - Dynamic Moment vs. Frequency Number
33 Thrust Bearing - Moment Phase Angle vs. Frequency Number

ABSTRACT

This report presents a summary of the work performed by Mechanical Technology Incorporated under Contract NAS8-2588 (Subcontract 213-03-72120-6244 with the General Electric Company), entitled "Gas Lubricated Gimbal Bearing Investigation," with the National Aeronautics and Space Administration, Huntsville, Alabama.

The investigation is an analytical study of the static and dynamic load carrying capacity and the flow for the externally pressurized, gas lubricated journal and thrust bearing with orifice restricted feeding.

The investigation comprises the following analyses:

1. An approximate analysis of the static load and the flow for the journal and thrust bearing, restricted to small values of the eccentricity ratio. The number of orifice restricted feeding holes is assumed to be large such that the feeding planes become line sources. The solution is a first order perturbation calculation on the eccentricity ratio.
2. An analysis of the static load and the flow for the thrust bearing where the orifices are represented by point sources.
3. An approximate analysis of the static load and the flow for the journal bearing with the orifices as point sources. The analysis is a first order perturbation calculation on the eccentricity ratio ϵ , i.e., the results are valid for small ϵ only.
4. An approximate analysis of the static load for the journal bearing, valid for all eccentricity ratios. The feeding planes are taken as line sources and the bearing is assumed to be infinitely short.
5. An approximate analysis of the dynamic stiffness for the journal and the thrust bearing. The feeding planes are represented by line sources and the solution is a first order perturbation calculation on

the amplitude, i.e., the results are limited to motions with small amplitude. The motion is a harmonic vibration around the concentric position and is either a pure translation or a pure transverse rotation.

All five analyses have been programmed for the IBM 704 computer. Numerical results are obtained and compared to test data.

INTRODUCTION

The externally pressurized, gas lubricated gimbal axis bearing for a gyroscope in a missile must meet a series of severe specifications. As specifically related to the pressurized gas bearing the most important of these specifications are:

1. The bearing must be capable of withstanding high static and dynamic loads imposed by acceleration and vibrations during launching and space flight conditions.
2. The bearing and its auxiliary equipment should have minimum weight, volume and power consumption.
3. The error drift rate caused by turbine torque should be as low as possible.
4. The bearing must be stable.

The design problems arising from these specifications require for their solution a development of manufacturing techniques, experimental methods and theoretical analysis. It is the purpose of this report to describe the analytical methods which have been developed to assist in the design of the gimbal gas bearing. The present analysis has three objectives:

- a) to furnish methods for optimization of the design
- b) to calculate the load carrying capacity and air flow of the bearing,
- c) to calculate the dynamic bearing stiffness for use in a resonant frequency calculation.

In formulating the theoretical analysis the two basic equations are:

1. Reynolds equation which represents the bearing gas film (see eq. (A.5) and (A.17), Appendix A). This means that gas inertia, turbulence and shock conditions are not considered. Furthermore, the gas film is assumed to be isothermal.

2. The thermodynamic, one-dimensional orifice flow equation (eq. (A.22), Appendix A). The equation contains a vena contracta coefficient to define the effective flow area through the orifice. This coefficient is determined experimentally.

Hence the basic requirement of the analysis is to find methods for solving Reynolds equation and the orifice equation simultaneously. In general, these equations are too complex to permit an exact solution so that instead various approximate solutions have been obtained, each serving its particular purpose.

The first solution assumes that the number of feeding holes in a feeding plane is sufficiently large to let the feeding planes become line sources. This simplification allows a direct solution of the thrust bearing whereas the journal bearing with its circumferentially varying film thickness is solved by a first order perturbation on the eccentricity ratio ϵ (i.e., the results are valid for small ϵ values only). The advantage of the solution is that the results for the load and the flow are functions of only three parameters: the L/D ratio, the pressure ratio P_s/P_a and the feeding parameter Λ_t (see Figs. 3-6). Hence the analysis provides an easily interpreted, yet comprehensive picture of the bearing performance so that the effect of a change in any design parameter is readily evaluated.

The second solution uses a more accurate representation of the orifices by making them discreet point sources. For the thrust bearing, Reynolds equation reduces to Laplace's equation and an exact solution can be obtained for all eccentricity ratios (i.e., for all values of the film thickness). The journal bearing, however, does not have a uniform film thickness and therefore an exact solution cannot be obtained. Restricting the analysis to small eccentricity ratios a first order perturbation calculation is performed which gives an accurate evaluation of the bearing stiffness at $\epsilon = 0$. To find the journal bearing load vs. eccentricity ratio relationship for large values of ϵ an

approximate analysis is made. The analysis assumes the orifice feeding to be a line source and in addition that the bearing is infinitely short (i.e., that the axial flow gradient is much larger than the circumferential flow gradient). This results in a load vs. ϵ curve which may be improved by normalizing it with respect to the accurately calculated slope (stiffness) at $\epsilon = 0$.

The last part of the analysis is concerned with the dynamic stiffness of the bearings. In this case Reynolds equation becomes non-linear. Limiting the analysis to harmonic vibrations with small amplitude around the concentric journal position, a numerical calculation is carried out by means of a first order perturbation solution. The analysis assumes two vibratory motions: either a pure translation or a pure transverse rotation. Hence the increase in bearing stiffness caused by the squeeze film effect can be estimated (see Figs. 26-33) and included in a resonant frequency calculation.

All the above analyses have been programmed for the IBM 704 computer. Numerical results have been obtained and compared to experimental data (see Figs. 7-14 and Figs. 20-25).

RESULTS

The scope of the investigation is outlined in the preceding section. The general theoretical background and all the analyses are given in detail in the appendices. This section is concerned with the numerical results of the investigation as they are given in Figs. 1-33. The results are of two categories: a) general dimensionless data from which the effect of a change in design parameters may be evaluated, and b) specific numerical data for comparison with test data.

1. Orifice and Millipore Characteristics

The thermodynamic, one dimensional orifice flow equation is given by eq. (A.22). To account for the effective orifice area the equation contains a vena contracta coefficient λ which is evaluated by fitting the theoretical equation to NASA test data 2588-1 to -4 giving the orifice flow as a function of downstream pressure for a fixed supply pressure. The results for the sleeve and the endplate are given in Fig. 2 and serve as a basis for the subsequent calculations. In addition to using orifice restricted feeding, tests have also been conducted with millipore restriction. The millipore restrictor is a filter of five layers: 2 screens, 2 cement wafers and a membrane filter. An empirical expression is used to describe the characteristics of the millipore, eq. (A.29), which contains five experimentally evaluated coefficients. From NASA test data 2588-21 to -27 of the millipore flow as a function of supply pressure for a fixed downstream pressure these coefficients are found to be:

| | <u>Sleeve No. 4</u> | <u>Endplate No. 2 and No. 4</u> |
|----------------------|-------------------------|---------------------------------|
| a_o | = 3.892 | 3.859 |
| B | = 1.406 | 1.267 |
| $C(\text{psi}^{-1})$ | = .101 | .198 |
| D(psi) | = -.335 | -.40 |
| $a^2(\text{in}^2)$ | = $1.399 \cdot 10^{-6}$ | $1.348 \cdot 10^{-6}$ |

2. Bearing Dimensions and Air Data

The general bearing geometry is shown in Fig. 1. The actual bearing dimensions are summarized below as taken from NASA drawings:

orifice bearing: D10581725, C10582503, F10582504, F10582710

millipore bearing: D10582619, FX1783550, BX1796031, BX1796032, FX1796040

| | <u>Orifice Bearing</u> <u>Sleeve No. 5256</u> <u>Endplate No. E339, E445</u> | <u>Millipore Bearing</u> <u>Sleeve No. 4</u> <u>Endplate No. 2&4</u> |
|--------------------|--|--|
| Journal Bearing | Length outside feeding planes : L .724 .724 | Length between feeding planes : L_1 1.2532 1.2532 |
| | Bearing dia. : D ₁ 2.1622 2.1625 | Radial clearance: C .00055, .000925 .0005, .00074, .00095 |
| | Orifice radius : a .0025 - | Feeding hole diameter : d .028 .028 |
| | Number of feed- ing holes : N 32 48 | Outer radius : R ₁ 1.057 1.0676 |
| | Inner radius : R ₂ .650 .650 | Inner radius : R ₂ .650 .650 |
| Thrust Bearing | Orifice circle radius : R _c .835 .835 | Axial clearance : C ^c .00085 .00055, .00075, .001 |
| | Orifice radius : a .0035 - | Orifice radius : a .0035 - |
| | Feeding hole diameter : d .018 .028 | Feeding hole diameter : d .018 .028 |
| | Number of feed- ing holes : N 12 18 | Number of feed- ing holes : N 12 18 |
| | Depth of recess : h _r .0002 .0002 | Radius of recess: R _r .109 .109 |

(all dimensions in inches)

The air is at 75° F with:

| | |
|------------------------------|--|
| Viscosity | : $\mu = 2.83 \cdot 10^{-9}$ lbs.sec/in ² |
| (Gas constant).(Total temp.) | : RT = 342,500 in |

Four ratios of supply pressure to ambient pressure have been tested:

| Ambient Pressure P_a psia | Supply Pressure ΔP_s psig | Supply Pressure P_s psia | Pressure Ratio $V = P_s / P_a$ |
|-----------------------------------|---|----------------------------------|-----------------------------------|
| 14.7 | 12.8 | 27.5 | 1.87075 |
| 14.7 | 1.25 | 15.95 | 1.08503 |
| 7.0 | 1.25 | 8.25 | 1.17857 |
| 1.0 | 1.25 | 2.25 | 2.25 |

3. Bearing Stiffness and Flow at Eccentricity = 0

The first part of the investigation is based on an analysis which is a first order perturbation solution on the eccentricity ratio ϵ around the concentric journal position (Appendix B and C). Hence the analysis gives results for the stiffness and the flow at $\epsilon = 0$ for the journal bearing and the double acting thrust bearing. In dimensionless form the results are given in Figs. 3-6 as function of the feeding parameter Λ_t . This parameter may be visualized as expressing the ratio between the bearing flow resistance and the orifice flow resistance. When the bearing resistance is very high (f. inst. for a very small clearance) or the orifice resistance is low, then there is no pressure drop through the orifice. Hence, the pressure is uniform around the circumference of the journal bearing and there is no load carrying capacity. In other words, as $\Lambda_t \rightarrow \infty$, the load $\rightarrow 0$. Conversely, when the bearing resistance is small (f. inst for a very large clearance) or the orifice resistance is high, the pressure downstream from the orifice reduces to ambient pressure and again there is no load carrying capacity, i.e., as $\Lambda_t \rightarrow 0$, the load $\rightarrow 0$. Therefore, the load has a maximum value for a given bearing geometry and a given pressure ratio, corresponding to a particular value of Λ_t . This is the case for both the journal bearing and the double acting thrust bearing as shown by Figs. 3 and 5. Thus, in general the bearing clearance and the orifice

area should be chosen to give a A_t which corresponds to the maximum load. This is illustrated in Figs. 7, 9, 11 and 13 where the orifice area is held fixed while varying the clearance. It should furthermore be observed that for a fixed A_t and a given ambient pressure, the flow increases with the cube of the bearing clearance. Hence, from the point of view of minimizing the flow, and still have a maximum load, i.e., A_t unchanged, the clearance should be as small as consistent with manufacturing considerations. However, the bearings capacity for shock absorption is diminished by reducing the clearance so that a need for a compromise is indicated.

In applying the above approximate line source analysis to an actual bearing design it is apparent that there is a need for introducing a correction to account for the difference between the idealized model and the actual bearing. Experience has shown that the analysis is able to predict the bearing flow rather accurately, from which it can be deduced that the analysis also calculates the downstream orifice pressure correctly. However, the analysis ignores the reduction of pressure between the orifices so that the calculated load tends to be too large. The load is generated by the circumferential pressure variation set up by the eccentric journal, or expressed in terms of the analysis, by the pressure perturbation on the symmetrical, concentric-position pressure. This variation (or perturbation) is governed by the slope of the orifice flow vs. downstream pressure relationship at the operating concentric journal position (see. Fig. 4, Appendix B). Therefore, it seems reasonable to attempt to apply an empirical correction factor to the slope while recognizing that a formal justification is lacking. A correction factor of 2.0 has been used in calculating Figs. 3, 5, 7, 9, 11 and 13, i.e., m'_o in Appendix B has been multiplied by 2.0. The

analysis is programmed for the IBM 704 computer.

Figs. 7-14 show a comparison between NASA test data (2588-5 to 20, -38 to 50 and data of June 26, June 28 and July 10, 1962) and theoretical results obtained as explained above. The agreement is quite satisfactory.

The same analysis is used to study the effect of the axial position of the feeding planes in the journal bearing. The results are shown in Fig. 15 where the abscissa is the ratio of the distance between the feeding planes and the total bearing length. The curves give the maximum obtainable dimensionless load together with the corresponding values of the dimensionless flow and the feeding parameter Λ_t . Within a practical range for the feeding plane distance the load does not exhibit a maximum as long as Λ_t is changed according to the given curves. If Λ_t is kept constant, though, while one distance is changed, an optimum feeding plane position can be determined. The ratio of load to flow is maximum with one feeding plane in the middle of the bearing. It should be noted that these results are concerned with the load for an aligned journal only, or in approximation with the stiffness for translatory journal motion. If instead the stiffness for journal rotation around a transverse axis was considered, it would be expected that an optimum feeding plane position existed. This calculation has not been performed

4. Bearing Load vs. Eccentricity Ratio

Since the preceding line source analysis is restricted to small values of the eccentricity ratio ϵ and predicts a linear relationship between load and ϵ , additional analyses are required to determine the load for large values of ϵ .

The thrust bearing presents the simplest case because the gas film thickness is uniform. Even the line source analysis need not be limited to small ϵ although this was done above in order to simplify the results for the double acting thrust bearing. For the present analysis a more accurate representation of the orifices is introduced by making them point sources. This is a logical method since Reynolds equation for the thrust bearing reduces to Laplace's equation in the square of the pressure. The orifices are taken as logarithmic singularities and the physical boundary conditions are satisfied by means of image sources and sinks (Appendix E). The general dimensionless results are given in Figs. 16 and 17 for the thrust bearing with a recess around the feeding hole and in Figs. 18 and 19 for the bearing without a recess. Figs. 16 and 18 give the dimensionless orifice downstream pressure P_i as a function of the feeding hole radius r_o and the orifice source strength C . The effect of recess depth h_r or number of feeding holes N is also shown. Combining this data with the orifice flow equation (see eq. (E.6), Appendix E), the actual downstream pressure and source strength can be determined for any particular case with a given film thickness and bearing geometry. Knowing the source strength the bearing load is found directly from Fig. 17 or 19. Such a calculation has been carried out for four specific test conditions and the results are compared to the experimental data in Figs. 20, 21 and 22. The agreement is good. The pressure distribution has also been computed and compared to measurements in a few cases. The correlation was very satisfactory, but no results are given here. It should be noted that in performing the calculations, the effective feeding hole radius r_o was taken as .007 inch instead of the actual dimension of .009 inch to account for the orifice jet not filling out the entire feeding hole.

area. This value of the effective radius is in agreement with the measurements of the velocity head of the orifice jet as it enters the bearing.

The corresponding analysis for the journal bearing is vastly more difficult since the film thickness varies circumferentially when the journal is in an eccentric position. Instead of attempting a complete solution the analysis has been limited to finding the bearing stiffness (i.e., the slope of the load curve) at $\epsilon = 0$. This is done by perturbing the pressure and the orifice source strength with respect to ϵ around the concentric position. The orifices are point sources expressed mathematically by the impulse function (the Dirac delta function). Performing a first order perturbation, Reynolds equation reduces to two equations of the Laplacian type, the first equation being for the pressure in the concentric portion and the second equation being for the pressure perturbation which determines the load. The equations are solved in terms of infinite series (see Appendix C and D) and calculated on the IBM 704 computer. Due to the many parameters and the lengthy computation time no general results have been given. However, the program is used to obtain the stiffness for four particular test conditions (Figs. 23-25) in connection with the subsequent analysis.

In order to extend the analysis of the journal bearing to larger values of the eccentricity ratio an approximate analysis has been set up, see Appendix F. The orifice feeding is again represented by line sources and in addition the bearing is considered infinitely short (or in other words the axial flow gradient \gg the circumferential flow gradient). A similar approach has been successfully employed for the hydrodynamic bearing (Ref. 6). Solving the equations results in the load as a

function of ϵ . This curve is scaled down so that its slope at $\epsilon = 0$ becomes equal to the previously calculated, accurate slope (stiffness). The results are shown and compared to NASA test data in Figs. 23-25. The agreement is reasonably good.

5. Dynamic Bearing Stiffness

If the gyroscope is subjected to time changing accelerations the journal will perform vibratory motions. The velocity of the motion will "squeeze" the gas film thereby increasing the film pressure and hence increase the bearing load and the stiffness. Since the velocity is proportional to the vibratory frequency the dynamic stiffness is frequency dependent. This effect is important in a resonant frequency calculation.

The dynamic Reynolds equation (eq. (A.6) and (A.17), Appendix A) is non-linear and only an approximate solution is attempted. The equation is linearized by assuming the journal motion to be harmonic with small amplitude around the concentric position. Two vibrating modes are studied for both the journal and the thrust bearing: a pure translation with amplitude $\epsilon \cos \omega t$ and a pure rotation around a transverse symmetry axis with angular amplitude $\alpha \cos \omega t$, where ω is the frequency. Assuming ϵ and α small, a first order perturbation calculation is performed. In addition, the feeding planes are treated as line sources. The resulting equations are rewritten in terms of finite difference equations and integrated numerically on the computer. Results for the dimensionless translatory stiffness, the dimensionless rotational stiffness and the phase angle (i.e., the angle by which the stiffness lags the amplitude) are given in Figs. 26-33 as function of frequency. As would be expected, the stiffness increases with increasing frequency.

but the effect is first noticeable at high frequencies, f. iust. for an ambient pressure $P_a = 1$ psia at 3 - 40 cps and for $P_a = 14.7$ at 200 to 400 cps. At low frequencies the dynamic stiffness is equal to the static stiffness.

Three distinct resonant frequencies may be visualized: a) a pure translatory mode governed by the journal bearing stiffness, b) a pure translatory mode governed by the thrust bearing stiffness, and c) a pure rotational mode (i.e., a rotation around an axis through the center of gravity of the journal perpendicular to the journal axis) governed by the combined journal and thrust bearing rotational stiffness. Denoting the translatory stiffness: K (lbs/in) and the rotational stiffness: m (lbs.in/rad) the resonant frequencies ω are given by:

$$\text{translatory } \omega = \sqrt{\frac{K}{M}} \frac{\text{rad}}{\text{sec}}$$

$$\text{rotational } \omega = \sqrt{\frac{m}{I}} \frac{\text{rad}}{\text{sec}}$$

where M is the journal mass in $\text{lbs} \cdot \text{sec}^2/\text{in}$ and I is the transverse mass moment of inertia in $\text{lbs} \cdot \text{in} \cdot \text{sec}^2$. Hence:

$$K = M\omega^2$$

$$m = I\omega^2$$

where K and m are found from Figs. 26, 30, 28 and 32 by:

$$K = \frac{W_D}{C\epsilon}$$

$$m = \frac{M_D}{C}$$

Thus K and m may be plotted as functions of frequency ω for a given bearing and a given operating condition. On the same graphs the parabolic curves $M\omega^2$ and $I\omega^2$ can be plotted and their intersection with the corresponding stiffness curves define the resonant frequencies.

The actual calculations have not been carried out. It should be noted that the dynamic stiffness actually is a combination of a stiffness term and a damping term. Let it be assumed that the journal is in static equilibrium at an eccentricity ratio ϵ_0 . If the journal is given a small displacement X and a corresponding velocity \dot{X} the restoring force becomes:

$$F = \frac{1}{C} \left(\frac{\partial F}{\partial \epsilon} \right)_{\epsilon_0} X + \frac{1}{C} \left(\frac{\partial F}{\partial \dot{\epsilon}} \right)_{\epsilon_0} \dot{X}$$

For a translatory journal motion with amplitude $C \cos \omega t$ the restoring force is from the analysis (see Eq. (G.62), Appendix G)

$$F = W_D = P_a D(L+L_1) W'_D \epsilon \cos(\omega t - \phi_w) = \frac{P_a D(L+L_1) W'_D}{C} (\cos \phi_w X - \frac{\sin \phi_w}{\omega} \dot{X})$$

where $W'_D = \frac{W_D}{P_a D(L+L_1) \epsilon}$ is given in Fig. 26 and ϕ_w is given in Fig. 27.

Pence we may introduce:

$$\text{the stiffness: } K_D = \frac{1}{C} \left(\frac{\partial F}{\partial \epsilon} \right)_{\epsilon_0} = \frac{P_a D(L+L_1) W'_D}{C} \cos \phi_w$$

$$\text{the damping: } C_D = \frac{1}{C} \left(\frac{\partial F}{\partial \dot{\epsilon}} \right)_{\epsilon_0} = - \frac{P_a D(L+L_1) W'_D}{\omega C} \sin \phi_w$$

where K_D is the actual dynamic stiffness. Both K_D and C_D are functions of frequency because W' and ϕ_w are. If the sleeve is subjected to a forced vibration with amplitude $b \cos \omega t$, then the journal will vibrate with an amplitude y relative to the sleeve, where:

$$y = \frac{M \omega^2 b}{\sqrt{(K_D - M \omega^2)^2 + (\omega C_D)^2}} \cos(\omega t - \psi_w) \quad \psi_w = \tan^{-1} \left(\frac{\omega C_D}{K_D - M \omega^2} \right)$$

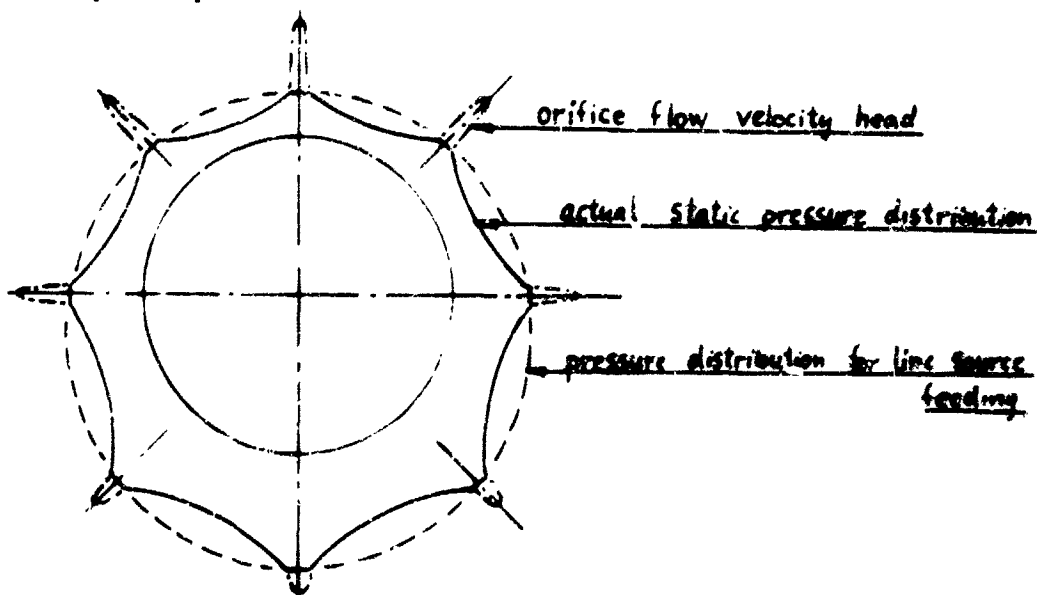
Thus for a given value of the frequency ω , the amplitude of the journal motion can be determined.

v. Turbine Torque

The actual bearing and orifice dimensions will always deviate slightly from the ideal drawing dimensions. Thus there will always be dissymmetries in the flow through the bearing and the circumferential component of those dissymmetries will exert a net torque on the journal.

For the function of the gyroscope this torque is highly undesirable and must be kept to a minimum. The torque depends on the eccentricity ratio and on the journal motion and is not constant over the operating range of the bearing. This makes it impossible to eliminate the torque by any simple compensation.

In the following a few simple calculations are made to bring out some of the important factors contributing to turbine torque. Limiting the discussion to the journal bearing the circumferential pressure distribution is in principle as shown below:



Three possible sources for turbine torque may be identified:

- a) The orifice jet impinging on the journal, i.e., the orifice flow velocity head above.
- b) The overall circumferential flow from the bottom towards the top caused by the eccentric journal. This flow may be considered to come from the distribution labeled: "pressure distribution for line source feeding" above, since this distribution represents the orifice downstream pressure.
- c) The local circumferential flow variation between the orifices caused by the above "scalloped" pressure distribution.

Let the total bearing flow over all N orifices be Q_T in³/sec at ambient pressure P_a . The orifice downstream pressure is P_o and the orifice jet is assumed to have the same radius, a , as the orifice. If all orifice centerlines pass the journal center by the distance δ inch, then the total torque caused by orifice jet impingement becomes:

$$T_1 = \frac{1}{2} \frac{P_a^2}{P_o(RT)} \frac{Q_T^2}{N\pi a^2} \delta$$

where RT is the (gas constant).(total temperature) in in²/sec². To convert the torque to dyn.cm, multiply by $1.130 \cdot 10^6$. For the particular test condition of a supply pressure = 12.8 psig and an ambient pressure of 14.6 psia the flow is 7.63 in³/sec at an orifice downstream pressure $P_o = 21.4$ psia. If furthermore the orifice centerline eccentricity δ due to both tolerances and journal eccentricity is set to $\delta = .001$ in. for all orifices (conservative) the torque becomes:

$$T_1 = 3.94 \text{ dyn}\cdot\text{cm}$$

Let the gas film pressure be P so that the circumferential shear stress on the journal at an angle Θ from the top of the bearing is:

$$\tau = \frac{1}{2} \frac{C}{R} \frac{\partial P}{\partial \theta} (1 + \epsilon \cos \theta) \quad \frac{\text{lbf}}{\text{in}^2}$$

where C is the radial clearance and R is the journal radius. The total torque on one bearing half becomes:

$$T_2 = RC \int_0^{\frac{\pi}{2}} \int_0^{\pi} \frac{\partial P}{\partial \theta} (1 + \epsilon \cos \theta) d\theta dz$$

When the feeding planes are line sources and the eccentricity ratio ϵ is small, a first order perturbation calculation shows that the pressure may be expressed by:

$$P = P_o(z) + \epsilon P_1(z) \cos \theta$$

Hence the torque becomes:

$$T_2 = -2\epsilon RC \int_0^{\frac{\pi}{2}} P_1(z) dz$$

The bearing load W lbs is:

$$W = -2 \int_0^{\frac{L}{2}} \int_0^{2\pi} P(z) \cos \theta R d\theta dz = -2\pi \epsilon R \int_0^{\frac{L}{2}} P_i(z) dz$$

so that the shear torque is given by:

$$T_2 = \frac{1}{4} CW$$

For the same test condition as used in arriving at the above value for the orifice jet torque T_1 , the shear torque becomes:

$$T_2 = 1380 \text{ dyn}\cdot\text{cm}$$

at an eccentricity ratio $\epsilon = .1$, a load of 4.16 lbs and a radial clearance $C = .000925$ in. The net torque on the journal is the balance between the torques on the two bearing halves, i.e.,

$$T_{2,\text{net}} = \text{error in } (1380 - 1380) \text{ dyn}\cdot\text{cm}$$

On the other hand the net orifice jet torque is

$$T_{1,\text{net}} = \text{error in } (4) \text{ dyn}\cdot\text{cm}$$

Hence it may be concluded that the jet impingement effect is small compared to the circumferential flow effect.

The third contribution to the turbine torque from the pressure variation between the orifices can be shown to be of the same order of magnitude as the shear torque T_2 . Thus this effect is very important but no numerical calculations will be given.

7. Summary of Results

Briefly summarized, the results of the investigation are:

- a) A simplified analysis of the bearing load and the flow for use in selecting the design parameters. The results are dimensionless and may readily be presented in convenient graphs as shown in Figs. 3-6. The validity of the results is established in Figs. 7-14 by a comparison with test data.
- b) A calculation method for determining the load as a function

of journal eccentricity for both the journal and the thrust bearing. Comparison with test data is shown in Figs. 20-25.

The form of the general theoretical results, from which the numerical data is calculated, is illustrated by Figs. 16-19.

- c) A simplified analysis for the dynamic stiffness. The results may be given in dimensionless charts as in Figs. 26-33 and are used for calculating the resonant frequencies of the bearing and the amplitude.
- d) Computer programs have been written for all the analyses.

DISCUSSION

Having presented the scope and the results of the analysis it remains to discuss the implications of the results and the limitations of the analysis.

One of the basic design requirements of the gimbal gas bearing is to obtain maximum stiffness and load with a minimum of flow and power. Since the stiffness is not constant over the operating range the design specifications must give information leading to a definition of where the stiffness should be optimized. No such explicit specifications exist at the present time (i.e., for steady state acceleration, vibratory acceleration, frequency spectrum, impulse loading etc.), but it is the current feeling that the stiffness should be optimized at a large eccentricity ratio (approximately $\epsilon = .9$) to ensure that the bearings load carrying capacity may be utilized to its limit. This is clearly not sufficient since the load curve may be such that the stiffness is large at $\epsilon = .9$ and relatively small at $\epsilon = 0$, the latter case being a possible space flight condition at zero g. Furthermore the area under the load curve cannot be neglected since it is a measure of the bearings capacity for shock absorption. Also, the gas film damping is important in establishing the vibratory amplitude at resonance where the cylinder must not touch the bearing sleeve. However, in any case an analysis is needed to give a rather accurate calculation of the load curve and the present investigation has been partially successful in doing so. It is apparent, though, that the journal bearing analysis need to be refined. In addition it seems clear that a more detailed and more physically correct orifice representation would improve the analysis. It is hardly to be expected that a one dimensional orifice model can account accurately for the complex three dimensional flow existing around the feeding hole entrance to the bearing. It is essential for future progress to explore this area.

Another problem is the dynamics of the bearing. The investigation has analyzed the dynamic stiffness but only for the concentric journal position and

based on a simplified orifice feeding representation. A more extensive analysis is needed which includes the effect of eccentricity ratio and, if at all possible, allows for the influence of the bearing on the orifice under dynamic conditions. This is an extremely difficult problem since it involves both a method for solving the non-linear Reynolds equation and in addition a method for solving the time dependent orifice characteristic, a problem which has not yet been well defined. A study of this type is necessary not only for a more accurate frequency response calculation but it is also an essential prerequisite for a stability analysis.

The investigation has ignored the possible existence of shock conditions in the bearing. Such conditions may occur around the feeding hole entrance and in the gas film when the ambient pressure is low. Since the analysis assumes isothermal conditions it is not suited to investigate shock. Therefore, a new analysis is needed if this problem becomes important.

The analysis is limited to the bearing geometry of Fig. 1, whereas an actual design analysis should consider all possible configurations. Thus it would seem natural to attempt a more uniformly distributed gas feeding to reduce turbine torque, f. inst. by a porous sleeve wall or by suitable grooving of the bearing surface. Obviously this requires a new analysis.

CONCLUSIONS

1. The investigation has demonstrated that analytical methods can be used in selecting the optimum bearing dimensions and design parameters.
2. A method has been developed to calculate the load as a function of journal displacement for both the thrust and the journal bearing. This is needed for evaluating the bearing performance over the entire operating range.
3. An analysis has been set up for calculating the dynamic stiffness of both the thrust and the journal bearing and, hence, for calculating the resonant frequencies of the bearing. The analysis provides for determining the vibration amplitude caused by a forced vibration of the bearing.
4. The investigation has demonstrated the need for a detailed study of the flow through the orifice and around the feeding hole entrance.
5. Calculations have been made to show that the orifice jet impingement plays a minor role in producing turbine torque. The circumferential flow, caused by the eccentric journal and by the pressure drop between the orifices, is a major factor.

RECOMMENDATIONS

1. A study of the pressure and velocity distribution around the orifice and the feeding hole should be undertaken. Preferably the study should include time dependent effects. Such an analysis is necessary for obtaining closer agreement between experimental and theoretical results and also for setting up a realistic stability analysis.
2. A more comprehensive analysis of the dynamic behavior of the bearing is desirable both for calculating the vibratory response and the stability. It may be necessary to resort to a numerical solution based on finite difference equations. Since the simultaneous solution of the Reynolds equation with the orifice equation is a highly non-linear problem, a separate mathematical study of related numerical techniques is indicated.
3. Other promising bearing configurations should be analyzed similarly to the present investigation. Thus f.inst. the bearing, where the gas feeding takes place through narrow slits or grooves, may have a reduced turbine torque and the same may be true for the porous wall bearing.
4. A study should be undertaken to establish the operating specifications for the bearing, i.e., specifications for steady acceleration, dynamic acceleration, frequency spectrum, impulse loading, allowable turbine torque, etc.

ACKNOWLEDGEMENT

This investigation is sponsored by the National Aeronautics and Space Administration, Huntsville, Alabama, through the General Electric Company, Pittsfield, Massachusetts under Contract NAS8-2588 (Subcontract 213-03-72120-6244). The authors wish to thank NASA and the General Electric Company for their support.

Also, the authors wish to thank Dr. Häusserman, Mr. R. E. Beyer, Mr. W. Kimmmons and Mr. E. Martz of the Astronics Division of NASA for their kind cooperation and assistance in the investigation and for supplying all the experimental data.

Dr. C. H. T. Pan has served as advisor on several parts of the theoretical analysis, Mr. F. Walsh has assisted in obtaining the numerical calculations and the graphs and Mr. R. Geguzys has written the computer program for the journal bearing with source feeding. Their contributions are appreciated by the authors.

REFERENCES

1. Pinkus, O. and Sternlicht, B., "Theory of Hydrodynamic Lubrication," McGraw-Hill Book Company (1961)
2. Heinrich, G., "The Theory of the Externally-Pressurized Bearing with Compressible Lubricant," First International Symposium on Gas Lubricated Bearings, ONR/ACR-49 (1959).
3. Friedman, Bernard, "Principles and Techniques of Applied Mathematics," Wiley, New York (1956).
4. Streeter, V. L., "Fluid Dynamics," McGraw-Hill Book Company (1948).
5. Kober, H., "Dictionary of Conformal Representations," Dover Publications \$160.
6. Dubois, G. B. and Ocvirk, F. W., "Analytical Derivation and Experimental Evaluation of Short Bearing Approximation for Full Journal Bearing," NACA Report 1157 (1953).

APPENDIX A

General Equations

A. Journal Bearing

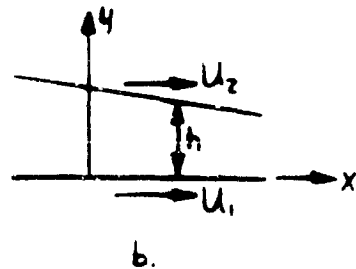
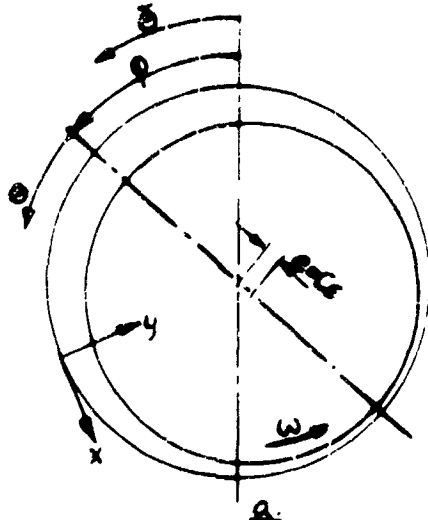


Fig. 1

If fluid film inertia is neglected and if the gas film is considered so thin that pressure, density and viscosity may be considered constant across the film and velocity gradients across the film much greater than gradients along the film, Navier-Stokes equations reduce to:

$$\frac{\partial^2 u}{\partial y^2} = \frac{1}{\mu} \frac{\partial p}{\partial x}$$

$$\frac{\partial^2 w}{\partial y^2} = \frac{1}{\mu} \frac{\partial p}{\partial z}$$

where u and w are the velocities in the x - and z -direction, μ is the viscosity and p is the pressure. Integrating twice making use of Fig. 1b:

$$(A.1) \quad u = \frac{1}{2\mu} \frac{\partial p}{\partial x} y(y-h) + \frac{h-y}{h} U_1 + \frac{y}{h} U_2$$

$$(A.2) \quad w = \frac{1}{2\mu} \frac{\partial p}{\partial z} y(y-h)$$

Hence the mass flow per inch becomes:

$$(A.3) \quad Q_x = \int_0^h g u dy = - \frac{h^3}{12\mu} g \frac{\partial p}{\partial x} + \frac{1}{2} gh(U_1 + U_2)$$

$$(A.4) \quad Q_z = \int_0^h g w dy = -\frac{h^3}{12\mu} \int \frac{\partial P}{\partial z}$$

These equations are used to establish the flow balance for an infinitesimal prism $h \cdot dx \cdot dz$ where external gas feeding is introduced as the mass flow M over the area A . Hence we get:

$$\frac{\partial Q_x}{\partial x} \cdot dx dz + \frac{\partial Q_z}{\partial z} dz dx + \frac{\partial (gh)}{\partial t} dx dz = \frac{M}{A} dx dz$$

Introducing eq. (A.3)-(A.4) we obtain Reynolds equation:

$$(A.5) \quad \frac{\partial}{\partial x} \left[\frac{h^3}{12\mu} g \frac{\partial P}{\partial x} \right] + \frac{\partial}{\partial z} \left[\frac{h^3}{12\mu} g \frac{\partial P}{\partial z} \right] = \frac{1}{2} \frac{\partial}{\partial x} \left[gh (U_1 + U_2) \right] + \frac{\partial (gh)}{\partial t} - \frac{M}{A}$$

This equation is made dimensionless by setting:

$$\bar{P} = \frac{P}{P_a} \quad \bar{h} = \frac{h}{C} = 1 + \epsilon \cos \theta \quad \epsilon = \frac{\epsilon}{C}, \text{ see fig. 1a}$$

$$\Theta = \frac{x}{R} \quad \zeta = \frac{z}{R} \quad \tau = \omega t$$

$$U_2 = R\omega \quad U_1 = 0$$

Assuming isothermal conditions such that μ is constant and $g = \frac{P}{RT}$, eq. (5) becomes upon neglecting the bar notation:

$$(A.6) \quad \frac{\partial}{\partial \Theta} \left[h^3 P \frac{\partial P}{\partial \Theta} \right] + \frac{\partial}{\partial \zeta} \left[h^3 P \frac{\partial P}{\partial \zeta} \right] = \Lambda \left[\frac{\partial (Ph)}{\partial \Theta} + 2 \frac{\partial (Ph)}{\partial T} \right] - 2 \Lambda_t V_m \frac{\pi R^2}{NA}$$

where:

$$(A.7) \quad \Lambda = \frac{6\mu\omega}{P_a} \left(\frac{C}{C} \right)^2$$

$$(A.8) \quad \Lambda_t = \frac{6\mu N \alpha a^2 \sqrt{RT}}{P_a C^3} \quad \alpha: \text{orifice coefficient}$$

$$(A.9) \quad V = \frac{P_s}{P_a}$$

(A.10) N : number of feeding holes

$$(A.11) \quad m = \frac{M \sqrt{RT}}{\alpha \pi a^2 P_s}$$

Since $\Theta = \bar{\Theta} - \phi$, where ϕ may vary with time, we can write:

$$\frac{\partial}{\partial \tau} = \frac{\partial}{\partial \tau}|_0 - \dot{\phi} \frac{\partial}{\partial \theta} \quad \text{where} \quad \dot{\phi} = \frac{\partial \phi}{\partial \tau} = \omega \frac{\partial \phi}{\partial t}$$

Hence, if $\frac{\partial}{\partial \tau}$ refers to the time derivative only, Reynolds equation becomes:

$$(A.12) \frac{\partial}{\partial \theta} \left[h^3 P \frac{\partial P}{\partial \theta} \right] + \frac{\partial}{\partial \zeta} \left[h^3 P \frac{\partial P}{\partial \zeta} \right] = \Lambda \left[(1-2\dot{\phi}) \frac{\partial (Ph)}{\partial \theta} + 2 \frac{\partial (Ph)}{\partial \tau} \right] - 2 \Lambda_t V_m \frac{\pi R^2}{NA}$$

For the hydrostatic bearing there is no journal rotation. However, the journal center may still have motion and assuming this motion to be periodic with frequency ω eq. (A.12) becomes:

$$(A.13) \frac{\partial}{\partial \theta} \left[h^3 \frac{\partial P^2}{\partial \theta} \right] + \frac{\partial}{\partial \zeta} \left[h^3 \frac{\partial P^2}{\partial \zeta} \right] = 4 \Lambda \left[-\dot{\phi} \frac{\partial (Ph)}{\partial \theta} + \frac{\partial (Ph)}{\partial \tau} \right] - 4 \Lambda_t V_m \frac{\pi R^2}{NA}$$

which is the general Reynolds equation for the hydrostatic journal bearing.

For steady state operation it reduces to:

$$(A.14) \frac{\partial}{\partial \theta} \left[h^3 \frac{\partial P^2}{\partial \theta} \right] + \frac{\partial}{\partial \zeta} \left[h^3 \frac{\partial P^2}{\partial \zeta} \right] = -4 \Lambda_t V_m \frac{\pi R^2}{NA}$$

B. Thrust Bearing

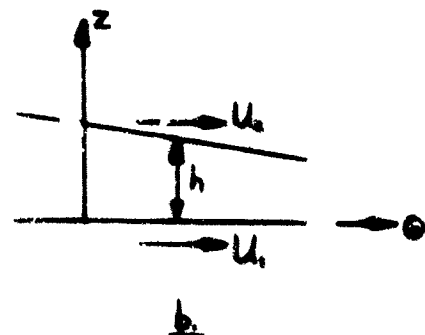
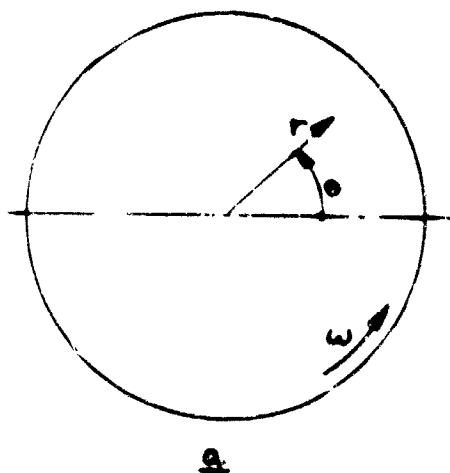


Fig. 2

Under the previous assumptions Navier-Stokes equations reduce to:

$$\frac{\partial u}{\partial z^2} = \frac{1}{\mu} \frac{\partial p}{\partial r}$$

$$\frac{\partial v}{\partial z^2} = \frac{1}{\mu} \frac{\partial p}{r \partial \theta}$$

where u and v are the velocities in the radial and tangential direction.

The mass flow per inch becomes:

$$(A.15) \quad Q_r = -\frac{h^3}{12\mu} g \frac{\partial p}{\partial r}$$

$$(A.16) \quad Q_\theta = -\frac{h^3}{12\mu} g \frac{\partial p}{r \partial \theta} + \frac{1}{2} gh(U_1 + U_2)$$

A mass flow balance gives:

$$\frac{\partial(rQ_r)}{\partial r} dr d\theta + \frac{\partial Q_\theta}{\partial \theta} r d\theta dr + \frac{\partial(gh)}{\partial t} r d\theta dr = \frac{M}{A} r d\theta dr$$

where M is the external gas feeding over the area A . Introducing eq. (A.15)- (A.16) we obtain Reynolds equation in polar coordinates:

$$(A.17) \quad \frac{\partial}{\partial r} \left[r \frac{h^3}{12\mu} g \frac{\partial p}{\partial r} \right] + \frac{\partial}{\partial \theta} \left[\frac{h^3}{12\mu} g \frac{\partial p}{r \partial \theta} \right] = \frac{1}{2} \frac{\partial}{\partial \theta} [gh(U_2 + U_1)] + \frac{\partial(gh)}{\partial t} - \frac{M}{A}$$

In this equation the local film thickness h changes with time not only due to a normal velocity difference between the two plates but also by the rotation of the upper plate in Fig. 2b. For this reason Reynolds equation is normally given in coordinates stationary with respect to the lower plate. Thus the new $\bar{\theta}$ -coordinate becomes:

$$\bar{\theta} = \theta - \frac{U_1}{r} t$$

Therefore:

$$\frac{\partial(gh)}{\partial t} = \frac{\partial(gh)}{\partial t} \Big|_{\theta} + \frac{\partial(gh)}{\partial \bar{\theta}} \frac{\partial \bar{\theta}}{\partial t} = \frac{\partial(gh)}{\partial t} \Big|_{\bar{\theta}} - U_1 \frac{\partial(gh)}{r \partial \bar{\theta}}$$

Dropping the bar notation eq. (A.17) becomes:

$$(A.18) \frac{1}{r} \frac{\partial}{\partial r} \left[r \frac{h^3}{12\mu} g \frac{\partial P}{\partial r} \right] + \frac{1}{r d\theta} \left[\frac{h^3}{12\mu} g \frac{\partial P}{\partial \theta} \right] = \frac{1}{2} (U_2 - U_1) \frac{\partial (gh)}{r d\theta} + \frac{\partial (gh)}{\partial t} - \frac{M}{A}$$

To make dimensionless set:

$$\bar{P} = \frac{P}{P_a} \quad \bar{h} = \frac{h}{C}$$

$$\bar{r} = \frac{r}{R} \quad \tau = \omega t$$

$$U_2 = r\omega \quad U_1 = 0$$

Assuming isothermal conditions and a perfect gas with $g = \frac{P}{RT}$ and dropping the bar notation eq. (A.18) becomes:

$$(A.19) \frac{1}{r} \frac{\partial}{\partial r} \left[r h^3 P \frac{\partial P}{\partial r} \right] + \frac{1}{r d\theta} \left[h^3 P \frac{\partial P}{\partial \theta} \right] = \Lambda \frac{\partial (Ph)}{\partial \theta} + 2\Lambda \frac{\partial (Ph)}{\partial \tau} - 2\Lambda_t V_m \frac{\pi R^2}{NA}$$

where the dimensionless parameters are defined in eq. (A.7)-(A.11). For the purely hydrostatic bearing there is no rotation. Assuming the upper plate to have motion with frequency ω eq. (A.19) reduces to:

$$(A.20) \frac{1}{r} \frac{\partial}{\partial r} \left[r h^3 \frac{\partial P^2}{\partial r} \right] + \frac{1}{r d\theta} \left[h^3 \frac{\partial P^2}{\partial \theta} \right] = 2\Lambda \left[\dot{\phi} \frac{\partial (Ph)}{\partial \theta} + 2 \frac{\partial (Ph)}{\partial \tau} \right] - 4\Lambda_t V_m \frac{\pi R^2}{NA}$$

where $\dot{\phi} = \frac{\partial \phi}{\partial \tau} = \frac{1}{\omega} \frac{\partial \phi}{\partial t}$ and ϕ is the angular motion of the top plate.

For steady state operation eq. (A.20) becomes:

$$(A.21) \frac{1}{r} \frac{\partial}{\partial r} \left[r h^3 \frac{\partial P^2}{\partial r} \right] + \frac{1}{r d\theta} \left[h^3 \frac{\partial P^2}{\partial \theta} \right] = -4\Lambda_t V_m \frac{\pi R^2}{NA}$$

C. External Gas Feeding

In the above equations the external gas feeding is introduced directly into the Reynolds equation. In general gas is only fed to the bearing at discrete points. Hence, it is frequently convenient to solve Reynolds equation

without feeding and introduce the feeding through the boundary conditions as will be shown in later appendices. In accordance with eq. (A.11) we define the dimensionless mass flow from the external feeding as

$$m = \frac{M \sqrt{RT}}{\alpha \pi a^2 P_s}$$

where M is the mass flow, $\text{lbs.sec}^2/\text{in}$; α is a flow coefficient; πa^2 is the restrictor area, P_s is the supply pressure and RT is the gas constant-total temperature, in^2/sec^2 . The dimensionless mass flow m is in general a function of the downstream pressure P_i from the feeding hole, i.e.

$$m = m\left(\frac{P_i}{V}\right)$$

In the present analysis two kinds of feeding restrictors are used: the orifice restricted and the millipore restricted feeding.

1. Orifice Restriction

The mass flow through an orifice with radius a is given by:

$$M = \nu \pi a^2 \sqrt{\eta \frac{2K}{K-1}} \sqrt{RT} \left(\frac{P_i}{V}\right)^{1/K} \sqrt{1 - \left(\frac{P_i}{V}\right)^{\frac{K-1}{K}}}$$

Setting the orifice coefficient $\alpha = \sqrt{\eta}$ the dimensionless mass flow becomes:

$$(A.22) \quad m = \nu \sqrt{\frac{2K}{K-1}} \left(\frac{P_i}{V}\right)^{1/K} \sqrt{1 - \left(\frac{P_i}{V}\right)^{\frac{K-1}{K}}}$$

where K is the adiabatic gas exponent, ν is the vent contracta coefficient and η is the adiabatic efficiency. For later use:

$$(A.23) \quad m' = \frac{\partial m}{\partial \left(\frac{P_i}{V}\right)} = \frac{1}{\nu} \frac{\partial \nu}{\partial \left(\frac{P_i}{V}\right)} m - \frac{2\nu^2}{K-1} \frac{\left(\frac{P_i}{V}\right)^{1/K} \left[\frac{K+1}{2} - \left(\frac{P_i}{V}\right)^{\frac{K-1}{K}}\right]}{m}$$

Eq. (A.22) and (A.23) apply to the unchoked orifice. When the orifice is choked, i.e.,

$$(A.24) \quad \left(\frac{P_i}{V}\right) \leq \left(\frac{2}{K+1}\right)^{\frac{K}{K-1}}$$

then eq. (A.22) and (A.23) become:

$$(A.25) \quad m = \nu \sqrt{\frac{2K}{K+1}} \left(\frac{2}{K+1}\right)^{\frac{1}{K-1}}$$

$$(A.26) \quad m' = \frac{\partial m}{\partial (\frac{P_i}{V})} = \frac{1}{\nu} \frac{\partial \nu}{\partial (\frac{P_i}{V})} m$$

Because of the discontinuity in the above equations at the critical pressure ratio, it is sometimes convenient to replace the exact orifice equation by an approximate expression. This can be done by setting:

$$M = \frac{\pi a^2}{\sqrt{RT}} P_s \sqrt{1 - \left(\frac{P_i}{V}\right)^2}$$

so that

$$(A.27) \quad m = \sqrt{1 - \left(\frac{P_i}{V}\right)^2}$$

$$(A.28) \quad m' = \frac{\partial m}{\partial (\frac{P_i}{V})} = \frac{-P_i}{\sqrt{V^2 - P_i^2}}$$

2. Millipore Restriction

The millipore restrictor is a filter consisting of 5 layers: 2 screens, 2 cement wafers and a membrane filter. No theoretical expression is available for the flow through this filter and instead the following empirical formula is used:

$$(A.29) \quad M = \frac{\pi a^2 P_s}{\sqrt{RT}} \frac{1}{V} \left[C P_i^2 + P_i + D \right] \frac{(V - P_i)(V - P_i + B)}{V - P_i + a_0}$$

where the coefficients a_0, B, C and D are determined experimentally.

In dimensionless form:

$$(A.36)m = \frac{1}{V} [CP_i^2 + P_i + D] \frac{(V - P_i)(V - P_i + B)}{V - P_i + a_s}$$

$$(A.37)m' = \frac{\partial m}{\partial (V)} = -[CP_i^2 + P_i + D] \left[1 + \frac{a(B-a)}{(V - P_i + a)^2} \right] + \frac{(V - P_i)(V - P_i + B)}{V - P_i + a_s} [2CP_i + 1]$$

3. Orifice Restriction with Inherent Compensation

If the diameter d of the feeding hole from the orifice to the bearing is small, the annular restrictor area between the journal and the rim of the feeding hole becomes important.

For two orifices in series the mass flow equation becomes:

$$(A.32) \frac{MVRT}{A_1 \sqrt{\eta_{1,2-1}} P_s \left(\frac{P_i}{P_s}\right)} = \frac{\left(\frac{P_i}{P_s}\right)^{k_*} \sqrt{1 - \left(\frac{P_i}{P_m}\right)^{\frac{k-1}{k}}}}{\left(\frac{P_m}{P_s}\right)} = \frac{A_2 \sqrt{\eta_2}}{A_1 \sqrt{\eta_1}} \left(\frac{P_i}{P_m}\right)^{k_*} \sqrt{1 - \left(\frac{P_i}{P_m}\right)^{\frac{k-1}{k}}}$$

where A_1 is the area of the first orifice, A_2 of the second orifice, η is the adiabatic efficiency, P_s is the pressure before the first orifice, P_m is the pressure between the orifices and P_i is the pressure after the second orifice.

When $\frac{A_2 \sqrt{\eta_2}}{A_1 \sqrt{\eta_1}}$ is known this equation may be solved numerically to give $m = \frac{MVRT}{A_1 P_s}$ as a function of $\frac{P_i}{P_s}$. If the orifice radius is a , the feeding hole diameter is d and the film thickness is h we get:

$$\frac{A_2 \sqrt{\eta_2}}{A_1 \sqrt{\eta_1}} = \frac{V \sqrt{\eta_2} d h}{V \sqrt{\eta_1} a^2}$$

where V is the vena contracta coefficient. Since V is a function of the orifice pressure ratio and h varies around the circumference in the journal bearing an exact solution is cumbersome and an approximate expression is more convenient. If it is assumed that h does not vary too much (i.e., for small

eccentricity ratios in the journal bearing) and if $\alpha = \sqrt{\eta_1}$ may be considered the same for the two restrictors we get:

$$\frac{A_2\sqrt{\eta_2}}{A_1\sqrt{\eta_1}} = \frac{dC(1+\epsilon\cos\theta)}{a^2} = \frac{1+\epsilon\cos\theta}{\sigma} \quad (A.33)$$

$$\sigma = \frac{a^2}{dC}$$

where C is the radial clearance. Then a reasonable approximation to eq. (A.32) is:

$$(A.34) \quad m = \frac{M\sqrt{RT}}{\alpha\pi a^2 P_s} = \frac{1}{\sqrt{1 + \frac{\sigma^2}{(1+\epsilon\cos\theta)^2}}} \sqrt{1 - \left(\frac{P_i}{V}\right)^2}$$

where α depends on σ .

When σ is small the bearing is predominantly orifice restricted whereas a large σ indicates a predominantly inherent compensated bearing.

APPENDIX B

The Static Load Carrying Capacity of Hydrostatic Bearings With Orifice Restricted Line Feeding

Frequently the number of orifices in a feeding plane is sufficiently large to permit representing the orifices by a line feed. This considerably simplifies the analysis, since the gas feeding does not enter Reynolds equation directly but instead becomes one of the boundary conditions.

A. Journal Bearing

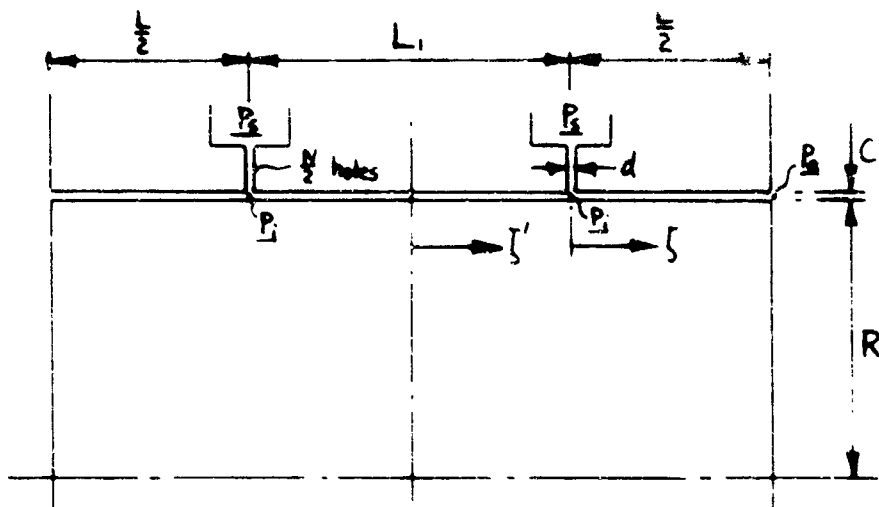


Fig. 3

The journal bearing is fed from two feeding planes, each with $\frac{1}{2} N$ equidistant orifice restricted feeding holes around the circumference. The supply pressure is P_s , the downstream orifice pressure is P_t and the ambient pressure at the ends of the bearing is P_a . The dimensionless axial coordinate is ζ , defined as $\zeta = \frac{z}{R}$ in Appendix A, and the circumferential

coordinate is Θ . The gas film between and outside the feeding planes is described by Reynolds equation which in dimensionless form is (see eq. A 14):

$$(B.1) \quad \frac{\partial}{\partial \Theta} \left[h^3 \frac{\partial P^2}{\partial \Theta} \right] + \frac{\partial}{\partial \xi} \left[h^3 \frac{\partial P^2}{\partial \xi} \right] = 0$$

where P is the dimensionless pressure with respect to ambient pressure and $h = 1 + \epsilon \cos \Theta$ is the dimensionless film thickness. To solve the equation set:

$$(B.2) \quad \begin{aligned} P &= P_0 + \epsilon P_1 + \epsilon^2 P_2 + \dots \\ P^2 &= P_0^2 + 2\epsilon P_0 P_1 + \dots \end{aligned}$$

Substituting eq. (B.2) into eq. (B.1) and setting the coefficients to $\epsilon, \epsilon, \epsilon^2, \dots$ equal to zero yields an infinite number of equations of which the first two become:

$$(B.3) \quad \frac{\partial^2 P_0^2}{\partial \Theta^2} + \frac{\partial^2 P_0^2}{\partial \xi^2} = 0$$

$$(B.4) \quad \frac{\partial^2 (P_0 P_1)}{\partial \Theta^2} + \frac{\partial^2 (P_0 P_1)}{\partial \xi^2} = 0$$

Thus the analysis is limited to small values of ϵ . Since P_0 is the pressure when the journal is concentric in the bearing, P_0 is independent of Θ and eq. (B.3) gives:

$$(B.5) \quad 0 \leq \xi \leq \xi \quad P_0^2 = 1 + q(\xi - \xi)$$

$$(B.6) \quad 0 \leq \xi' \leq \eta \quad P_0^2 = 1 + q\xi$$

where

$$(B.7) \quad \xi = \frac{L}{D} \quad \text{see fig. 3}$$

$$(B.8) \quad \eta = \frac{L_1}{D}$$

and q will be determined later.

Eq. (B.5) satisfies the boundary condition of ambient pressure at the end of the bearing, i.e., where $P=1$. At the feeding plane ($\zeta=0, \zeta'=\gamma$) the flow entering the bearing from the orifices must equal the flow into the bearing film. The orifice flow per inch circumference is $\frac{1}{2\pi R} NM$ whereas the flow into the film is given by eq. (A.4). Equating the two flows:

$$-\frac{h^3}{12\mu} \oint \frac{\partial P}{\partial z} |_i = \frac{NM}{4\pi R}$$

Make this equation dimensionless as defined in Appendix A:

$$(B.9) \quad (1+\epsilon \cos\theta)^3 \left[-\frac{\partial r^2}{\partial \zeta} + \frac{\partial P^2}{\partial \zeta'} \right]_i = \Lambda_t V m$$

where Λ_t , V and m are defined in eq. (A.8), (A.9) and (A.11). Expand m in a Taylor series around the operating point for concentric journal:

$$(B.10) \quad m = m_o + \frac{\partial m}{\partial (\frac{P}{V})} \Big|_o \left(\frac{P}{V} - \frac{P_o}{V} \right) + \dots$$

Substitute eq. (B.2) into the equations and collect coefficients according to powers of ϵ :

$$(B.11) \quad \left(\frac{\partial P_o^2}{\partial \zeta} - \frac{\partial P_o^2}{\partial \zeta'} \right)_i = -\Lambda_t V m_o$$

$$(B.12) \quad \left(\frac{\partial(P_o P_i)}{\partial \zeta} - \frac{\partial(P_o P_i)}{\partial \zeta'} \right)_i = \frac{3}{2} \cos\theta \Lambda_t V m_o - \frac{1}{2} \Lambda_t m'_o P_{i,i}$$

where

$$m'_o = \frac{\partial m}{\partial (\frac{P}{V})} \Big|_o$$

Introducing eq. (B.5)-(B.6) into eq. (B.11) gives

$$(B.13) \quad q = \Lambda_t V m_o$$

Eq. (B.12) serves as a boundary condition to eq. (B.4). The remaining boundary conditions are:

$$P_1(\theta, \xi) = P_1(\theta + 2\pi, \xi)$$

$$P_1(\theta, \xi) = 0$$

$$\frac{\partial P_1}{\partial \xi}(\theta, 0) = 0$$

Setting

$$(B.14) \quad P_0 P_1 = H(\xi) \cos \theta$$

and substituting into eq. (B.4) gives:

$$\frac{d^2 H}{d\xi^2} - H = 0$$

with the solution:

$$0 \leq \xi \leq \xi \quad H = C_1 \sinh(\xi - \xi)$$

$$0 \leq \xi' \leq \eta \quad H = C_2 \cosh \xi'$$

where C_1 and C_2 are integration constants to be determined from the boundary conditions.

Setting $H_{\xi=0} = h_{\xi'=\eta}$ and using eq. (B.12) yields:

$$(B.15) \quad \underline{0 \leq \xi \leq \xi} \quad P_1 = \frac{H \cos \theta}{P_0} = \frac{-\frac{3}{2} q \cos \theta}{[\cosh \xi + (\tanh \eta - \frac{A_{\text{min}}}{2\sqrt{1+q\xi}}) \sinh \xi]} \frac{\sinh(\xi - \xi)}{\sqrt{1+q(\xi - \xi)}}$$

$$(B.16) \quad \underline{0 \leq \xi' \leq \eta} \quad P_1 = \frac{H \cos \theta}{P_0} = \frac{-\frac{3}{2} q \sinh \xi \cos \theta}{[\cosh \xi + (\tanh \eta - \frac{A_{\text{min}}}{2\sqrt{1+q\xi}}) \sinh \xi] \sqrt{1+q\xi}} \frac{\cosh \xi'}{\cosh \eta}$$

The load carrying capacity is given by:

$$\underline{0 \leq \xi \leq \xi} \quad W_2 = -2P_a R^2 \int_0^\xi \int_0^{2\pi} P \cos \theta d\theta d\xi$$

$$0 \leq \xi' \leq \eta \quad W_1 = -2\pi R^2 \int_0^\eta \int_0^{2\pi} P \cos \theta d\theta d\xi'$$

Substituting for P from eq. (B.2) gives

$$(B.17) \quad 0 \leq \xi \leq \xi' \quad \frac{4W_1}{\pi D L P_a \epsilon} = \frac{3q}{\xi [\cosh \xi + (\tanh \eta - \frac{A_m}{2\sqrt{1+q\xi}}) \sinh \xi]} \int_0^\xi \frac{\sinh(\xi-\xi') d\xi'}{\sqrt{1+q(\xi-\xi')}}$$

$$(B.18) \quad 0 \leq \xi' \leq \eta \quad \frac{4W_1}{\pi D L P_a \epsilon} = \frac{3q \cdot \sinh \xi}{[\cosh \xi + (\tanh \eta - \frac{A_m}{2\sqrt{1+q\xi}}) \sinh \xi] \sqrt{1+q\xi}} \frac{\tanh \eta}{\eta}$$

The integral in eq. (B.17) may be solved by the substitution:

$$t = \sqrt{\frac{1}{q}} + (\xi - \xi')$$

so that:

$$(B.19) \quad \int_0^\xi \frac{\sinh(\xi-\xi') d\xi'}{\sqrt{1+q(\xi-\xi')}} = \frac{e^{-\frac{t}{\sqrt{q}}}}{\sqrt{q}} [\Psi(\sqrt{\frac{1}{q}} + \xi) - \Psi(\sqrt{\frac{1}{q}})] - \frac{\sqrt{\pi}}{2} \frac{e^{-\frac{t}{\sqrt{q}}}}{\sqrt{q}} [\text{erf}(\sqrt{\frac{1}{q}} + \xi) - \text{erf}(\sqrt{\frac{1}{q}})]$$

where:

$$(B.20) \quad \begin{aligned} \Psi(x) &= \int_0^x e^{-t^2} dt \\ \text{erf}(x) &= \frac{2}{\sqrt{\pi}} \int_0^x e^{-t^2} dt \end{aligned}$$

$\Psi(x)$ is tabulated in Jahnke and Emde: Table of Functions. However, in most cases it is more convenient to evaluate the integrals by numerical integration. Since the axial flow per inch circumference is given by eq. (A.4) the total flow from both ends of the bearing is given by:

$$M_T = -2 \int_0^{2\pi} \frac{h^3}{12\mu} q \frac{dp}{dz} R d\theta$$

Substituting dimensionless expressions from Appendix A and making use of

eq. (B.2), (B.5) and (B.15) gives:

$$(B.21) \quad M_T = \frac{C^3 P_a^2}{12 \mu R T} \int_0^{2\pi} \left[-\frac{\partial P_a^2}{\partial \xi} - 2\varepsilon \frac{\partial (P_a P_i)}{\partial \xi} \right] (1 - 3\varepsilon \cos \theta) d\theta = \frac{\pi C^3 P_a^2}{6 \mu R T} \cdot q$$

Hence q may be denoted the dimensionless bearing flow. To determine q use is made of eq. (B.13). This shall be illustrated for the case of the orifice bearing. The solution for the millipore bearing is analogous.

For the orifice bearing m_o is given by eq. (A.22) and (A.25):

$$(B.22) \quad \begin{aligned} \left(\frac{2}{K+1}\right)^{\frac{K}{K-1}} &\leq \left(\frac{P_{oi}}{V}\right) \leq 1 \\ \frac{1}{V} &\leq \left(\frac{P_{oi}}{V}\right) \leq \left(\frac{2}{K+1}\right)^{\frac{K}{K-1}} \end{aligned} \quad m_o = V \sqrt{\frac{2K}{K+1}} \left(\frac{P_{oi}}{V}\right)^{\frac{1}{K-1}}$$

From eq. (B.5) or (B.6) we get at $\xi=0$:

$$(B.23) \quad \begin{aligned} i.e. \quad \frac{P_{oi}^2}{V^2} &= 1 + q \xi \\ q &= \frac{V^2}{\xi} \left[\left(\frac{P_{oi}}{V}\right)^2 - \frac{1}{V^2} \right] \end{aligned}$$

Thus eq. (B.13) becomes:

$$(B.24) \quad \frac{V}{\xi A_t} \left[\left(\frac{P_{oi}}{V}\right)^2 - \frac{1}{V^2} \right] = m_o$$

This relationship may be shown graphically:

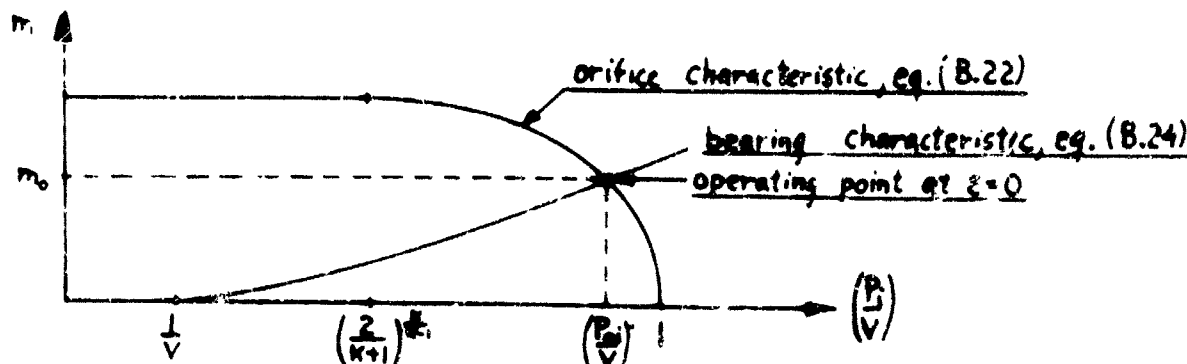


Fig. 4

Hence eq. (B.24) can be solved graphically or by iterations when using a computer.

If the approximate orifice formula is used(eq. (A.27)) a closed form solution can be obtained as follows:

$$q = A_t V m_o = A_t V \sqrt{1 - \left(\frac{P_o}{V}\right)^2} = A_t \sqrt{V^2 - 1 - q\xi}$$

or

$$(B.25) \quad q = \frac{1}{2} \xi A_t^2 \left[-1 + \sqrt{1 + \frac{4(V^2 - 1)}{\xi^2 A_t^2}} \right]$$

and from eq. (A.28):

$$(B.26) \quad -\frac{dL_t m'_o}{2V! + q\xi} = \frac{A_t^2}{2q}$$

for use in the calculation of the load.

When the feeding hole diameter is small, we may use the approximate eq. (A.34) to estimate the effect of inherent compensation. Substituting eq. (A.34) into eq. (B.9), then eq. (B.11) and (B.12) becomes:

$$\left(\frac{\partial P_o^2}{\partial \xi} - \frac{\partial P_o'^2}{\partial \xi'} \right) = - \frac{A_t}{\sqrt{1+\sigma^2}} \sqrt{V^2 - 1 - q\xi}$$

$$\left(\frac{\partial(P_o P_i)}{\partial \xi} - \frac{\partial(P_o' P_i)}{\partial \xi'} \right)_i = \frac{3}{2} q \cos \theta \frac{1 + \frac{3}{4} \sigma^2}{1 + \sigma^2} + \frac{1}{2q} \left(\frac{A_t}{\sqrt{1+\sigma^2}} \right)^2 (P_o P_i)_i$$

where $\sigma = \frac{d^2}{dc}$

Hence when inherent compensation is important, i.e., $\sigma > 4-5$, the journal bearing load becomes:

$$(B.27) \quad \frac{4W_d}{\pi P_a D L C} = \frac{1 + \frac{3}{4} \sigma^2}{1 + \sigma^2} \frac{4W_{d=0}}{\pi P_a D L C}$$

where $W_{d=0}$ is given by eq. (B.17) and (B.18). In calculating $W_{d=0}$, set

$$(B.28) \quad A_{t,d=0} = \frac{A_t}{\sqrt{1+\sigma^2}}$$

where A_t is as previously defined.

B. Single Acting Thrust Bearing

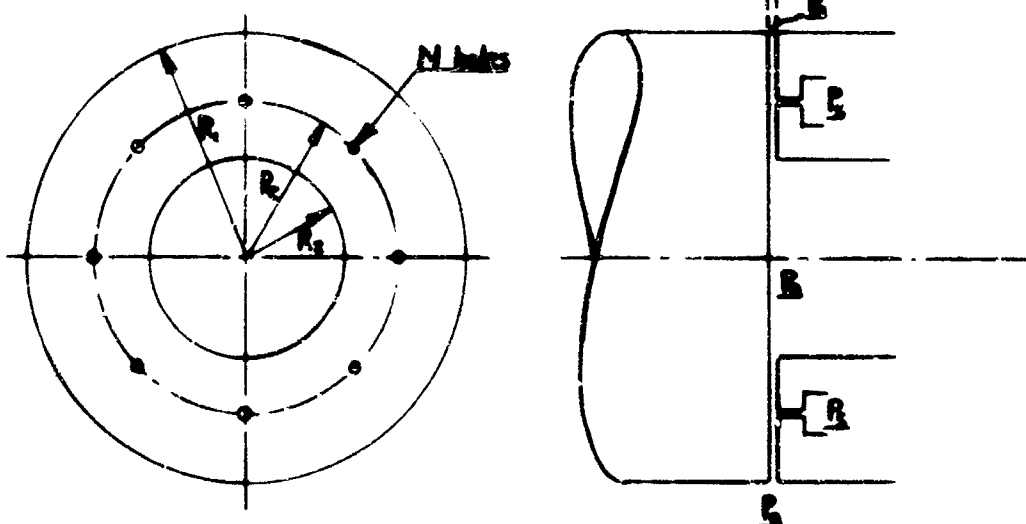


Fig. 5

The thrust bearing consists of an annular flat plate with inner and outer radius R_2 and R_1 . It is fed through N orifice restricted feeding holes located at radius R_c .

For static load and uniform film thickness the dimensionless Reynolds equation on both side of the feeding plane is obtained from eq. (A.21):

$$(B.29) \quad \frac{1}{r} \frac{d}{dr} \left[r \frac{dP^2}{dr} \right] + \frac{d^2 P^2}{r^2 d\theta^2} = 0$$

where the second term is zero due to axial symmetry. Hence the solution for the dimensionless pressure becomes:

$$P^2 = 1 + C_1 \ln r$$

where C_1 is an integration constant. Introducing the dimensionless bearing dimensions:

$$(B.30) \quad \eta = \frac{R_1}{R_c}$$

$$(B.31) \quad \gamma = \frac{R_{r_2}}{R_c}$$

$$(B.32) \quad \beta = \frac{\ln \eta}{\ln \gamma}$$

C_1 can be evaluated to give the dimensionless pressure:

$$(B.33) \quad 1 \leq r \leq \eta \quad P^2 = 1 + q_T \ln\left(\frac{\eta}{r}\right)$$

$$(B.34) \quad \frac{1}{\gamma} \leq r \leq 1 \quad P^2 = 1 + \beta q_T \ln(\gamma r)$$

where r is the radius made dimensionless by dividing by R_c . q_T is determined by equating the orifice and the bearing flow analogous to the analysis for the journal bearing. Thus:

$$\left(-\frac{\partial P^2}{\partial r} \Big|_{r=1} + \frac{\partial P^2}{\partial r} \Big|_{r=\frac{1}{\gamma}} \right) = \frac{12 \mu N \alpha a^2 \sqrt{RT}}{P_a h^3} V_m$$

Inserting eq. (B.33) we get:

$$(B.35) \quad q_T = \Lambda_T V_m$$

where

$$(B.36) \quad \Lambda_T = \frac{12 \mu N \alpha a^2 \sqrt{RT}}{P_a h^3 (1+\beta)}$$

To determine q_T substitute eq. (B.33) into eq. (B.35), setting $r=1$:

$$(B.37) \quad \frac{V}{\Lambda_T \ln \eta} \left[\left(\frac{P_1}{V} \right)^2 - \frac{1}{V^2} \right] = m$$

This equation is analogous to eq. (B.24) and is solved in the same way. If the approximate orifice formula (eq. (A.27)) is used we get:

$$(B.38) \quad q_T = \frac{1}{2} \ln \eta \lambda_T^2 \left[-1 + \sqrt{1 + \frac{4(V^2-1)}{\ln \eta \cdot \lambda_T^2}} \right]$$

The load is found by integrating the pressure:

$$W = P_a R_c^2 \int_0^{2\pi} \int_{\frac{1}{2}}^{\eta} r(P-1) dr d\theta$$

i.e.

$$(B.39) \quad \frac{W}{\pi R_c^2 P_a} = \frac{2 \sqrt{1+q_T \ln \eta}}{\eta^2} \int_1^{\eta} r \sqrt{1 - \frac{q_T}{1+q_T \ln \eta} \ln r} dr + \frac{2}{(\eta \gamma)^2} \int_1^{\eta} r' \sqrt{1+\beta q_T \ln r'} dr' + \frac{1}{(\eta \gamma)^2} - 1$$

The two integrals may be solved in closed form by the substitutions:

$$t = \sqrt{2 \left(\frac{1}{q_T} + \ln \eta - \ln r \right)}$$

$$t = \sqrt{2 \left(\frac{1}{q_T \beta} + \ln r' \right)}$$

to get:

$$(B.40) \quad \frac{W}{\pi R_c^2 P_a} = \frac{\sqrt{\pi}}{2} \sqrt{\frac{q_T}{2}} e^{\frac{q_T^2}{4}} \left[\operatorname{erf} \left(\sqrt{2 \left(\frac{1}{q_T} + \ln \eta \right)} \right) - \operatorname{erf} \left(\sqrt{\frac{2}{q_T}} \right) \right] - \frac{1}{(\eta \gamma)^2} e^{-\frac{q_T^2}{4}} \sqrt{\frac{\beta q_T}{2}} \left[\Psi \left(\sqrt{2 \left(\frac{1}{q_T \beta} + \ln \eta \right)} \right) - \Psi \left(\sqrt{\frac{2}{q_T \beta}} \right) \right]$$

where $\operatorname{erf}(x)$ and $\Psi(x)$ are defined in eq. (B.20). Frequently, it is more convenient to evaluate the integrals in eq. (B.39) by numerical integration. The total mass flow from the thrust bearing is determined by:

$$M_T = \frac{C^3 P_a^2}{24 \mu R T} \int_0^{2\pi} \left[-\gamma \frac{dP^2}{dr} \Big|_{r=\eta} + \frac{1}{\gamma} \frac{dP^2}{dr} \Big|_{r=\frac{1}{2}} \right] d\theta$$

or

$$(B.41) \quad M_T = \frac{\pi C^3 P_a^2}{12 \mu R T} (1+\beta) q_T$$

so that q_T denotes the dimensionless flow.

If inherent compensation is important λ_T should be divided by $\sqrt{1+\sigma^2}$ where $\sigma = \frac{a^2}{dh}$, see. eq. (A.34).

C. Double Acting Thrust Bearing

The double acting thrust bearing consists of two thrust bearings as shown on Fig. 5, one bearing at each end of the cylinder. From eq. (B.29) Reynolds equation is:

$$(B.42) \quad \frac{1}{r} \frac{\partial}{\partial r} \left[r h^3 \frac{\partial P^2}{\partial r} \right] = 0$$

In the center position of the cylinder the clearance in both bearings is C . If the cylinder is displaced a small distance ϵC the dimensionless film thickness in the bearings becomes $h = 1 \pm \epsilon$. Limiting the analysis to $\epsilon \ll 1$ we may express the pressure as:

$$(B.43) \quad \begin{aligned} P &= P_0 \pm \epsilon P_i \\ P^2 &= P_0^2 \pm 2\epsilon P_0 P_i \end{aligned}$$

Substituting eq. (B.43) into eq. (B.42) and collecting terms according to powers of ϵ we get:

$$(B.44) \quad \begin{aligned} \frac{1}{r} \frac{\partial}{\partial r} \left[r \frac{\partial P_0^2}{\partial r} \right] &= 0 \\ \frac{1}{r} \frac{\partial}{\partial r} \left[r \frac{\partial (P_0 P_i)}{\partial r} \right] &= 0 \end{aligned}$$

with the solutions (see eq. (B.33)-(B.34)):

$$(B.45) \quad 1 \leq r \leq \gamma \quad P_0^2 = 1 + q_T \ln \left(\frac{\gamma}{r} \right)$$

$$(B.46) \quad \frac{1}{\gamma} \leq r \leq 1 \quad P_0^2 = 1 + \beta q_T \ln (\gamma r)$$

$$(B.47) \quad 1 \leq r \leq \gamma \quad P_0 P_i = C_1 \ln \left(\frac{\gamma}{r} \right)$$

$$(B.48) \quad \frac{1}{\gamma} \leq r \leq 1 \quad P_0 P_i = \beta C_1 \ln (\gamma r)$$

where C_1 is an integration constant. q_T and C_1 are determined by equating the orifice flow with the flow through the bearing:

$$\frac{C^3 P_0^2 (1 \pm \epsilon)^3}{24 \mu R T R_c} \left[- \frac{\partial P^2}{\partial r} \Big|_{r=1} + \frac{\partial P^2}{\partial r} \Big|_{r=\frac{1}{\gamma}} \right]_{r=r_1} = \frac{N M}{2 \pi R_c}$$

Substituting from eq. (B.43) and using eq. (A.8), (A.9) and (A.11), we get:

$$\left(-\frac{\partial P_0^2}{\partial r} \Big|_{r=1} + \frac{\partial P_0^2}{\partial r} \Big|_{r=1} \right)_{r=1} = 2 \Lambda_t V m_0$$

$$\left(\frac{\partial(P_0 P_i)}{\partial r} \Big|_{r=1} - \frac{\partial(P_0 P_i)}{\partial r} \Big|_{r=1} \right)_{r=1} = 3 \Lambda_t V m_0 - \frac{\Lambda_t m_0}{P_{0,r=1}} (P_0 P_i)_{r=1}$$

Inserting eq. (B.45)-(B.48) we get:

$$(B.49) \quad q_T = \Lambda_T V m_0$$

$$(B.50) \quad C_1 = \frac{-\frac{3}{2} q_T}{1 - \frac{\Lambda_t m_0}{2V1+q_T \ln \eta} \ln \eta}$$

where $\Lambda_T = \frac{2 \Lambda_t}{1+\beta}$ is defined in eq. (E.36) by setting $h=C$. Thus in total:

$$(B.51) \quad 1 \leq r \leq \eta \quad P^2 = 1 + q_T \left[1 + \varepsilon \frac{3}{1 - \frac{\Lambda_t m_0}{2V1+q_T \ln \eta} \ln \eta} \right] \ln \left(\frac{\eta}{r} \right)$$

$$(B.52) \quad \frac{1}{\eta} \leq r \leq 1 \quad P^2 = 1 + \beta q_T \left[1 + \varepsilon \frac{3}{1 - \frac{\Lambda_t m_0}{2V1+q_T \ln \eta} \ln \eta} \right] \ln (\eta r)$$

The combined load for the double acting bearing is:

$$W = P_a R_c^2 \int_0^{2\pi} \int_{\frac{1}{\eta}}^{\eta} r [P(-\varepsilon) - P(+\varepsilon)] dr d\theta$$

or

$$(B.53) \quad \frac{W}{\pi R_c^2 P_a \varepsilon} = \frac{6 q_T}{1 - \frac{\Lambda_t m_0}{2V1+q_T \ln \eta} \ln \eta} \left\{ \frac{\beta}{(\eta \eta)^2} \int_{\frac{1}{\eta}}^{\eta} \frac{r' \ln r' dr'}{\sqrt{1+\beta q_T \ln r'}} - \int_{\frac{1}{\eta}}^{\eta} \frac{r' \ln r' dr'}{\sqrt{1-q_T \ln r'}} \right\}$$

The two integrals on the right hand side may be evaluated by means of the substitutions:

$$t = \sqrt{2(\frac{1}{\beta q_T} + \ln r')}$$

$$t = \sqrt{2(\frac{1}{q_T} - \ln r')}$$

to get:

$$(B.54) \quad \frac{W}{\pi R^2 P_a \epsilon} = \frac{\frac{6q_T}{1 - \frac{\Lambda_{T,\epsilon}}{2\sqrt{1+q_T}\ln\eta} \ln\eta}}{\left\{ \frac{1}{2q_T} \left(1 - \frac{1}{(\gamma\eta)^2}\right) + \frac{\sqrt{\pi}}{2} e^{\frac{-2}{\beta q_T}} \sqrt{\frac{2}{q_T}} \left(\frac{1}{4} - \frac{1}{q_T}\right) [\operatorname{erf}(\sqrt{2}(\frac{1}{q_T} + \ln\eta)) - \operatorname{erf}(\sqrt{\frac{2}{q_T}})] \right.} \\ \left. - e^{-\frac{2}{\beta q_T}} \sqrt{\frac{2}{\beta q_T}} \frac{\beta}{(\gamma\eta)^2} \left(\frac{1}{4} + \frac{1}{\beta q_T}\right) [\psi(\sqrt{\frac{2}{\beta q_T}}(\frac{1}{q_T} + \ln\eta)) - \psi(\sqrt{\frac{2}{\beta q_T}})] \right\}$$

where $\psi(x)$ and $\operatorname{erf}(x)$ are given by eq. (B.20). The mass flow from each thrust bearing is given by eq. (B.41).

If inherent compensation is important we may use the approximate equation (A.34) to get

$$\frac{W_\epsilon}{\pi R^2 P_a \epsilon} = \frac{1 + \frac{2}{3} \delta^2}{1 + \delta^2} \frac{W_{\delta=0}}{\pi R^2 P_a \epsilon}$$

where $W_{\delta=0}$ is given by eq. (B.53) and

$$\Lambda_{T,\epsilon} = \frac{\Lambda_{T,\delta=0}}{\sqrt{1+\delta^2}}$$

Appendix C

Static Load Carrying Capacity of Hydrostatic Journal Bearing with Orifice Source Feeding

The dimensionless steady state Reynolds equation with feeding is derived in Eq. (14), Appendix A. In this derivation it is assumed that the gas feeding takes place over a finite area A . However, the present analysis assumes that the orifice is represented by a point source. Hence, the feeding term is replaced by the source strength C , and Eq. (A.14) becomes:

$$(C.1) \quad \frac{\partial}{\partial \theta} \left[h^3 \frac{\partial (p^2)}{\partial \theta} \right] + \frac{\partial}{\partial \xi} \left[h^3 \frac{\partial (p^2)}{\partial \xi} \right] = - \delta(\xi - \xi_0) \sum_{j=1}^N C_j \delta(\theta - \varphi_j),$$

where

$\delta(x)$ = the Dirac delta function,

ξ_0 = the ξ - coordinate of the point sources,

φ_j = the angular position of the jth source,

N = the number of sources on each side of the ξ - origin
(See Figure 6 below),

C_j = the strength of the jth point source.

The solution of the problem is then that of finding a Green's function for the equation

$$\frac{\partial}{\partial \theta} \left[h^3 \frac{\partial (p^2)}{\partial \theta} \right] + \frac{\partial}{\partial \xi} \left[h^3 \frac{\partial (p^2)}{\partial \xi} \right] = 0,$$

subject to certain boundary conditions

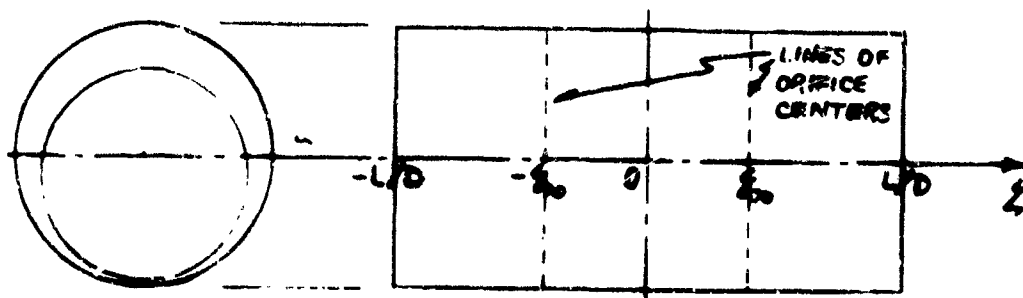


Figure 6

Since the orifices are assumed uniformly spaced with respect to θ , then

$$\varphi_j = (2j-1)\pi/N, \quad j=1, 2, \dots, N.$$

Moreover, since the problem is symmetric in ξ , we need consider only that portion of the bearing for which $0 \leq \xi \leq \frac{L}{D}$. Figure 7 shows the bearing unfolded and the boundary conditions.

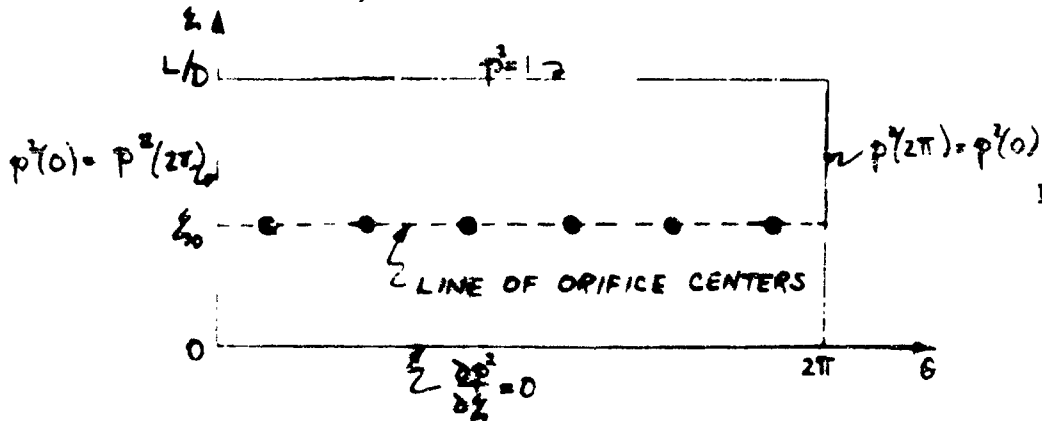


Figure 7

We note that $\xi = 1 + \epsilon \cos \theta$. If we expand p and C_j in perturbation series in powers of ϵ and retain only first degree terms, we have

$$(C.2) \quad \begin{aligned} p^2 &= p_0^2 + 2\epsilon p_0 p_1, \\ \xi^3 &= 1 + 3\epsilon \cos \theta, \\ C_j &= C_j^{(0)} + \epsilon C_j^{(1)}. \end{aligned}$$

Substitution of Eq. (C.2) in (C.1), retaining again only terms of first degree in ϵ , yields

$$\nabla^2(p_0^2) = -8(\xi - \xi_0) \sum_{j=1}^N C_j^{(0)} \delta(\theta - \varphi_j),$$

as the equation of zeroth degree in ϵ . Since this corresponds to the symmetric case, we note that all values of $C_j^{(0)}$ are identical ($=C^{(0)}$) for a uniform source pressure; therefore, we need only consider the sector

$$\frac{2(i-1)\pi}{N} \leq \theta \leq \frac{2i\pi}{N},$$

and the above equation reduces to

$$(C.3a) \quad \nabla^2(p_0^2) = \frac{\partial^2}{\partial \xi^2}(p_0^2) + \frac{\partial^2}{\partial \theta^2}(p_0^2) = -C^{(0)} \delta(\xi - \xi_0) \delta(\theta - \varphi_j),$$

with the boundary conditions

$$(C.3b) \quad \left\{ \begin{array}{l} p_0^2 = 1 \text{ at } \xi = L/D; \quad \frac{\partial}{\partial \xi}(p_0^2) = 0 \text{ at } \xi = 0; \\ p_0^2|_{\theta=0} = p_0^2|_{\theta=2\pi}; \quad \theta_j = \frac{j\pi}{N}; \quad j = 1, 2, \dots, N. \end{array} \right.$$

The first degree terms in ϵ yield the equation

$$(C.4a) \quad \nabla^2(p_0 p_1) = \nabla^2(U_1 + U_2 + U_3),$$

where

$$\nabla^2 U_1 = \frac{3}{2} \sin \theta \frac{\partial}{\partial \theta}(p_0^2),$$

$$\nabla^2 U_2 = \frac{3}{2} C^{(0)} \cos \theta \delta(\xi - \xi_0) \sum_{j=1}^N \delta(\theta - \varphi_j),$$

$$\nabla^2 U_3 = -\frac{1}{2} \delta(\xi - \xi_0) \sum_{j=1}^N C_j^{(0)} \delta(\theta - \varphi_j).$$

The boundary conditions on $p_0 p_1$ (and U_1, U_2, U_3) are:

$$(C.4b) \quad \left\{ \begin{array}{l} p_0 p_1 = 0 \text{ at } \xi = L/D, \quad \frac{\partial}{\partial \xi}(p_0 p_1) = 0 \text{ at } \xi = 0; \\ p_0 p_1|_{\theta=0} = p_0 p_1|_{\theta=2\pi}. \end{array} \right.$$

Solution of the Zeroth Degree Equation

We write (C.3a) as

$$(C.5) \quad p_0^2 = 1 + U_0.$$

We then have the equation

$$(C.6) \quad \nabla^2 U_0 = -C^{(0)} \delta(\xi - \xi_0) \delta(\theta - \varphi_j),$$

with the boundary conditions as in Eq. (C.3b), except that at $\xi = L/D$, $U_0 = 0$. Eq. (C.6) is then the equation for a Green's function:

$$U_0 = U_0(\xi, \theta; \xi_0, \varphi_j)$$

It is found by separation of variables in a direct product function space (See Reference 3.)

We write U_0 as a Fourier series:

$$(C.7) \quad U_0(\xi, \theta) = \frac{N}{\pi} \left\{ \frac{1}{2} Y_0(\xi) + \sum_{n=1}^{\infty} \chi_n(\xi) \cos nN\theta \right\},$$

where

$$\chi_n(\xi) = \int_{2\pi(j-1)/N}^{2\pi j/N} U_0(\xi, \theta) \cos nN\theta d\theta; \quad n = 0, 1, 2, \dots$$

Eq. (C.7) satisfies the boundary conditions in the θ direction. We now multiply Eq. (C.6) by $\cos nN\theta$ and integrate with respect to θ from $\frac{2\pi(j-1)}{N}$ to $\frac{2\pi j}{N}$. The result is

$$(C.8) \quad \frac{d^2}{d\xi^2} \chi_n(\xi) = -C^{(0)} \delta(\xi - \xi_0), \quad n = 0,$$

$$(C.9) \quad \frac{d^2}{d\xi^2} \chi_n(\xi) - (nN)^2 \chi_n(\xi) = -C^{(0)} \delta(\xi - \xi_0) \cos nN\varphi_j, \quad n = 1, 2, \dots$$

The solutions to both (C.8) and (C.9) must obey the remaining boundary conditions, must be continuous across $\xi = \xi_0$, and must have the proper jump in their first derivative at that point. The solution of the homogeneous part of (C.8) is $\gamma_0 = A\xi + \text{const.}$ Thus,

$$\gamma_0(\xi) = \begin{cases} A_0 \left(\frac{\xi}{D} - \xi_0 \right), & \xi < \xi_0 \\ A_0 \left(\frac{\xi}{D} - \xi_0 \right)^0, & \xi > \xi_0 \end{cases}$$

The jump in $\gamma'_0(\xi)$ at ξ_0 is $-C^{(o)}$; thus

$$\left. \frac{d}{d\xi} \left[A_0 \left(\frac{\xi}{D} - \xi_0 \right) \right] \right|_{\xi=\xi_0} - \left. \frac{d}{d\xi} \left[A_0 \left(\frac{\xi}{D} - \xi_0 \right)^0 \right] \right|_{\xi=\xi_0} = -C^{(o)}$$

and

$$A_0 = C^{(o)}$$

Hence, if we write

$$\xi_c = \min \text{ of } (\xi, \xi_0),$$

$$\xi_s = \max \text{ of } (\xi, \xi_0),$$

then we obtain

$$(C.10) \quad \gamma_0(\xi) = C^{(o)} \left(\frac{\xi}{D} - \xi_s \right).$$

The solution of the homogeneous part of (C.9) is given by hyperbolic functions. To satisfy the boundary conditions, our solution (continuous at $\xi = \xi_0$) is given by

$$\gamma_n(\xi) = \begin{cases} A_n \cosh nN \xi_c \sinh nN \left(\frac{\xi}{D} - \xi_0 \right), & \xi < \xi_0, \\ A_n \cosh nN \xi_0 \sinh nN \left(\frac{\xi}{D} - \xi_s \right), & \xi > \xi_0. \end{cases}$$

The constant A_n is chosen to satisfy the jump condition across $\xi = \xi_0$:

$$\begin{aligned} -nN A_n \left[\cosh nN \left(\frac{\xi}{D} - \xi_0 \right) \cosh nN \xi_c + \sinh nN \xi_0 \sinh nN \left(\frac{\xi}{D} - \xi_0 \right) \right] &= \\ = -nN A_n \cosh \frac{nN \omega}{D} &= -C^{(o)} e^{-nN \omega}, \end{aligned}$$

Therefore,

- 53 -

$$A_n = \frac{C^{(0)} \cos nN\varphi_j}{nN \cosh(nNL/D)}.$$

But $\varphi_j = (2j-1)\pi/N$, and $\cos nN\varphi_j = \cos n\pi(2j-1) = (-1)^n$. Hence, A_n is independent of j , and is given by

$$A_n = (-1)^n C^{(0)} / (nN \cosh \frac{nNL}{D}), \quad n=1, 2, \dots$$

Thus,

$$Y_n(\xi) = \frac{(-1)^n C^{(0)}}{nN} \frac{\cosh nN\xi_2 \sinh nN(\frac{L}{D}-\xi_2)}{\cosh(nNL/D)}, \quad n=1, 2, \dots$$

The solution for U_0 is then

$$(C.11) \quad U_0(\xi, \theta; \xi_0) = \frac{C^{(0)}}{\pi} \left[\frac{N(L-D-\xi_2)}{2(D-\xi_2)} + \sum_{n=1}^{\infty} (-1)^n \frac{\cosh nN\theta \cosh nN\xi_2 \sinh nN(\frac{L}{D}-\xi_2)}{n \cosh(nNL/D)} \right],$$

and p_0^2 is obtained by adding 1 to Eq. (C.1).

The method for determining $C^{(0)}$ will be described later.

Solution of the First Degree Equations

To obtain the functions U_1 , U_2 , and U_3 whose sum is the solution of Eq. (C.4a), we must first obtain the Green's function $G(\xi, \theta; \xi, \psi)$ for the Laplacean with boundary conditions (C.4b). From the fact that

$$(C.12) \quad \nabla_{\xi, \theta}^2 G(\xi, \theta; \xi, \psi) = -\delta(\xi-\xi) \delta(\theta-\psi),$$

(where the subscripts or the Laplacean operator indicate the variables with respect to which we differentiate), we find that

$$(C.13) \quad U_1 = -\frac{3}{2} \int_0^{L/D} \int_0^{2\pi} G(\xi, \theta; \xi, \psi) \frac{\partial}{\partial \psi} [p_0^2(\xi, \psi; \xi_0)] \sin \psi \, d\psi \, d\xi.$$

Moreover, since U_2 and U_3 are also Green's functions satisfying the same boundary conditions as G , we may obtain U_2 and U_3 by a comparatively simple modification of G .

To obtain G , then, we follow the same procedure as in the solution for p_0^2 , expanding this time in Fourier series in integers. Thus,

$$(C.14) \quad G(\xi, \theta; \xi, \psi) = \frac{1}{\pi} \left\{ \frac{1}{2} \left(\frac{L}{D} - y \right) + \sum_{n=1}^{\infty} \left[\frac{\cos n\psi \cos n\theta}{n} \cdot \frac{\cosh nx \sinh n(\frac{L}{D} - y)}{\cosh(nL/D)} \right] \right\},$$

where

$$y = \max(\xi, \xi),$$

$$x = \min(\xi, \xi),$$

If we exclude the source points we may show uniform convergence of both the series p_0^2 and its term-by-term derivative with respect to θ . Therefore, from Eqs. (C.11), (C.13), and (C.14)

$$U_1(\xi, \theta; \xi_0) = \frac{3NC^{(0)}}{2\pi^2} \int_0^{L/D} \int_0^{2\pi} \left\{ \frac{1}{2} \left(\frac{L}{D} - y \right) + \sum_{n=1}^{\infty} \left[\frac{\cos n\psi \cos n\theta \cosh nx \sinh n(\frac{L}{D} - y)}{n \cosh(nL/D)} \right] \right\} \times \\ \times \left\{ \sum_{m=1}^{\infty} (-1)^m \frac{\sin mN\psi \cosh mN\bar{x} \sinh mN(\frac{L}{D} - \bar{y})}{\cosh(mNL/D)} \right\} \sin \psi \, d\psi \, d\xi$$

where

$$\bar{y} = \max(\xi_0, \xi),$$

$$\bar{x} = \min(\xi_0, \xi).$$

(NOTE: U_1 takes on a slightly different form in the case $N = 1$ (i.e., a single orifice). The analysis given herein includes this case, but the computer program assumes $N > 1$.)

Integration of the above gives

$$(C.15) \quad U_1(\xi, \theta; \xi_0) = \frac{3NC^{(a)}}{4\pi} \sum_{m=1}^{\infty} (-1)^m \left\{ \frac{\cos d_m \theta}{d_m(2mN-1)} \left[\frac{mN \cosh d_m \xi_c \sinh d_m \left(\frac{L}{D} - \xi_2\right)}{\cosh(d_m L/D)} - \frac{d_m \cosh mN \xi_c \sinh mN \left(\frac{L}{D} - \xi_2\right)}{\cosh(mNL/D)} \right] \right. \\ \left. + \frac{\cos \beta_m \theta}{\beta_m(2mN+1)} \left[\frac{mN \cosh \beta_m \xi_c \sinh \beta_m \left(\frac{L}{D} - \xi_2\right)}{\cosh(\beta_m L/D)} - \frac{\beta_m \cosh mN \xi_c \sinh mN \left(\frac{L}{D} - \xi_2\right)}{\cosh(mNL/D)} \right] \right\},$$

(For the special case $N = 1$,

$$U_1(\xi, \theta; \xi_0) = \frac{3C^{(a)}}{4\pi} \left\{ \left[\frac{\cosh \xi_c \sinh \left(\frac{L}{D} - \xi_2\right)}{\cosh(L/D)} - \left(\frac{L}{D} - \xi_2\right) \right] \right. \\ \left. + \sum_{m=2}^{\infty} (-1)^m \left\{ \frac{\cos d_m \theta}{d_m(2m-1)} \left[\frac{m \cosh d_m \xi_c \sinh d_m \left(\frac{L}{D} - \xi_2\right)}{\cosh(d_m L/D)} \right. \right. \right. \\ \left. \left. \left. - \frac{d_m \cosh m \xi_c \sinh m \left(\frac{L}{D} - \xi_2\right)}{\cosh(mL/D)} \right] \right\} \right. \\ \left. + \frac{\cos \beta_m \theta}{\beta_m(2m+1)} \left[\frac{m \cosh \beta_m \xi_c \sinh \beta_m \left(\frac{L}{D} - \xi_2\right)}{\cosh(\beta_m L/D)} \right. \right. \\ \left. \left. - \frac{\beta_m \cosh m \xi_c \sinh m \left(\frac{L}{D} - \xi_2\right)}{\cosh(mL/D)} \right] \right\} \cdot \right)$$

where

$$\alpha_m = mN - 1$$

$$\beta_m = mN + 1$$

As noted above, the function U_2 is also a Green's function satisfying the same boundary conditions as G , but with a different jump in the first derivative:

$$(C.16) \quad U_2 = -\frac{3C^{(0)}}{2\pi} \sum_{j=1}^N \cos \theta_j \left\{ \frac{1}{2} \left(\frac{L}{D} - \xi_j \right) + \sum_{n=1}^{\infty} \left[\frac{\cos n\theta_j \cos n\theta \cosh n\xi_j \sinh n\left(\frac{L}{D} - \xi_j\right)}{n \cosh(nL/D)} \right] \right\}.$$

(For the special case $N=1$, where $\theta = \pi$, we obtain

$$U_2 = \frac{3C^{(0)}}{4\pi} \left[\left(\frac{L}{D} - \xi_j \right) - \sum_{m=1}^{\infty} (-1)^m \frac{\cos m\theta \cosh m\xi_j \sinh m\left(\frac{L}{D} - \xi_j\right)}{m \cosh(mL/D)} \right].)$$

We note that $\theta_j = (2j-1)\pi/N$. Interchanging the order of summation, we make use of the orthogonality of trigonometric functions under summation to obtain

$$(C.17a) \quad \sum_{j=1}^N \cos \frac{(2j-1)\pi}{N} = 0,$$

$$(C.17b) \quad \sum_{j=1}^N \cos \frac{(2j-1)\pi}{N} \cos \frac{n(2j-1)\pi}{N} = \begin{cases} 0, & \frac{n}{2} \neq mN \pm 1 \\ (-1)^m \frac{N}{2}, & n = mN \pm 1 \end{cases}$$

Hence,

$$(C.18) \quad U_2(\xi, \theta; \xi_0) = -\frac{3NC^{(o)}}{4\pi} \sum_{m=1}^{\infty} (-1)^m \left[\frac{\cos \alpha_m \theta \cosh \alpha_m \xi_0 \sinh \alpha_m (\frac{L}{D} - \xi)}{\alpha_m \cosh(\alpha_m L/D)} \right. \\ \left. + \frac{\cos \beta_m \theta \cosh \beta_m \xi_0 \sinh \beta_m (\frac{L}{D} - \xi)}{\beta_m \cosh(\beta_m L/D)} \right].$$

Combination of Eqs. (C.15) and (C.18) results in

$$(C.19) \quad [U_1 + U_2](\xi, \theta; \xi_0) = -\frac{3NC^{(o)}}{4\pi} \sum_{m=1}^{\infty} (-1)^m \left\{ \frac{\cos \alpha_m \theta \left[\cosh \alpha_m \xi_0 \sinh \alpha_m (\frac{L}{D} - \xi) \right]}{(2mN-1) \cosh(\alpha_m L/D)} : \frac{\cosh mN \xi_0 \sinh mN (\frac{L}{D} - \xi)}{\cosh(mNL/D)} \right. \\ \left. + \frac{\cos \beta_m \theta \left[\cosh \beta_m \xi_0 \sinh \beta_m (\frac{L}{D} - \xi) \right]}{(2mN+1) \cosh(\beta_m L/D)} : \frac{\cosh mN \xi_0 \sinh mN (\frac{L}{D} - \xi)}{\cosh(mNL/D)} \right\}.$$

In a similar fashion we may write

$$(C.20) \quad U_3(\xi, \theta; \xi_0) = \frac{1}{2\pi} \sum_{j=1}^N C_j^{(1)} \left[\frac{1}{2} \left(\frac{L}{D} - \xi \right) + \sum_{n=1}^{\infty} \frac{\cos n \varphi_j \cos n \theta \cosh n \xi_0 \sinh n (\frac{L}{D} - \xi)}{n \cosh(nL/D)} \right].$$

(For the special case $N=1$, Eq. (C.20) becomes

$$U_3(\xi, \theta; \xi_0) = \frac{C^{(1)}}{2\pi} \left[\frac{1}{2} \left(\frac{L}{D} - \xi \right) + \sum_{m=1}^{\infty} (-1)^m \frac{\cos m \theta \cosh m \xi_0 \sinh m (\frac{L}{D} - \xi)}{m \cosh(mL/D)} \right].$$

The solution for $p_0 p_1$ is given by the sum of U_1 , U_2 , and U_3 , i.e., by the sum of Eqs. (C.19) and (C.20).

This result depends on the symmetric source strength $C^{(o)}$ and the perturbed source strengths $C_j^{(1)}$ ($j=1, 2, \dots, N$). In the next section we describe the procedure for their calculation.

Calculations of Source Strengths from the Equations of Mass Flow

From Eqs. (A.3) and (A.4), we may obtain the mass flow at the jth source as

$$(C.21a) \quad M = -\frac{\rho_0^2 c^3}{24 \mu R T} \oint_j A^3 \frac{\partial}{\partial n} (p^2) ds,$$

where

$\oint_j [] ds$ denotes the line integral about the jth source,
 $\frac{\partial}{\partial n}$ = the outward normal derivative.

If we use the perturbation series in Eq. (C.21), we obtain, at the jth orifice

$$(C.21b) \quad M = M_0 + \epsilon M_1 = -\frac{\rho_0^2 c^3}{24 \mu R T} \oint_j \left\{ \frac{\partial}{\partial n} (p_0^2) + \epsilon \left[2 \frac{\partial}{\partial n} (p_0 p_1) + 3 \cos \theta \frac{\partial}{\partial n} (p_0^2) \right] \right\} ds.$$

From Eq. (A.22), we obtain the mass flow at the jth orifice to be

$$(C.22) \quad M = \frac{\pi a^2 \gamma^{1/2} \sqrt{\frac{2k}{k-1}} \rho_0 V \cdot [\nu(p/V)]}{\sqrt{RT}} \left(\frac{p}{V}\right)^{1/k} \sqrt{1 - \left(\frac{p}{V}\right)^{\frac{k-1}{k}}}$$

Expanding Eq. (C.22) in a Taylor's series about $p=p_0$ and retaining only the first two terms yields

$$M = M(p_0) + (p-p_0) \left. \frac{dM}{dp} \right|_{p=p_0} .$$

But,

$$p-p_0 = \epsilon p_1;$$

Therefore,

$$(C.23) \quad M = M(p_0) + \epsilon p_1 \left. \frac{dM}{dp} \right|_{p=p_0} .$$

We note that Eq. (C.23) holds at the j th orifice. Equating the coefficients like powers of ϵ in Eqs. (C.21b) and (C.23) at the j th orifice gives

$$(C.24a) \quad M_0 = M(p_0) = -\frac{p_0^2 c^3}{24 \mu R T} \oint_j \frac{\partial}{\partial n} (p_0^2) ds,$$

$$(C.24b) \quad M_1 = M'(p_0) \cdot [p_1]_j = -\frac{p_0^2 c^3}{24 \mu R T} \oint_j [2 \frac{\partial}{\partial n} (p_0 p_1) + 3 \cos \theta \frac{\partial}{\partial n} (p_0^2)] ds,$$

where $M(p_0)$ and $M'(p_0)$ are obtained from Eq. (C.22).

Consider first the integral on the right hand side of Eq. (C.24a).

By Green's theorem and Eq. (C.3a),

$$(C.25) \quad \oint_j \frac{\partial}{\partial n} (p_0^2) ds = \iint \nabla^2 (p_0^2) d\theta d\eta = -C^{(0)}.$$

Applying Green's theorem and Eq. (C.4a) to the integral in Eq. (C.24b) we find

$$(C.26) \quad \oint_j [2 \frac{\partial}{\partial n} (p_0 p_1) + 3 \cos \theta \frac{\partial}{\partial n} (p_0^2)] ds = -C_j^{(1)}$$

We now define the following quantities:

$$(C.27) \quad \left\{ \begin{array}{l} x = p_0/V, \\ \Lambda_t = 6\mu\eta^{1/2}a^2\sqrt{RT} N/p_0 c^3, \\ f(x) = \sqrt{\frac{2k}{k-1}} [V(x)]^{1/k} \sqrt{1-x^{\frac{k-1}{k}}}. \end{array} \right.$$

To solve for $C^{(0)}$, we consider Eq. (C.24a). Using Eqs. (C.22), (C.25), and (C.27), Eq. (C.24a) becomes

$$(C.28) \quad \Lambda_t V f(x) = \frac{N}{4} \left[\frac{C^{(0)}}{\pi} \right].$$

At the jth orifice, $\theta = (2j-1)\pi/N$. Substituting this value in Eq. (C.11), we have

$$\begin{aligned} \left. \frac{P_0^2}{S_0} \right|_{\theta=\theta_j} &= 1 + \frac{C^{(0)}}{\pi} \left[\frac{N}{2} \left(\frac{L}{D} - \xi_j \right) + \sum_{m=1}^{\infty} \frac{\cosh mNL \xi_j \sinh mN \left(\frac{L}{D} - \xi_j \right)}{m \cosh(mNL/D)} \right], \\ &= 1 + \frac{C^{(0)}}{\pi} S_0(\xi_j, \xi_0). \end{aligned}$$

To represent S_0 at the orifice we choose

$$\bar{S}_0 = \frac{1}{2} [S_0(\xi_0 + a, \xi_0) + S_0(\xi_0 - a, \xi_0)].$$

(In Appendix D, a transformation is made in the series S_0 to obtain quicker convergence.) Hence, at the jth orifice we have

$$\frac{C^{(0)}}{\pi} = \frac{P_0^2 - 1}{\bar{S}_0} = \frac{V^2}{\bar{S}_0} \left[x^2 - \frac{1}{V^2} \right].$$

Eq. (C.28) becomes

$$(C.29) \quad \Lambda_t f(x) = \frac{NV}{4\bar{S}_0} \left[x^2 - \frac{1}{V^2} \right].$$

The above equation has one and only one root for positive $x \leq 1$.

Calling this root x^* , we then obtain

$$C^{(0)} = \frac{\pi V^2}{\bar{S}_0} \left[(x^*)^2 - \frac{1}{V^2} \right].$$

The root x^* also defines the value of $\psi(x)$ and $\psi'(x)$ to be used subsequently.

We next solve for $C_j^{(1)}$. From Eq. (C.22),

$$(C.30) \quad M'_0 = M_0 \Psi/V,$$

where

$$\Psi = \frac{\nu'(x^*)}{\nu(x^*)} + \frac{1}{k} \left\{ \frac{1}{x^*} - \frac{k-1}{2(x^*)^{1/k} [1 - (x^*)^{(k-1)/k}]} \right\}.$$

We multiply and divide the left hand side of (C.24b) by $(p_0)_j$, and use Eqs. (C.27) and (C.30) to obtain

$$f(x) \frac{\lambda_k \Psi}{\sqrt{x^*}} [p_0 p_j]_j = \frac{N}{4} \left[\frac{C_j^{(1)}}{\pi} \right].$$

Clearing of fractions gives

$$(C.31) \quad [p_0 p_j]_j = \frac{N \sqrt{x^*}}{4 \pi \lambda_k \Psi f(x)} C_j^{(1)}, \quad j = 1, 2, \dots, N.$$

The above equation is a linear system wherein the unknowns are the source strengths $C_j^{(1)}$. Therefore, it can be put in the equivalent form

$$(C.32) \quad [\mathbf{A}] \quad \widehat{\mathbf{C}}^{(1)} = \widehat{\mathbf{B}},$$

where

$[\mathbf{A}]$ is a matrix of order $N \times N$ whose elements are A_{jk} ,

$\widehat{\mathbf{C}}^{(1)}$ is a column vector whose N elements are the unknowns $C_j^{(1)}$,

$\widehat{\mathbf{B}}$ is a column vector containing N elements.

In the following, it is assumed that all expressions are evaluated first for $\xi = \xi_0 - a$, then for $\xi = \xi_0 + a$, and an average taken.

We recall first that

$$r_0 p_1 = U_1 + U_2 + U_3.$$

Moreover, at the jth orifice, the angular coordinate is given by

$$(2j-1)\pi/N.$$

From Eq. (C.19), at the jth orifice

$$(C.33a) \quad (U_1 + U_2)_j = (\bar{S}_1)_j, \quad j = 1, 2, \dots, N$$

where

$(\bar{S}_1)_j$ is the right hand side of (C.19) with $\theta = (2j-1)\pi/N$.

Also, from Eq. (C.20), at the jth orifice

$$(C.33b) \quad (U_3)_j = \sum_{k=1}^N C_k^{(1)} T_{jk}, \quad j = 1, 2, \dots, N,$$

where

$$T_{jk} = \frac{1}{2\pi} \left[\frac{1}{2} \left(\frac{L}{D} - \xi_j \right) + \sum_{n=1}^{\infty} \frac{\cos \frac{n\pi(2k-1)}{N} \cos \frac{n\pi(j-1)}{N} \cosh n\xi_j \sinh n \left(\frac{L}{D} - \xi_j \right)}{n \cosh(nL/D)} \right].$$

(This series is also put into more easily calculable form by the transformation described in Appendix D.) Therefore, the elements of the matrix $[A]$ and the vector \vec{B} of Eq. (C.31) are given by

$$(C.34) \quad \begin{cases} A_{jk} = T_{jk} - \left[\frac{NV^2 x^*}{4\pi A_t \Psi} \right] \delta_{jk} = A_{kj}, \\ B_j = -(\bar{S}_1)_j. \end{cases}$$

where

$$\delta_{jk} = \begin{cases} 0, & j \neq k \\ 1, & j = k \end{cases}$$

The $C^{(1)}$ vector is then found by inverting $[A]$ and multiplying \vec{B} by $[A]^{-1}$.

Appendix D

Reformulation of an Infinite Series Encountered in the
Analysis Performed in Appendix C

Several expressions in the previous Appendix (e.g., Eqs. (C.11), (C.20)) involve infinite series containing several parameters, of the form

$$(D.1) \quad S = \sum_{n=1}^{\infty} \frac{\cos n\alpha \cosh n\beta \cosh nx \sinh n(R-y)}{n \cosh nR},$$

where

$$R > y > x \geq 0.$$

The series is absolutely convergent.

We make the following substitutions:

$$(D.2) \quad \begin{aligned} a_1 &= \alpha + \beta \\ a_2 &= \alpha - \beta \\ \delta &= y - x \\ \sigma &= y + x \end{aligned}$$

after which Eq. (D.1) becomes

$$(D.3) \quad S = \frac{1}{4} \sum_{n=1}^{\infty} \frac{[\cos na_1 + \cos na_2][\sinh n(R-\delta) + \sinh n(R-\sigma)]}{n \cosh nR},$$

noting that

$$2R > \sigma > \delta > 0.$$

We represent a typical part of the series as

$$(D.4) \quad T = \sum_{n=1}^{\infty} \frac{\cos n\varphi \sinh n(R-\xi)}{n \cosh nR},$$

where

$$2R > \xi > 0.$$

Then, writing the trigonometric and hyperbolic functions as sums of exponentials, we have

$$T = \frac{1}{2} \sum_{n=1}^{\infty} \frac{[e^{-n(\xi+i\varphi)} + e^{-n(\xi-i\varphi)} - e^{-n(2R-\xi+i\varphi)} - e^{-n(2R-\xi-i\varphi)}]}{n(1+e^{-2nR})}.$$

But,

$$(1+e^{-2nR})^{-1} = \sum_{k=0}^{\infty} (-1)^k e^{-2knR} \quad (nR > 0);$$

hence,

$$(D.5) \quad T = \frac{1}{2} \sum_{n=1}^{\infty} \frac{1}{n} \sum_{k=0}^{\infty} (-1)^k \left[e^{-n(2kR+\xi+i\varphi)} + e^{-n(2kR+\xi-i\varphi)} - e^{-n(2kR+2R-\xi+i\varphi)} - e^{-n(2kR+2R-\xi-i\varphi)} \right].$$

Interchanging the order of summation yields

$$T = \frac{1}{2} \sum_{k=0}^{\infty} (-1)^k \sum_{n=1}^{\infty} \frac{1}{n} \left[e^{-n(2kR+\xi+i\varphi)} + e^{-n(2kR+\xi-i\varphi)} - e^{-n(2kR+2R-\xi+i\varphi)} - e^{-n(2kR+2R-\xi-i\varphi)} \right].$$

Since

$$\sum_{n=1}^{\infty} \frac{z^n}{n} = -\log(1-z) \quad (|z|^2 < 1),$$

we then have

$$T = \frac{1}{2} \sum_{k=0}^{\infty} (-1)^k \log \left\{ \frac{[1-e^{-(2kR+2R-\xi+i\varphi)}][1-e^{-(2kR+2R-\xi-i\varphi)}]}{[1-e^{-(2kR+\xi+i\varphi)}][1-e^{-(2kR+\xi-i\varphi)}]} \right\},$$

which is still absolutely convergent. We now convert the expressions within the curly brackets back to trigonometric and hyperbolic functions:

$$T = \frac{1}{2} \sum_{k=0}^{\infty} (-1)^k \log \left\{ e^{-2(R-\xi)} \left[\frac{\sinh^2(kR+R-\frac{\xi}{2}) \cos^2 \frac{\varphi}{2} + \cosh^2(R+R-\frac{\xi}{2}) \sin^2 \frac{\varphi}{2}}{\sinh^2(kR+\frac{\xi}{2}) \cos^2 \frac{\varphi}{2} + \cosh^2(kR+\frac{\xi}{2}) \sin^2 \frac{\varphi}{2}} \right] \right\}$$

$$= \frac{1}{2} \sum_{k=0}^{\infty} (-1)^k \log \left\{ e^{-2(R-\xi)} \left[\frac{\cosh^2(kR+R-\frac{\xi}{2}) - \cos^2 \frac{\varphi}{2}}{\cosh^2(kR+\frac{\xi}{2}) - \cos^2 \frac{\varphi}{2}} \right] \right\}$$

Finally,

$$(D.6) \quad T = \frac{1}{2} \sum_{k=0}^{\infty} (-1)^k \log \left\{ \frac{e^{-(2R-\xi)}}{e^{-\xi}} \left[\frac{\cosh(2R-\xi) + \tanh 2kR \sinh(2R-\xi) - \frac{\cos \varphi}{\cosh 2kR}}{\cosh \xi + \tanh 2kR \sinh \xi - \frac{\cos \varphi}{\cosh 2kR}} \right] \right\}.$$

Eq. (D.6) is then substituted in Eq. (D.3), for $\xi = \sigma$, $\xi = \delta$, $\varphi = \alpha_1$, $\varphi = \alpha_2$.

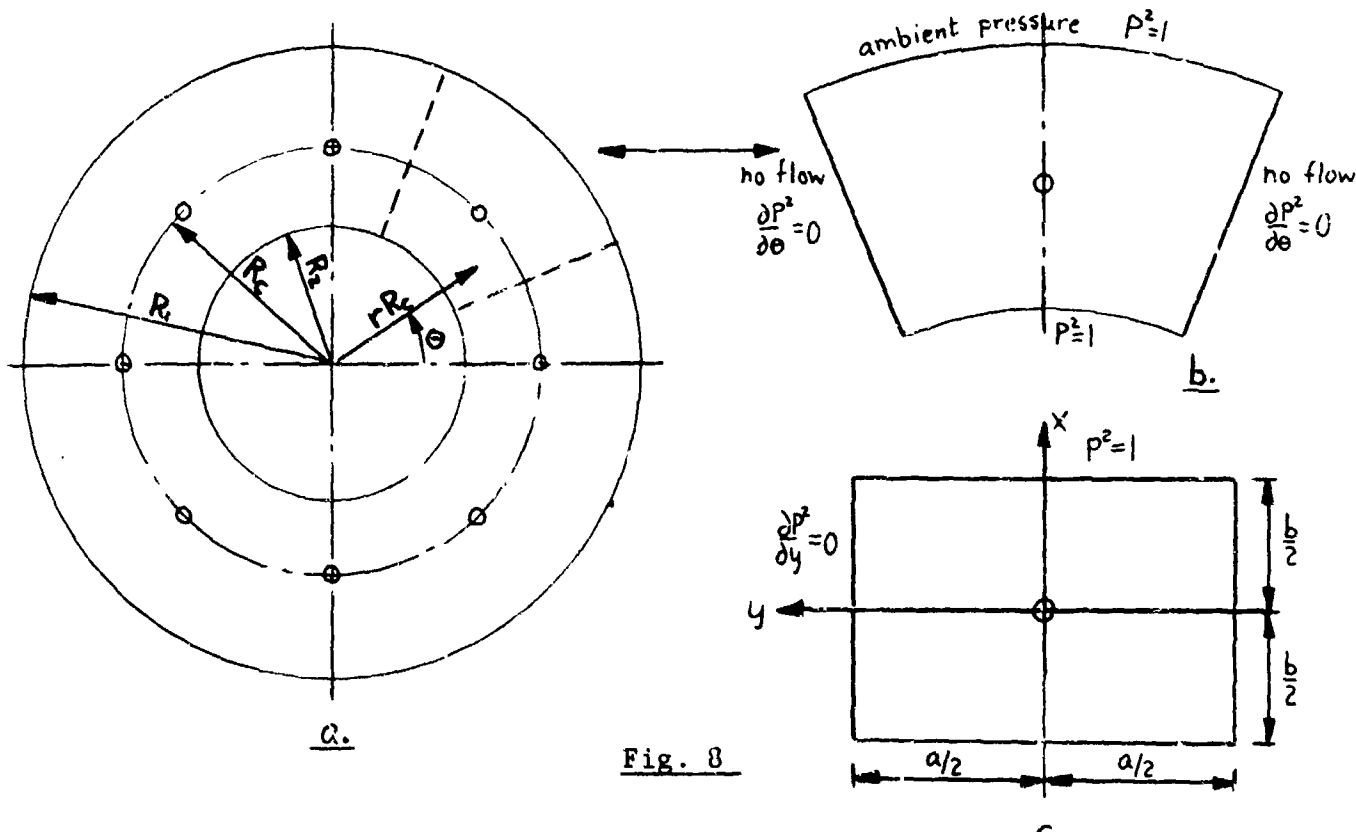
The computational advantages of the new form Eq. (D.6) are as follows:

- 1) In the initial formulation Eq. (D.1), both trigonometric and three hyperbolic functions are required for each value of the summation index n. Even if these are calculated from recurrence formulas, the form (D.6) is more efficient, since after an initial calculation of entry values, only two hyperbolic functions are necessary at each step.
- 2) The new formulation is alternating, and the rate of convergence can be increased by means of Euler's method.

APPENDIX E

Static Load Carrying Capacity of Hydrostatic Thrust Bearing with Orifice Source Feeding

Reynolds equation for the hydrostatic annular thrust bearing with feeding is given in eq. (A.21). If the feeding is represented by a point source instead of a flow over a finite area, eq. (A.21) reduces to Laplaces equation with singularities at the orifices. Assuming that the orifice may be described by a simple source (a logarithmic singularity) use can be made of the methods of conformal mapping. (See f. inst. Ref. 4 and 5) Thus in the present case it is most convenient first to consider a rectangular pad with a source in the center, ambient pressure at two sides and no flow from the other two sides. This pad is equivalent to a radial sector of the annular thrust bearing.



The boundary condition of zero flow at $y = \pm \frac{a}{2}$ is satisfied if we along the y-axis take a infinite number of equidistant sources of equal strength. Similarly we need an infinite number of alternating sources and sinks in the x-direction to satisfy the ambient pressure condition. Such an array is represented by

$$(E.1) \quad P^2 = 1 + \operatorname{Re} \left\{ -C \sum_{n=-\infty}^{\infty} (-1)^n \cdot \ln \left[\frac{\sinh \pi(\bar{z}+nb)}{K_n} \right] \right\}$$

where P is the dimensionless pressure (with respect to ambient), C is the source strength, $\bar{b} = \frac{b}{a}$, b is the length of the rectangle in the x-direction, a is the length in the y-direction, K_n is a constant and $\bar{z} = \frac{1}{a}(x+iy)$.

Taking the real part as indicated gives:

$$(E.2) \quad P^2 = 1 - \frac{1}{2} C \sum_{n=-\infty}^{\infty} (-1)^n \cdot \ln \left[\frac{\cosh 2\pi(\frac{x}{a}+nb) - \cos(2\pi \frac{y}{a})}{\cosh \pi b(2n+1) - 1} \right]$$

which satisfies the boundary conditions:

$$x = \pm \frac{b}{2} : \quad P^2 = 1$$

$$y = \pm \frac{a}{2} : \quad \frac{\partial P^2}{\partial y} = 0$$

From eq. (E.2) we get:

$$(E.3) \quad \frac{\partial P^2}{\partial (\frac{x}{a})} = -\pi C \sum_{n=-\infty}^{\infty} (-1)^n \frac{\sinh 2\pi(\frac{x}{a}+nb)}{\cosh 2\pi(\frac{x}{a}+nb) - \cos(2\pi \frac{y}{a})}$$

To determine the source strength C the bearing flow must be equated to the orifice mass flow M :

$$(E.4) \quad M = -\frac{P_a^2 h^3}{24 \mu R T} \oint \frac{\partial P^2}{\partial n} ds$$

where $\oint ds$ is a closed line integral around the source and n is the outward directed normal.

Using the boundaries of the rectangle as the integration path, where $\frac{\partial P^2}{\partial y} = 0$ along $y = \pm \frac{a}{2}$, eq. (E.4) reduces to:

$$M = - \frac{P_a^2 h^3}{12\mu RT} \int_{-\frac{1}{2}}^{\frac{1}{2}} \left. \frac{\partial P^2}{\partial(x/a)} \right|_{x=\frac{1}{2}} d(\frac{y}{a})$$

Introducing eq. (E.3) gives:

$$(E.5) \quad M = \frac{\pi P_a^2 h^3}{12\mu RT} \cdot C$$

Substituting the dimensionless mass flow m from eq. (A.11) and the feeding parameter Λ_t from eq. (A.8) (setting $h = C(1+\epsilon)$) gives:

$$(E.6) \quad \frac{CN(1+\epsilon)^3}{2\Lambda_t V} = m$$

This equation may be solved graphically or numerically as shown in Appendix B, Fig. 4, where C is known as a function of the downstream orifice pressure P_i . This relationship is calculated from eq. (E.2) based on a known feeding hole diameter (i.e. known values of x and y).

The rectangular pad is transformed into the radial sector shown in Fig. 8b by the transformation:

$$(E.7) \quad \bar{z} = \frac{1}{a}(x+iy) = \frac{N}{2\pi} \ln(re^{i\theta})$$

$$(E.8) \quad \text{i.e. } \frac{x}{a} = \frac{N}{2\pi} \ln r$$

$$(E.9) \quad \frac{y}{a} = \frac{N}{2\pi} \theta$$

where N is the number of orifices, r is the dimensionless radius with respect to the orifice circle radius R_c and θ is the angular coordinate.

Substituting eq. (E.8) and (E.9) into eq. (E.2) gives:

$$(E.10) \quad P^2 = 1 - \frac{1}{2}C \sum_{n=-\infty}^{\infty} (-1)^n \ln \left[\frac{\cosh N(\ln r + n \ln(\frac{R}{R_c})) - \cos N\theta}{\cosh(N(n+\frac{1}{2}) \cdot \ln(\frac{R}{R_c})) - 1} \right]$$

where C still is given by eq. (E.5) or (E.6). Thus C is determined as the intersection between the orifice flow curve and the C vs. (P_i/V) relationship

determined from eq. (E.10) for a given feeding hole diameter.

It should be noted that since the isobars are not circles this relationship is determined by taking the average pressure along the rim of the feeding hole. However, this is not a serious assumption since the isobars tend to circle in the limit of approaching the singularity. The load carrying capacity is calculated by integrating the pressure:

$$(E.11) \quad W = 2N P_a R_c^2 \int_0^{\frac{\pi}{N}} \int_{\frac{R_c}{R_2}}^{\frac{R_1}{R_2}} r(P-1) dr d\theta$$

Since the orifice was located in the center of the rectangular pad, the transformation given by eq. (E.7) results in:

$$(E.12) \quad R_c = \sqrt{R_1 R_2}$$

i.e., the analysis is only valid for this particular value of R_c . Hence eq. (E.11) becomes:

$$(E.13) \quad \frac{W}{\pi R_1^2 P_a} = \frac{2N}{\pi} \cdot \frac{R_2}{R_1} \int_0^{\frac{\pi}{N}} \int_{\sqrt{\frac{R_2}{R_1}}}^{\sqrt{\frac{R_1}{R_2}}} r \cdot (P-1) dr d\theta$$

where P is given by eq. (E.10). The integration is performed numerically.

Rearranging eq. (E.10) we get:

$$(E.14) \quad P^2 = 1 - \frac{1}{2} \left(\left\{ \ln \left[\frac{\cosh(N \ln r) - \cos N\theta}{\cosh(\frac{N}{2} \ln(\frac{R_1}{R_2})) - 1} \right] + \sum_{n=1}^{\infty} (-1)^n \ln \left[\frac{\cosh^2(nN \ln(\frac{R_1}{R_2})) - 2 \cosh(nN \ln(\frac{R_1}{R_2})) \cosh(N \ln r) \cos N\theta + \cosh^2(N \ln r) + (\cos^2 N\theta)}{\left[\cosh(nN \ln(\frac{R_1}{R_2})) - \cosh(\frac{N}{2} \ln(\frac{R_1}{R_2})) \right]^2} \right] \right\} \right)$$

It can be shown that this series is absolute convergent except at the source.

Since the series is alternating, the truncation error after n terms is less than the absolute value of the $(n+1)^{\text{st}}$ term. The series converges very fast so that only the two first terms are necessary for an evaluation.

If the bearing has a circular recess around the orifice with depth h_r and radius R_r eq. (E.10) and (E.14) still describes the pressure outside the

recess. Inside the recess the pressure becomes:

$$(E.15) \quad P_r^2 = 1 + C_2 - \frac{1}{2} \left(\frac{1}{1 + \frac{h_r}{h}} \right)^3 C \sum_{n=-\infty}^{\infty} (-1)^n \ln \left[\frac{\cosh N(\ln r + n \ln (\frac{R_i}{R_s})) - \cos N\theta}{\cosh(N(n+\frac{1}{2}) \ln (\frac{R_i}{R_s})) - 1} \right]$$

where C_2 is determined from the condition that $P = P_r$ along the circumference of the recess. This solution is only approximate since the isobars are not exactly circular. An average value is used.

When the orifices are not located as given by eq. (E.12) the above analysis is no longer valid. Instead we may use the method developed in Appendix C. Let us again start with a rectangular pad where the location of the orifice in this case is not restricted to the center of the pad.

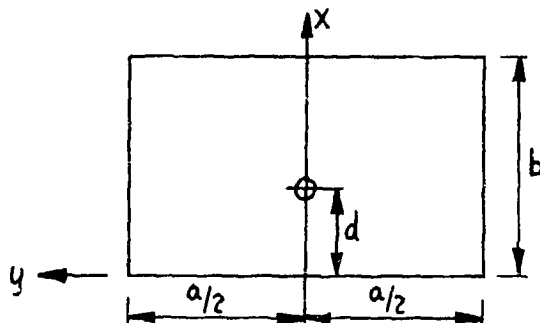


Fig. 9

If the gas feeding is represented by a point source of strength C it can be written $C \cdot \delta(x-d) \cdot \delta(y)$ where δ is the Dirac delta function. Thus Reynolds equation, eq. (A.14) becomes, in dimensionless form:

$$(E.16) \quad \frac{\partial^2 P^2}{\partial \xi^2} + \frac{\partial^2 P^2}{\partial \phi^2} = -C \cdot \delta(\xi - 2\pi x) \delta(\phi)$$

where:

$$(E.17) \quad \xi = 2\pi \frac{x}{a} \quad \phi = 2\pi \frac{y}{a} \quad \xi = \frac{b}{a} \quad x = \frac{d}{a}$$

The boundary conditions for eq. (E.16) are:

$$(E.18) \quad \phi = \pm \pi : \quad \frac{\partial P^2}{\partial \phi} = 0$$

$$(E.19) \quad \zeta = 0 \quad \text{and} \quad \zeta = 2\pi x : \quad P^2 = 1$$

To make the boundary conditions homogenous set:

$$(E.20) \quad P^2 = 1 + U(\zeta, \phi)$$

and express U in a Fourier expansion:

$$(E.21) \quad U(\zeta, \phi) = \frac{1}{2\pi} \gamma_0 + \frac{1}{\pi} \sum_{n=1}^{\infty} \gamma_n(\zeta) \cos n\phi$$

where the coefficients $\gamma_n(\zeta)$ are determined by the inverse Fourier transform:

$$(E.22) \quad \gamma_n(\zeta) = \int_{-\pi}^{\pi} U(\zeta, \phi) \cos n\phi \, d\phi$$

Substituting eq. (E.20) into eq. (E.16) gives:

$$\frac{\partial^2 U}{\partial \zeta^2} + \frac{\partial^2 U}{\partial \phi^2} = -C \delta(\zeta - 2\pi x) \delta(\phi)$$

Then

$$(E.23) \quad \int_{-\pi}^{\pi} \left[\frac{\partial^2 U}{\partial \zeta^2} + \frac{\partial^2 U}{\partial \phi^2} \right] \cos n\phi \, d\phi = -C \delta(\zeta - 2\pi x) \int_{-\pi}^{\pi} \delta(\phi) \cos n\phi \, d\phi = -C \delta(\zeta - 2\pi x)$$

The left hand side may be evaluated by:

$$\int_{-\pi}^{\pi} \frac{\partial^2 U}{\partial \zeta^2} \cos n\phi \, d\phi = \frac{\partial^2}{\partial \zeta^2} \left[\int_{-\pi}^{\pi} U \cos n\phi \, d\phi \right] = \frac{\partial^2 \gamma_n}{\partial \zeta^2}$$

$$\int_{-\pi}^{\pi} \frac{\partial^2 U}{\partial \phi^2} \cos n\phi \, d\phi = \frac{\partial U}{\partial \phi} \cos n\phi \Big|_{-\pi}^{\pi} + n \int_{-\pi}^{\pi} \frac{\partial U}{\partial \phi} \sin n\phi \, d\phi = n U \sin n\phi \Big|_{-\pi}^{\pi} - n^2 \int_{-\pi}^{\pi} U \cos n\phi \, d\phi = -n^2 \gamma_n$$

making use of eq. (E.18). Therefore eq. (E.23) becomes:

$$(E.24) \quad \frac{\partial^2 \gamma_n}{\partial \zeta^2} - n^2 \gamma_n = -C \delta(\zeta - 2\pi x)$$

Integrating:

$$(E.25) \quad \frac{d\gamma_n}{d\xi} \Big|_{2\pi\xi=0} - \frac{d\gamma_n}{d\xi} \Big|_{2\pi\xi=0} = -C$$

The general solution of eq. (E.24) is:

$$(E.26) \quad \begin{aligned} \gamma_0 &= A_0 + B_0 \xi \\ \gamma_n &= A_n \cosh(n\xi) + B_n \sinh(n\xi) \end{aligned}$$

Introducing the boundary conditions eq. (E.18) and (E.19) together with eq. (E.20) and using eq. (E.25) yields the values of the coefficients A_n and B_n .

Substituting into eq. (E.21) and (E.20) gives:

$$(E.27) \quad \underline{0 \leq \xi \leq 2\pi x} \quad P^2 = 1 + \frac{C}{\pi} \left\{ \frac{\xi-x}{2\xi} \xi + \sum_{n=1}^{\infty} \frac{1}{n} \frac{\sinh(2\pi n(\xi-x))}{\sinh(2\pi n\xi)} \sinh(n\xi) \cos(n\phi) \right\}$$

$$(E.28) \quad \underline{2\pi x \leq \xi \leq 2\pi \xi} \quad P^2 = 1 + \frac{C}{\pi} \left\{ \frac{x}{2\xi} (2\pi\xi-\xi) + \sum_{n=1}^{\infty} \frac{1}{n} \frac{\sinh(2\pi n x)}{\sinh(2\pi n\xi)} \sinh(n(2\pi\xi-\xi)) \cos(n\phi) \right\}$$

To find the flow we must take the derivative of the above equations:

$$\begin{aligned} \underline{0 \leq \xi \leq 2\pi x} \quad \frac{\partial P^2}{\partial \xi} &= \frac{C}{\pi} \left\{ \frac{\xi-x}{2\xi} + \sum_{n=1}^{\infty} \frac{\sinh(2\pi n(\xi-x))}{\sinh(2\pi n\xi)} \cosh(n\xi) \cos(n\phi) \right\} \\ \underline{2\pi x \leq \xi \leq 2\pi \xi} \quad \frac{\partial P^2}{\partial \xi} &= \frac{C}{\pi} \left\{ -\frac{x}{2\xi} + \sum_{n=1}^{\infty} -\frac{\sinh(2\pi n x)}{\sinh(2\pi n\xi)} \cosh(n(2\pi\xi-\xi)) \cos(n\phi) \right\} \end{aligned}$$

The mass flow M is given by eq. (E.4). Let the integration path be around the boundaries of the rectangle so that:

$$M = -\frac{P_a^2 h^3}{24\mu RT} \int_{-\pi}^{\pi} \left[-\frac{\partial P^2}{\partial \xi} \Big|_{\xi=2\pi\xi} + \frac{\partial P^2}{\partial \xi} \Big|_{\xi=0} \right] d\phi$$

Thus:

$$(E.29) \quad M = \frac{P_a^2 h^3}{24\mu RT} C$$

Analogous to eq. (E.6) we get:

$$(E.30) \quad \frac{CN(1+\epsilon)^3}{4\pi \lambda_t V} = m$$

The transformation from rectangular to polar coordinates is:

$$(E.31) \quad \xi + i\phi = N \cdot \ln(r'e^{i\theta})$$

i.e.

$$(E.32) \quad \xi = N \cdot \ln r'$$

$$(E.33) \quad \phi = N\theta$$

where r' is the dimensionless radius with respect to the inner radius R_2 .

Therefore

$$(E.34) \quad \xi = \frac{N}{2\pi} \cdot \ln\left(\frac{R_1}{R_2}\right)$$

$$(E.35) \quad \alpha = \frac{N}{2\pi} \cdot \ln\left(\frac{R_c}{R_2}\right)$$

Substituting eq. (E.32)-(E.35) into eq. (E.27)-(E.28) and introducing the previous nomenclature

$$(E.36) \quad \gamma = \frac{R_1}{R_c} \quad \gamma = \frac{R_c}{R_2} \quad \beta = \frac{\ln \gamma}{\ln \alpha}$$

yields:

$$(E.37) \quad \underline{1 \leq r' \leq \gamma} \quad P^2 = 1 + \frac{C}{\pi} \left\{ \frac{N}{2} \frac{\beta}{1+\beta} \ln r' + \sum_{n=1}^{\infty} \frac{1}{n} \frac{\sinh(nN \ln \gamma)}{\sinh(nN \ln \alpha)} \sinh(nN \ln r') \cos(nN\theta) \right\}$$

$$(E.38) \quad \underline{\gamma < r' < \alpha} \quad P^2 = 1 + \frac{C}{\pi} \left\{ \frac{N}{2} \frac{1}{1+\beta} \ln\left(\frac{\alpha}{r'}\right) + \sum_{n=1}^{\infty} \frac{1}{n} \frac{\sinh(nN \ln \alpha)}{\sinh(nN \ln \gamma)} \sinh(nN \ln\left(\frac{\alpha}{r'}\right)) \cos(nN\theta) \right\}$$

The load is determined by eq. (E.11) and is evaluated numerically.

Since it is more convenient to have the above series in the same general form as the series in eq. (E.14), eq. (E.37)-(E.38) shall be rearranged. These series have the form:

$$(E.39) \quad T = \sum_{n=1}^{\infty} \frac{1}{n} \frac{\sinh(na)}{\sinh(nb)} \sinh(nc) \cos(nd)$$

Rewrite to get:

$$(E.40) \quad T = \frac{1}{4} \sum_{n=1}^{\infty} \frac{e^{-n(b-a-c)}}{n} \cdot (1-e^{-2nb})^{-1} [e^{ind} + e^{-ind} - e^{-n(2a-id)} - e^{-n(2a+id)} - e^{-n(2c-id)} - e^{-n(2c+id)} + e^{-n(2a+2c-id)} + e^{-n(2a+2c+id)}]$$

From the binomial expansion:

$$(1-x)^{-1} = \sum_{k=0}^{\infty} x^k \quad |x^k| < 1$$

we get

$$(E.41) \quad (1-e^{-2nb})^{-1} = \sum_{k=0}^{\infty} e^{-2kb} \quad b > 0$$

Substituting eq. (E.41) into eq. (E.40) and interchange order of summation gives:

$$(E.42) \quad T = \frac{1}{4} \sum_{k=0}^{\infty} \sum_{n=1}^{\infty} \frac{1}{n} [e^{-n(2kb+b-a-c-id)} + e^{-n(2kb+b-a-c+id)} - e^{-n(2kb+b+a-c-id)} - e^{-n(2kb+b+a-c+id)} \\ - e^{-n(2kb+b-a+c-id)} - e^{-n(2kb+b-a+c+id)} + e^{-n(2kb+b+a+c-id)} + e^{-n(2kb+b+a+c+id)}]$$

Introduce the expansion:

$$\sum_{n=1}^{\infty} \frac{x^n}{n} = -\ln(1-x) \quad |x| < 1$$

Since $b > a+c$ and a, b and c are positive all the exponentials in eq. (E.42) are less than 1. Therefore eq. (E.42) becomes

$$(E.43) \quad T = \frac{1}{4} \sum_{k=0}^{\infty} \ln \left[\frac{\sinh \frac{1}{2}(2kb+b+a-c-id) \cdot \sinh \frac{1}{2}(2kb+b+a-c+id) \cdot \sinh \frac{1}{2}(2kb+b-a+c-id) \cdot \sinh \frac{1}{2}(2kb+b-a+c+id)}{\sinh \frac{1}{2}(2kb+b+a+c-id) \cdot \sinh \frac{1}{2}(2kb+b+a+c+id) \cdot \sinh \frac{1}{2}(2kb+b-a-c-id) \cdot \sinh \frac{1}{2}(2kb+b-a-c+id)} \right]$$

From the relationships:

$$\sinh \frac{1}{2}(x+iy) \cdot \sinh \frac{1}{2}(x-iy) = \frac{1}{2} [\cosh x - \cosh y]$$

$$\cosh(x \pm iy) = \cosh x \cdot \cos y \pm i \sinh x \cdot \sin y$$

eq. (E.43) reduces to:

$$(E.44) \quad T = \frac{1}{4} \sum_{k=0}^{\infty} \ln \left[\frac{\cosh^2(2k+1)b - 2\cosh(2k+1)b \cdot \cosh(a-c) \cdot \cos d + \cosh^2(a-c) + \cos^2 d - 1}{\cosh^2(2k+1)b - 2\cosh(2k+1)b \cdot \cosh(a+c) \cdot \cos d + \cosh^2(a+c) + \cos^2 d - 1} \right]$$

Comparing eq. (E.37) and (E.38) with eq. (E.39) we get:

$$(E.45) \quad 1 \leq r' \leq \gamma \quad \frac{1}{\gamma} \leq r \leq 1 \quad a-c = N \cdot \ln \left(\frac{\gamma}{r'} \right) \quad a+c = N \cdot \ln \left(\frac{\gamma}{r} \right) \quad b = N \cdot \ln \left(\eta_{\gamma} \right) \quad d = N \theta$$

$$(E.46) \quad \gamma \leq r' \leq \eta_{\gamma} \quad 1 \leq r \leq \eta \quad a-c = N \cdot \ln \left(\frac{\eta}{r'} \right) \quad a+c = N \cdot \ln \left(\frac{\eta}{r} \right) \quad b = N \cdot \ln \left(\eta_{\gamma} \right) \quad d = N \theta$$

where r' is the dimensionless radius with respect to R_c whereas r' is dimensionless with respect to R_2 , i.e., $r' = \gamma r$. Thus eq. (E.37)-(E.38) become:

$$(E.47) \quad \underline{\frac{1}{\gamma} \leq r \leq 1} \quad P^2 = 1 + \frac{C}{4\pi} \left\{ 2N \frac{\beta}{1+\beta} \ln(\gamma r) + 4T \right\}$$

$$(E.48) \quad \underline{1 \leq r \leq \eta} \quad P^2 = 1 + \frac{C}{4\pi} \left\{ 2N \frac{1}{1+\beta} \ln \left(\frac{\eta}{r} \right) + 4T \right\}$$

where T is determined from eq. (E.44) in combination with eq. (E.45) and (E.46).

APPENDIX F

Effect of Eccentricity Ratio on Load Carrying Capacity of Hydrostatic Journal Bearing

The analyses of the hydrostatic journal bearing in Appendix B and C are limited to small values of the eccentricity ratio and predict a linear relationship between load and eccentricity ratio. The present appendix is concerned with an approximate analysis of the journal bearing where the eccentricity ratio is not small. If it is assumed that the orifice feeding may be represented by line feeding as in Appendix B, the Reynolds equation outside the feeding planes is given by eq. (A.14) without local feeding:

$$(F.1) \quad \frac{\partial}{\partial \theta} \left[h^3 \frac{\partial P^2}{\partial \theta} \right] + \frac{\partial}{\partial \zeta} \left[h^3 \frac{\partial P^2}{\partial \zeta} \right] = 0$$

where $h = 1 + \epsilon \cos \theta$. If it is assumed that the bearing is short so that $\frac{\partial P^2}{\partial \zeta} \gg \frac{\partial P^2}{\partial \theta}$, eq. (F.1) can be approximated by:

$$(F.2) \quad \frac{\partial}{\partial \zeta} \left[(1 + \epsilon \cos \theta)^3 \frac{\partial P^2}{\partial \zeta} \right] = 0$$

with the solution (see Fig. 3, Appendix B, and eq. (B.7) and (B.8)):

$$(F.3) \quad 0 \leq \zeta \leq \xi \quad P^2 = 1 + f(\theta) \cdot \left(1 - \frac{\zeta}{\xi} \right)$$

$$(F.4) \quad 0 \leq \zeta' \leq \eta \quad P^2 = 1 + f(\theta)$$

where $f(\theta)$ is a function of θ only. A similar approximation has been employed successfully for the hydrodynamic bearing, see Ref. 6.

Eq. (F.3) satisfies the boundary condition of ambient pressure at the end of the bearing, i.e., $P=1$ for $\zeta=\xi$. At $\zeta=0$ the bearing flow must equal the orifice flow as given by eq. (B.9):

$$(F.5) \quad (1 + \epsilon \cos \theta)^3 \left[-\frac{\partial P^2}{\partial \zeta} \Big|_{\zeta=0} + \frac{\partial P^2}{\partial \zeta'} \Big|_{\zeta'=\eta} \right] = A_t V_m$$

Substitute eq. (F.3) and (F.4) into eq. (F.5):

$$(F.6) \quad (1+\varepsilon \cos \theta)^3 \cdot f = \xi \Lambda_t V m$$

If m is replaced by the approximate orifice flow equation eq. (A.27):

$$m = \sqrt{1 - \left(\frac{P_i}{V}\right)^2}$$

where in the present case $P_i^2 = 1 + f(\theta)$ from eq. (F.3) we get:

$$(1+\varepsilon \cos \theta)^3 \cdot f = \xi \Lambda_t \sqrt{V^2 - 1 - f}$$

or

$$(F.7) \quad f(\theta) = \frac{1}{2} \frac{\xi^2 \Lambda_t^2}{(1+\varepsilon \cos \theta)^6} \left[-1 + \sqrt{1 + \frac{4(V^2-1)}{\xi^2 \Lambda_t^2} (1+\varepsilon \cos \theta)^6} \right]$$

The load carrying capacity W is found by integrating the pressure:

$$W = -4 P_a R^2 \int_0^\pi \left[\int_0^\xi P d\zeta + \int_\xi^\eta P d\zeta' \right] \cos \theta d\theta$$

Using eq. (F.3) and (F.4) we get:

$$(F.8) \quad \frac{W}{P_a D(L+L_1)} = -\frac{\xi}{\xi+\eta} \cdot \frac{2}{3} \int_0^\eta \frac{(1+f)^{3/2}-1}{f} \cos \theta d\theta - \frac{\eta}{\xi+\eta} \int_0^\pi \sqrt{1+f} \cos \theta d\theta$$

The integration is carried out numerically.

The total mass flow is given by:

$$(F.9) \quad M_T = \frac{P_a^2 C^3}{12 \mu R T} \frac{1}{\xi} \int_0^\pi f \cdot (1+\varepsilon \cos \theta)^3 d\theta$$

APPENDIX G

The Dynamic Load Carrying Capacity of the Hydrostatic Journal Bearing with Orifice Restricted Line Feeding

When the journal performs harmonic vibrations, pressure will be generated in the gas film due to the compressibility of the gas as indicated in Appendix A. The present appendix is concerned with an analysis of this dynamic load when the eccentricity ratio and the vibration amplitude is small.

The governing equation is Reynolds equation (A.13) and the bearing configuration is shown in Fig. 3, Appendix B. If it is assumed that the journal perform harmonic vibrations with frequency ω such that the motion is either purely translatory or a rotation around a transverse axis, then outside and between the feeding planes eq. (A.13) becomes:

$$(G.1) \quad \frac{\partial}{\partial \theta} \left[h^3 \frac{\partial P^2}{\partial \theta} \right] + \frac{\partial}{\partial \zeta} \left[h^3 \frac{\partial P^2}{\partial \zeta} \right] = 2\sigma \frac{\partial (Ph)}{\partial \tau}$$

where σ is the frequency number:

$$(G.2) \quad \sigma = \frac{12 \mu \omega}{P_a} \left(\frac{R}{C} \right)^2$$

When the journal performs translatory motion with amplitude $\text{Re}\{C e^{i\omega t}\}$ around the concentric position the dimensionless film thickness is:

$$(G.3) \quad h = \text{Re}\{1 + \epsilon e^{i\tau} \cos \theta\}$$

Expanding the pressure in a power series of the amplitude and assuming $\epsilon \ll 1$ so that only the two first terms are retained, we get:

$$(G.4) \quad P = P_0 + \text{Re}\{\epsilon e^{i\tau} P_1\}$$

$$(G.5) \quad P^2 = P_0^2 + \text{Re}\{2\epsilon e^{i\tau} P_0 P_1\}$$

Also:

$$(G.6) \quad h^3 = 1 + \text{Re}\{3\epsilon e^{i\tau} \cos \theta\}$$

Set:

$$(G.7) \quad \zeta P_1 = H(\zeta) \cos \theta$$

and substitute eq. (G.4)-(G.6) into eq. (G.1) to get:

$$(G.8) \quad \frac{\partial P_o^2}{\partial \theta^2} + \frac{\partial P_o^2}{\partial \zeta^2} = 0$$

where $\frac{\partial P_o}{\partial \theta} = 0$ because of symmetry

$$(G.9) \quad \frac{d^2 H}{d \zeta^2} - \left(1 + \frac{i\sigma}{P_o} \right) H = i\sigma P_o$$

Referring to Fig. 3, Appendix B, the solution of eq. (G.8) is:

$$(G.10) \quad 0 \leq \zeta \leq \xi \quad P_o^2 = 1 + q(\xi + \zeta)$$

$$(G.11) \quad 0 \leq \zeta' \leq \eta \quad P_o^2 = 1 + q\xi$$

At $\zeta = 0$ the bearing flow must equal the orifice flow as expressed by eq. (B.9):

$$(G.12) \quad (1 + \epsilon e^{i\tau} \cos \theta)^3 \left[-\frac{\partial P^2}{\partial \zeta} \Big|_{\zeta=0} + \frac{\partial P^2}{\partial \zeta'} \Big|_{\zeta'=\eta} \right] = \Lambda_t V_m$$

Insert eq. (G.4)-(G.7) and expand m as in eq. (B.10) to get:

$$(G.13) \quad -\frac{\partial P_o^2}{\partial \zeta} \Big|_{\zeta=0} + \frac{\partial P_o^2}{\partial \zeta'} \Big|_{\zeta'=\eta} = \Lambda_t V_{m_o}$$

$$(G.14) \quad \frac{dH}{d\zeta} \Big|_{\zeta=0} - \frac{dH}{d\zeta'} \Big|_{\zeta'=\eta} = \frac{3}{2} \Lambda_t V_{m_o} - \frac{\Lambda_t m'_o}{2 P_{o,i}} H_i$$

Eq. (G.13) gives:

$$(G.15) \quad q = \Lambda_t V_{m_o}$$

For $0 \leq \zeta' \leq \eta$ eq. (G.9) may be solved since P_o is constant, see eq. (J.11).

From symmetry $\frac{dH}{d\zeta'} \Big|_{\zeta'=0} = 0$ and therefore the solution of eq. (G.9) is:

$$(G.16) \quad 0 \leq \zeta' \leq \eta \quad H = \left[H_i + \frac{i\sigma P_o}{1 + \frac{i\sigma}{P_o}} \right] \frac{\cosh \zeta' (\alpha + i\beta)}{\cosh \eta (\alpha + i\beta)} - \frac{i\sigma P_o}{1 + \frac{i\sigma}{P_o}}$$

where $H_i = H_{\zeta'=\eta}$ and:

$$(G.17) \quad \alpha + i\beta = \sqrt{1 + \frac{i\sigma}{P_{o,i}}}$$

i.e.

$$(G.18) \quad \alpha = \sqrt{\frac{1}{2} \left[1 + \sqrt{1 + \left(\frac{\sigma}{P_{oi}} \right)^2} \right]}$$

$$(G.19) \quad \beta = \sqrt{\frac{1}{2} \left[-1 + \sqrt{1 + \left(\frac{\sigma}{P_{oi}} \right)^2} \right]}$$

Substituting eq. (G.16) and (G.15) into eq. (G.14) gives:

$$(G.20) \quad \frac{dH}{d\zeta} \Big|_{\zeta=0} = \frac{3}{2} q + \frac{i\sigma P_{oi}}{1 + \frac{q}{P_{oi}}} (\alpha + i\beta) \tanh \eta(\alpha + i\beta) + \left[(\alpha + i\beta) \tanh \eta(\alpha + i\beta) - \frac{A_t m_a}{2 P_{oi}} \right] H_i$$

where:

$$(G.21) \quad P_{oi} = \sqrt{1 + q\zeta}$$

Thus eq. (G.9) should be solved in $0 \leq \zeta \leq \xi$ with eq. (G.20) as one boundary condition and $H(\xi) = 0$ as the other boundary condition. The solution is obtained numerically as shown later, but first the equations for rotational vibrations will be derived.

When the journal performs rotational motion with the angular displacement $\text{Re}\{de^{i\omega t}\}$ around a transverse axis perpendicular to the journal axis at $\zeta' = 0$ (see Fig. 3, Appendix B) the dimensionless film thickness becomes:

$$(G.22) \quad h = 1 + \left(\frac{R}{C} \right) \zeta' de^{i\tau} \cos \theta$$

Proceeding as in the translatory case we get:

$$(G.23) \quad P = P_o + \text{Re}\{de^{i\tau} P_i\}$$

$$(G.24) \quad P^2 = P_o^2 + \text{Re}\{2de^{i\tau} P_o P_i\}$$

$$(G.25) \quad h^3 = 1 + \text{Re}\left\{ 3 \left(\frac{R}{C} \right) de^{i\tau} \zeta' \cos \theta \right\}$$

Set:

$$(G.26) \quad P_o P_i = \left(\frac{R}{C} \right) H(\zeta) \cdot \cos \theta$$

so that eq. (G.1) becomes in addition to eq. (G.8):

$$(G.27) \quad \frac{d^2 H}{d\zeta^2} - \left(1 + \frac{i\sigma}{P_o} \right) H = - \frac{3}{2} \frac{\partial P_o^2}{\partial \zeta} + i\sigma P_o \zeta'$$

Since $\frac{\partial P_o^2}{\partial \theta} = 0$. P_o is given by eq. (G.10) and (G.11). As P_o is

constant for $0 \leq \zeta' \leq \eta$ eq. (G.27) may be solved between the feeding planes.

From symmetry $H_{\zeta'=0} = 0$ so that eq. (G.27) gives:

$$(G.28) \quad \underline{0 \leq \zeta' \leq \eta} \quad H = \left[H_i + \frac{i\sigma P_0 \eta}{1 + \frac{i\sigma}{P_0}} \right] \frac{\sinh \zeta'(\alpha + i\beta)}{\sinh \eta(\alpha + i\beta)} \sim \frac{i\sigma P_0 \zeta'}{1 + \frac{i\sigma}{P_0}}$$

where α and β are given by eq. (G.18) and (G.19). The boundary condition at $\zeta = 0$ is given analogous to eq. (G.12) by:

$$(G.29) \quad \left(1 + 3 \left(\frac{R}{C} \right) \eta \alpha e^{i\tau} \cos \theta \right) \left(- \frac{\partial P^2}{\partial \zeta} \Big|_{\zeta=0} + \frac{\partial P^2}{\partial \zeta'} \Big|_{\zeta'=\eta} \right) = \Lambda_t \left(V_m_0 + \left(\frac{R}{C} \right) \alpha e^{i\tau} \frac{m'_0}{P_{0i}} H_i \cos \theta \right)$$

Introducing eq. (G.28) we get in addition to eq. (G.13) and (G.15):

$$(G.30) \quad \frac{dH}{d\zeta} \Big|_{\zeta=0} = \frac{3}{2} q \eta + \frac{i\sigma P_{0i}}{1 + \frac{i\sigma}{P_{0i}}} \left[\eta(\alpha + i\beta) \coth \eta(\alpha + i\beta) - 1 \right] + \left[(\alpha + i\beta) \coth \eta(\alpha + i\beta) - \frac{\Lambda_t m'_0}{2 P_{0i}} \right] H_i$$

Hence eq. (G.27) should be solved in $0 \leq \zeta \leq \xi$ where eq. (G.30) serves as one boundary condition and $H(\xi) = 0$ as the other condition.

Eq. (G.9) and (G.27) has the general form:

$$(G.31) \quad \underline{0 \leq \zeta \leq \xi} \quad \frac{d^2 H}{d\zeta^2} - \left(1 + \frac{i\sigma}{P_0} \right) H = F = \begin{cases} i\sigma P_0 & \text{translatory} \\ \frac{3}{2} q + i\sigma P_0(\xi + \eta) & \text{rotational} \end{cases}$$

where P_0 is given by eq. (G.10) and H and F are complex:

$$(G.32) \quad H = h_r + i h_i$$

$$(G.33) \quad F = f_r + i f_i$$

The boundary conditions are:

$$(G.34) \quad H(\xi) = 0$$

$$(G.35) \quad H'_0 = \frac{dH}{d\zeta} \Big|_{\zeta=0} = \alpha + ib + (c + id) H_0$$

Eq. (G.31) is solved numerically. To get it in finite difference form, integrate

twice:

$$(G.36) \quad H = \int_0^{\zeta} \left(\int_0^x \left[\left(1 + \frac{i\zeta}{P_0} \right) H + F \right] dy \right) dx + \zeta H'_0 + H_0$$

Set:

$$(G.37) \quad G = \left(1 + \frac{i\zeta}{P_0} \right) H + F$$

and integrate the double integral by parts to get:

$$(G.38) \quad H = \int_0^{\zeta} (\zeta - x) G dx + \zeta H'_0 + H_0$$

To write this equation in finite difference form subdivide the interval $0 \rightarrow \zeta$ in m increments of length $\Delta\zeta = \frac{\zeta}{m}$ and integrate by the trapezoidal rule:

$$(G.39) \quad 0 \leq n \leq m-1 \quad H_{n+1} = H_n + (\Delta\zeta)^2 \left[\frac{1}{2} G_0 + G_1 + G_2 + \dots + G_n \right] + \Delta\zeta \cdot H'_0$$

For computer calculations it is convenient to set:

$$(G.40) \quad H_n = S_{rn} + iS_{in} + (t_{rn} + it_{in}) H_0$$

$$(G.41) \quad (\Delta\zeta)^2 \left[\frac{1}{2} G_0 + G_1 + G_2 + \dots + G_n \right] = p_{rn} + ip_{in} + (q_{rn} + iq_{in}) H_0$$

Then from eq. (G.39), (G.35), (G.37) and (G.33):

$$(G.42) \quad P_{on} = \sqrt{1 + q(m-n) \Delta\zeta}$$

$$(G.43) \quad p_{rn} = p_{r,n-1} + (\Delta\zeta)^2 \left[S_{rn} - \frac{q}{P_{on}} S_{in} + f_{rn} \right]$$

$$(G.44) \quad p_{in} = p_{i,n-1} + (\Delta\zeta)^2 \left[S_{in} + \frac{q}{P_{on}} \cdot S_{rn} + f_{in} \right]$$

$$(G.45) \quad q_{rn} = q_{r,n-1} + (\Delta\zeta)^2 \left[t_{rn} - \frac{q}{P_{on}} \cdot t_{in} \right]$$

$$(G.46) \quad q_{in} = q_{i,n-1} + (\Delta\zeta)^2 \left[t_{in} + \frac{q}{P_{on}} t_{rn} \right]$$

$$(G.47) \quad S_{r,n+1} = S_{rn} + p_{rn} + a \cdot \Delta\zeta$$

$$(G.48) \quad S_{i,n+1} = S_{in} + p_{in} + b \cdot \Delta\zeta$$

$$(G.49) \quad t_{r,n+1} = t_{rn} + q_{rn} + c \cdot \Delta\zeta$$

$$(G.50) \quad t_{i,n+1} = t_{in} + q_{in} + d \cdot \Delta\zeta$$

To initiate calculations set:

$$(G.51) \quad P_{ro} = \frac{1}{2} (\Delta \zeta)^2 f_{ro}$$

$$(G.52) \quad P_{io} = \frac{1}{2} (\Delta \zeta)^2 f_{io}$$

$$(G.53) \quad q_{ro} = \frac{1}{2} (\Delta \zeta)^2$$

$$(G.54) \quad q_{io} = \frac{1}{2} (\Delta \zeta)^2 \frac{\phi}{P_{eo}}$$

$$(G.55) \quad S_{ro} = S_{io} = t_{io} = 0$$

$$(G.56) \quad t_{ro} = 1$$

Thus the method of calculation is: 1) preset $P_{ro}, P_{io}, q_{ro}, \dots, t_{ro}$ from eq. (G.51)-(G.56); 2) set $n=0$ and calculate eq. (G.47)-(G.50); 3) increase n by 1 and repeat the cycle eq. (G.42)-(G.50) to $n=m-1$, where the boundary condition eq. (G.34) gives:

$$H_m = S_{rm} + iS_{im} + (t_{rm} + it_{im}) H_0 = 0$$

or:

$$(G.57) \quad H_0 = -\frac{S_{rm} + iS_{im}}{t_{rm} + it_{im}} = h_{ro} + ih_{io}$$

Having determined H_0 we may find $H_n = h_{rn} + ih_{in}$ from eq. (G.40). The pressure is calculated from eq. (G.7) and (G.4) or eq. (G.26) and (G.23):

$$(G.58) \quad \text{translatory} \quad P_n = P_{on} + \frac{E}{P_{on}} (h_{rn} \cos \omega t - h_{in} \sin \omega t) \cos \theta$$

$$(G.59) \quad \text{rotational} \quad P_n = P_{on} + \left(\frac{R}{C}\right) \frac{d}{P_{on}} (h_{rn} \cos \omega t - h_{in} \sin \omega t) \cos \theta$$

The dynamic load carrying capacity W_D and the restoring moment M_D are obtained by integration:

$$(G.60) \quad \text{translatory} \quad W_D = -2P_a R^2 \int_0^{2\pi} \left[\int_0^{\zeta} (P_0 + \varepsilon e^{i\tau} \frac{H}{P_0} \cos \theta) d\zeta + \int_0^{\eta} (P_0 + \varepsilon e^{i\tau} \frac{H}{P_0} \cos \theta) d\zeta' \right] \cos \theta d\theta$$

$$(G.61) \quad \text{rotational} \quad M_D = -2P_a R^3 \int_0^{2\pi} \left[\int_0^{\zeta} \left((\zeta + \eta) \left(P_0 + \left(\frac{R}{C}\right) d e^{i\tau} \frac{H}{P_0} \cos \theta \right) d\zeta + \int_0^{\eta} \left(P_0 + \left(\frac{R}{C}\right) d e^{i\tau} \frac{H}{P_0} \cos \theta \right) d\zeta' \right) \right] \cos \theta d\theta$$

In dimensionless form:

$$(G.62) \frac{W_D}{P_a D(L+L_i)E} = \frac{\pi}{2(\xi+\eta)} \left\{ -\cos \omega t \left[\int_0^\xi \frac{h_{rn}}{P_{on}} d\xi + \int_0^\eta \frac{h_r}{P_o} d\xi' \right] + \sin \omega t \left[\int_0^\xi \frac{h_{rn}}{P_{on}} d\xi + \int_0^\eta \frac{h_r}{P_o} d\xi' \right] \right\} = W'_D \cos(\omega t - \phi_w)$$

$$(G.63) \frac{M_D}{P_a D^2(L+L_i)\left(\frac{B}{c}\right)d} = \frac{\pi}{4(\xi+\eta)} \left\{ -\cos \omega t \left[\int_0^\xi ((\xi+\eta) \frac{h_{rn}}{P_{on}} d\xi + \int_0^\eta \frac{h_r}{P_o} d\xi') \right] + \sin \omega t \left[\left((\xi+\eta) \frac{h_{rn}}{P_{on}} d\xi + \int_0^\eta \frac{h_r}{P_o} d\xi' \right) \right] \right\} = M'_D \cos(\omega t - \phi_M)$$

The integrals $\int_0^\xi d\xi$ are calculated numerically from the above obtained values of H_{rn} . The integrals $\int_0^\eta d\xi'$ can be evaluated from eq. (G.16) and (G.28):

$$(G.64) \text{translatory} \quad -\frac{e^{i\omega t}}{P_o} \int_0^\eta H d\xi' = -\frac{\cos \omega t + i \sin \omega t}{P_o + i\sigma} \left\{ \left(H_0 + \frac{i\sigma P_o}{1 + \frac{i\sigma}{P_o}} \right) (\alpha + i\beta) \tanh \eta(\alpha + i\beta) - i\sigma P_o \eta \right\}$$

$$(G.65) \text{rotational} \quad -\frac{e^{i\omega t}}{P_o} \int_0^\eta \xi' H d\xi' = -\frac{\cos \omega t + i \sin \omega t}{P_o + i\sigma} \left\{ \left(H_0 + \frac{i\sigma P_o \eta}{1 + \frac{i\sigma}{P_o}} \right) (\eta(\alpha + i\beta) \coth \eta(\alpha + i\beta) - 1) - i\frac{1}{3} \sigma P_o \eta^3 \right\}$$

where:

$$(G.66) (\alpha + i\beta)^2 = 1 + \frac{i\sigma}{P_o} \quad (\text{see eq. (G.17)})$$

$$(G.67) (\alpha + i\beta) \tanh \eta(\alpha + i\beta) = \frac{\alpha \sinh(2\eta\alpha) - \beta \sin(2\eta\beta) + i(\alpha \sin(2\eta\beta) + \beta \sinh(2\eta\alpha))}{\cosh(2\eta\alpha) + \cos(2\eta\beta)}$$

$$(G.68) (\alpha + i\beta) \coth \eta(\alpha + i\beta) = \frac{\alpha \sinh(2\eta\alpha) + \beta \sin(2\eta\beta) - i(\alpha \sin(2\eta\beta) - \beta \sinh(2\eta\alpha))}{\cosh(2\eta\alpha) - \cos(2\eta\beta)}$$

$$(G.69) \frac{i\sigma P_{oi}}{1 + \frac{i\sigma}{P_{oi}}} = \frac{\sigma^2 + i\sigma P_{oi}}{1 + \left(\frac{\sigma}{P_{oi}}\right)^2}$$

APPENDIX H

The Dynamic Load Carrying Capacity of the Hydrostatic Thrust Bearing with Orifice Restricted Line Feeding

When one face of the thrust bearing performs harmonic vibrations, pressure will be generated in the gas film due to the compressibility of the gas. The present appendix is concerned with an analysis of this dynamic load when the vibration amplitude is small.

The governing equation is Reynolds equation (A.20) and the bearing geometry is shown in Fig. 5, Appendix B. If it is assumed that the vibrational motion with frequency ω is either purely translatory or a rotation around a diameter, then outside the feeding planes eq. (A.20) becomes:

$$(H.1) \quad \frac{1}{r} \frac{\partial}{\partial r} \left[r h^3 \frac{\partial P^2}{\partial r} \right] + \frac{\partial}{\partial \theta} \left[h^3 \frac{\partial P^2}{\partial \theta} \right] = 2 \sigma \frac{\partial (Ph)}{\partial T}$$

where σ is the frequency number:

$$\sigma = \frac{12 \mu \omega}{P_a} \left(\frac{R_c}{C} \right)^2$$

and R_c is the radius of the orifice circle.

Let the vibration be purely translatory with amplitude $\text{Re}\{C \epsilon e^{i\omega t}\}$ where C denotes the equilibrium film thickness. Then the dimensionless film thickness is:

$$(H.2) \quad h = 1 + \text{Re}\{\epsilon e^{i\tau}\}$$

Performing a first order perturbation in ϵ we get:

$$(H.3) \quad P = P_0 + \text{Re}\{\epsilon e^{i\tau} P_1\}$$

$$(H.4) \quad P^2 = P_0^2 + \text{Re}\{2\epsilon e^{i\tau} P_0 P_1\}$$

$$(H.5) \quad h^3 = 1 + 3\epsilon e^{i\tau}$$

Set:

$$(H.6) \quad P_0 P_1 = H(r)$$

and substitute eq. (H.2)-(H.6) into eq. (H.1) to get:

$$(H.7) \quad \frac{1}{r} \frac{\partial}{\partial r} \left[r \frac{\partial P^2}{\partial r} \right] + \frac{\partial^2 P^2}{r^2 \partial \theta^2} = 0$$

$$(H.8) \quad \frac{1}{r} \frac{\partial}{\partial r} \left[r \frac{\partial H}{\partial r} \right] - \frac{i\omega}{P_0} H = i\omega P_0$$

Since $\frac{\partial P^2}{\partial \theta} = 0$ because of symmetry eq. (H.7) gives:

$$(H.9) \quad \underline{1 \leq r \leq \gamma} \quad P_0^2 = 1 + q_T \ln\left(\frac{\gamma}{r}\right)$$

$$(H.10) \quad \underline{\gamma \leq r \leq 1} \quad P_0^2 = 1 + \beta q_T \ln(\gamma r)$$

where $r = \frac{R}{R}$, and γ , γ and β are defined in eq. (B.30)-(B.32). At $r=1$ the bearing flow must equal the orifice flow:

$$(H.11) \quad (1+3\varepsilon e^{i\tau}) \left(-\frac{\partial P^2}{\partial r} \Big|_{r=R_0} + \frac{\partial P^2}{\partial r} \Big|_{r=1} \right) = (1+\beta) \Lambda_T V_m = (1+\beta) \Lambda_T \left(V_{m_0} + \frac{m'_0}{P_{0i}} \varepsilon e^{i\tau} H_{r=1} \right)$$

where Λ_T is as defined in eq. (B.36):

$$(H.12) \quad \Lambda_T = \frac{12 \mu N \alpha^2 \sqrt{RT}}{P_a C^3 (1+\beta)}$$

Hence:

$$(H.13) \quad q_T = \Lambda_T V_{m_0}$$

$$(H.14) \quad \frac{\partial H}{\partial r} \Big|_{r=1+0} - \frac{\partial H}{\partial r} \Big|_{r=1-0} = (1+\beta) \left(\frac{3}{2} q_T - \frac{\Lambda_T m'_0}{2 P_{0i}} H_i \right)$$

Thus eq. (H.8) is to be solved with eq. (H.14) as one boundary condition and

$$(H.15) \quad H\left(\frac{1}{\gamma}\right) = H(\gamma) = 0$$

as the other boundary condition. This will be done numerically as shown later.

If the vibration is pure rotational with angular displacement $\text{Re}\{de^{i\omega t}\}$ around a diameter, the dimensionless film thickness becomes:

$$(H.16) \quad h = 1 + \text{Re}\left\{ \left(\frac{R}{C}\right) \alpha e^{i\tau} r \sin\theta \right\}$$

A first order perturbation gives:

$$(H.17) \quad P = P_0 + \operatorname{Re}\{de^{i\tau} P_i\}$$

$$(H.18) \quad P^2 = P_0^2 + \operatorname{Re}\{2de^{i\tau} P_0 P_i\}$$

$$(H.19) \quad h^3 = 1 + 3\left(\frac{R_c}{C}\right)de^{i\tau} r \sin\theta$$

Set:

$$(H.20) \quad P_0 P_i = \left(\frac{R_c}{C}\right) H(r) \sin\theta$$

and substitute eq. (H.16)-(H.20) into eq. (H.1) to get in addition to eq. (H.7):

$$(H.21) \quad \frac{1}{r} \frac{d}{dr} \left[r \frac{dH}{dr} \right] - \left(\frac{1}{r^2} + \frac{i\zeta}{P_0} \right) H = -\frac{3}{2} \frac{\partial P^2}{\partial r} + i\delta P_0 r$$

where P_0 is given by eq. (H.5)-(H.10). At $r=1$ the boundary condition is given by eq. (H.14) and the other boundary condition is eq. (H.15). Eq. (H.8) and (H.21) are solved numerically. They have the general form:

$$(H.22) \quad \frac{1}{r} \frac{d}{dr} \left[r \frac{dH}{dr} \right] - EH = F$$

where:

$$(H.23) \quad E = e_r + ie_i = \begin{cases} \frac{i\zeta}{P_0} \\ \frac{1}{r^2} + \frac{i\zeta}{P_0} \end{cases}$$

$$(H.24) \quad F = f_r + if_i = \begin{cases} i\delta P_0 \\ -\frac{3}{2} \frac{\partial P^2}{\partial r} + i\delta P_0 r \end{cases}$$

$$(H.25) \quad H = h_r + ih_i$$

The boundary conditions are:

$$H(\eta) = H\left(\frac{1}{\delta}\right) = 0$$

$$(H.26) \quad \left. \frac{dH}{dr} \right|_{r=1+0} - \left. \frac{dH}{dr} \right|_{r=1-0} = a + b H_i$$

where:

$$(H.27) \quad a = \frac{3}{2}(1+\beta)q_T$$

$$(H.28) \quad b = -(1+\beta)\frac{\Lambda_T m'_0}{2P_{0i}}$$

To get eq. (H.22) into finite difference form, integrate twice:

$$H = \int_1^r \left(\int_1^x y(EH+F) dy \right) dx + \ln r \cdot H'_i + H_i$$

where $H'_i = \frac{dH}{dr} \Big|_{r=1}$ and $H_i = H_{r=1}$. Set:

$$G = EH + F$$

and integrate the double integral by parts to get:

$$(H.29) \quad H = \int_1^r x \cdot \ln\left(\frac{r}{x}\right) G dx + \ln r \cdot H'_i + H_i$$

Set

$$(H.30) \quad H'_0 = \frac{dH}{dr} \Big|_{r=1+0}$$

$$(H.31) \quad H_0 = H_i = H_{r=1}$$

Then eq. (H.29) by use of eq. (H.26) becomes:

$$(H.32) \quad \underline{1 \leq r \leq m} \quad H = \int_1^r x \ln\left(\frac{r}{x}\right) \cdot G dx + \ln r \cdot H'_0 + H_0$$

$$(H.33) \quad \underline{\frac{1}{x} \leq r \leq 1} \quad H = \int_1^r x \ln\left(\frac{r}{x}\right) G dx - a \cdot \ln r + \ln r \cdot H'_0 + (1 - b \cdot \ln r) H_0$$

Subdivide the integration interval in m increments of length

$$(H.34) \quad \Delta r = \begin{cases} \frac{m-1}{m} & \underline{1 \leq r \leq m} \\ \frac{1-\frac{1}{m}}{m} & \underline{\frac{1}{m} \leq r \leq 1} \end{cases}$$

and integrate eq. (H.32)-(H.33) numerically by the trapezoidal rule to obtain their finite difference form:

$$(H.35) \quad \underline{1 \leq r \leq m} \quad H_{n+1} = H_n + \ln\left(\frac{1+(n+1)\Delta r}{1+n\Delta r}\right) \Delta r \left[\frac{1}{2} G_0 + (1+\Delta r) G_1 + \dots + (1+n\Delta r) G_n \right] + H'_0 \ln\left(\frac{1+(n+1)\Delta r}{1+n\Delta r}\right)$$

$$(H.36) \quad \underline{1 \geq r \geq \frac{1}{m}} \quad H_{n+1} = H_n + \ln\left(\frac{1-(n+1)\Delta r}{1-n\Delta r}\right) \Delta r \left[\frac{1}{2} G_0 + (1-\Delta r) G_1 + \dots + (1-n\Delta r) G_n \right] + (-a + H'_0 - b H_0) \cdot \ln\left(\frac{1-(n+1)\Delta r}{1-n\Delta r}\right)$$

To calculate eq. (H.35) on the computer set:

$$(H.37) \quad H_n = s_{rn} + i s_{in} + (t_{rn} + i t_{in}) H'_0 + (v_{rn} + i v_{in}) H_0$$

$$(H.38) \quad \Delta r [\frac{1}{2} G_0 + (1 + \Delta r) G_1 + \dots + (1 + n \Delta r) G_n] = p_{rn} + i p_{in} + (q_{rn} + i q_{in}) H'_0 + (w_{rn} + i w_{in}) H_0$$

$$(H.39) \quad G_n = E_n H_n + F_n = e_{rn} s_{rn} - e_{in} s_{in} + f_{rn} + i(e_{rn} s_{in} + e_{in} s_{rn} + f_{in}) + [e_{rn} t_{rn} - e_{in} t_{in} + i(e_{rn} t_{in} + e_{in} t_{rn})] H'_0 \\ + [e_{rn} v_{rn} - e_{in} v_{in} + i(e_{rn} v_{in} + e_{in} v_{rn})] H_0$$

Therefore:

$$(H.40) \quad P_{on} = \sqrt{1 + q_r \ln(\frac{\gamma}{1 + n \Delta r})}$$

$$(H.41) \quad e_{rn} = 0 \quad (\text{translatory}) \quad \left(\frac{1}{1 + n \Delta r} \right)^2 \quad (\text{rotational})$$

$$(H.42) \quad e_{in} = \frac{q}{P_{on}} \quad (\text{---"---}) \quad \frac{q}{P_{on}} \quad (\text{---"---})$$

$$(H.43) \quad f_{rn} = 0 \quad (\text{---"---}) \quad \frac{3}{2} \frac{q_r}{(1 + n \Delta r)} \quad (\text{---"---})$$

$$(H.44) \quad f_{in} = q P_{on} (1 + n \Delta r) \quad (\text{---"---})$$

$$(H.45) \quad p_{rn} = p_{r,n-1} + \Delta r (1 + n \Delta r) (e_{rn} s_{rn} - e_{in} s_{in} + f_{rn})$$

$$(H.46) \quad p_{in} = p_{i,n-1} + \Delta r (1 + n \Delta r) (e_{rn} s_{in} + e_{in} s_{rn} + f_{in})$$

$$(H.47) \quad q_{rn} = q_{r,n-1} + \Delta r (1 + n \Delta r) (e_{rn} t_{rn} - e_{in} t_{in})$$

$$(H.48) \quad q_{in} = q_{i,n-1} + \Delta r (1 + n \Delta r) (e_{rn} t_{in} + e_{in} t_{rn})$$

$$(H.49) \quad w_{rn} = w_{r,n-1} + \Delta r (1 + n \Delta r) (e_{rn} v_{rn} - e_{in} v_{in})$$

$$(H.50) \quad w_{in} = w_{i,n-1} + \Delta r (1 + n \Delta r) (e_{rn} v_{in} + e_{in} v_{rn})$$

$$(H.51) \quad s_{r,n+1} = s_{rn} + \ln\left(\frac{1 + (n+1) \Delta r}{1 + n \Delta r}\right) p_{rn}$$

$$(H.52) \quad S_{i,n+1} = S_{in} + \ln\left(\frac{1+(n+1)\Delta r}{1+n\Delta r}\right) p_{in}$$

$$(H.53) \quad t_{r,n+1} = t_{rn} + \ln\left(\frac{1+(n+1)\Delta r}{1+n\Delta r}\right) (1+q_{rn})$$

$$(H.54) \quad t_{i,n+1} = t_{in} + \ln\left(\frac{1+(n+1)\Delta r}{1+n\Delta r}\right) q_{in}$$

$$(H.55) \quad v_{r,n+1} = v_{rn} + \ln\left(\frac{1+(n+1)\Delta r}{1+n\Delta r}\right) w_{rn}$$

$$(H.56) \quad v_{i,n+1} = v_{in} + \ln\left(\frac{1+(n+1)\Delta r}{1+n\Delta r}\right) w_{in}$$

To initiate the calculations we have:

$$(H.57) \quad S_{ro} = S_{io} = t_{ro} = t_{io} = v_{ro} = v_{io} = 0$$

$$(H.58) \quad v_{ro} = 1$$

$$(H.59) \quad p_{ro} = \frac{1}{2} \Delta r f_{ro}$$

$$(H.60) \quad p_{io} = \frac{1}{2} \Delta r f_{io}$$

$$(H.61) \quad q_{ro} = q_{io} = 0$$

$$(H.62) \quad w_{ro} = \frac{1}{2} \Delta r e_{ro}$$

$$(H.63) \quad w_{io} = \frac{1}{2} \Delta r e_{io}$$

The calculations proceed as follows: 1) preset $S_{ro}, S_{io}, t_{ro}, \dots, w_{io}$ from eq. (H.57)-(H.63); 2) set $n=0$ and calculate eq. (H.51)-(H.56); 3) advance n by 1 and repeat the cycle eq. (H.40)-(H.56) till $n=m-1$. The test calculation results in:

$$(H.64) \quad H_\eta = H_m = S_{rm} + i s_{rm} + (t_{rm} + i t_{rm}) H'_0 + (v_{rm} + i v_{rm}) H_0 = 0$$

A similar calculation is performed for $\frac{1}{2} \leq r \leq 1$ from eq. (H.36). The previous eq. (H.37)-(H.56) are used by replacing n by $-n$ and $(n+1)$ by

$-(n+1)$ and making the following changes:

$$(H.40a) \quad P_{on} = \sqrt{1 + \beta q_r \ln(\gamma(1-n\Delta r))}$$

$$(H.43a) \quad f_r = 0 \quad (\text{translatory}) \quad -\frac{3}{2} \frac{\beta q_r}{1-n\Delta r} \quad (\text{rotational})$$

$$(H.51a) \quad s_{r,n+1} = s_{rn} + \ln\left(\frac{1-(n+1)\Delta r}{1-n\Delta r}\right) (P_{rn}-a)$$

$$(H.55a) \quad v_{r,n+1} = v_{rn} + \ln\left(\frac{1-(n+1)\Delta r}{1-n\Delta r}\right) (w_{rn}-b)$$

Proceeding as above we get:

$$(H.65) \quad H_\delta = H_m = s_{ry} + i s_{iy} + (t_{ry} + i t_{iy}) H'_o + (v_{ry} + i v_{iy}) H_o$$

Solve eq. (H.64) and (H.65) together:

$$(H.66) \quad H'_o = - \frac{(s_{ry} + i s_{iy})(v_{ry} + i v_{iy}) - (s_{ry} + i s_{iy})(v_{r\eta} + i v_{i\eta})}{(t_{ry} + i t_{iy})(v_{ry} + i v_{iy}) - (t_{ry} + i t_{iy})(v_{r\eta} + i v_{i\eta})} = h'_{ro} + i h'_{io}$$

$$(H.67) \quad H_o = - \frac{(t_{ry} + i t_{iy})(s_{ry} + i s_{iy}) - (t_{ry} + i t_{iy})(s_{r\eta} + i s_{i\eta})}{(t_{ry} + i t_{iy})(v_{ry} + i v_{iy}) - (t_{ry} + i t_{iy})(v_{r\eta} + i v_{i\eta})} = h_{ro} + i h_{io}$$

Having determined H'_o and H_o , we can calculate $H_n = h_{rn} + i h_{in}$ from eq. (H.37). The pressure is obtained from eq. (H.6) and (H.3) or eq. (H.20) and (H.17):

$$(H.68) \quad \text{translatory} \quad P_n = P_{on} + \frac{\epsilon}{P_{on}} (h_{rn} \cos \omega t - h_{in} \sin \omega t)$$

$$(H.69) \quad \text{rotational} \quad P_n = P_{on} + \left(\frac{R_c}{C}\right) \frac{\alpha}{P_{on}} (h_{rn} \cos \omega t - h_{in} \sin \omega t) \sin \theta$$

The dynamic load carrying capacity W_D and the restoring moment M_D are obtained by integration over the thrust bearing:

$$(H.70) \quad W_D = -P_a R_c^2 \int_0^{2\pi} \int_{\frac{\pi}{2}}^{\eta} r P dr d\theta$$

$$(H.71) \quad M_D = -P_a R_c^3 \int_0^{2\pi} \int_{\frac{\pi}{2}}^{\eta} r^2 P \sin \theta dr d\theta$$

If, in calculating W_D , the static load is disregarded we get:

$$(H.72) \quad \frac{W_D}{\pi R_i^3 P_a E} = -\frac{2}{\eta^2} \left[\cos \omega t \int_{\frac{1}{2}}^{\eta} r \frac{h_r}{P_0} dr - \sin \omega t \int_{\frac{1}{2}}^{\eta} r \frac{h_i}{P_0} dr \right] = W'_D \cos(\omega t - \phi_w)$$

$$(H.73) \quad \frac{M_D}{\pi R_i^3 P_a R_c (\frac{R_c}{C}) \alpha} = -\frac{1}{\eta^2} \left[\cos \omega t \int_{\frac{1}{2}}^{\eta} r^2 \frac{h_r}{P_0} dr - \sin \omega t \int_{\frac{1}{2}}^{\eta} r^2 \frac{h_i}{P_0} dr \right] = M'_D \cos(\omega t - \phi_M)$$

The integration is carried out numerically.

COMPUTER PROGRAM PN0020

Static Load and Flow for Journal and
Thrust Bearing with Line Source Feeding

C MECHANICAL TECHNOLOGY, INC. JORGEN W. LUND
C PNO020=HYDROSTATIC JOURNAL AND THRUST BEARING
DIMENSION FLAM(100), AREA(100), VLST(100), PSL(100), PAL(100), EPS(50),
1EPS3(50), PZ(21), P1(21), GAML(100), DGAL(100), QST(50), PRST(50),
2PR2ST(50), DUMMY(500)

200 READ 100
RFAD 101
WRITE OUTPUT TAPE 3,102
WRITE OUTPUT TAPE 3,103
WRITE OUTPUT TAPE 3,100
WRITE OUTPUT TAPE 3,101
READ 104, LMB, NV, NJT, MIL, MDIM, NDIAG, INP, NPRT
READ 107, PCFC
WRITE OUTPUT TAPE 3,105
WRITE OUTPUT TAPE 3,106, LMB, NV, NJT, MIL, MDIM, NDIAG, INP, NPRT
WRITE OUTPUT TAPE 3,136
WRITE OUTPUT TAPE 3,137, PCFC
IF(MDIM) 204, 201, 204

201 READ 107, (FLAM(I), I=1, LMB)
READ 107, (VLST(I), I=1, NV)
IF(NJT) 203, 202, 203

202 READ 107, FLD, FLID
GO TO 207

203 READ 107, RTA, GAM
IF(NJT) 207, 202, 245

245 READ 107, (EPS(I), I=1, NJT)
GO TO 207

204 READ 107, VISC, RT, HN, CLRZ
READ 107, (PSL(I), PAL(I), I=1, NV)
RFAD 107, (ARFA(I), I=1, LMB)
IF(NJT) 206, 205, 206

205 RFAD 107, RD, RL, BL1
GO TO 207

206 READ 107, R1, R2, RC
IF(NJT) 207, 205, 245

207 IF(MIL) 220, 209, 208

208 RFAD 107, CB, SA, CAC, CAD
GO TO 209

220 IF(MIL+1) 214, 247, 209

247 READ 139, ADC, LVC
IF(LVC) 254, 255, 254

254 READ 107, (GAML(I), I=2, 261)
GAMZ=1.0
DGAMZ=0.0
GAML(1)=1.0
WRITE OUTPUT TAPE 3,138
WRITE OUTPUT TAPE 3,112, (GAML(I), I=1, 251)
GO TO 256

255 READ 107, (GAML(I), DGAL(I), I=1, NV)
256 EX6=2.0/(ADC+1.0)
EX1=1.0/(ADC-1.0)
EX7=(EX6**EX1)*SQRTF(EX6*ADC)
EX4=2.0*EX1
EX1=ADC*EX1
CRP=EX6**EX1
EX3=SQRTF(2.0*EX1)
EX2=1.0/EX1
EX5=-EX2
EX6=1.0/EX6
EX1=1.0/ADC
DIT=(1.0-CRP)/50.0
CX=CRP
DO 258 I-1 50

```

CX=C/-DIT
C5=C*FX1
DST(I)=FX3*C5*SORTF(1.0-CX/C5)
PQ2ST(I)=CX*CX
258 PR5(I)=CX
C INITIAL CONDITIONS
209 IF(MDIM) 210,214,210
210 DO 211 I=1,NV
211 VEST(I)=PSL(I)/PAL(I)
IF(NJT) 213,212,213
212 BET1=2.0
FLD=BL/BD
FL1D=BL1/BD
GO TO 217
213 FTA=R1/RC
GAM=RC/R2
214 IF(NJT) 215,217,215
215 FLFTA=LOGF(FTA)
C1=LOGF,GAM!
BETA=FLFTA/C1
BET1=1.0+BETA
IF(NJT) 249,217,248
248 DO 216 I=1,NJT
C1=1.0+EPS(I)
216 EPS3(I)=C1**3
IF(MDIM) 218,300,218
217 C1=EXP(FLD)
C2=1.0/C1
SHKS=(C1-C2)/2.0
CHKS=(C1+C2)/2.0
IF(FL1D) 276,277,276
276 C1=-2.0*FL1D
C1=EXP(C1)
TAH=(1.0-C1)/(1.0+C1)
THFT=TAH/FL1D
GO TO 249
277 FAH=0.0
THFT=1.0
249 EPS3(I)=1.0
EPS=1.0.0
IF(MDIM) 218,300,218
218 C1=1.0*VISC
C1=FFT1/C1
C2=SORTF(386.069*RT)
CLAM=HN*C2/C1
CFLWZ=3.415927*C1/RT
C INITIATE LAMBDA AND V
300 DO 431 I=1,LMR
LMIL+1) 251,252,252
251 RL=FLAM(I)
FLM=RL
I=NL) 354,371,354
IF(FLM(M) 275,301,274
301 FLM=FLAM(I)
I=NL) 303
474 AR=ARFA(I)
AR=CLR2
AR=0.302
475 AR=CLR2
AR=ARFA(I)
302 RLMT=CLR**3
CFLWZ=FLMT*CFLWZ
FLMT=CLAM*AR/FLMT

```

```

303 DO 431 J=1,NV
  V=VLST(J)
  V2 = V*V
  VM1=V2-1.0
  IF(MDIM) 304,305,304
304 PA=PAL(J)
  PA2=PA*PA
  FLM=FLMT/PA
  FLFCT=CFLW*PA2
  CACP=CAC*PA
  CADP=CAD/PA
  GO TO 241
305 FLM=FLMT
241 IF(MIL+1) 306,242,306
242 IF(LVC) 306,257,306
257 GAMZ=GAML(J)
  DGAMZ=DGAL(J)
  IF(MDIM) 243,306,243
243 FLM=FLM*GAMZ
C   P2 CALCULATION
306 K=1
307 FLME=FLM/EPS3(K)
  FLFE=FLFCT*EPS3(K)
  IF(NJT) 309,308,309
308 P2LD=FLD
  GO TO 310
309 P2LD=FLETA
310 IF(MIL) 221,311,312
311 C1=FLME/2.0*P2LD
  C2=C1*C1
  C1=C1*FLME
  P2=C1*(-1.0+SQRTF(1.0+VM1/C2))
  C1=3.0*P2
  C2=FLMF/2.0*FLME/P2
  GO TO 325
312 C1=FLME*P2LD
  C2=VM1
  MTST=0
  C3=V-1.0
  C4=0.01*C3
  CX=C4
  IF(NPRT) 329,313,329
329 WRITE OUTPUT TAPE 3,108
313 C5=V-CX
  C5=C5+C5-1.0-C1*CX/(CX+SA)*(CX+CB)*(CACP*C5*C5+C5+CADP)
  IF(NPRT) 314,315,314
314 WRITE OUTPUT TAPE 3,109,CX,C5
315 IF(MTST) 316,316,319
316 C6=C5*C2
  IF(C6) 318,330,317
317 CX=CX+C4
  C7=C5
  IF(CX-C3) 313,313,440
318 MTST=1
  C7=C5
  CX=CX-0.5*C4
  GO TO 313
319 C1=C4*C4
  C1=2.0*(C2+C7-2.0*C5)/C1
  C3=(C7-C2)/C4
  IF(C1) 321,320,321
320 C6=-C5/C3
  GO TO 324

```

```

321 C4=0.5*C3/C1
    C6=SQRTF(C4*C4-C5/C1)
    IF(C4) 322,323,323
322 C6=-C6
323 C6=C6-C4
324 CX=CX+C6
330 C6=V-CX
    P2=(C6*C6-1.0)/P2LD
    C5=CX+SA
    C2=CX*(CX+CR)/C5
    C3=CACP*C6*C6+C6+CAPP
    C1=3.0*FLME*C2*C3
    C2=0.5*FLME/C6*((1.0+SA/C5*(CR-SA))/C5)*C3-C2*(2.0*CACP*C6+1.0))
    GO TO 325
?21 IF(MIL+1) 253,259,311
259 C1=FLME*P2LD*V
    CX=SQRTF(1.0+C1*EX7)/V
    IF(CRP-CX) 223,222,222
222 P2=FLME*V*EX7
    C1=3.0*P2
    C2=-0.5*FLME/V*EX7/CX*DGMZ/GAMZ
    GO TO 244
223 C2=V2*CRP*CRP-1.0-C1*EX7
    MTST=0
    L=2
    C4=2.0*DIT
    IF(NPRT) 224,260,224
224 WRITE OUTPUT TAPE 3,132
260 IF(LVC) 261,225,261
225 C5=V2*PR2ST(L)-1.0-C1*QST(L)
    CX=PRST(L)
    IF(NPRT) 226,227,226
226 WRITE OUTPUT TAPE 3,109,CX,C5
227 IF(MTST) 228,228,231
228 C6=C5*C2
    IF(C6) 230,237,229
229 L=L+2
    C2=C5
    IF(L=50) 225,225,441
230 MTST=1
    C7=C5
    L=L-1
    GO TO 225
?61 M=2
262 VC=GAML(M)
263 C5=V2*PR2ST(L)-1.0-C1*VC*QST(L)
    CX=PRST(L)
    IF(NPRT) 264,265,264
264 WRITE OUTPUT TAPE 3,109,CX,C5
265 IF(MTST) 266,266,231
266 C6=C5*C2
    IF(C6) 268,237,267
267 L=L+2
    M=M+1
    C2=C5
    IF(L=50) 262,262,441
268 MTST=1
    C7=C5
    L=L-1
    VCM=GAML(M-1)
    VCS=VC
    DVC=(VC-VCM)/C4
    VC=(VC+VCM)/2.0

```

```

      GO TO 263
231 C1=C4*C4
      C1=2.0(C2+C7-2.0*C5)/C1
      C3=(C7-C2)/C4
      IF(C1) 233,232,233
232 C6=-C5/C3
      GO TO 236
233 C4=0.5*C3/C1
      C6=SQRTF(C4*C4-C5/C1)
      IF(C4) 234,235,235
234 C6=-C6
235 C6=C6-C4
236 CX=CX+C6
237 P2=(V2*CX*CX-1.0)/P2LD
      EX2=CX**EX1
      C1=3.0*P2
      IF(LVC) 270,269,270
269 C4=P2/FLME/V
      C5=-DGAMZ/GAMZ
      C6=0.5
      GO TO 271
270 VC=VC+C6*DVC
      C4=VC*FLME*V
      C4=P2/C4
      C5=-DVC/VC
      C6=0.5*VC
271 C2=C6/V*FLME/CX*(C5*C4+EX4*EX2/C4*(EX6-EX2/CX))
244 IF(NPRT) 238,325,238
238 WRITE OUTPUT TAPE 3,109,CX,C1
      GO TO 325
253 C1=3.0*P2
      C2=SQRTF(1.0+P2*P2LD)
      C2=0.5*V/C2
325 IF(NJT) 350,326,340
C JOURNAL BEARING FORCE CALCULATION
326 SLP=C2
      C2=C2+TAH
      C5=FLD*(CHKS+C2*PCFC*SHKS)
      PFCT=C1/C5
      C5=FLD*(CHKS+C2*SHKS)
      P1FC=C1/C5
      IF(MIL+1) 372,371,371
372 FRC=PFCT*FINT1
      FRCM=FLD*PFCT*P1(1)*THET
      GO TO 400
C THRUST BEARING FORCE CALCULATION
340 C1=ETA*ETA
      C2=1.0/GAM/GAM/C1
      C3=1.0+P2*FLETA
      C4=SQRTF(C3)/C1
      C3=P2/C3
      C5=HETA*P2
      C8=(ETA-1.0)/20.0
      CX=1.0
      DO 341 L=1,21
      C7=LOGF(CX)
      C7=1.0-C3*C7
      PZ(L)=CX*SQRTF(C7)
341 CX=CX+C8
      C9=(GAM-1.0)/20.0
      CX=1.0
      DO 342 L=1,21
      C7=LOGF(CX)

```

```

C7=1.0+C5*C7
P1(L)=CX*SQRTF(C7)
342 CX=CX+C9
C6=PZ(1)-PZ(21)
C7=P1(1)-P1(21)
DO 343 L=2,20,2
C6=C6+4.0*PZ(L)+2.0*PZ(L+1)
343 C7=C7+4.0*P1(L)+2.0*P1(L+1)
FINT1=C6*C8/3.0
FINT2=C7*C9/3.0
FRC=(C4*FINT1+C2*FINT2)*2.0+C2-1.0
FRCM=P1(21)/GAM
GO TO 400
350 PFCT=1.0+C2*PCFC*FLFTA
PFCT=2.0*C1/PFCT
P1FC=1.0+C2*FLETA
P1FC=0.5*C1/P1FC
SLP=C2
IF(MIL+1) 355,354,354
355 FRC=PFCT*(FINT1+FINT2)
FRCM=P1FC*P2(1)*ETA
C OUTPUT
400 DPW=P2*LOGF(V)
IF(NJT) 402,401,402
401 WRITE OUTPUT TAPE 3,110,FLD,FL1D
GO TO 403
402 WRITE OUTPUT TAPE 3,111
WRITE OUTPUT TAPE 3,115
WRITE OUTPUT TAPE 3,112,EP(S(K)),ETA,GAM,FLETA,BETA
403 WRITE OUTPUT TAPE 3,114
WRITE OUTPUT TAPE 3,113,FLME,V,P2,FRC,FRCM,DPW
IF(MIL) 240,405,404
240 IF(MIL+1) 405,246,405
246 WRITE OUTPUT TAPE 3,133
IF(LVC) 272,273,272
272 WRITE OUTPUT TAPE 3,122,ADC,VC,DVC
GO TO 405
273 WRITE OUTPUT TAPE 3,122,ADC,GAMZ,DGAMZ
GO TO 405
404 WRITE OUTPUT TAPE 3,116
WRITE OUTPUT TAPE 3,117,SA,CB,CAC,CAD
405 IF(MDIM) 406,415,406
406 WRITE OUTPUT TAPE 3,118
WRITE OUTPUT TAPE 3,113,PSL(J),PA,VISC,RT,HN,AR
FLW-FLFE*P2
PW=RT*FLFE/6600.0*DPW
IF(NJT) 411,407,411
407 WRITE OUTPUT TAPE 3,120
WRITE OUTPUT TAPE 3,119,BD,BL,BL1,CLR
CX=0.78539816*BD*PA
C7=CX*BL1
CX=CX*BL
FRC=FRC*CX
FRCM=FRCM*C7
TFR=FRC+FRCM
STF=TFR/CLR
WRITE OUTPUT TAPE 3,121
WRITE OUTPUT TAPE 3,113,FLW,PW,FRC,FRCM,TFR,STF
CX=PA*FLD/2.0*P1FC
C6=PA*PZ(1)
C7=CX*P1(1)
SLP=-2.0*PZ(1)/FLME*SLP
CRT=PZ(1)/V

```

```

      WRITE OUTPUT TAPE 3,123
      WRITE OUTPUT TAPE 3,112,C6,C7,FINT1,SLP,CRT
      IF(NDIAG) 408,410,408
  408 WRITE OUTPUT TAPE 3,124
      C6=BL/40.0
      C7=0.0
      DO 409 L=1,21
      PZ(L)=PA*PZ(L)
      P1(L)=CX*P1(L)
      WRITE OUTPUT TAPE 3,125,C7,PZ(L),P1(L)
  409 C7=C7+C6
  410 GO TO 430
  411 CX=(1.0+EPS(K))*CLR
      WRITE OUTPUT TAPE 3,126
      WRITE OUTPUT TAPE 3,112,R1,R2,RC,CLR,CX
      CX=3.1415927*PA*R1*R1
      FRC=CX*FRC
      FRCM=PA*FRCM
      IF(NJT) 424,430,423
  423 WRITE OUTPUT TAPE 3,127
      WRITE OUTPUT TAPE 3,119,FLW,PW,FRC,FRCM
      IF(NDIAG) 412,414,412
  412 WRITE OUTPUT TAPE 3,129
      C1=C4*C1*PA*RC
      C4=PA*R2
  426 C2=(R1-RC)/20.0
      C3=RC
      C5=(RC-R2)/20.0
      C6=R2
      DO 413 L=1,21
      PZ(L)=PZ(L)*C1/C3
      P1(L)=P1(L)*C4/C6
      WRITE OUTPUT TAPE 3,128,C6,P1(L),C3,PZ(L)
      C3=C3+C2
  413 C6=C6+C5
  414 GO TO 430
  424 STF=FRC/CLR
      C3=PA*SQRTF(1.0+P2*FLETA)
      WRITE OUTPUT TAPE 3,134
      WRITE OUTPUT TAPE 3,113,FLW,PW,FRC,STF,C3,FRCM
      IF(NDIAG) 425,430,425
  425 WRITE OUTPUT TAPE 3,129
      C1=P1FC*PA
      C4=R2*BETA*C1
      C1=C1*R1
      GO TO 426
  415 IF(NJT) 427,416,420
  416 WRITE OUTPUT TAPE 3,123
      CX=FLD/2.0*P1FC
      C6=P1(1)*CX
      SLP=-2.0*PZ(1)/FLME*SLP
      CRT=PZ(1)/V
      WRITE OUTPUT TAPE 3,112,PZ(1),C6,FINT1,SLP,CRT
      IF(NDIAG) 417,419,417
  417 WRITE OUTPUT TAPE 3,124
      C5=FLD/20.0
      C6=0.0
      DO 418 L=1,21
      C1=P1(L)*CX
      WRITE OUTPUT TAPE 3,125,C6,PZ(L),C1
  418 C6=C6+C5
  419 GO TO 430
  420 IF(NDIAG) 421,430,421

```

```

421 WRITE OUTPUT TAPE 3,129
C1=C1*C4
C2=(FTA-1.0)/20.0
C3=1.0
C4=(GAM-1.0)/20.0
C5=1.0
DO 422 L=1,21
C6=C1*PZ(L)/C3
C7=P1(L)/C5
WRITE OUTPUT TAPE 3,128,C5,C7,C3,C6
C3=C3+C2
422 C5=C5+C4
GO TO 430
427 WRITE OUTPUT TAPE 3,135
C4=SQRTF(1.0+P2*FLFTA)
SLP=-2.0*C4/FLME*SLP
C5=C4/V
WRITE OUTPUT TAPE 3,113,C4,FRCM,FINT1,FINT2,SLP,C5
IF(NDIAG) 428,430,428
428 C1=P1FC*BFTA
C2=(FTA-1.0)/20.0
C3=1.0
C4=(GAM-1.0)/20.0
C5=1.0
WRITE OUTPUT TAPE 3,129
DO 429 L=1,21
C6=C3*PZ(L)*P1FC
C7=C1/C5*P1(L)
WRITE OUTPUT TAPE 3,128,C5,C7,C3,C6
C3=C3+C2
429 C5=C5+C4
C START A NEW LOOP
430 K=K+1
IF(K-NJT) 307,307,431
431 CONTINUE
IF(INP) 432,200,432
432 END FILE 3
STOP 77777
440 WRITE OUTPUT TAPE 3,130
GO TO 430
441 WRITE OUTPUT TAPE 3,131
GO TO 430
371 CX=FLD
C3=FLD/20.0
DO 327 L=1,21
C4=EXPFC(CX)
C6=0.5*(C4-1.0/C4)
C4=SQRTF(1.0+P2*CX)
PZ(L)=C4
CX=CX-C3
327 P1(L)=C6/C4
C7=P1(1)
DO 328 L=2,20,2
328 C7=C7+4.0*P1(L)+2.0*P1(L+1)
FINT1=C7*C3/3.0
IF(MIL+1) 303,372,372
354 C1=GAM*ETA
C1=BFTA/C1/C1
CX=1.0/ETA
C8=(1.0-CX)/20.0
C5=BETA*P2
DO 351 L=1,21
C7=-LOGF(CX)

```

$PZ(L) = CX * C7 / \text{SQRT}(1.0 + PZ * C7)$ -102-

 351: $CX = CX + C8$
 $C9 = (\text{GAM} - 1.0) / 20.0$
 $CX = 1.0$
 DO 352 L=1,21
 $C7 = \text{LOGF}(CX)$
 $P1(L) = CX * C7 / \text{SQRT}(1.0 + C5 * C7)$
 352: $CX = CX + C9$
 $C6 = P7(1) - PZ(21)$
 $C7 = P1(1) - P1(21)$
 DO 353 L=2,20,2
 $C6 = C6 + 4.0 * PZ(L) + 2.0 * PZ(L+1)$
 353: $C7 = C7 + 4.0 * P1(L) + 2.0 * P1(L+1)$
 $FINT1 = C6 * C8 / 3.0$
 $FINT2 = C1 * C7 / 3.0 * C9$
 IF(MIL+1) 303,355,355
 100 FORMAT(72H0
 1)
 101 FORMAT(72H
 1)
 102 FORMAT(84H1
 1 LOGY, INC. JORGEN W.LUND) MECHANICAL TECHNO
 103 FORMAT(84H
 1C JOURNAL AND THRUST BEARING)
 104 FORMAT(8I5)
 105 FORMAT(120H0 NO,LAMBDA NO,PRESS,RAT. JOURN/THRUST ORIF/MILL
 1IPOR DIMENSIONLESS PRESS.OUTPUT LAST INPUT ITERAT,PRINT)
 106 FORMAT(18,7!15)
 107 FORMAT(1P4E15.7)
 108 FORMAT(30H0 V-PO F(V-PO))
 109 FORMAT(1P2E16.7)
 110 FORMAT(56H0 JOURNAL BEARING,L/D=
 11PE15.7)
 111 FORMAT(66H0 THRUST BE
 1ARING)
 112 FORMAT(1P5E18.7)
 113 FORMAT(1P6E18.7)
 114 FORMAT(108H0 LAMBDA PRESS.RATIO DIM.FLOW
 1 DIM.FORCE DIM.ORIF.PRESS. DIM.POWER)
 115 FORMAT(90H0 FCC.RATIO OUT.R/ORIF.R ORIF.R/INNER R
 1 LOG(R1/RC) BETA)
 116 FORMAT(36H0 MILLIPORE FLOW COEFFICIENTS)
 117 FORMAT(13H COEFF.A=1PF14.7,12H COEFF.B=1PE14.7,12H COFFF
 1.C=1PE14.7,12H COEFF.D=1PE14.7)
 118 FORMAT(108H0 SUPPLY PRESS. AMB.PRESSURE VISCOSITY
 1 GAS CONST*TEMP. NO.FFFD.HOLES FFFDER AREA)
 119 FORMAT(1P4F18.7)
 120 FORMAT(72H0 BRG.DIAMETER BRG.LENGTH FFFD.PL.DIST.
 1 RAD.CLEAR.)
 121 FORMAT(108H0 FLOW POWER END FORCE
 1 CENTER FORCE TOTAL FORCE STIFFNESS)
 122 FORMAT(1P3F18.7)
 123 FORMAT(90H0 P0 AT ORIFICE P1 AT ORIFICE INTEGRAL
 1 SLOPE ORIF.PR.RATIO)
 124 FORMAT(48H0 DISTANCE P0 P1)
 125 FORMAT(F12.6,1P2E17.7)
 126 FORMAT(90H0 OUTER RADIUS INNER RADIUS ORIF.RADIUS
 1 CLEARANCE FILM THICKN.)
 127 FORMAT(72H0 FLOW POWER FORCE
 1 ORIF.PRESSURE)
 128 FORMAT(F12.6,1PE15.7,0PF12.6,1PF15.7)
 129 FORMAT(54H0 RADIUS PRESSURE RADIUS PRESSURE)
 130 FORMAT(42H0 NO ROOT FOUND IN MILLIPORE CALCULATION)

131 FORMAT(36HONO ROOT FOUND IN ORIFICE ITERATION) -103-
132 FORMAT(30H0 PO/V F(PO/V))
133 FORMAT(54H0 ADIAB.FXP. ARFA COFF. DFRIV.ARFA CF.)
134 FORMAT(108H0 FLOW POWFR FORCE
1 STIFFNESS PO AT ORIFICE PI AT ORIFICE)
135 FORMAT(108H0 PO AT ORIFICE PI AT ORIFICE OUT.INTEGRAL
1 INN.INTEGRAL SLOPF ORIF.PR.RATIO)
136 FORMAT(18H0 PR.CORR.FACT.)
137 FORMAT(1PE18.7)
138 FORMAT(32H0 VENA CONTRACTA COEFFICIENTS)
139 FORMAT(1PE15.7,I5)
END(0,1,0,1,1)

COMPUTER PROGRAM PN0031

Static Load for Thrust Bearing with Point Source Feeding

```

C      CALCULATION OF PRESSURE DISTRIBUTION FOR GAS LUBRICATED GIMBAL
C      BEARING RD 3 ROR BURGESS FOR STAN MALANOSKI
C      DIMENSION P(10,10),PSQ(10,10),A(10,10),THETA(10),RHO(10)
10 FORMAT(3F6.3,2I2)
20 FORMAT (8H1 C(1)=F6.3,8H R(1)=F6.3,8H R(2)=F6.3,
1      5H N=I2,8H R(I)=F6.3,8H WRAR=F9.5,8H C(2)=F6.3,
2      8H C(3)=F7.4)
30 FORMAT (3FH0 RHO(L) THETA(K) P(K,L))
40 FORMAT(F10.5,F16.5,F14.5/(9H F16.5,F14.5))
50 FORMAT (3I2,F5.2)
55 FORMAT (56H1PRESSURE DISTRIBUTION FOR GAS LUBRICATED GIMBAL BEAR!
1NG1
60 FORMAT (45H0      MECHANICAL TECHNOLOGY INC.,LATHAM,N.Y.)
61 WRITE OUTPUT TAPE 3,55
62 WRITE OUTPUT TAPE 3,60
-105-
80 READ 10,CONF,RONF,RTWO,N,I
81 IF (6-I) 160,300,85
85 AN=N
DTHETA = 3.14159265/(10.0*AN)
RI=SQRTF(RONF*RTWO)
DRHO1= .22222222*(RI-RTWO)/RI
DRHO2= .18181818*(RONE-RI)/RI
THETA(1)= DTHETA/2.0
DO 100 K=2,10
100 THETA(K)= THETA(K-1)+ DTHETA
RHO(1)= RTWO/RI + .5*DRHO1
DO 110 L=2,5
110 RHO(L)= RHO(L-1)+ DRHO1
RHO(6)= 1.0 + DRHO2
DO 120 L=7,10
120 RHO(L) = RHO(L-1) + DRHO2
Z=AN * LOGF(RONE/RTWO)
COSHZ =COSH(Z)
COSHZZ = COSH(.5*Z)
E = COSHZZ -1.0
G = (COSHZ - COSHZZ)**2
H= G/E
DO 130 L=1,10
X= AN * LOGF(RHO(L))
COSHX = COSH(X)
COSH2X = COSH(2.0*X)
DO 130 K=1,10
Y= AN * THETA(K)
COSY = COSF(Y)
COS2Y = COSF(2.0*Y)
D = COSHX - COSY
F = COSHZ**2 -2.0*COSHZ * COSHX * COSY + .5 *(COSH2X + COS2Y)
130 A(K,L) = LOGF(H * (D/F))
DO 140 L= 1,10
DO 140 K= 1,10
PSQ(K,L) = 1.0 - .5 * CONF * A(K,L)
140 P(K,L) = SQRTF(PSQ(K,L))
J=1
GO TO 541
C      DO RECESS CALCULATION IF I=2, QUIT IF I=1
150 GO TO (80,155),I
155 READ 50,LONE,LTWO,KONE,CTWO
IF (LTWO-LONE) 160,160,165
160 STOP
165 AM=LTWO-LONE-1+2*KONE
PAVG1=0.0
KMAX=KONE-1
DO 170 K=1,KMAX

```

```

170 PAVG1=PAVG1+PSQ(K,LONE)+PSQ(K,LTWO) -106-
    DO 180 L=LONE,LTWO
180 PAVG1=PAVG1+PSQ(KONE,L)
    PAVG1=PAVG1/AM
    DO 190 K=1,KMAX
        PSQ(K,LONE)=1.0-.5*CTWO*A(K,LONE)
190 PSQ(K,LTWO)=1.0-.5*CTWO*A(K,LTWO)
    DO 200 L=LONE,LTWO
200 PSQ(KONE,L)=1.0-.5*CTWO*A(KONE,L)
    PAVG2=0.0
    DO 210 K=1,KMAX
210 PAVG2=PAVG2+PSQ(K,LC,F)+PSQ(K,LTWO)
    DO 220 L=LONE,LTWO
220 PAVG2=PAVG2+PSQ(KONE,L)
    PAVG2=PAVG2/AM
    CTHREF=PAVG1-PAVG2
    DO 230 L=LONE,LTWO
    DO 230 K=1,KONE
        PSQ(K,L)=1.0-.5*CTWO*A(K,L)+CTHREF
230 P(K,L)=SQRTF(PSQ(K,L))
    J=2
    GO TO 541
300 STOP
541 WBAR=0.0
    DO 550 L=1,5
        T=0.0
        DO 545 K=1,10
545 T=T+P(K,L)
550 WBAR=WBAR+RHO(L)*(T-10.0)
    WBAR=WBAR*DRHO1
    TT=0.0
    DO 570 L=6,10
        T=0.0
        DO 560 K=1,10
560 T=T+P(K,L)
570 TT=TT+RHO(L)*(T-10.0)
    WBAR=(WBAR+TT*DRHO2)/5.0
    WRITE OUTPUT TAPE 3,20,CONE,RONE,RTWO,N,RI,WBAR,CTWO,CTHREE
    WRITF OUTPUT TAPE 3,30
    DO 580 L=1,10
580 WRITE OUTPUT TAPE 3,40,RHO(L),(THFTA(K),P(K,L),K=1,10)
    GO TO (150,80),J
    END (0,1,0,1,1)
    FUNCTION COSH(X)
    EX=EXP(X)
    COSH=.5*(EX+1.0/EX)
    RETURN
    END (0,1,0,1,1)

```

COMPUTER PROGRAM PN0040

Static Load for Journal Bearing with Point Source Feeding

ANALYSIS OF NASA AIR BEARING (MAIN PROG) PNO040
 PROGRAMMED FOR R. WERNICK BY R. GEGUZYS MTI STS-58RF 7-25-62
 DIMENSION ALFA(511,11,ND(10)),AMDAL(100),V(100),F(51),X(51),T(12),
 ND(51,61),DUMMY(100),C1(200),PAM(61),ZN(3),YM(4),XT(5),CH(3),SH
 13,(CHP(3),SHP(3),CHM(3),SHM(3),CHN(3),SHN(3),RVFC(50)
),XCOS1(200),COS1(50,50),COS2(50,50),EPASE(50),AMAT(50,50),CCOS1
 45,CS1(61,3),CSIN(50),SINT(61,3),TFMP(51,61)
 COMMON PA,C,A,ZTA,AK,RT12,N,NA,NLD,NAA,NV,ALFA,ALOD,AMDAL,V,F,X,M
 ,MDAG,MORCS,RS,XS,YS,COSA1,COSA2,CS,SD,T,SINHK,SINHDK,COSHK,COSHDK,
 22,NTH,PO2,AAB,B,CR,D,ICOUNT,F,FM,ALODI,WK,TAR,ZTAM,ALFP,ALFSP,DFL
 3,CD,DFLT,H,C1,DIN,NDIN,CN,SN,S1,IS1,ZH,ZL,RVFC,ANAT,COS1,C
 4S2,RASE,XCOS,TAP,ZTAM,CCOS,COST,CSIN,SINT,TFMP
 500 READ 150,PA,C,A,ZTA,AK,RT12,DIN
 READ AND PRINT INPUT
 WRITE OUTPUT TAPE 3,151
 WRITE OUTPUT TAPE 3,152,PA,C,A,ZTA,AK,RT12,DIN
 READ 153,N,NA,NLD,NAA,NV,MDAG,MORCS,N7,NTH,NDIN,ND
 READ 150,(ALFA(I),I=1,NA)
 WRITE OUTPUT TAPE 3,154,N,NA,NLD,NAA,NV,N7,NTH
 WRITE OUTPUT TAPE 3,155,(ALFA(I),I=1,NA)
 READ 150,(ALOD(I),I=1,NLD)
 READ 150,(AMDAL(I),I=1,NAA)
 WRITE OUTPUT TAPE 3,156,(ALOD(I),I=1,NLD)
 WRITE OUTPUT TAPE 3,157,(AMDAL(I),I=1,NAA)
 READ 150,(V(I),I=1,NV)
 WRITE OUTPUT TAPE 3,158,(V(I),I=1,NV)
 WRITE OUTPUT TAPE 3,166,MDAG,MORCS,NDIN,ND
 WRITE OUTPUT TAPE 3,159
 C INITIAL CALCULATIONS -- PO/V AND F TABLE
 FX1 = AK/(AK+1.0)
 FX2 = 1.0/FX1
 FX3 = 1.0/AK
 FX4 = SQRTF((AK+AK)/(AK+1.0))
 ZTAP = ZTA+A
 ZTAM = ZTA-A
 FM = N
 ZTAN = ZTA*FM
 FNA = NA
 POVCR = (2.0/(AK+1.0))**FX1
 DFLX = (1.0-POVCR)/(FNA-1.0)
 NAM = NA-1
 F1 = ((2.0/(AK+1.0))**((1.0/(AK-1.0)))*SQRTF((AK+AK)/(AK+1.0))
 X(1) = POVCR
 DO1 I=2,NAM
 X(I)=X(I-1)+DFLX
 VAR = SQRTF(1.0-X(I)**FX2)
 F1 = ALFA(I)*VAR*(X(I)**FX3)*FX4
 X(NA) = 1.0
 F(NA) = 0.0
 FN2 = NM
 FNTH = NTH
 DFL = 6.2831853/(FNTH-1.0)
 C HERE WE SET UP THE COSINE MATRICES WHICH WILL BE USED IN THE
 C CALCULATION OF THE C1 VECTOR AND P1 MATRIX
 TAR = 0.0
 ICOUNT = 2
 F = 3.1415927/EN
 AAB = SIN(F)
 CR=AAB
 RE = COS(F)
 DEG
 NAM=4*N
 C1(1)=CB

```

XCOS(1)=D
DO 7 I=2,NAM
CALL SINCOS
C(I)=CR
7 XCOS(I)=D
DO 120 I=1,N
DO 120 J=1,N
K1=(I+J-1)*2
K2=XARSF((I-J)*2)
1F(K2)122,121,122
121 COS2(I,J)=1.
GO TO 120
122 COS2(I,J)=XCOS(K2)
120 COS1(I,J)=XCOS(K1)
C          THE ARRAYS COS1, AND COS2, CONTAIN
C          COS(2(I+J-1)PI/N)      AND
C          COS(2(I-J)PI/N)  RESPECTIVELY
C
DO 603 I= 1,N
K2=2*I-1
CSIN(I)= C(I,K2)
603 CCOS(I) = XCOS(K2)
C          THE ARRAYS CCOS, CSIN, CONTAIN COS, SIN OF (2I-1)*PI/( N).
ICOUNT = 1
TAR = 0.0
F= DFLTH
AAR = SINF(F)
B= COSF(E)
CB = 0.0
D= 1.0
COST(1,2)= D
COST(1,3)= D
SINT(1,2)=0.0
SINT(1,3)=0.0
DO 601 I=2,NTH
CALL SINCOS
COST(I,2)= D
601 SINT(I,2)= CB
TAR = 0.0
F= FN*DFLTH
AAR= SINF(E)
B= COSF(E)
CB= 0.0
D= 1.0
ICOUNT = 1
DO 604 I=2,NTH
CALL SINCOS
COST(I,3)=D
604 SINT(I,3)= CR
C          THE ARRAYS SINT(I,J), COST(I,J) CONTAIN SIN , COS RSPCTVLY OF
C          0.5*THETA(I) FOR J= 1
C          THETA(I)    FOR J=2
C          N*THETA(I)  FOR J=3 .
C
IF (MDIAG) 102,101,102
102 WRITE OUTPUT TAPE 4, 151
      WRITE OUTPUT TAPE 4,161
      WRITE OUTPUT TAPE 4,162,EX1,EX2,FX3,ZTAN,POVCR,DELX,DELTH,FX4,ZTAF
      1,7TAM
      WRITE OUTPUT TAPE 4,163,(X(I),F(I),I=1,NA)
      WRITE OUTPUT TAPE 4,162,(BCOS(I) ,I=1,N)
C          THE L/D LOOP BEGINS HERE -- SO IS CALCULATED IN SUBROUTINE SOR
101 DO' 2 I=1,NLD
      RS = FN*ALOD(I)
      YS = FN*ZIA

```

XS = FN*(ZTA-A)
 CS = 1.0
 COSA1=CS
 COSA2=COSA1
 ALODI=ALOD(I)
 DELZ = ALODI / (FN2-1.0)
 CALL SOR
 VAR = SO
 XS =YS
 YS = FN*(ZTA +A)
 CALL SOR
 SO =(SO +VAR)*0.5
 TESO=SO
 C SO IS GIVEN BY THE AVERAGE OF SOI AND SOII
 C THE LAMBDA(T)/ALPHA LOOP BEGINS HERE ENDS WITH STATEMENT 3
 DO 3 J=1,NAA
 A1= 4.0*AMDAL(J)/FN
 CRM0 = A1 * F(1)
 C THE V LOOP BEGINS HERE
 DO 4 K=1,NV
 XSTR=SQRTE((TESO*CRM0+1.0/V(K))/V(K))
 IF(XSTR-POVCR) 5,5,6
 C IF XSTAR LARGER THAN PO/V CRIT GO TO 6 IF NOT GO TO 5
 5 PO = V(K)*XSTR
 ALFP =0.0
 ALFSR=1.0
 GO TO 75
 C LOOP6 USED TO FIND ROOT XSTR BETWEEN X(I) AND X(I-1)
 6 VSO = V(K)/TESO
 RV2 = 1.0/V(K)**2
 Y1 = CRM0 -VSO*(X(I)**2-RV2)
 DO 8 L=2,NA
 L=L
 Y3 = A1*F(L)-VSO*(X(L)**2-RV2)
 C IF Y3=0 PO = V*X(L), IF PLUS CONTINUE, IF MINUS PUT QUADRATIC
 C THRU Y1,Y2,Y3
 IF (Y3) 9,10,11
 11 Y1=Y3
 GO TO 8
 10 PO =V(K)*X(L)
 ALFSR=ALFA(L)
 IF (L-NA) 76,77,77
 77 ALFP =(ALFA(L)-ALFA(L-1))/DFLX
 GO TO 75
 76 ALFP=0.5*(ALFA(L+1)-ALFA(L-1))/DFLX
 GO TO 75
 9 VAR = (X(L)+X(L-1))**2/2.0-RV2
 Y2 = A1*(F(I)+F(L-1))/2.0 - VSO*VAR
 AA=X(L-1)*Y3
 BB=X(L)*Y1
 CC=0.25*(X(L-1)*Y1+X(L)*Y3)
 AAA=0.5*(Y1+Y3)-Y2
 BBB=Y2*(X(L-1)+X(L))-CC-0.75*(AA+BB)
 CCC =(AA+BB)*(X(L-1)+X(L))/4.0-Y2*X(L) *X(L-1)
 VAR = BBB **2 -4.0*AAA+CCC
 IF(VAR) 12,13,13
 12 WRITE OUTPUT TAPE 3,160
 GO TO 99
 14 ROOT1=(-BBB +SQRTE(VAR))/2.0/AAA
 ROOT2=(-BBB -SQRTE(VAR))/2.0/AAA
 IF(ROOT1-X(L-1)) 14,14,15
 15 IF(ROOT1-X(L)) 15,14,14
 14 IF(ROOT12-X(L-1)) 17,17,18

```

17 WRITE OUTPUT TAPE 3,160
GO TO 99
18 IF( ROOT2-X(L))19,17,17
19 XSTR =ROOT1
GO TO 20
19 XSTR =ROOT2
GO TO 20
C CONTINUE
GO TO 100
20 PO= V(K)*XSTR
ALFP =(ALFA(L)-ALFA(L-1))/DFLX
ALFSR =(XSTR-X(L))/DFLX*(ALFA(L)-ALFA(L-1))+ ALFA(L)
GO TO 75
C THESE CALCULATIONS ARE MADE ON THE ASSUMPTION THAT THERE IS ONLY
C ONE ROOT BETWEEN X(L-1) AND X(L). THE FUNCTION IS ALSO ASSUMED TO
C BE QUADRATIC. LINEAR INTERPOLATION IS USED TO DETERMINE ALPHA STAR
C IF PROGRAM GOES TO N99 IT WILL INCLUE AN ERROR STOP. THIS MEANS A
C COMPLEX ROOT HAS BEEN FOUND OR THE REAL ROOTS ARE NOT IN THE
C PROPER RANGE. N100 WILL BE REACHED ON AN INPUT ERROR
99 STOP 77772
100 STOP 77773
75 CO = (PC**2-1.0)*3.1415927/TE50
IF (MDIAG) 103,104,103
103 WRITE OUTPUT TAPE 4,162,RS,XS,YS,CS,COSA1,COSA2,S0,A1,CRMO,XSTR,PO
    1,V50,RV2,Y1,Y2,Y3,VAR,ALFP,ALFSR,AA,BB,CC,AAA,BBB,CCC,ROOT1,ROOT2
104 WRITE OUTPUT TAPE 3,165, ALODI,AMDAL(J),V(K)
    WRITE OUTPUT TAPE 3,164,CO,ALFSR,ALFP,XSTR
C COMPUTATION OF PO AT EACH MESH POINT
PO=FN*ALODI
CS= 1.0
K1=(NTH+1)/2
DO 78 M=1,K1
K2= NTH+1
COSA1=-CO 1(M,3)
82 COSA1=COSA1
Z=0.0
YS =ZTAN
DO 78 L=1,NZ
IF (L-NZ) 80,81,81
81 PO2(L,M)=1.0
PO2(L,K2)= 1.0
GO TO 78
80 ZN = FN* Z
IF (ZN -ZTAN) 84,84,85
84 XS =ZN
GO TO 86
85 IF(Z-ZTAP) 126,127,127
126 YS=ZTAN
XS=FN*ZTAN
CALL SOR
PO2(L,M)=S0
YS= FN/ZTAP
XS =ZTAN
CALL SOR
S0= 0.5*(S0+PO2(L,M))
GO TO 128
127 YS =ZN
XS =ZTAN
86 CALL SOR
128 PO2(L,M) = SQRTF(1.0 + (-3.1415927*S0)
    PO2(L,K2) PO2(L,M)
    (END) 105 178,105

```

```

178 Z = ? +DFLZ          -112-
78 CONTINUE
    NGO=1
    IF(NP) 106,107,106
106 WRITE OUTPUT TAPE 3,167
    WRITE OUTPUT TAPE 3,177,DELTH,ALODI,DELZ
137 NAM=NTH-10
    LL=-9
    L=0
    GO TO 1088
108 WRITE OUTPUT TAPE 3, 178
108P IF(NAM) 109,110,110
109 L=NTH
    LL=10+LL
    M11=2
    GO TO 111
110 L=10+L
    LL=10+LL
    NAM=NAM-10
    M11=1
    GO TO 111
111 DO 112 M=1,NZ
112 WRITE OUTPUT TAPE 3,168,(PO2(M,JJ),JJ=LL,L)
    GO TO( 108,107),M11
107 GO TO (134,135 ) ,NGO
134 VAR=1.0-XSTR**EX2
    XSTRR= XSTR**EX1
    PHI= ALFP/ALFSR+EX3/XSTR-((0.5/XSTRR)*(AK-1.)/VAR)*EX3
    CAPK=((6.2831853/PHI)*PO/C0)*V(K)
C HERE WE BEGIN THE CALCULATION OF THE C1 VECTOR BY SETTING UP
C WHAT SHALL BE CALLED THE B VECTOR AND THE A MATRIX
    RS= ALODI
    CS= 1.
    IS1=1
    ZH= ZTA
    ZL=ZTAM
    CALL S1
    VAR= S1
    ZH= ZTAP
    ZL= ZTA
    CALL S1
    S1=(S1+VAR)/2.0
    TEM = C0*FN*S1*1.5
    YS=ZTA
    XS=ZTAM
    DO 123 L=1,N
    BVFC(L)= CCOS(L)*TEM
    DO 123 M=L,N
    COSA1=COS1(L,M)
    COSA2=COS2(L,M)
    CALL SOR
123 AMAT(L,M)= S0+0.5*(RS-YS)
    XS=YS
    YS= ZTAP
    IF (MDIAG) 132,133,132
132 WRITE OUTPUT TAPE 4,171, (BVEC(L),L=1,N)
    WRITE OUTPUT TAPE 4,172,((AMAT(L,M), L=1,N),M=1,N)
    WRITE OUTPUT TAPE 4,162, VAR,XSTRR,PHI,CAPK,ZH,ZL,S1,TEM ,XS,YS
133 DO 124 L=1,N
    DO 124 M=L,N
    COSA1= COS1(L,M)
    COSA2= COS2(L,M)
    CALL SOR

```

-113-

```

124 AMAT(L,M)=(AMAT(L,M)+SO+0.5*(RS-Y5))*0.5
125 AMAT(M,L)= AMAT(L,M)
DO 125 L=1,N
125 AMAT(L,L)= AMAT(L,L)- CAPK
C   SURROUTINF XSIMEQ IS USED TO SOLVE AX=B WHERE X IS THE C1 VECTOR
SCALF = 1.
IFRR= XSIMEOF(50,N,],AMAT,RVFC,SCALF,ERASE)
IF (IERR-2)129,130,131
C   IFRR IS AN ASSIGNED FIXED POINT VARIABLE
C       1 IF SOLUTION SUCESSFUL -- CONTINUE
C       2 IF UNDERFLOW OR OVERFLOW -- PRINT ERROR PROCEED
C       3 IF AMAT IS SINGULAR -- PRINT ERROP PROCEED
130 WRITE OUTPUT TAPE 3,169
GO TO 4
131 WRITE OUTPUT TAPE 3,170
GO TO 4
129 WRITE OUTPUT TAPE 3, 173, (AMAT(L,1),L=1,N)
DO 140 L=1,N
140 C1(L)=AMAT(L,1)
CALL SURP1
IF(NP) 138,135,138
138 WRITE OUTPUT TAPE 3,174
WRITE OUTPUT TAPE 3,177,DELTH,ALODI,DELZ
NGO =2
GO TO 137
135 CALL LCALC
WK=WK+WK
WRITE OUTPUT TAPE 3,175,WK
IF (NDIN) 136,4,136
136 DWK= WK*PA*ALODI*DIN*DIN
WRITE OUTPUT TAPE 3,176, DWK
4 CONTINUE
3 CONTINUE
2 CONTINUE
IF (MORCS) 500,501,500
501 STOP
C   FORMAT STATEMENTS
150 FORMAT (6E12.5)
151 FORMAT( 30H1 ANALYSIS OF NASA AIR BEARING/ 39H R.WERNICK MTI LAT
1HAM,NY ST 5-5886 )
152 FORMAT( 7HO INPUT/117H      P(A)          C          A
1           ZETA          K          SQRT(RT)        DIA
2 METER / 1P7F17.7 )
154 FORMAT( 87HO N    NO OF ALPHAS    NO OF L/D    NO OF LAMBDA(T)
1 NO OF V  NO OF Z  NO OF THETA / 1I5,1I10,3I15,2I10)
155 FORMAT(23HO TABLE OF ALPHA VALUES/(1P7F17.7))
156 FORMAT(21HO TABLE OF L/D VALUES/(1P7E17.7))
157 FORMAT(33HO TABLE OF LAMBDA(T) VALUES    /(1P7E17.7))
158 FORMAT(19HO TABLE OF V VALUES/(1P7E17.7))
159 FORMAT( 8HO OUTPUT)
160 FORMAT(29HO OOPS SOMETHING IS WRONG )
161 FORMAT(22HO DIAGNOSTIC PRINTOUT )
162 FORMAT(1P7E17.7)
163 FORMAT(24HO X(I)          F(I) /(1P2F15.7))
164 FORMAT(90HO CO          ALFA STAR          ALFA STR PRIM
1PO/V          /1D4F17.7)
165 FORMAT(44HO L/D(I)          LAMBDA(T)          V(I) / 1P3F17.7)
153 FORMAT(11I5)
166 FORMAT( 29HO (1) MEANS YES, (0) MEANS NO/59H PRINT DIAG MORE
1CASES DIMENS. LOAD PRESS. PRINTOUT / 1I7,3I15)
167 FORMAT (61HO DIMENSIONLESS ZEROTH ORDER PRESSURE PROFILE PO(Z,THE
1ETA). )
168 FORMAT (1P10E12.4)

```

169 FORMAT(38H0 UNDERFLOW OR OVERFLOW IN XSIMFO) -114-
170 FORMAT(24H0 A MATRIX IS SINGULAR)
171 FORMAT(13H0 R VECTO R /(1P7F17.7))
172 FORMAT(13H0 A MATRIX /(1P7F17.7))
173 FORMAT(13H0 C1 VECTO R /(1P7F17.7))
174 FORMAT(61H0 DIMENSIONLESS FIRST ORDER PRESSURE PROFILE PI(7,1H
1ETA).)
175 FORMAT(36H0 FULL BEARING DIMENSIONLESS LOAD /1P1F17.7)
176 FORMAT(31H0 FULL BEARING LOAD IN POUNDS /1P1F17.7)
177 FORMAT(104H EACH COLUMN BELOW GIVES PRESSURE FOR A GIVEN VALUE OF
1THETA(THETA GOES FROM 0 TO 2*PI IN INCREMNTS OF 1P1E14.5, 2H)./
234H IN EACH COLUMN, Z GOES FROM 0 TO 1P1E14.5, 21H , IN INCREMENT
3S OF 1P1E14.5, 3H .)
178 FORMAT(31H0CONTINUATION OF PRESSURE FIFLD)
END(0,1,0,1,1)

SUBROUTINE SOR

-115-

DIMENSION ALFA(51),ALOD(10),AMDAL(100),V(100),F(51),X(51),T(12),P
102(51,61),DUMMY(100),C1(200),DAM(61),ZN(3),XN(4),X7(5),CH(3),SH(13),
CHP(3),SHP(3),CHM(3),SHM(3),CHN(3),SHN(3),RVFC(50)
2, XCOS(200),COS1(50,50),COS2(50,50),FRASE(50),AMAT(50,50),CCOS(5
30),COST(61,3),CSIN(50),SINT(61,3),TEMP(51,61)
COMMON PA,C,A,ZTA,AK,RT12,N,NA,NLD,NAA,NV,ALFA,ALOD,AMDAL,V,F,X,MD
1IAG,MORCS,RS,XS,YS,COSA1,COSA2,CS,SO,T,SINHK,SINHDK,COSHK,COSHDK,N
2Z,NTH,P02,AAB,B,CR,D,ICOUNT,E,FN,ALODI,WK,TAR,ZTAN,ALFP,ALFSR,DFL7
3,CO,DEFLTH,CI,DIN,NDIN,CN,SN,S1,IS1,ZH,ZL,RVEC,AMAT,COS1,CO
4S2,ERASE,XCOS,ZTAP,ZTAM,CCOS,COST,CSIN,SINT,TEMP

DELTA = YS-XS

SIGMA = XS+YS

TR = 2.0*RS

IF(TR) 14,15,15

15 IF(SIGMA) 14,16,16

16 IF(DELTA) 14,17,17

17 IF(TR-SIGMA)14,18,18

18 IF(SIGMA-DELTA)14,19,19

C IF PROGRAM GOES TO N14 AN ERROR HAS OCCURRED. EITHER 2R SIGMA OR
C DELTA ARE MINUS

14 STOP 77771

19 EX2R = EXPF(-TR)

EXSG = EXPF(-SIGMA)

EXDT = EXPF(-DELTA)

EX2RS = EX2R/EXSG

EX2RD = FX2R/FXDT

SINHK = 0.0

COSHK = 1.0

TRMSG = TR-SIGMA

TRMDT=TR-DELTA

COHRS = 0.5*(EX2RS+ 1.0/EX2RS)

SIHRS = 0.5*(-EX2RS+ 1.0/FX2RS)

COHRD = 0.5*(EX2RD+ 1.0/EX2RD)

SIHRD = 0.5*(-EX2RD+ 1.0/FX2RD)

COHSG = 0.5*(FYSG + 1.0/FXSG)

SIHSG = 0.5*(-EXSG + 1.0/FXSG)

COHDT = 0.5*(EXDT + 1.0/FXDT)

SIHDT = 0.5*(-EXDT + 1.0/FXDT)

COSHDK = 0.5*(EX2R + 1.0/FX2R)

SINHDK = 0.5*(-EX2R+ 1.0/FX2R)

C IF THE ARGUMENT (EXCLUDING THOSE CONTAINING THE INCRFMNT K) OF
C ANY HYPERBOLIC FUNCTION FXCEEDS 5.0 AN ASYMTOTIC APPROXIMATION
C IS USED TO COMPUTE T(K)

IF (COSA1-COSA2) 63,64,63

64 M11 = 2

GO TO 163

63 M11 = 1

163 DO 50 K=1,12

IF (K-1) 51,51,52

51 T21N =0.0

T22N =0.0

T21D =0.0

T22D =0.0

TM31=COSA1

TM32=COSA2

TANHK= 0.0

GO TO 53

52 AKK=K -1

IF (TR*AKK -60.0) 54,54,55

55 T(K)=T(K-1)

GO TO 50

54 CALL SINH

TANHK = SINHK/COSHK
T21N = TANHK * SIHRS
T22N = TANHK * SIHRD
T21D = TANHK * SIHSG
T22D = TANHK * SIHDT
IF QUOTIENT OVRFLOW 56,56
56 TM31 = COSA1/COSHK
IF QUOTIENT OVRFLOW 57,58
57 TM31=0.0
GO TO (58,53),M11
58 TM32 = COSA2/COSHK
IF QUOTIENT OVRFLOW 59,53
59 TM32 =0.0
C IF PRK IS GREATER THAN 60.0 WE ASSUME THE SERIES HAS CONVERGED
C SINCE REMAINING FORWARD DIFFERENCES ARE ESSENTIALLY ZERO
53 IF (TRMSG -5.0) 20,21,21
20 T1N = (COHRS + T21N - TM31) * FX2RS
GO TO(65,22), M11
65 T3N = (COHRS + T21N - TM32) * FX2RS
GO TO 22
21 IF ACCUMULATOR OVERFLOW 23,23
23 TM1 = EX2RS * TM31
IF ACCUMULATOR OVRFLOW 24,255
24 TM1 = 0.0
255 GO TO (25,27), M11
25 TM2 = EX2RS * TM32
IF ACCUMULATOR OVERFLOW 26,27
26 TM2 =0.0
27 T1N = 0.5*(1.0+TANHK)-TM1
GO TO (66,22),M11
66 T3N = 0.5*(1.0+TANHK)-TM2
22 IF (TRMDT-5.0) 28,29,29
28 T2N =(COHRD+ T22N-TM31)* EX2RD
GO TO (67,49),M11
67 T4N = (COHRD +T22N-TM32)*FX2RD
GO TO 49
29 TM1 = EX2RD *TM31
IF ACCUMULATOR OVRFLOW 30,311
30 TM1 = 0.0
311 GO TO (31,33),M11
31 TM2 = EX2RD * TM32
IF ACCUMULATOR OVERFLOW 32,33
32 TM2 =0.0
33 T2N =0.5*(1.0+TANHK)-TM1
GO TO (68,49),M11
68 T4N = 0.5*(1.0+TANHK)-TM2
49 IF (SIGMA -5.0) 34,35,35
34 T1D =(COHSG +T21D -TM31)*EXSG
GO TO (69,37),M11
69 T3D = (COHSG + T21D -TM32)*EXSG
GO TO 37
35 IF ACCUMULATOR OVRFLOW 36,36
36 TM1 = FXSG * TM31
IF ACCUMULATOR OVRFLOW 38,399
38 TM1 =0.0
399 GO TO (39,41),M11
39 TM2=FXSG*TM32
IF ACCUMULATOR OVRFLOW 40,41
40 TM2 = 0.0
41 T1D = 0.5*(1.0+TANHK)- TM1
GO TO (70,37),M11
70 T3D = 0.5 *(1.0+TANHK) -TM2
37 IF (DELTA -5.0) 42,43,43

```

42 T2D = (COHDT + T22D - TM31)* FXDT
    GO TO (71,72),M11
71 T4D = (COHDT + T22D - TM32)* FXDT
    GO TO 60
43 IF ACCUMULATOR OVFRELOW 44,44
44 TM1 = FXDT * TM31
    IF ACCUMULATOR OVFRELOW 45,466
45 TM1 =0.0
46 GO TO (46,48),M11
46 TM2 = EXDT * TM32
    IF ACCUMULATOR OVFRELOW 47,48
47 TM2 =0.0
48 T2D =0.5*(1.0+TANHK) -TM1
    GO TO (73,72),M11
73 T4D = 0.5*(1.0+TANHK)-TM2
    GO TO 60
72 VAR =(T1N/T1D *T2N/T2D)**2
    GO TO 74
60 VAR = T1N/T1D*T2N/T2D*T3N/T3D*T4N/T4D
74 T(K) =LOGF(VAR)
    IF (MDIAG) 113,50,113
113 WRITE OUTPUT TAPE 4,169, DELTA,SIGMA,TR,COHRS,COHRD,SIHSG,SIHDT,CO
    1SHDK,T21N,T21D,TANHK,TM1,T1N,T2N,T3N,T4N,T1D,T2D,T3D,T4D,T(K),VAR
169 FORMAT(16H0 50 SUBROUTINE /(1P7E16.7))
50 CONTINUE
    VAR = T(1)-T(2)+T(3)-T(4)+T(5)/2.0
    OM= 1.0
    DIV= 2.0
    DO 61 J=1,7
    OM=-OM
    DIV=DIV*2.0
    M=8 -J
    DO 62 K=1,M
62 T(K+4)=T(K+4)-T(K+5)
    VAR= VAR +OM*T(5)/DIV
61 CONTINUE
    SO = 0.5*(RS-Y5 + (CS *VAR)/4.)
    RETURN
    END(0,1,0,1,0)

```

SUBROUTINE S1
 DIMENSION ALFA(51),ALOD(10),AMDAL(100),V(100),F(51),X(51),T(12),P
 102(51,61),DUMMY(100),C1(200),DAM(61),ZN(3),XN(4),XZ(5),CH(3),SH(13),
 CHP(3),SHP(3),CHM(3),SHM(3),CHN(3),SHN(3),
 XCOS(200),COS1(50,50),COS2(50,50),FRASF(50), AMAT(50,50),CCOS(50),
 COST(61,3),CSIN(50),SINT(61,3),TEMP(51,61)

COMMON PA,C,A,ZTA,AK,RT12,N,NA,NLD,NAA,NV,ALFA,ALOD,AMDAL,V,F,X,MD
 11AG,MORCS,RS,XS,YS,COSA1,COSA2,CS,SO,T,SINHK,SINHDK,COSHDK,COSHDK,N
 22,NTH,P02,AAB,R,CR,D,ICOUNT,E,FN,ALODI,WK,TAR,ZTAN,ALFP,ALFSR,DFL
 3,CO, DFLTH,C1,DIN,NDIN,CN,SN,S1,IS1,ZH,ZL,
 BVEC,AMAT,COS1,CO
 452,ERASE,XCOS,ZTAP,ZTAM,CCOS,COST,CSIN,SINT,TEMP

C ENTER WITH

C FN= NO. ORIFICES, ZH= MAX(Z,ZFTA), ZL= MIN(Z,ZFTA),
 C ALODI= CURRENT (L/D).

C IS1= 1 FOR C1 CALCULATION,
 = 2 REQUIRES SINF, COSINF N*THETA, THETA.

C F=N THETA ICOUNT=1

C R=COS(F) TAR= 0

C AAB=SIN(F) CN=COS(THETA)

C CR= 0. SN= SIN(THETA)

C D= 1.

C FIRST COMPUTE ARGUMENTS AND INITIAL VALUES.

1 ZN(1)=FN*ZL
 ZN(2)=FN*(ALODI- ZH)
 ZN(3)=FN*ALODI
 ENN= FN+ FN
 EMNZ1= ZN(1)
 FMNZ2= FN*ZH
 FNZH=EMNZ2
 EMNZ3= ZN(3)
 BOTM= ENN- 1.
 BOTP= FNN+ 1.

C COMPUTE EXPONENTIAL FUNCTIONS.

3 DO 4 IQ=1,3
 4 XN(IQ)= EXPF(ZN(IQ))
 XZ(1)= EXPF(ZL)
 XZ(2)= EXPF(ALODI- ZH)
 XZ(3)= EXPF(ALODI)
 XZ(5)= XZ(2)/XZ(3)
 XN(4)= XN(2)*XN(1)/XN(3)
 XZ(4)= XZ(5)*XZ(1)

C COMPUTE HYPERBOLIC FUNCTIONS

5 DO 6 IQ=1,3
 VA= 1./XN(IQ)
 VR= 1./XZ(IQ)
 CHN(IQ)= (XN(IQ) + VA)/2.
 SHN(IQ)= (XN(IQ) - VA)/2.
 CH(IQ)= (XZ(IQ) + VR)/2.
 6 SH(IQ)= (XZ(IQ) - VR)/2.

C STORE HYPERBOLIC FUNCTIONS FOR M= 0.

DO 7 IQ=1,3
 CHP(IQ)= 1.
 7 SHP(IQ)= 0.
 OM = -1.0
 STS= 0.

C NOW COMPUTE COSH, SINH OF- MN*ZL, MN*(L/D-ZH), MN*(L/D)
 ASSIGN 8 TO NHA
 GO TO 500

C RETURN WITH HYPERBOLIC FUNCTS IN CHM, SHM ARRAYS. NEXT COMPUTE
 UAR1, UAR2, UAR3 USING HYPERBOLIC FUNCTS.

8 ASSIGN 9 TO NUARA

GO TO 600

C RETURN WITH UAR,S.

9 $S_1 = UAR1 + UAR3 + UAR2/ROTM + UAR2/ROTP$
 $SPR = S_1$
 GO TO 11,101,151
 C FOLLOWING COMPUTES SUM WHEN THETA TERM ENTERS- CASE 2.
 10 ASSIGN 12 TO NIS12
 CALL SINCOS
 $SMN = D*CN$
 $SMP = CR*SN$
 $C1 = SMN + SMP$
 $C2 = SMN - SMP$
 11 $STS = OM * (C1 * (UAR1 + UAR2/ROTM) + C2 * (UAR3 + UAR2/ROTP)) + STS$
 $OM = -OM$
 GO TO NIS12, 12,26
 12 $FMNZ3 = FMNZ3 + ZN(3)$
 $EMNZ2 = EMNZ2 + FNZH$
 $FMNZ1 = FMNZ1 + ZN(1)$
 $ROTM = ROTM + FNN$
 $ROTP = ROTP + FNN$
 C ABOVE STATEMENTS ADVANCE SUMMATION INDEX M BY 1.
 13 IF (FMNZ3= 8.0) 14,14,17
 C FOLLOWING COMPUTE UAR1-3 BY HYPERBOLIC FUNCTIONS.
 14 ASSIGN 16 TO NHA
 GO TO 500
 16 ASSIGN 24 TO NUARA
 GO TO 600
 C FOLLOWING FOR MN*(L/D) GREATER 8. TEST MN*7L.
 17 IF (FMNZ1= 8.0) 18,18,23
 18 IF (FMNZ3= 50.0) 21,19,19
 19 $CHM(1) = CHN(1)*CHP(1) + SHN(1)*SHP(1)$
 $SHM(1) = SHN(1)*CHP(1) + CHN(1)*SHP(1)$
 $CHP(1) = CHM(1)$
 $SHP(1) = SHM(1)$
 $X5 = EXPF(FMNZ2)$
 $UAR2 = CHM(1)/X5$
 $T(1) = CHM(1)*CH(1)$
 $T(2) = SHM(1)*SH(1)$
 20 $UAR1 = (T(1) - T(2))/(X5* X7(5)*ROTM)$
 $UAR3 = (T(1) + T(2))/X5*X7(5)/ROTP$
 GO TO 24
 C FOLLOWING COMPUTE UAR1-3 BY HYPERBOLIC FUNCTIONS.
 21 ASSIGN 22 TO NHA
 GO TO 500
 22 ASSIGN 24 TO NUARA
 GO TO 600
 C FOLLOWING EVALUATE UAR1-3 BY ASYMPTOTIC FORMULAS.
 23 $UAR2 = 0.5*EXP(FMNZ1-FMNZ2)$
 $UAR1 = UAR2/(X7(4)*ROTM)$
 $UAR3 = UAR2*X7(4)/ROTP$
 C FOLLOWING CALCULATE SUMS AND CHECK CONVERGENCE.
 24 $S1 = S1 + UAR1 + UAR3 + UAR2/ROTM + UAR2/ROTP$
 GO TO 12,25,151
 25 ASSIGN 26 TO NIS12
 GO TO 11
 26 IF (SPR/S1= 0.9999127,28,28
 27 SPR = S1
 GO TO 12
 28 GO TO 130,291,151
 29 $S1 = STS$
 30 RETURN
 C CALCULATION OF HYPERBOLIC FUNCTS OF MN*ARGUMENT.
 500 DO 501 IQ= 1,3
 $CHM(IQ) = CHN(IQ)*CHP(IQ) + SHN(IQ)*SHP(IQ)$
 $SHM(IQ) = SHN(IQ)*CHP(IQ) + CHN(IQ)*SHP(IQ)$

501 CHP(IQ)= CHM(IQ)
501 SHP(IQ)= SHM(IQ)
GO TO NHA, (8,16,22)

C CALCULATION OF UAR1-3 USING HYPERBOLIC FUNCTIONS.

600 UAR2 = CHM(1)*SHM(2)/CHM(3)
T(1)= CHM(1)*CH(1)
T(2)= SHM(1)*SH(1)
T(3)= SHM(2)*CH(2)
T(4)= CHM(2)*SH(2)
T(5)= CHM(3)*CH(3)
T(6)= SHM(3)*SH(3)

601 UAR1= ((T(1)-T(2))/(T(5)-T(6)))*(T(3)-T(4))/BOTM
UAR3= ((T(1)+T(2))/(T(5)+T(6)))*(T(3)+T(4))/BOTP
GO TO NUARA,(9,24)
END(0,1,0,1,0)

SUBROUTINE SURP1

-121-

THIS SUBROUTINE COMPUTES THE FIRST ORDER PRESSURE PROFILE WHICH UPON EXIT FROM THE ROUTINE IS STORED IN P02. THE S1 AND SOR SUBPROGRAMS ARE USED. POP1= (U1+U2)+U3 ,
 $POP1/(P02) = P1$

U1+U2 INVOLVES USE OF S1

DIMENSION ALFA(51),ALOD(10),AMDAL(100),V(100),F(51),X(51),T(12),P
 102(51,61) ,DUMMY(100),C1(200),DAM(61) ,ZN(3),XN(4),X7(5),CH(3),SH(13),CHP(3),SHP(3),CHM(3),SHM(3),CHN(3),SHN(3), BVFC(50)
 2, XCOS(200),COS1(50,50),COS2(50,50),FRASE(50) , AMAT(50,50),CCOS(5
 30),COST(61,3),CSIN(50),SINT(61,3),TEMP(51,61)

COMMON PA,C,A,ZTA,AK,RT12,N,NA,NLD,NAA,NV,ALFA,ALOD,AMDAL,V,F,X,MD
 1IAG,MORCS,RS,XS,YS,COSA1,COSA2,CS,SO,T,SINHK,SINHDK,COSHK,COSHDK,N
 2Z,NTH,P02,AAB,R,CB,D,ICOUNT,E,FN,ALODI,WK,TAR,ZTAN,ALFP,ALFSR,DFL2
 3,CO, DELTH,C1,DIN,NDIN,CN,SN,S1,IS1,ZH,ZL, BVEC,AMAT,COS1,CO
 4S2,ERASE,XCOS,ZTAP,ZTAM,CCOS,COST,CSIN,SINT,TFMP

VAR = FN*DELTH

E= -VAR

IS1=2

FMPT= -CO*FN/3.1415927*0.75

DO 2 J=1,NTH

E=E+VAR

Z= 0.0

CN=COST(J,2)

SN=SINT(J,2)

ZH= ZTA

DO 2 I=1,NZ

CB=0.0

D=1.0

ICOUNT = 1

TAR =0.

B= COST(J,3)

AAB= SINT(J,3)

IF(I-NZ) 3,2,2

3 IF(Z-ZTAM) 5,5,6

5 ZL=Z

GO TO 7

6 IF(Z-ZTAP) 8,9,9

8 ZH= ZTA

ZL=ZTAM

CALL S1

TEMP(I,J)= S1

ZH= ZTAP

ZL= ZTA

CB= 0.

D= 1.

ICOUNT = 1

TAR= 0.0

B= COST(J,3)

AAB= SINT(J,3)

CALL S1

S1= 0.5*(S1+TEMP(I,J))

GO TO 10

9 ZH= Z

ZL= ZTA

7 CALL S1

10 TEMP(I,J)= S1 #FMPT

Z=Z+DELZ

2 CONTINUE

RS= ALODI

DO 11 J=1,NTH

Z=0.0

YS=ZTA

```
DO 11 I=1,NZ
  IF(I-NZ) 12,91,91
12 IF (Z-ZTAM) 13,13,14
13 XS=Z
  M11=1
  GO TO 15
14 IF(Z-ZTAP) 16,17,17
16 YS= ZTA
  XS= ZTAM
  M11=2
  GO TO 15
17 YS= Z
  XS= ZTA
  M11=1
15 DO 21 K=1,N
  A1= COST(J,2)*CCOS(K)
  A2= SINT(J,2)*CSIN(K)
  COSA1= A1-A2
  COSA2= A1+A2
  GO TO 22
18 VAR= SO+ 0.5*(RS-YS)
  YS= ZTAP
  XS= ZTA
  M11=3
22 CALL SOR
  GO TO ( 19,18,20),M11
20 SO=IVAR+SO+(RS-YS)*0.5 1*0.5
  YS= ZTA
  XS= ZTAM
  M11=2
  GO TO 21
19 SO= SO+0.5*(RS-YS)
21 TEMP(I,J)= SO* C1(K)/6.2831853 + TEMP(I,J)
  PO2(I,J)= TEMP(I,J)/PO2(I,J)
  GO TO 11
91 PO2(I,J) = PO2(I,1)
11 CONTINUE
  RETURN
END (0+I,0+L+0)
```

```

SUBROUTINE SINH -123-
DIMENSION ALFA(51),ALOD(10),AMDAL(100),V(100),F(51),X(51),T(12),P
102(51,61) ,DUMMY(100),C1(200),DAM(61) ,ZN(3),XN(4),XZ(5),CH(3),SH(1
13),CHP(3),SHP(3),CHM(3),SHM(3),CHN(3),SHN(3), BVFC(50)
2, XCOS(200),COS1(50,50),COS2(50,50),ERASE(50) , AMAT(50,50),CCOS(5
30),COST(61,3),CSIN(50),SINT(61,3),TFMP(51,61)
COMMON PA,C,A,ZTA,AK,RT12,N,NA,NLD,NAA,NV,ALFA,ALOD,AMDAL,V,F,X,MD
1IAG,MORCS,RS,XS,YS,COSA1,COSA2,CS,SO,T,SINHK,SINHDK,COSHDK,COSHDK,N
2Z,NTH,P02,AAB,B,CR,D,ICOUNT,E,FN,ALODI,WK,TAR,ZTAN,ALFP,ALFSR,DFLZ
3,CO, DELTH,C1,DIN,NDIN,CN,SN,S1,IS1,ZH,ZL, BVEC,AMAT,COS1,CO
4S2,ERASE,XCOS,ZTAP,ZTAM,CCOS,COST,CSIN,SINT,TFMP
SINHK1= SINHK*COSHDK + SINHDK*COSHK
COSHK = SINHDK*SINHK + COSHDK*COSHK
SINHK =SINHK1
RETURN
END(0,1,0,1,0)

```

```

C SINE COS SUBROUTINE -- DUE TO POSSIBLE ROUNDOFF FRROR IN THIS
C ROUTINE EVERY TENTH SET OF VALUES IS COMPUTED USING A SERIES
C OR EXPONENTIAL APPROXIMATION ROUTINE AAB=SIN(DARG),B=COS(DARG)
C CB=SIN(ARG), D=COS(ARG)
SUBROUTINE SINCOS
DIMENSION ALFA(51),ALOD(10),AMDAL(100),V(100),F(51),X(51),T(12),P
102(51,61) ,DUMMY(100),C1(200),DAM(61) ,ZN(3),XN(4),XZ(5),CH(3),SH(1
13),CHP(3),SHP(3),CHM(3),SHM(3),CHN(3),SHN(3), BVFC(50)
2, XCOS(200),COS1(50,50),COS2(50,50),ERASE(50) , AMAT(50,50),CCOS(5
30),COST(61,3),CSIN(50),SINT(61,3),TEMP(51,61)
COMMON PA,C,A,ZTA,AK,RT12,N,NA,NLD,NAA,NV,ALFA,ALOD,AMDAL,V,F,X,MD
1IAG,MORCS,RS,XS,YS,COSA1,COSA2,CS,SO,T,SINHK,SINHDK,COSHDK,COSHDK,N
2Z,NTH,P02,AAB,B,CR,D,ICOUNT,E,FN,ALODI,WK,TAR,ZTAN,ALFP,ALFSR,DFLZ
3,CO, DELTH,C1,DIN,NDIN,CN,SN,S1,IS1,ZH,ZL, BVEC,AMAT,COS1,CO
4S2,ERASE,XCOS,ZTAP,ZTAM,CCOS,COST,CSIN,SINT,TEMP
IF (ICOUNT-10 ) 1,2,2
2 FIC = ICOUNT
TAR = 1.0+TAR
ICOUNT =1
CB = SIN(FIC *TAR*E)
D= COS(FIC*TAR*E)
GO TO 3
1 ICOUNT =ICOUNT +1
FIC = .B*CR + AAB*D
D = -AAB*CR + B*D
CB =FIC
3 RETURN
END(0,1,0,1,0)

```

C DOUBLE INTEGRATION OF WK =// PK COS(TH) DTH DZ • THE THETA RANGE
C IS APPROXIMATED BY TRAPEZOIDAL RULE. THE Z RANGE IS APPROXIMATED
C BY SIMPSONS RULE.

SUBROUTINE LCALC

```
DIMENSION ALFA(51),ALOD(10),AMDAL(100),V(100),F(51),X(51),T(12),P  
102(51,61),DUMMY(100),C1(200),DAM(61),ZN(3),XN(4),X7(5),CH(3),SH(13),  
CHP(3),SHP(3),CHM(3),SHM(3),CHU(3),SHN(3),BVEC(50)  
2, XCOS(200),COS1(50,50),COS2(50,50),ERASF(50),AMAT(50,50),CCOS(5  
30),COST(61,3),CSIN(50),SINT(61,3),TEMP(51,61)  
COMMON PA,C,A,ZTA,AK,RT12,N,NA,NLD,NAA,NV,ALFA,ALOD,AMDAL,V,F,X,MD  
1IAG,MORCS,RS,XS,YS,COSA1,COSA2,CS,SO,T,SINHK,SINHDK,COSHDK,COSHDK,N  
22,NTH,PO2,AAB,B,CB,D,ICOUNT,E,FN,ALODI,WK,TAR,ZTAN,ALFP,ALFSR,DFL7  
3,CO,DELTH,C1,DIN,NDIN,CN,SN,S1,IS1,ZH,ZL,BVEC,AMAT,COS1,CO  
4S2,ERASE,XCOS,ZTAP,ZTAM,CCOS,COST,CSIN,SINT,TEMP  
COSTH =1.0  
DZ3 = DELZ/3.0  
TDZ3= DZ3+DZ3  
FDZ3=TDZ3+TDZ3  
NX =NZ-2  
WK=0.0  
DO 1 I=1,NTH  
VAR=0.0  
VAR1= PO2(I,2)  
COSTH= COST(I,2)  
3 DAM(I) = DZ3*(PO2(I,1))  
DO 2 J=3,NX,2  
VAR = PO2(I,J) + VAR  
2 VAR1 = PO2(I,J+1) + VAR1  
DAM(I)= DAM(I)+TDZ3*VAR+FDZ3*VAR1  
DAM(I)=DAM(I)*COSTH  
1 WK=WK+DAM(I)  
WK= (WK-(DAM(1)+DAM(NTH))*0.5)*DELTH  
RETURN  
END(0,1,0,1,0)
```

-124-

COMPUTER PROGRAM PN0045

Static Load for Infinitely Short
Journal Bearing with Line Source Feeding

C MECHANICAL TECNOLOGY, INC. JORGEN W. LUND 12-8-1962
 C PN0045=INFINITELY SHORT HYDROSTATIC JOURNAL BEARING
 DIMENSION VLST(200),FLST(200),FPL(200),CS(200),DW(200),DUM(500),
 1DW1(200) -126-

```

200 READ INPUT TAPE 2,100
  READ INPUT TAPE 2,101
  READ INPUT TAPE 2,105,NV,NLL,NFP,NTH,NDIA,INP
  READ INPUT TAPE 2,106,(VLST(I),I=1,NV),(FLST(I),I=1,NLL)
  1,(EPL(I),I=1,NFP)
  WRITE OUTPUT TAPE 3,102
  WRITE OUTPUT TAPE 3,100
  WRITE OUTPUT TAPE 3,101
  WRITE OUTPUT TAPE 3,103
  WRITE OUTPUT TAPE 3,104,NV,NLL,NEP,NTH,NDIA,INP
  WRITE OUTPUT TAPE 3,107
  WRITE OUTPUT TAPE 3,108,(VLST(I),I=1,NV)
  WRITE OUTPUT TAPE 3,109
  WRITE OUTPUT TAPE 3,108,(FLST(I),I=1,NLL)
  WRITE OUTPUT TAPE 3,110
  WRITE OUTPUT TAPE 3,108,(FPL(I),I=1,NFP)
  DTH=NTH
  DTH=3.1415927/DTH
  NTHE=NTH+1
  TH=0.0
  DO 201 I=1,NTHE
    CS(I)=COSF(TH)
  201 TH=TH+DTH
  DO 205 J=1,NV
    V=VLST(J)
    V2=(V*V-1.0)*4.0
    DO 205 K=1,NLL
      FL=FLST(K)
      A=FL*FL
      A2=0.5*A
      DO 205 L=1,NEP
        EPS=EPL(L)
        W=0.0
        W2=0.0
        DO 202 I=1,NTHE
          CTH=CS(I)
          H6=(1.0+EPS*CTH)**6.0
          TH=V2/A*H6
          IF(TH-.0001) 207,208,208
        207 Q=V2/4.0
        GO TO 209
      208 Q=A2*(-1.0+SQRTF(1.0+TH))/H6
      209 Q1=Q+1.0
        QSR=SQRTF(Q1)
        DW(I)=(Q1*QSR-1.0)/Q*CTH
        DW1(I)=QSR*CTH
        W2=W2+DW1(I)
      202 W=W+DW(I)
        W=DTH*(DW(1)+DW(NTHE)-2.0*W)/3.0
        W2=DTH*(0.5*DW1(1)+0.5*DW1(NTHE)-W2)
        W1=1.2732395*W/EPS
        IF(NDIA) 203,204,203
      203 WRITE OUTPUT TAPE 3,111
        WRITE OUTPUT TAPE 3,112,V,FL,EPS,V2,A,A2,DTH,TH,CTH,H6,Q,Q1,QSR,
        1W,W1
        WRITE OUTPUT TAPE 3,113,(CS(I),DW(I),I=1,NTHE)
      204 WRITE OUTPUT TAPE 3,114
        WRITE OUTPUT TAPE 3,115,V,FL,EPS,W,W1,W2
      205 CONTINUE
  
```

```
205 IF(INPI) 206,200,206
206 END FILE 3
      STOP 77777
100 FORMAT(72H0
      1          )
101 FORMAT(72H
      1          )
102 FORMAT(84H1  PN0045=INFINITELY SHORT HYDROSTATIC JOURNAL BEARING
      1    JORGEN W.LUND 12-8-1962 )
103 FORMAT(90H0 NO.PR.RATIO   NO.L/D*LAMBDA   NO.EPSILON      NO.THETA
      1    DIAGNOSTIC      INPUT      )
104 FORMAT(18,5I15)
105 FORMAT(6I5)
106 FORMAT(1P4E15.7)
107 FORMAT(18H0  PRESSURF RATIOS)
108 FORMAT(1P7E16.7)
109 FORMAT(18H0  L/D*LAMBDA-T   )
110 FORMAT(12H0  EPSILONS   )
111 FORMAT(18H0  DIAGNOSTIC   )
112 FORMAT(1P6E16.7)
113 FORMAT(1P2E16.7)
114 FORMAT(108H0  PRESSURE RATIO   L/D*LAMBDA-T      EPSILON
      1    DIMENS LOAD     4/PI*LOAD/EPS.    CENTER LOAD )
115 FORMAT(1P6E18.7)
END (0,0,1)
```

COMPUTER PROGRAM PN0047

**Dynamic Load for Journal and Thrust
Bearing with Line Source Feeding**

C MECHANICAL TECHNOLOGY, INC. JORGEN W. LUND 9-2-62
C PN0047 DYNAMIC LOAD FOR HYDROSTATIC JOURNAL AND THRUST BEARING
DIMENSION FVFE(100),FLAM(100),FSIG(100),FALFA(26),FXI(50),FGAM(50)
1,QST(50),PR2ST(50),PRST(50),G(101),P0(101),PZG(101),PR1(101),
2PI1(101),PR2(101),PI2(101),SR(101),SI(101),TR(101),TI(101),VR(101)
3,VI(101),TSR(101),TSI(101),TTR(101),TTI(101),TVR(101),TVI(101),
4DUMMY(1000)

-129-

200 READ 100
READ 101
READ 102,NSIG,NLAM,NVEE,KOP1,NX,NGAM,MT,NDIAG,NPR,FKA
READ 103,(FXI(I),I=1,NX)
READ 103,(FGAM(I),I=1,NGAM)
READ 103,(FVEE(I),I=1,NVEE)
READ 103,(FLAM(I),I=1,NLAM)
READ 103,(FSIG(I),I=1,NSIG)
READ 103,(FALFA(I),I=2,26)
WRITE OUTPUT TAPE 3,115
WRITE OUTPUT TAPE 3,120
WRITE OUTPUT TAPE 3,100
WRITE OUTPUT TAPE 3,101
WRITE OUTPUT TAPE 3,136
WRITE OUTPUT TAPE 3,137,NX,NGAM,NVEE,NLAM,NSIG,KOP1,MT,NPR,NDIAG,

1FKA

WRITE OUTPUT TAPE 3,131
WRITE OUTPUT TAPE 3,124,(FXI(I),I=1,NX)
WRITE OUTPUT TAPE 3,132
WRITE OUTPUT TAPE 3,124,(FGAM(I),I=1,NGAM)
WRITE OUTPUT TAPE 3,125
WRITE OUTPUT TAPE 3,124,(FVEE(I),I=1,NVEE)
WRITE OUTPUT TAPE 3,123
WRITE OUTPUT TAPE 3,124,(FLAM(I),I=1,NLAM)
WRITE OUTPUT TAPE 3,126
WRITE OUTPUT TAPE 3,124,(FSIG(I),I=1,NSIG)
WRITE OUTPUT TAPE 3,127
WRITE OUTPUT TAPE 3,124,(FALFA(I),I=2,26)

C CALCULATION OF ORIFICE FLOW TABLE

FALFA(1)=1.0
EX6=2.0/(FKA+1.0)
EX1=1.0/(FKA-1.0)
EX7=(EX6**EX1)*SQRTF(EX6*FKA)
EX4 = 2.0 * EX1
EX1=FKA*EX1
CRP = EX6 ** EX1
EX3= SQRTF(2.0*EX1)
EX2= 1.0/EX1
EX5 = -EX2
EX6 = 1.0/EX6
EX1=1.0/FKA
DIT =(1.0 -CRP)/50.0
CX=CRP

DO 258 I=1,50
CX = CX+DIT
C5 = CX**EX1
QST(I)=EX3*C5*SQRTF(1.0-CX/C5)
PR2ST(I)=CX*CX

258 PRST(I)= CX

AME=MT
C INITIATE L/D LOOP
DO 242 IA=1,NX
FLD=FXI(IA)
DELTA=FLD/AMF
DELTAS=DELTA*DELTA
IF(KOP1) 202,201,202

201 P2LD=FLD
 GO TO 203
 202 P2LD=LOGF(FLD)
 C INITIATE L1/D-LOOP
 203 DO 242 IB=1,NGAM
 FL1D=FGAM(IB)
 IF(KOP1) 204,205,204
 204 FLG=LOGF(FL1D)
 BETAT=P2LD/FLG
 BP1=RFTAT+1.0
 GMNV=1.0/FL1D
 FRFT=1.0/(FLD*FLD)
 DELTA=(FLD-1.0)/AMF
 DELG=(1.0-GMNV)/AME
 C INITIATE PRESSURE RATIO LOOP
 205 DO 242 IC=1,NVEE
 V=FVFE(IC)
 V2=V*V
 VNv=1.0/V2
 C INITIATE LAMBDA-T LOOP
 DO 242 ID=1,NLAM
 FLT=FLAM(ID)
 C CALCULATE DIMENSIONLESS FLOW AND ORIFICE PRESSURE
 259 C1=FLT*P2LD*V
 CX=SQRTF(1.0+C1*EX7)/V
 IF(CRP-CX) 223,222,222
 222 P2=FLT*V*EX7
 C1=1.5*P2
 C2=0.0
 P00=CX*V
 SLP=0.0
 VC=1.0
 GO TO 244
 223 C2=V2*CRP*CRP-1.0-C1*EX7
 MTST =0
 L=2
 C4=2.0*DIT
 261 M=2
 262 VC= FALFA(M)
 263 C5=V2 * PR2ST(L)-1.0-C1*VC* QST(L)
 CX=PRST(L)
 265 IF (MTST) 266,266,231
 266 C6=C5* C2
 IF(C6) 268,268,267
 267 L=L+2
 M=M+1
 C2=C5
 IF(L=50) 262,262,275
 268 MTST =1
 C7=C5
 L=L-1
 VCM = FALFA(M-1)
 VCS=VC
 DVC=(VC- VCM)/C4
 VC = (VC+VCM)/2.0
 GO TO 263
 231 C1 = C4 * C4
 C1 = 2.0*(C2+C7-2.0*C5)/C1
 C3 =(C7-C2)/C4
 IF (C1) 233,232,233
 232 C6= -C5/C3
 GO TO 236
 233 C4= 0.5* C3/C1

$C_6 = \text{SQRTF}(C_4 * C_4 - C_5 / C_1)$
 IF(C4) 234,235,235
 234 $C_6 = -C_6$
 235 $C_6 = C_6 - C_4$
 236 $C_6 = C_X + C_6$
 237 $P_2 = (V_2 * C_X * C_X - 1.0) / P_{2LD}$
 $P_{00} = C_X * V$
 $EX_2 = C_X ** EX_1$
 $C_1 = 1.5 * P_2$
 $VC = VC + C_6 * DVC$
 $C_4 = VC * FLT * V$
 $C_4 = P_2 / C_4$
 $C_5 = -DVC / VC$
 $C_6 = 0.5 * VC$
 $C_2 = C_6 * FLT / P_{00} * (C_5 * C_4 + EX_4 * EX_2 / C_4 * (EX_6 - EX_2 / C_X))$
 $SLP = -2.0 * C_2 / FLT * P_{00}$
 244 IF(KOP1) 245,271,245

C JOURNAL BEARING CALCULATIONS

271 $P_0(1) = P_{00}$
 $MTST = 1 + MT$
 $C_4 = P_2 * DELTA$
 $C_6 = P_2 * FLD - C_4$
 DO 213 J=2,MTST
 $P_0(J) = \text{SQRTF}(1.0 + C_6)$

213 $C_6 = C_6 - C_4$

C INITIATE FREQUENCY NO. LOOP

DO 246 J=1,NSIG

$SIG = FSIG(J)$

C CALCULATE A,B,C AND D AND CENTER LOAD CONSTANTS

$SGPZ = SIG * P_{00}$

$FFCI = SIG / P_{00}$

$FUNK = 1.0 + FFCI * FFCI$

$AL = \text{SQRTE}(FUNK)$

$BETAJ = AL - 1.0$

$BETAJ = \text{SQRTE}(0.5 * BETAJ)$

$AL = AL + 1.0$

$AL = \text{SQRTE}(0.5 * AL)$

$FFCR = 1.0 / (FUNK * P_{00})$

$FFCI = -FFCI / (FUNK * P_{00})$

$FSPI = SIG / FUNK * SIG$

$FSPR = SIG / FUNK * SIG$

$SH2A = 2.0 * FL1D * AL$

$SH2A = EXPF(SH2A)$

$SN2B = 1.0 / SH2A$

$CH2A = (SH2A + SN2B) * 0.5$

$SH2A = (SH2A - SN2B) * 0.5$

$SN2B = 2.0 * FL1D * BETAJ$

$CS2B = COSF(SN2B)$

$SN2B = SINF(SN2B)$

$CTR = CH2A + CS2B$

$THR = (AL * SH2A - BETAJ * SN2B) / CTR$

$THI = (AL * SN2B + BETAJ * SH2A) / CTR$

IF(FL1D) 211,219,211

211 $CTR = 0.0$

$CTI = 0.0$

$FSPR = 0.0$

$FSPI = 0.0$

GO TO 212

211 $CTI = CH2A - CS2B$

$CTR = (AL * SH2A + BETAJ * SN2B) / CTI$

$CTI = (BETAJ * SH2A - AL * SN2B) / CTI$

212 $A = C_1 + THR * FSPR - THI * FSPI$

$R = THI * FSPI + THI * FSPR$

C = 1 HR+C2
 D=THI
 FINITE DIFFERENCE EQUATIONS
 FF=0.0
 K=1
 M=MT+1
 DO 207 N=1,M
 207 G(N)=SIG*PO(N)
 218 QR=0.5*DELTAS
 QI=QR/P00*SIG
 PR=QR*FF
 PI=QR*G(1)
 SR(1)=0.0
 SI(1)=0.0
 TI(1)=0.0
 TR(1)=1.0
 DO 209 N=2,M
 SR(N)=SR(N-1)+PR+DELTA*A
 SI(N)=SI(N-1)+PI+DELTA*B
 TR(N)=TR(N-1)+QR+DELTA*C
 TI(N)=TI(N-1)+QI+DELTA*D
 IF(N-MT) 208,208,210
 208 C6=SIG/P0(N)
 PR=PR+DELTAS*(SR(N)-C6*SI(N)+FF)
 PI=PI+DELTAS*(SI(N)+C6*SR(N)+G(N))
 QR=QR+DELTAS*(TR(N)-C6*TI(N))
 209 QI=QI+DELTAS*(TI(N)+C6*TR(N))
 210 DHRI=TR(M)*TR(M)+TI(M)*TI(M)
 H10=(TI(M)*SR(M)-TR(M)*SI(M))/DHRI
 HRO=-(TI(M)*SI(M)+TR(M)*SR(M))/DHRI
 GO TO (600,601),K
 C JOURNAL BEARING LOAD, TRANSLATION
 600 REL=0.0
 EEL=0.0
 DO 302 N=1,M
 PR1(N)=(SR(N)+TR(N)*HRO-TI(N)*H10)/P0(N)
 PI1(N)=(SI(N)+TR(N)*H10+TI(N)*HRO)/P0(N)
 REL=REL+PR1(N)
 302 EEL=EEL+PI1(N)
 REL=DELTA*(0.5*PR1(1)-REL)
 EEL=DELTA*(EEL-0.5*PI1(1))
 IF(FL1D) 214,215,214
 215 RCL=0.0
 ECL=0.0
 GO TO 216
 214 RF=HRO+FSPR
 EF=H10+FSP1
 C6=RF*THR-EF*THI
 EF=RF*THI+EF*THR-SGPZ*FL1D
 RCL=-FFCR*C6+FFCI*EF
 ECL=FFCR*EF+FFCI*C6
 216 C6=REL+RCL
 C4=-(EEL+ECL)
 W=1.5707963/(FLD+FL1D)*SQRTF(C6*C6+C4*C4)
 THETA=ANG(C6,C4)
 C JOURNAL BEARING MOMENT, ROTATION
 FF=C1
 K=2
 C4=FL1D
 DO 217 N=1,M
 G(N)=G(N)*C4
 217 C4=C4+DELTA
 A=FL1D*(C1+FSPR*CTR-FSP1*CTI)-FSPR

B=FL1D*(FSPR*CTI+FSPI*CTR)-FSPI

-133-

C=CTR+C2

D=CTI

HTRZ=HRO

HTEZ=HIO

GO TO 218

601 REM=0.0

EEM=0.0

C4=FL1D

DO 220 N=1,M

PR2(N)=(SR(N)+TR(N)*HRO-TI(N)*HIO)/PO(N)

PI2(N)=(SI(N)+TR(N)*HIO+TI(N)*HRO)/PO(N)

REM=REM+C4*PR2(N)

EEM=EEM+C4*PI2(N)

220 C4=C4+DELT

REM=DELT*(0.5*PR2(1)*FL1D-REM)

EEM=DELT*(EEM-0.5*PI2(1)*FL1D)

IF(FL1D) 224,221,224

221 RCM=0.0

ECM=0.0

GO TO 225

224 RF=HRO+FL1D*FSPR

EF=HIO+FL1D*FSPI

C4=FL1D*CTR-1.0

C6=FL1D*CTI

ECM=RF*C4-EF*C6

C4=RF*C6+EF*C4-SGPZ/3.0*(FL1D**3)

RCM=FFCI*C4-FFCR*ECM

ECM=FFCR*C4+FFCI*ECM

225 C6=REM+RCM

C4=-(EEM+ECM)

RMT=0.78539816/(FLD+FL1D)*SQRTF(C6*C6+C4*C4)

THMT=ANG(C6,C4)

C JOURNAL BEARING OUTPUT

WRITE OUTPUT TAPE 3,106

WRITE OUTPUT TAPE 3,107,FLD,FL1D,V,FLT,SIG,P2,CX

WRITE OUTPUT TAPE 3,108

WRITE OUTPUT TAPE 3,107,P00,VC,SLP,HTRZ,HTEZ,HRO,HIO

WRITE OUTPUT TAPE 3,109

WRITE OUTPUT TAPE 3,110,W,THETA,REL,EEL,RCL,ECL

WRITE OUTPUT TAPE 3,111

WRITE OUTPUT TAPE 3,110,RMT,THMT,REM,EEM,RCM,ECM

IF(NPR) 240,246,240

240 WRITE OUTPUT TAPE 3,112

WRITE OUTPUT TAPE 3,113

C4=FL1D

DO 241 N=1,M

WRITE OUTPUT TAPE 3,110,C4,PO(N),PR1(N),PI1(N),PR2(N),PI2(N)

241 C4=C4+DELT

246 CONTINUE

GO TO 242

C THRUST BEARING CALCULATION

245 A=BP1*C1

B=BP1*C2

M=1+MT

C3=RETAT*P2

C4=1.0

C5=1.0

C6=1.0+P2*P2LD

DO 247 N=1,M

C=LOGF(C4)

D=LOGF(C5)

P0(N)=SQRTF(C6-P2*C1)

```

PZG(N)=SQRTF(C6+C3*D)
C4=C4+DELTA
247 C5=C5-DELG
C INITIATE FREQUFNCE NO. LOOP
DO 290 J=1,NSIG
SIG=FSIG(J)
C FINITE DIFFERENCE EQUATIONS
K=1
ERC=0.0
FRC=0.0
ER=0.0
FR=0.0
248 ADR=DELTA
BDR=DELTA
C=0.0
D=0.0
DO 249 N=1,M
249 G(N)=PO(N)
250 C3=1.0
C4=1.0+BDR
SR(1)=0.0
SI(1)=0.0
TR(1)=0.0
TI(1)=0.0
VI(1)=0.0
VR(1)=1.0
C6=0.5*ADR
PR=C6*FRC
PI=C6*SIG*POO
WR=C6*ERC
WI=C6/POO*SIG
QR=0.0
QI=0.0
DO 254 N=2,M
C5=LOGF(C4/C3)
SR(N)=SR(N-1)+C5*(PR-C)
SI(N)=SI(N-1)+C5*PI
TR(N)=TR(N-1)+C5*(1.0+QR)
TI(N)=TI(N-1)+C5*QI
VR(N)=VR(N-1)+C5*(WR-D)
VI(N)=VI(N-1)+C5*WI
IF(N-M) 251,255,255
251 C3=C3+BDR
C4=C4+BDR
FE=G(N)
EE=SIG/FE
FE=SIG*FE
IF(K-2) 253,253,252
252 FE=FE*C3
FR=FRC/C3
ER=1.0/C3
ER=ER*ER
253 C5=ADR*C3
PR=PR+C5*(ER*SR(N)-FE*SI(N)+FR)
PI=PI+C5*(ER*SI(N)+FE*SR(N)+FE)
QR=QR+C5*(ER*TR(N)-EE*TI(N))
QI=QI+C5*(ER*TI(N)+FE*TR(N))
WR=WR+C5*(ER*VR(N)-FF*VI(N))
254 WI=WI+C5*(ER*VI(N)+FE*VR(N))
255 GO TO (256,278,270,278),K
270 FRC=-C1*RETAT
256 ADR=DELG
BDR=-DELG

```

C=A
D=B
DO 257 N=1,M
G(N)=PZG(N)
TSR(N)=SR(N)
TSI(N)=SI(N)
TTR(N)=TR(N)
TTI(N)=TI(N)
TVR(N)=VR(N)
257 TVI(N)=VI(N)
K=K+1
GO TO 250
278 D1=TSR(M)
D2=TSI(M)
D3=TTR(M)
D4=TTI(M)
D5=TVR(M)
D6=TVI(M)
G1=SR(M)
G2=SI(M)
G3=TR(M)
G4=TI(M)
G5=VR(M)
G6=VI(M)
C3=D4*G6+G3*D5-D3*G5-G4*D6
C4=D3*G6+D4*G5-G3*D6-G4*D5
C5=D1*G5-D2*G6-G1*D5+G2*D6
C6=D1*G6+D2*G5-G1*D6-G2*D5
C7=C3*C3+C4*C4
HPR=(C5*C3-C6*C4)/C7
HPE=(C5*C4+C6*C3)/C7
C5=D3*G1-D4*G2-G3*D1+G4*D2
C6=D3*G2+D4*G1-G3*D2-G4*D1
HR0=(C5*C3-C6*C4)/C7
HI0=(C5*C4+C6*C3)/C7
IF(K-2) 279,279,264
C THRUST BEARING LOAD,TRANSLATION
279 ERC=1.0
FRC=C1
K=3
STW=-0.5*(P00+FLD)
STC=-0.5*(P00+GMNV)
REL=0.0
EEL=0.0
RCL=0.0
ECL=0.0
C3=1.0
C4=1.0
DO 260 N=1,M
PR1(N)=(TSR(N)+TTR(N)*HPR-TTI(N)*HPE+TVR(N)*HR0-TVI(N)*HI0)/P0(N)
PI1(N)=(TSI(N)+TTR(N)*HPE+TTI(N)*HPR+TVR(N)*HI0+TVI(N)*HR0)/P0(N)
PR2(N)=(SR(N)+TR(N)*HPR-TI(N)*HPE+VR(N)*HR0-VI(N)*HI0)/PZG(N)
PI2(N)=(SI(N)+TR(N)*HPE+TI(N)*HPR+VR(N)*HI0+VI(N)*HR0)/PZG(N)
REL=REL+C3*PR1(N)
EEL=FEL+C3*PI1(N)
RCL=RCL+C4*PR2(N)
ECL=ECL+C4*PI2(N)
STW=STW+C3*P0(N)
STC=STC+C4*PZG(N)
C3=C3+DELTA
260 C4=C4-DELG
REL=DELTA*(REL-0.5*PR1(1))
FFI=FFI TA*(FFI-0.5*PI1(1))

```

RCL=DELG*(RCL-0.5*PR2(1))
ECL=DELG*(ECL-0.5*PI2(1))
STW=DELT A*STW*2.0*FRFT
STC=DELG*STC*2.0*FRFT
WST=STW+STC
C6=- (RFL+RCL)
C4=- EEL-ECL
W=2.0*FRFT*SQRTF(C6*C6+C4*C4)
THETA=ANG(C6,C4)
WRITE OUTPUT TAPE 3,114
WRITE OUTPUT TAPE 3,107,FLD,FLID,V,FLT,SIG,P2,CX
WRITE OUTPUT TAPE 3,116
WRITE OUTPUT TAPE 3,110,P00,VC,SLP,STW,STC,WST
WRITE OUTPUT TAPE 3,117
WRITE OUTPUT TAPE 3,110,W,THETA,REL,EEL,RCL,ECL
286 WRITE OUTPUT TAPE 3,118
WRITE OUTPUT TAPE 3,119,HRO,HIO,HPR,HPE
IF(NPR) 281,283,281
281 WRITE OUTPUT TAPE 3,128
C3=1.0
C4=1.0
DO 282 N=1,M
WRITE OUTPUT TAPE 3,121,C3,P0(N),PR1(N),PI1(N),C4,PZG(N),PR2(N)
  PI2(N)
  C3=C3+DELT A
282 C4=C4-DELG
283 IF(K-3) 248,248,290
C THRUST BEARING MOMENT,ROTATION
264 REM=0.0
EEM=0.0
RCM=0.0
ECM=0.0
C3=1.0
C4=1.0
DC 285 N=1,M
PR1(N)=(TSR(N)+TTR(N)*HPR-TTI(N)*HPE+TVR(N)*HRO-TV(N)*HIO)/P0(N)
PI1(N)=(TSI(N)+TTR(N)*HPE+TTI(N)*HPR+TVR(N)*HIO+VI(N)*HRO)/P0(N)
PR2(N)=(SR(N)+TR(N)*HPR-TI(N)*HPE+VR(N)*HRO-VI(N)*HIO)/PZG(N)
PI2(N)=(SI(N)+TR(N)*HPE+TI(N)*HPR+VR(N)*HIO+VI(N)*HRO)/PZG(N)
C5=C3*C3
C6=C4*C4
REM=REM+C5*PR1(N)
EEM=EEM+C5*PI1(N)
RCM=RCM+C6*PR2(N)
ECM=ECM+C6*PI2(N)
C3=C3+DELT A
285 C4=C4-DELG
REM=DELT A*(REM-0.5*PR1(1))
EEM=DELT A*(EEM-0.5*PI1(1))
RCM=DELG*(RCM-0.5*PR2(1))
ECM=DELG*(ECM-0.5*PI2(1))
C6=- (REM+RCM)
C4=- EEM-ECM
RMT=FRFT*SQRTF(C6*C6+C4*C4)
THMT=ANG(C6,C4)
WRITE OUTPUT TAPE 3,122
WRITE OUTPUT TAPE 3,110,RMT,THMT,REM,EEM,RCM,ECM
GO TO 286
290 CONTINUE
242 CONTINUE
IF(NDIAG) 243,200,243
243 END FILE 3
STOP 77777

```

275 WRITE OUTPUT TAPE 3,129

-137-

GO TO 242

100 FORMAT(72H)

1)

101 FORMAT(72H)

1)

102 FORMAT(9I5,1PE15.7)

103 FORMAT(1P4E15.7)

106 FORMAT(////120H L/D FREQUENCY NO. L1/D DIM.FLOW PRESS.RATIO
1 LAMBDA-T) ORIF.PR.RAT

210)

107 FORMAT(1P7E17.7)

108 FORMAT(120H0 ORIF.PRESS. VENA CONT.CF. DM/D(P/V)
1TRANS.RE(H0) TRANS.IM(H0) ROTAT.RE(H0) ROTAT.IM(H0))

109 FORMAT(102H0 LOAD PHASE ANGLE RE(END LOAD)
1IM(END LOAD) RF(CTR.LOAD) IM(CTR.LOAD))

110 FORMAT(1P6E17.7)

111 FORMAT(102H0 MOMENT PHASE ANGLE RE(END MOMT)
1IM(END MOMT) RE(CTR.MOMT) IM(CTR.MOMT))

112 FORMAT(96H0 ROTATIONAL) TRANSLATO
1RY)

113 FORMAT(102H DIST.FR.FD.PL. PO RE(P1)
1 IM(P1) RE(P1) IM(P1))

114 FORMAT(////120H OUT.R/ORIF.R. ORIF.R/INN.R. PRESS.RATIO
1 LAMBDA-T FREQUENCY NO. DIM.FLOW ORIF.PR.RAT

210)

115 FORMAT(84H1 MECHANICAL TECHNO

1LOGY, INC. JORGEN W.LUND)
116 FORMAT(102H0 ORIF.PRESS. VENA CONT.CF. DM/D(P/V)
1OUT.STAT.LOAD INN.STAT.LOAD STATIC LOAD)

117 FORMAT(102H0 DYNAMIC LOAD PHASE ANGLE RE(OUT.LOAD)
1IM(OUT.LOAD) RE(INN.LOAD) IM(INN.LOAD))

118 FORMAT(66H0 RE(H0) IM(H0) RE(HPRO)
1 IM(HPRO))

119 FORMAT(1P4E17.7)

120 FORMAT(108H PN0047 DYNAMIC LOAD FOR HYDROSTATIC JO
1URNAL AND THRUST BEARING-FIRST ORDER PERTURBATION)

121 FORMAT(1PE14.6,1P3F15.6,1PE16.6,1P3F15.6)

122 FORMAT(102H0 MOMENT PHASE ANGLE RE(OUT.MOMT)
1IM(OUT.MOMT) RF(INN.MOMT) IM(INN.MOMT))

123 FORMAT(23H0 FEEDING PARAMETERS)

124 FORMAT(1P7F17.7)

125 FORMAT(18H0 PRESS. RATIOS)

126 FORMAT(22H0 FREQUENCY NUMBERS)

127 FORMAT(32H0 VENA CONTRACTA COEFFICIENTS)

128 FORMAT(120H0 RADIUS/ORIF.R PO RE(P1) IM(P1)
1 RADIUS/ORIF.R PO RE(P1) IM(P1))

129 FORMAT(36H0 NO ROOT IN ORIFICE FLOW CALCULATION)

131 FORMAT(18H0 L/D-RATIO)

132 FORMAT(18H0 L1/D-RATIO)

136 FORMAT(120H0 NO.L/D NO.L1/D NO.PR.RATIO NO.LAMBDA NO.FR
1EQ. JOURN/THR. NO.INCR. PRESS.OUTP. INPUT ADIAB.EXP.)

137 FORMAT(17,8I12,1PF16.7)

END(0,1,0,1,1)

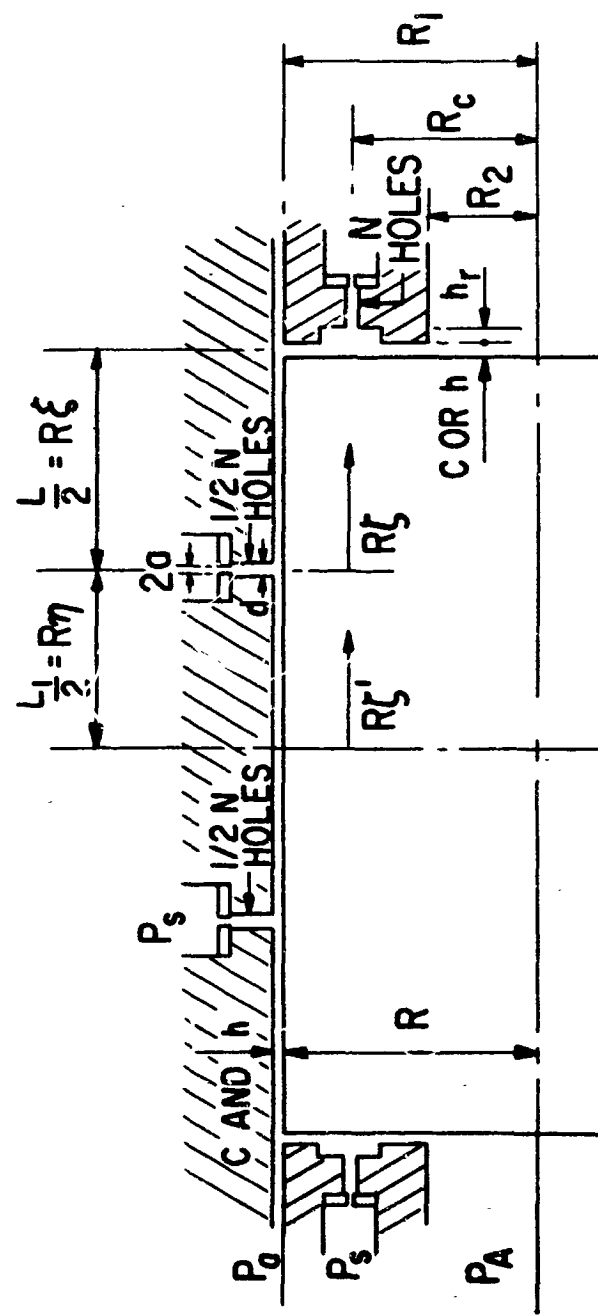
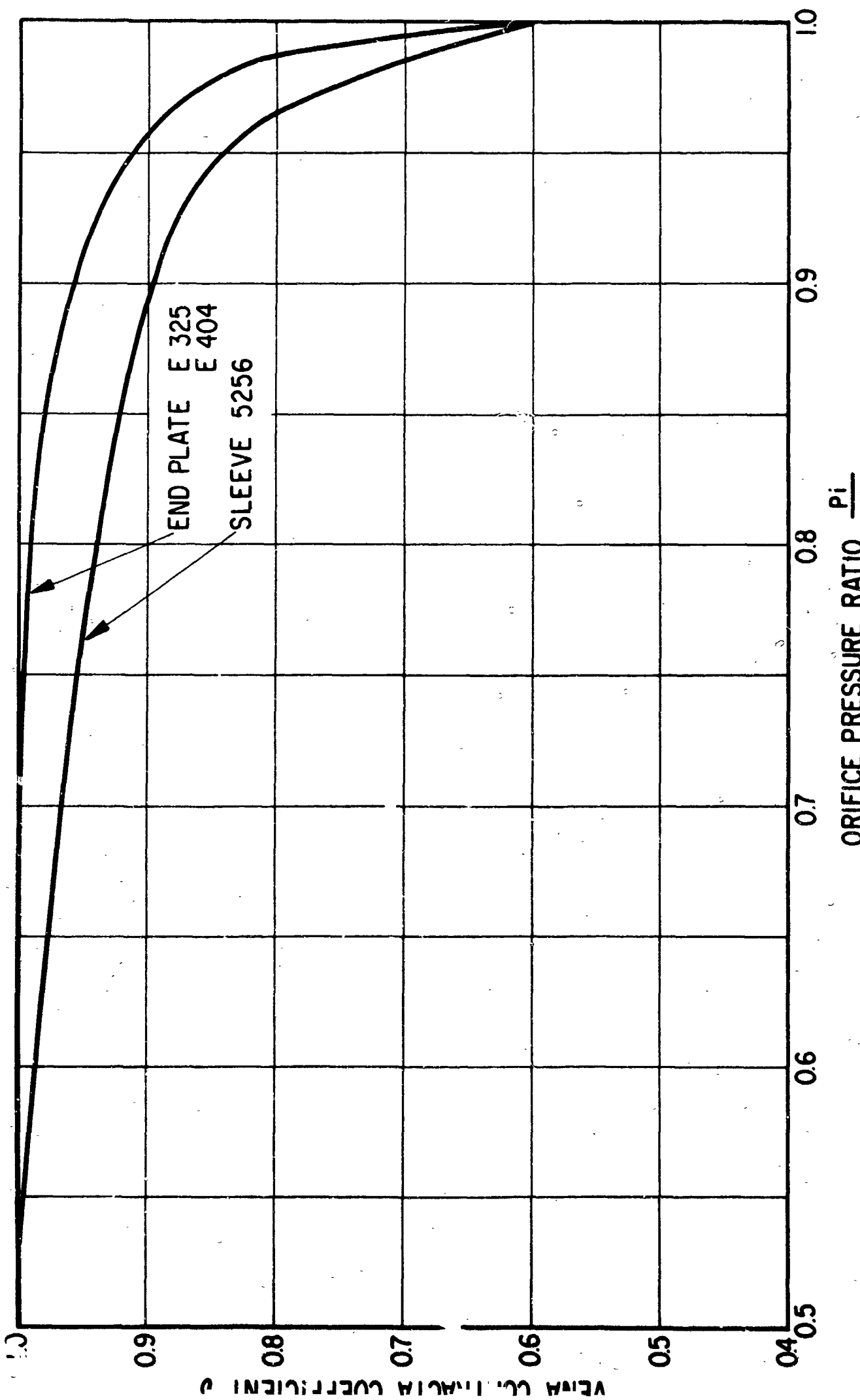


FIG. I GEOMETRY OF GIMBAL AIR BEARING

FIG. 2 VENA CONTRACTA COEFFICIENT



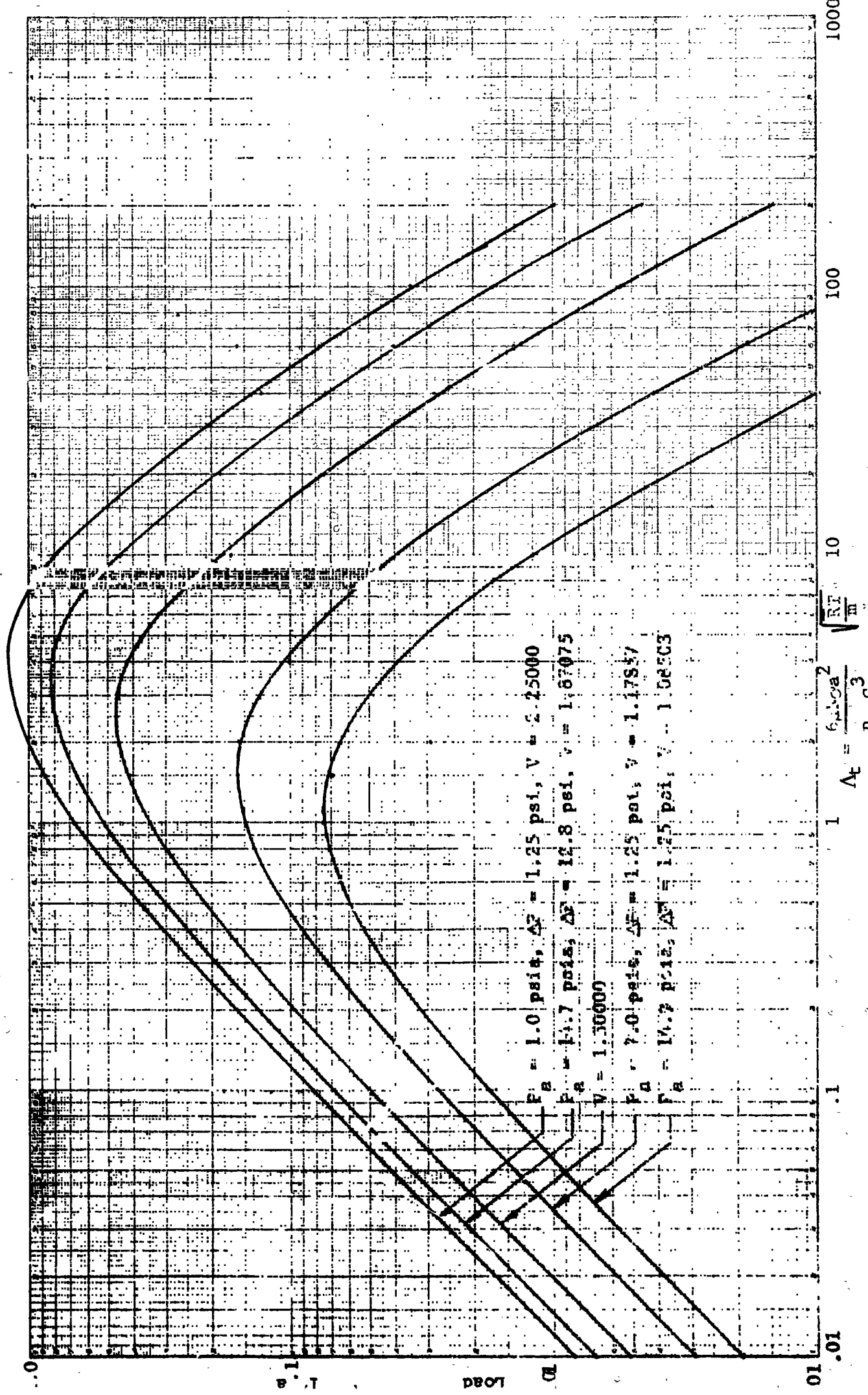


Fig. 3 Journal Bearing - Dimensionless Load vs. α_t

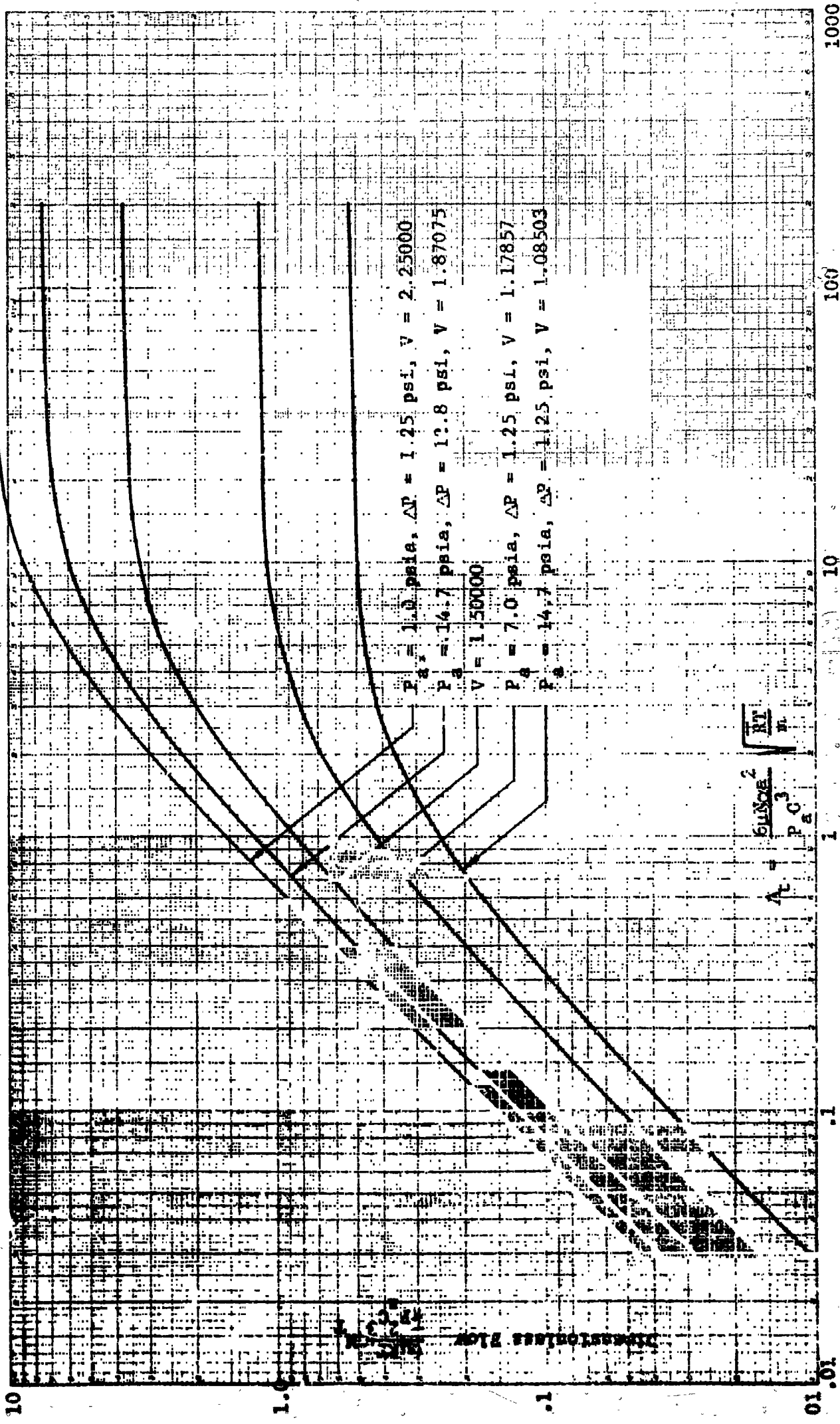


Fig. 4 Journal Bearing - Dimensionless Flow vs. Δ_t

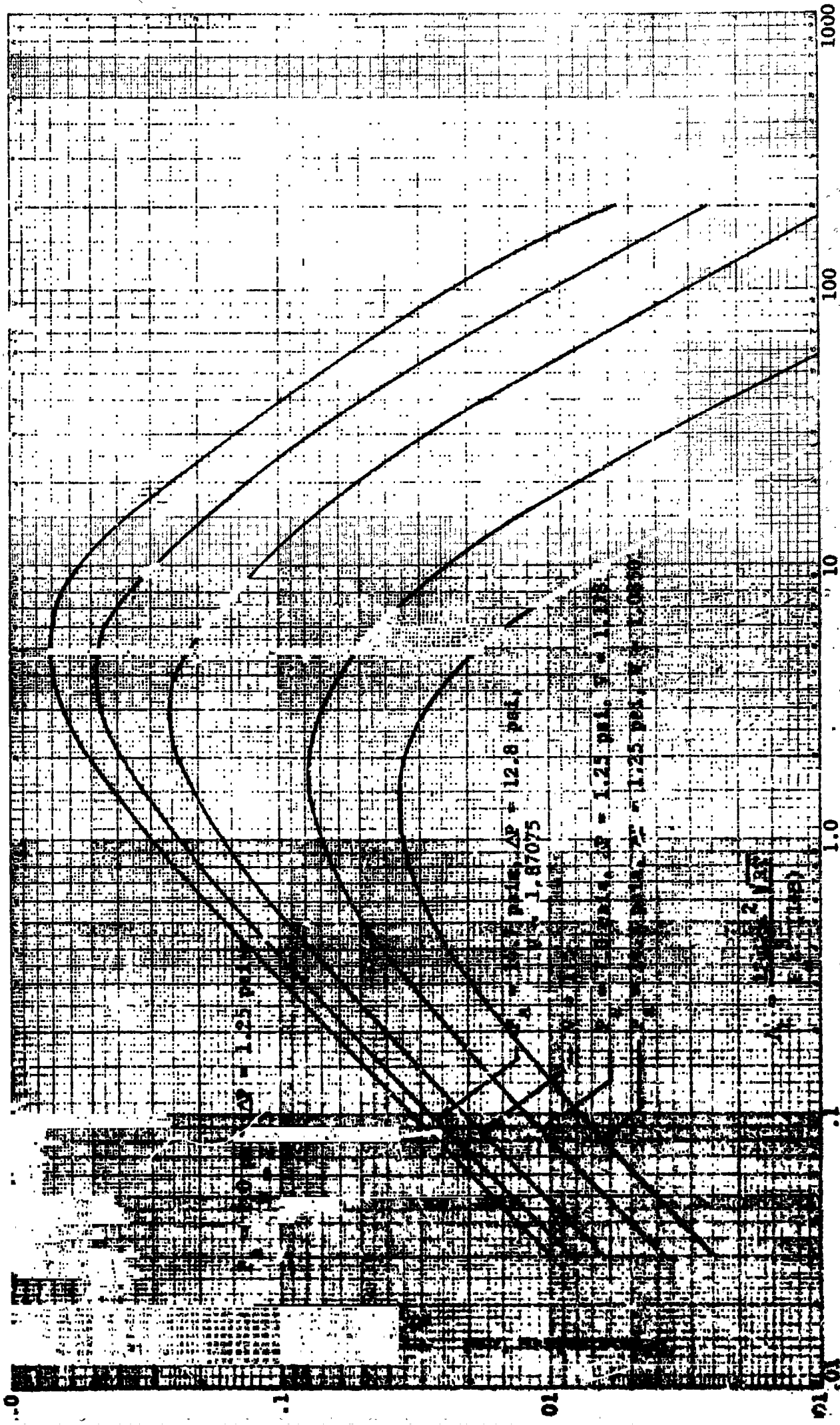


FIG. 5 Thrust Bearing - Dimensionless Load vs. Δ_t

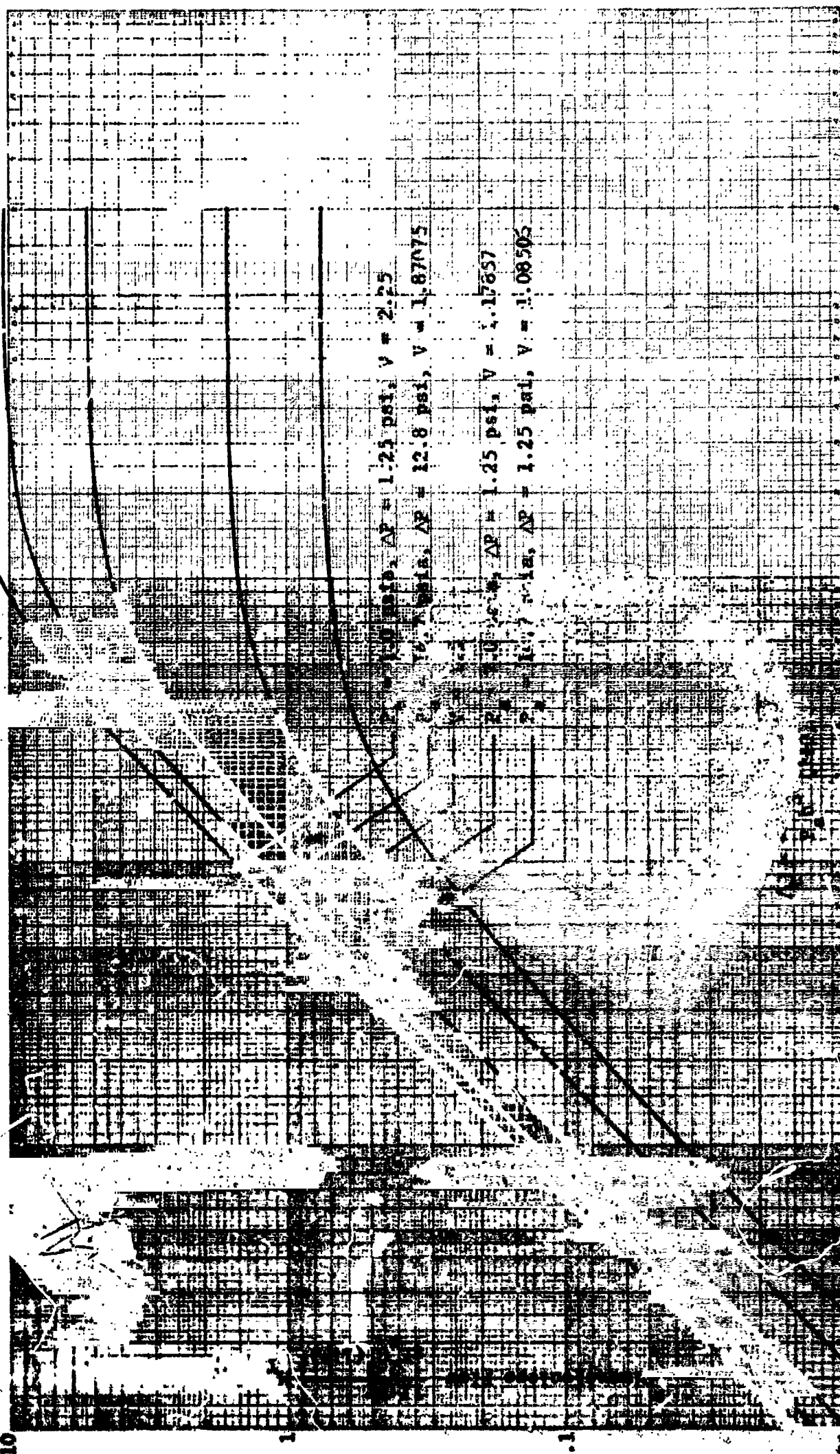
1000

100

10

1

0.1

FIG. 6 Thrust Bearing - Dimensionless Flow vs. A_t 

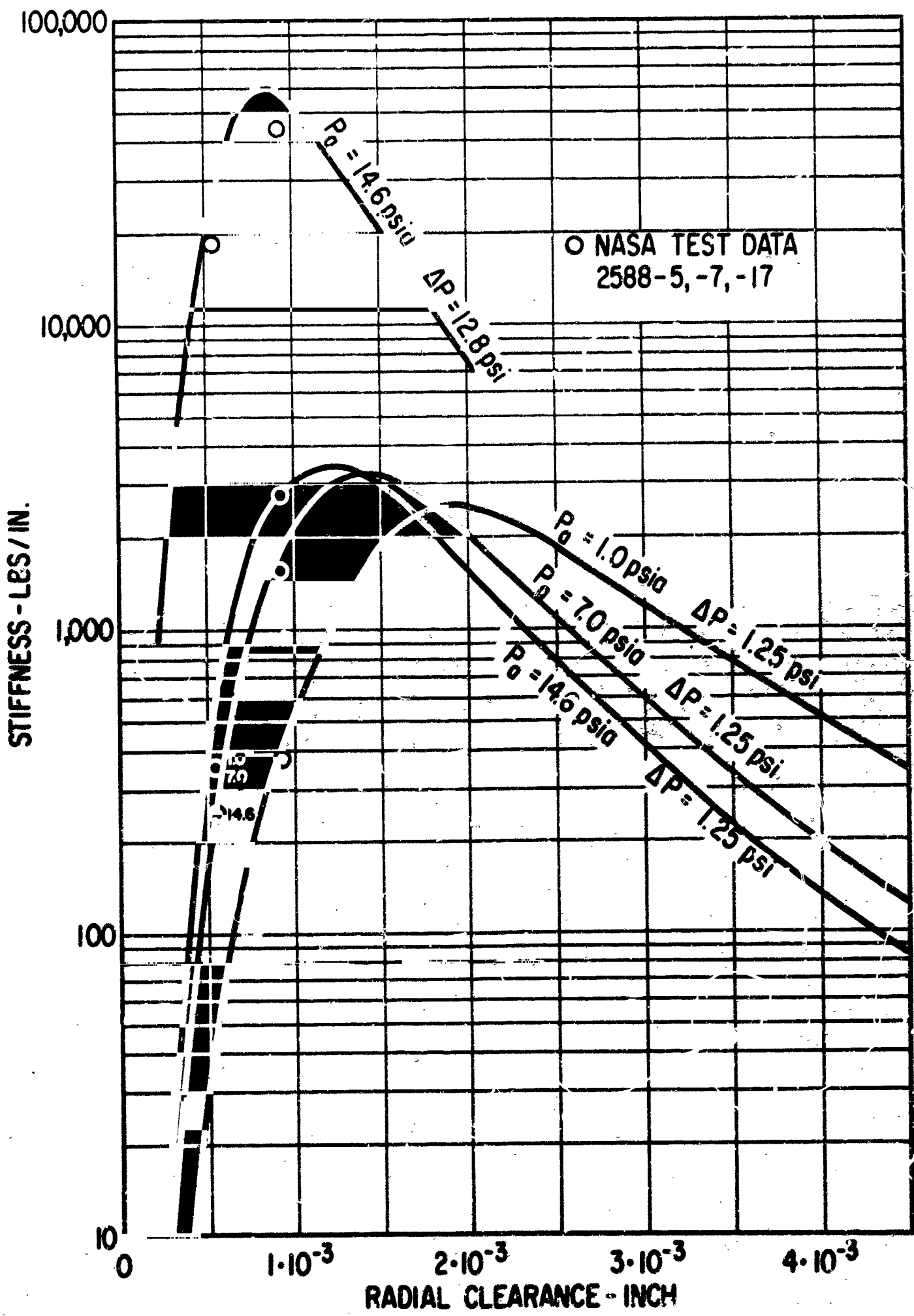
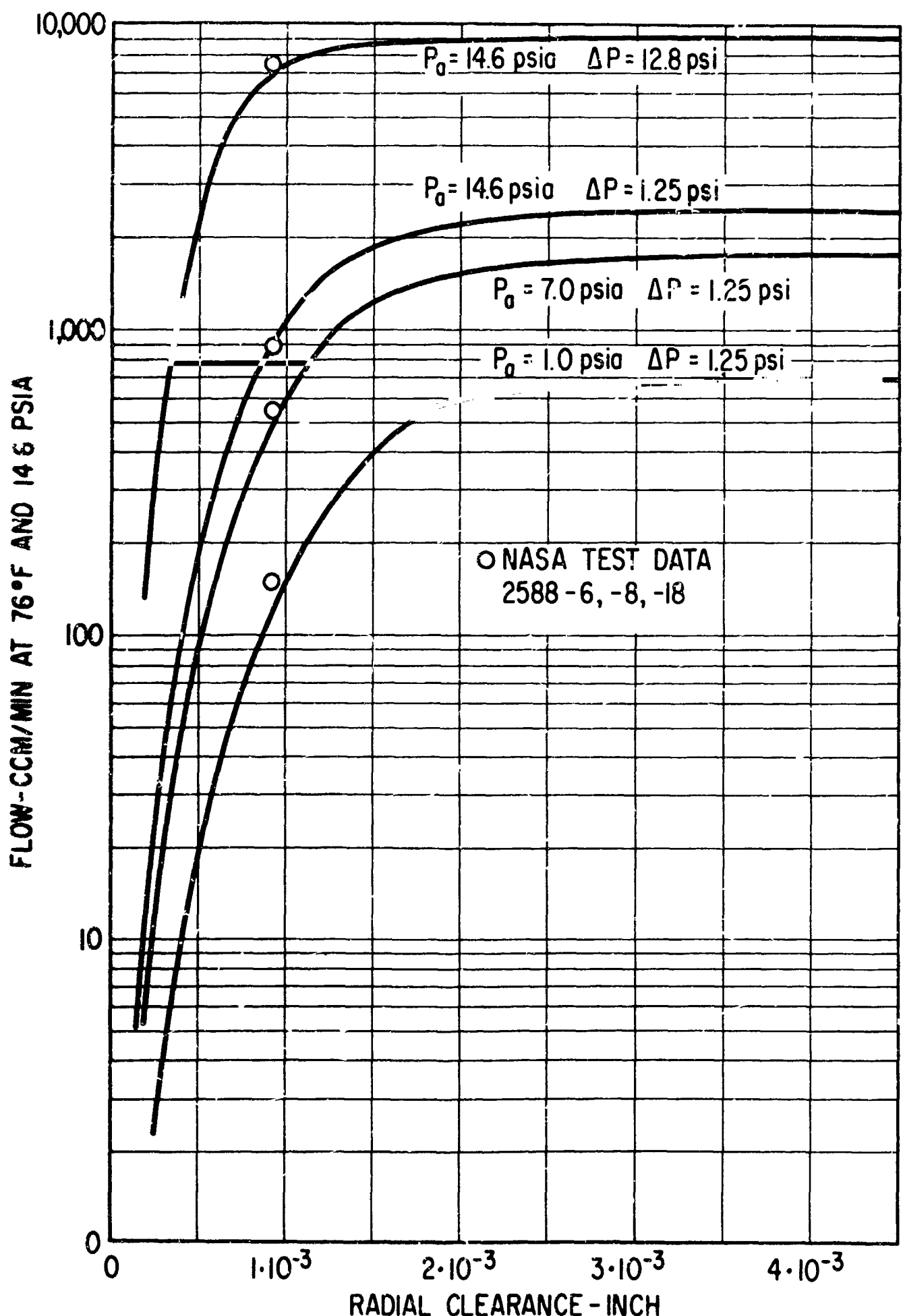
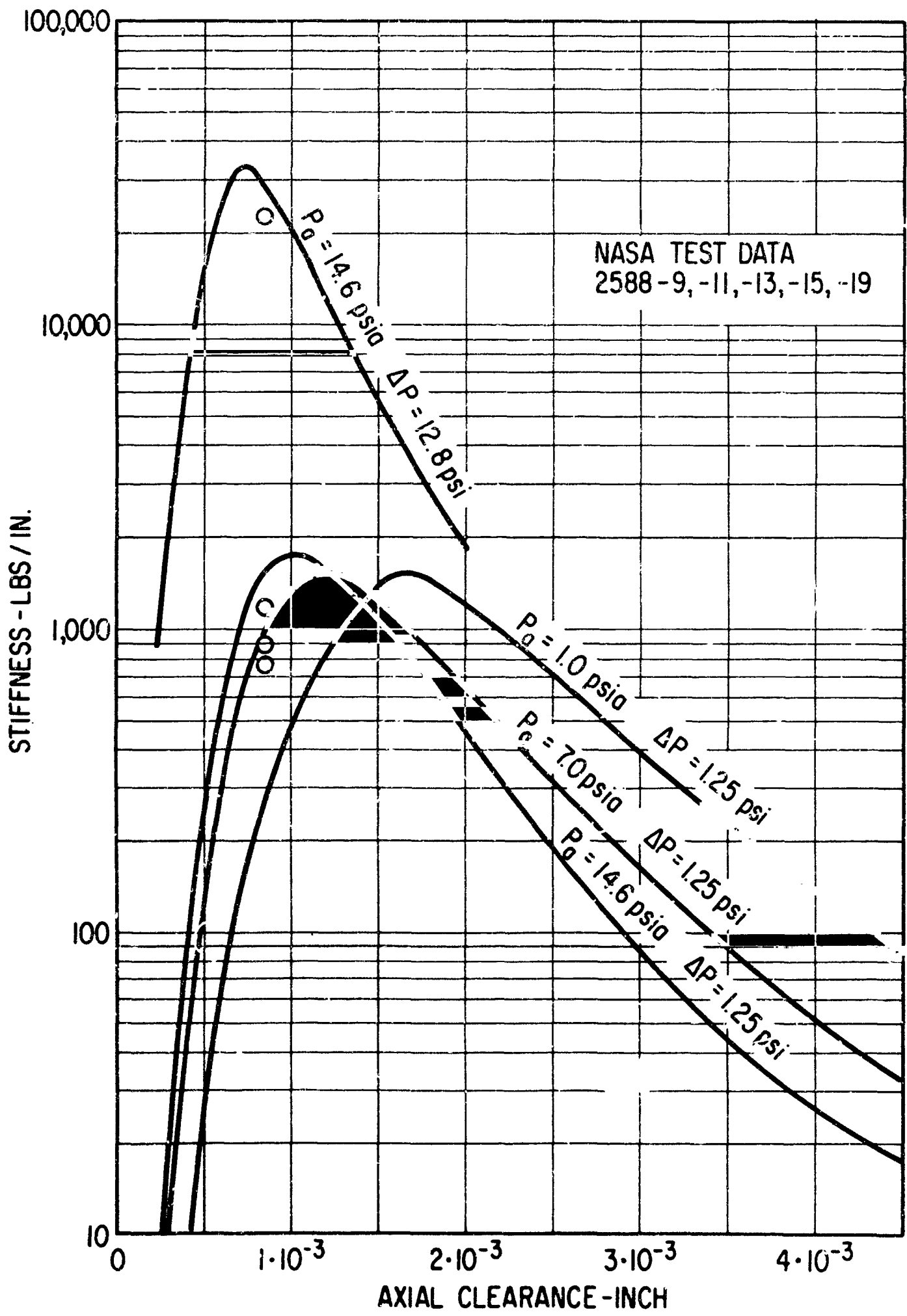


FIG. 7 AB-5 PIERCED HOLES AIRBEARING
RADIAL STIFFNESS vs CLEARANCE



**FIG. 8 AB-5 PIERCED HOLES AIRBEARING
RADIAL LOADING - SLEEVE FLOW
vs CLEARANCE**



**FIG. 9 AB-5 PIERCED HOLES AIRBEARING
AXIAL STIFFNESS vs CLEARANCE**

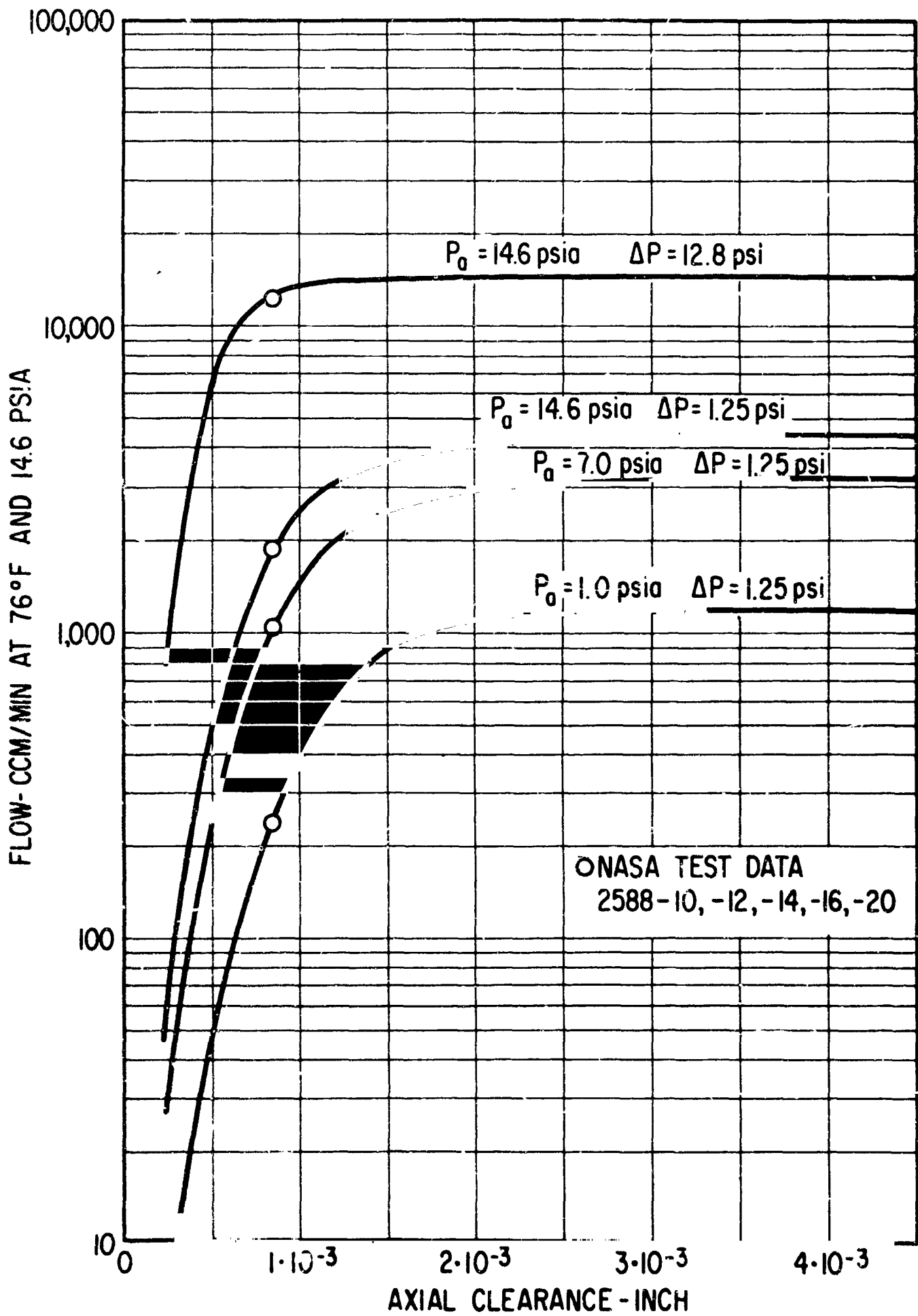


FIG. 10 AB-5 PIERCED HOLES AIRBEARING
AXIAL LOADING - ENDPLATE FLOW
vs CLEARANCE

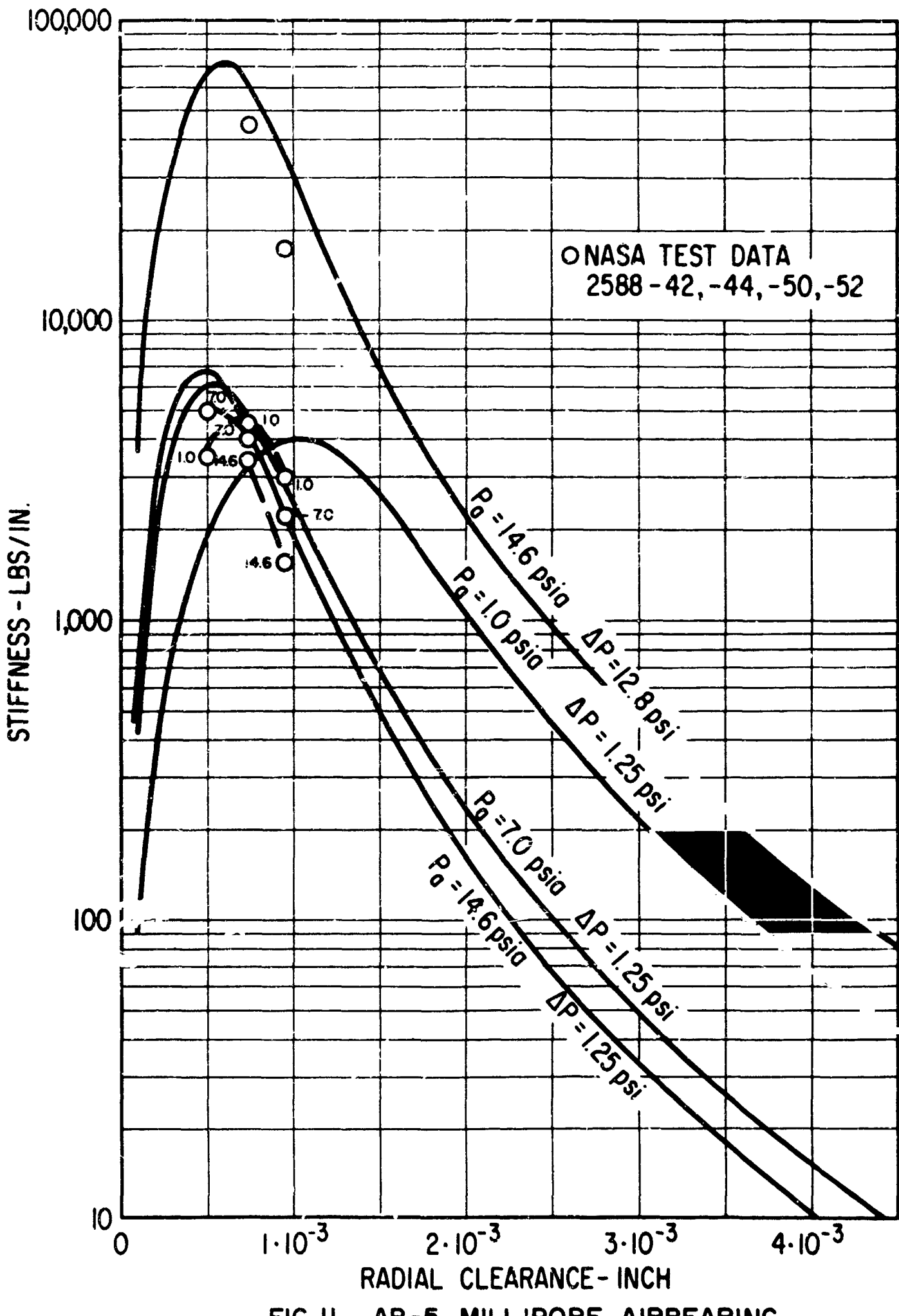


FIG. II AB-5 MILLIPORE AIRBEARING
RADIAL STIFFNESS vs CLEARANCE

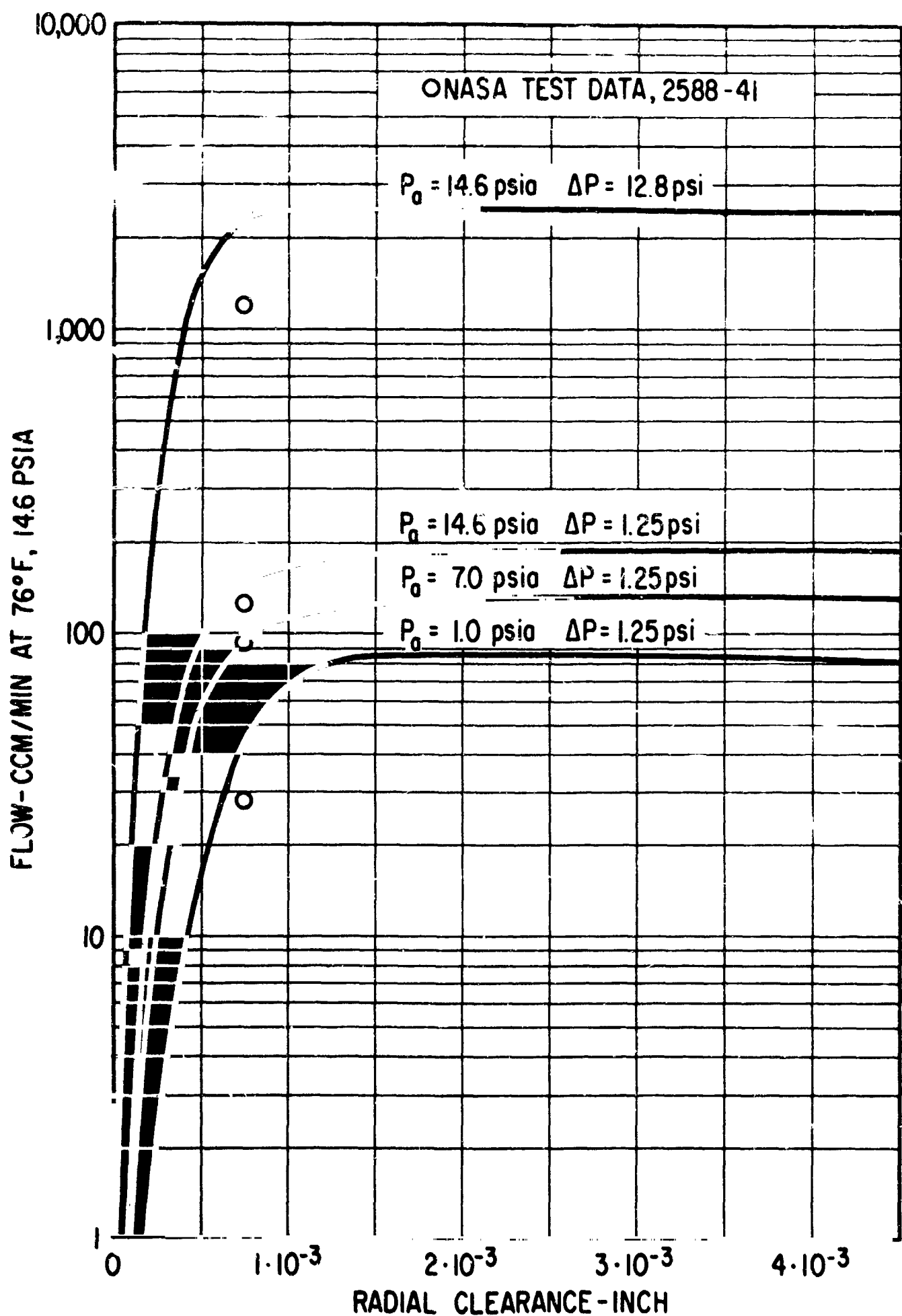


FIG. 12 AB-5 MILLIPORE AIRBEARING
RADIAL LOADING - SLEEVE
FLOW vs CLEARANCE

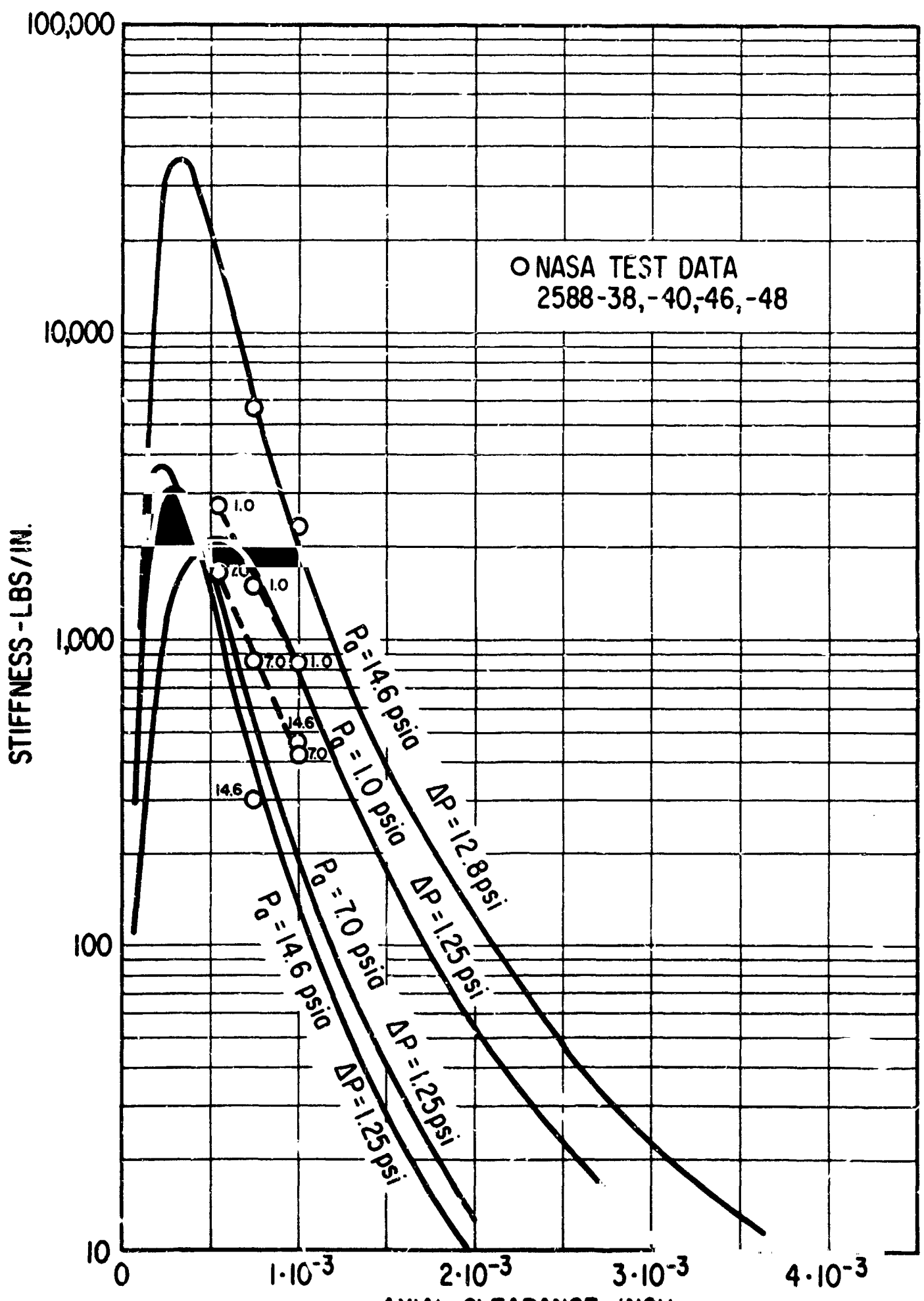


FIG. 13 AB-5 MILLIPORE AIRBEARING
AXIAL STIFFNESS vs CLEARANCE

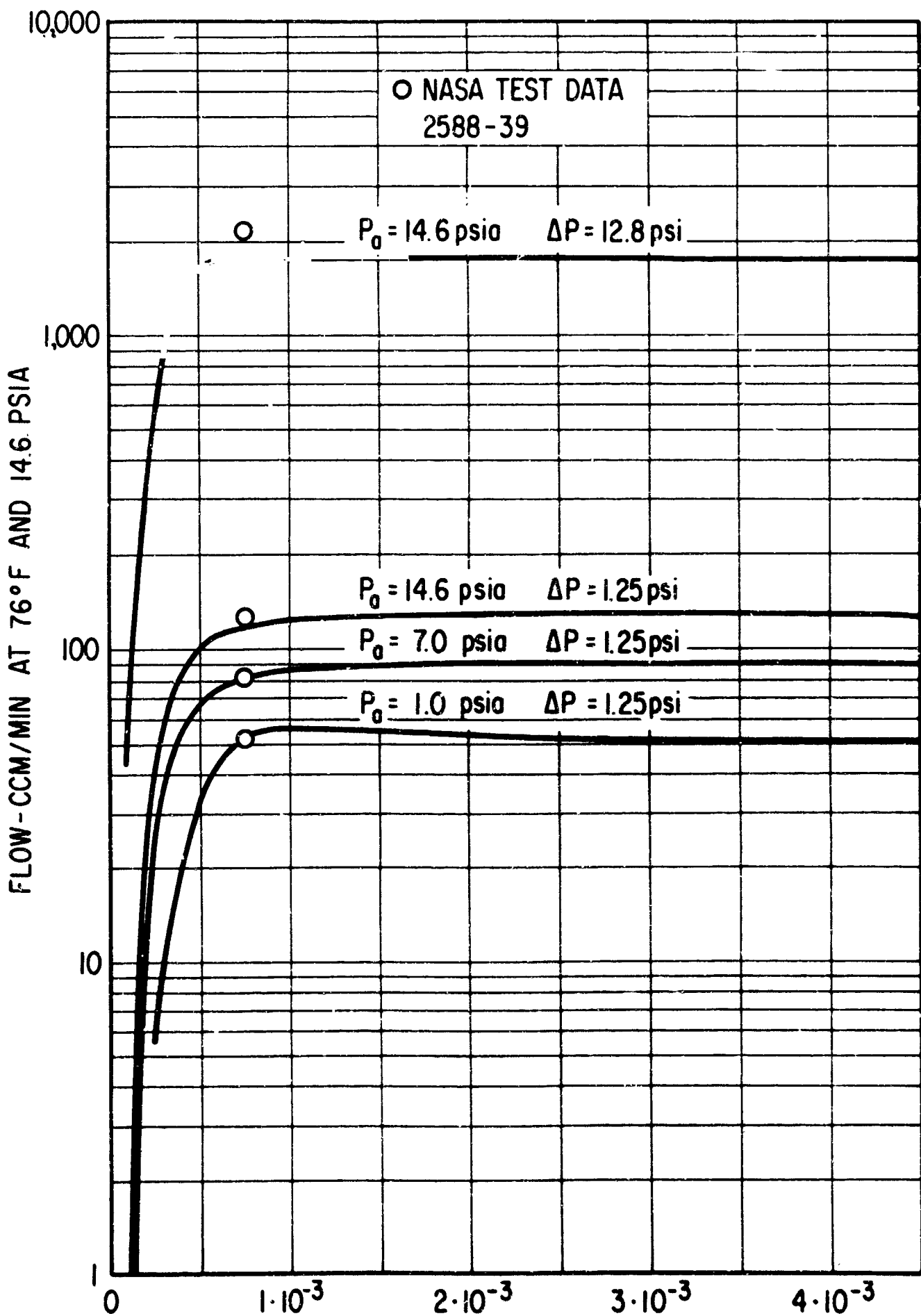


FIG. 14 AB-5 MILLIPORE AIRBEARING
AXIAL LOADING - ENDPLATE
FLOW vs CLEARANCE

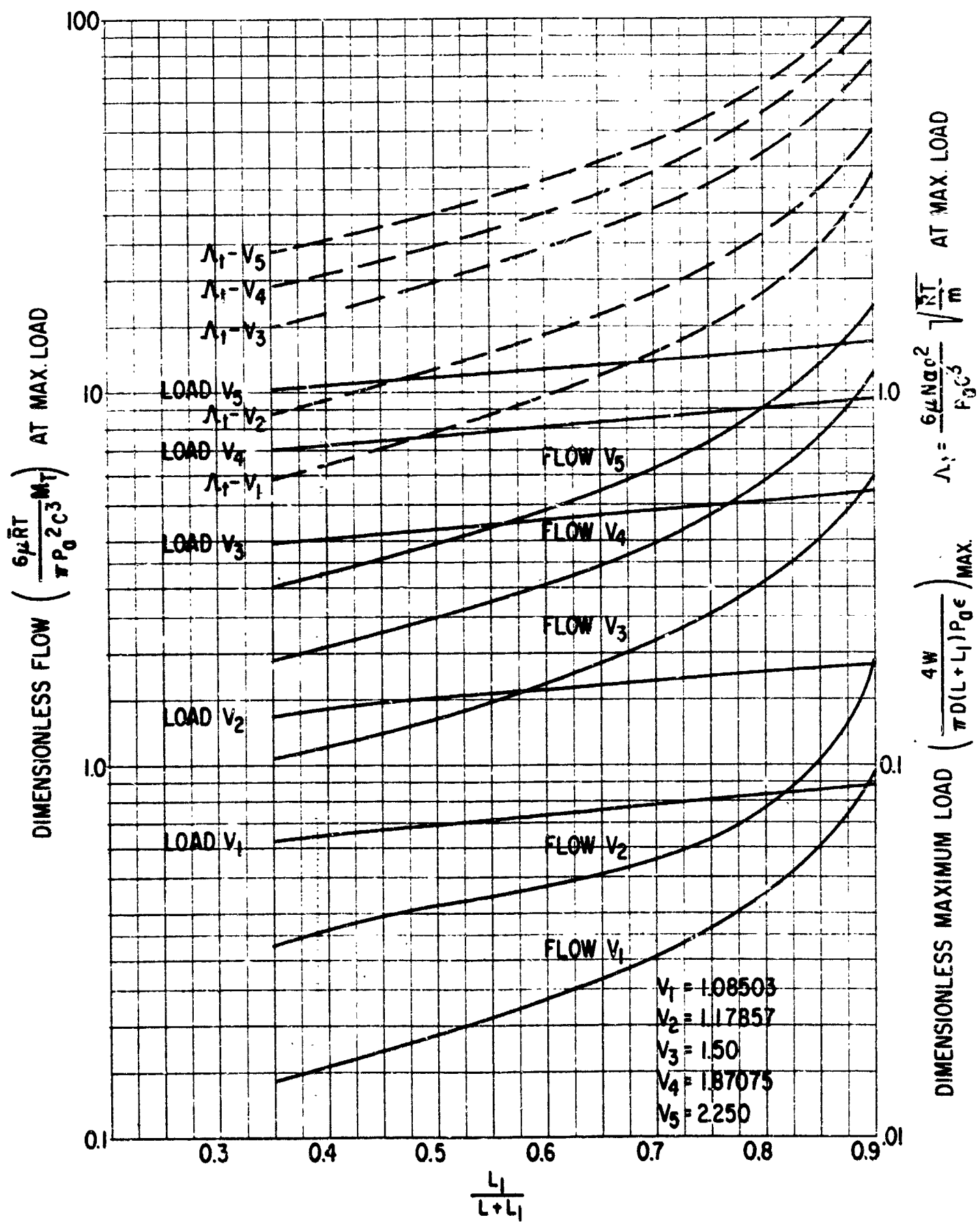


FIG.15 JOURNAL BEARING-LOAD AND FLOW OPTIMIZATION

2 CYCLES X 70 DIVISIONS

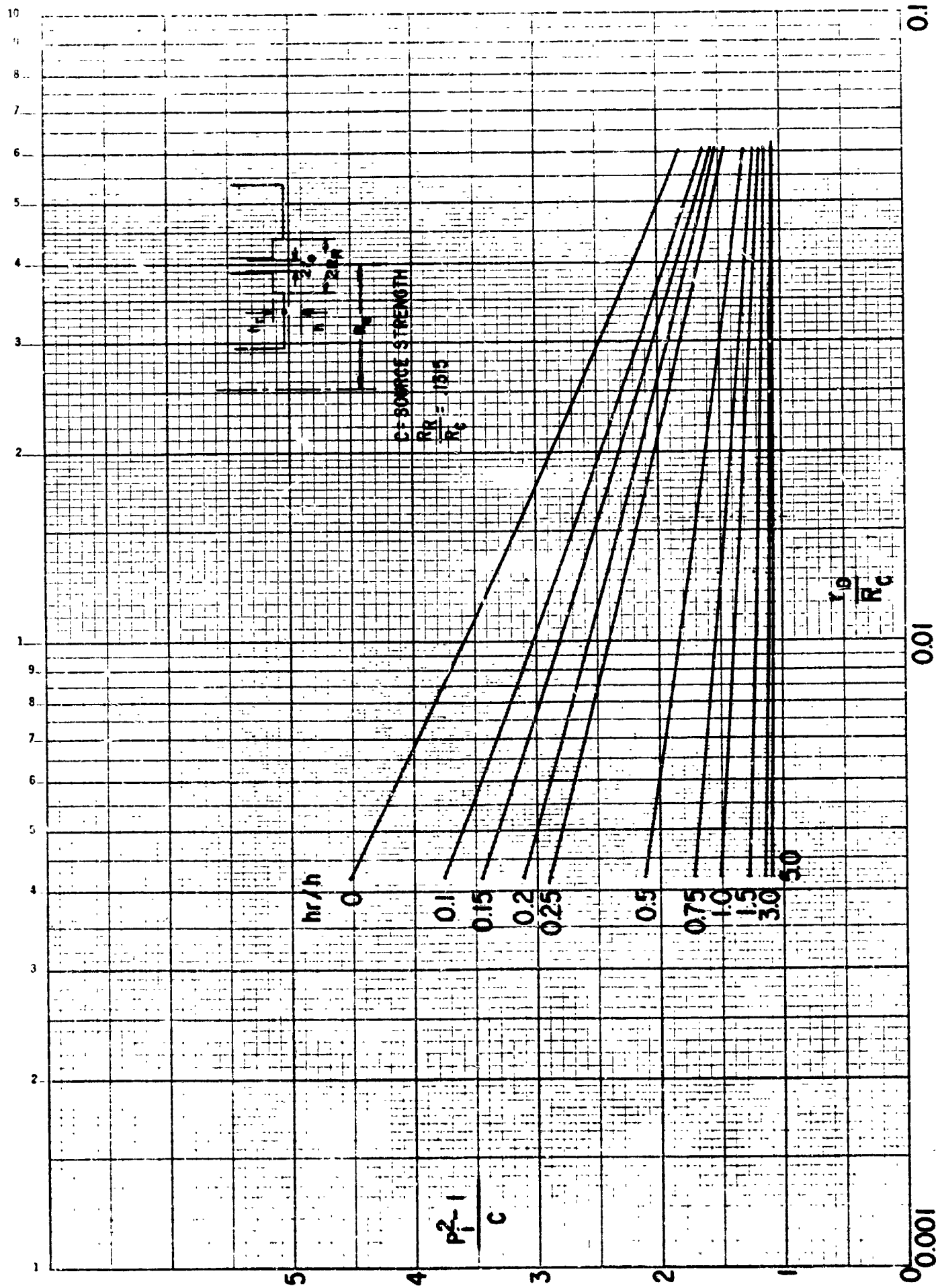


Fig. 17 Thrust: Bearing with Recess $N = 12$
Dimensionless Load vs. Source Strength

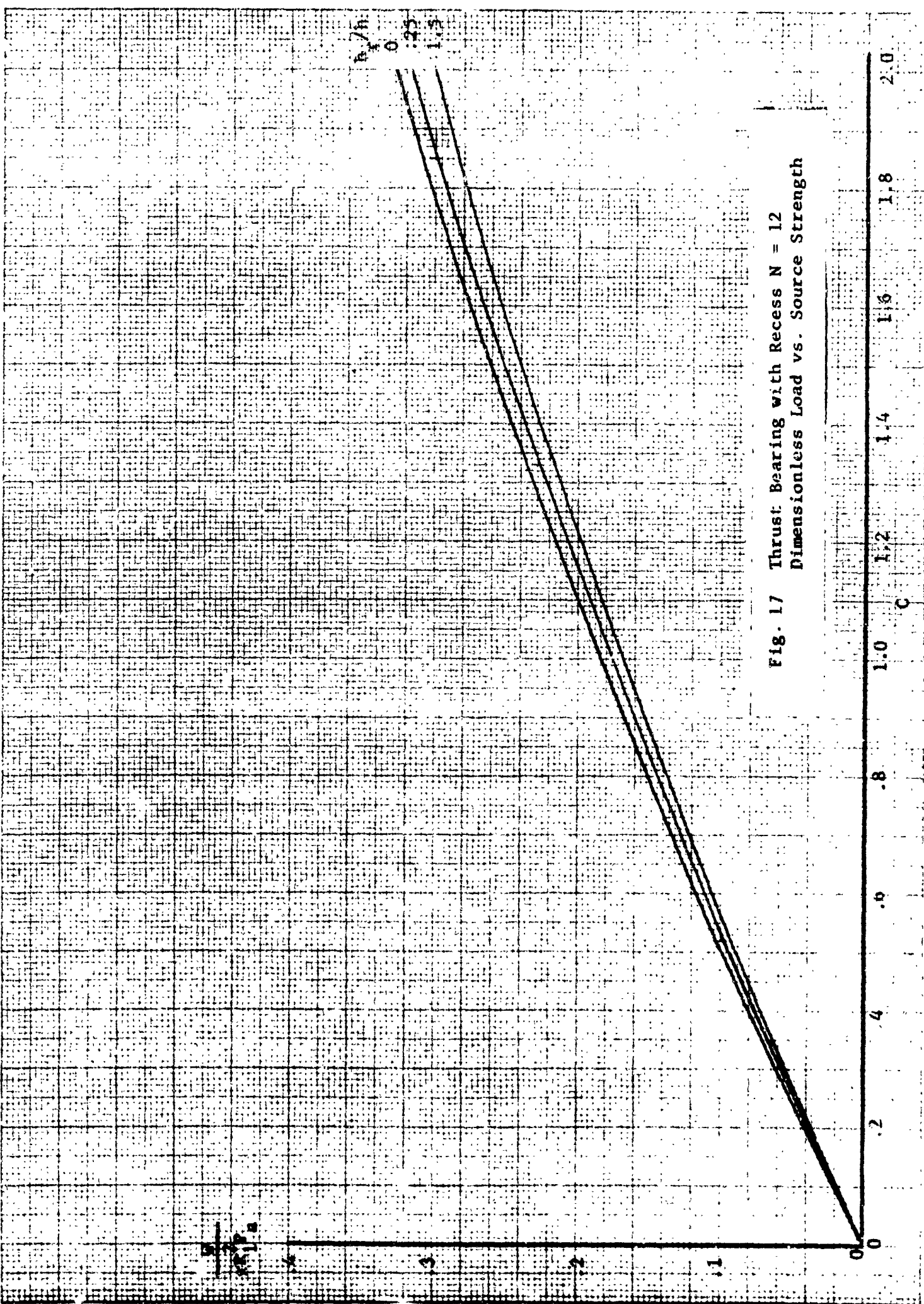


FIG. 18 THRUST BEARING WITHOUT RECESS N = 6, 12, 18

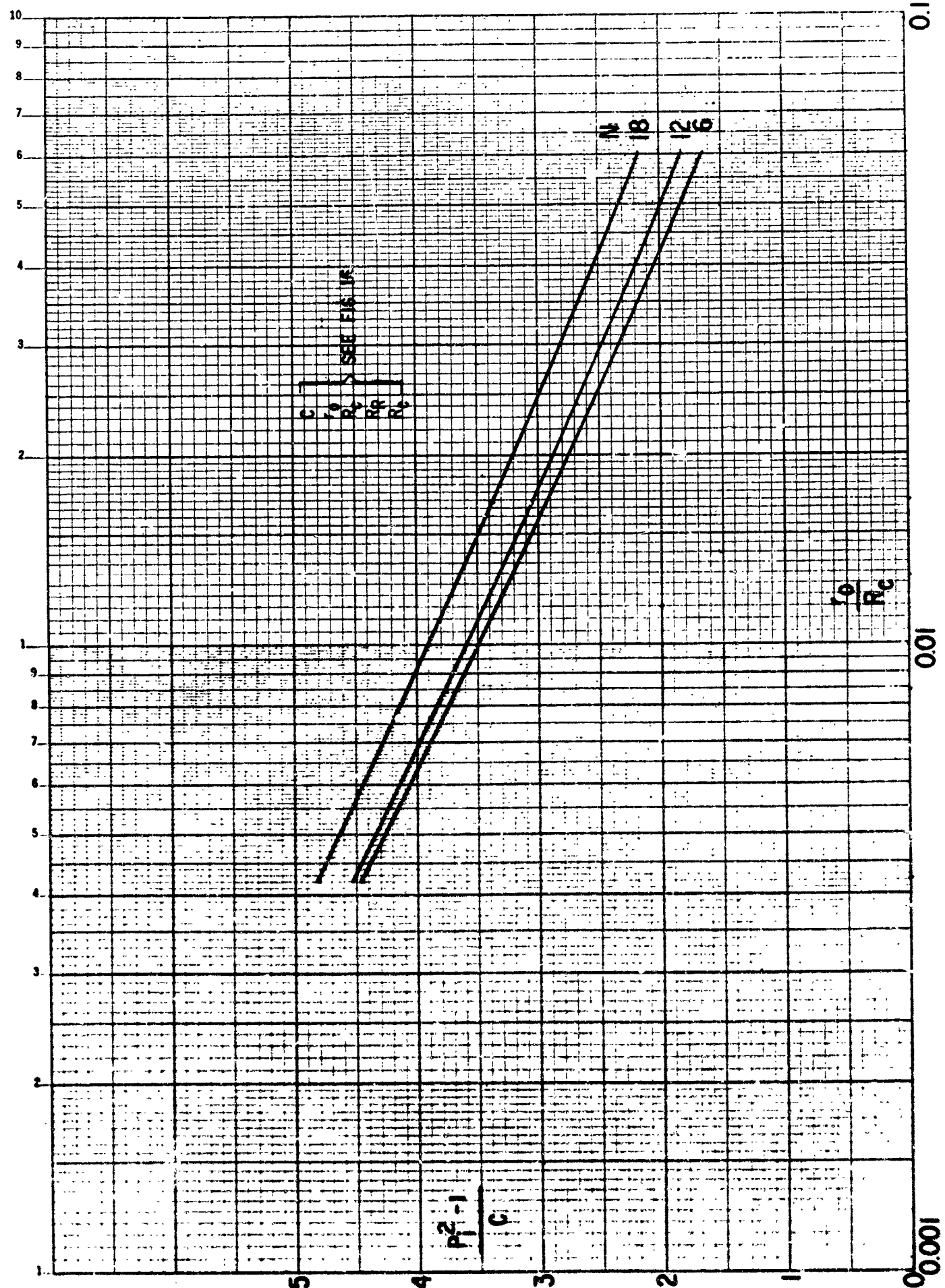


Fig. 15 Thrust Bearing without Recombination
Dimensions in feet v_s, Source Strength



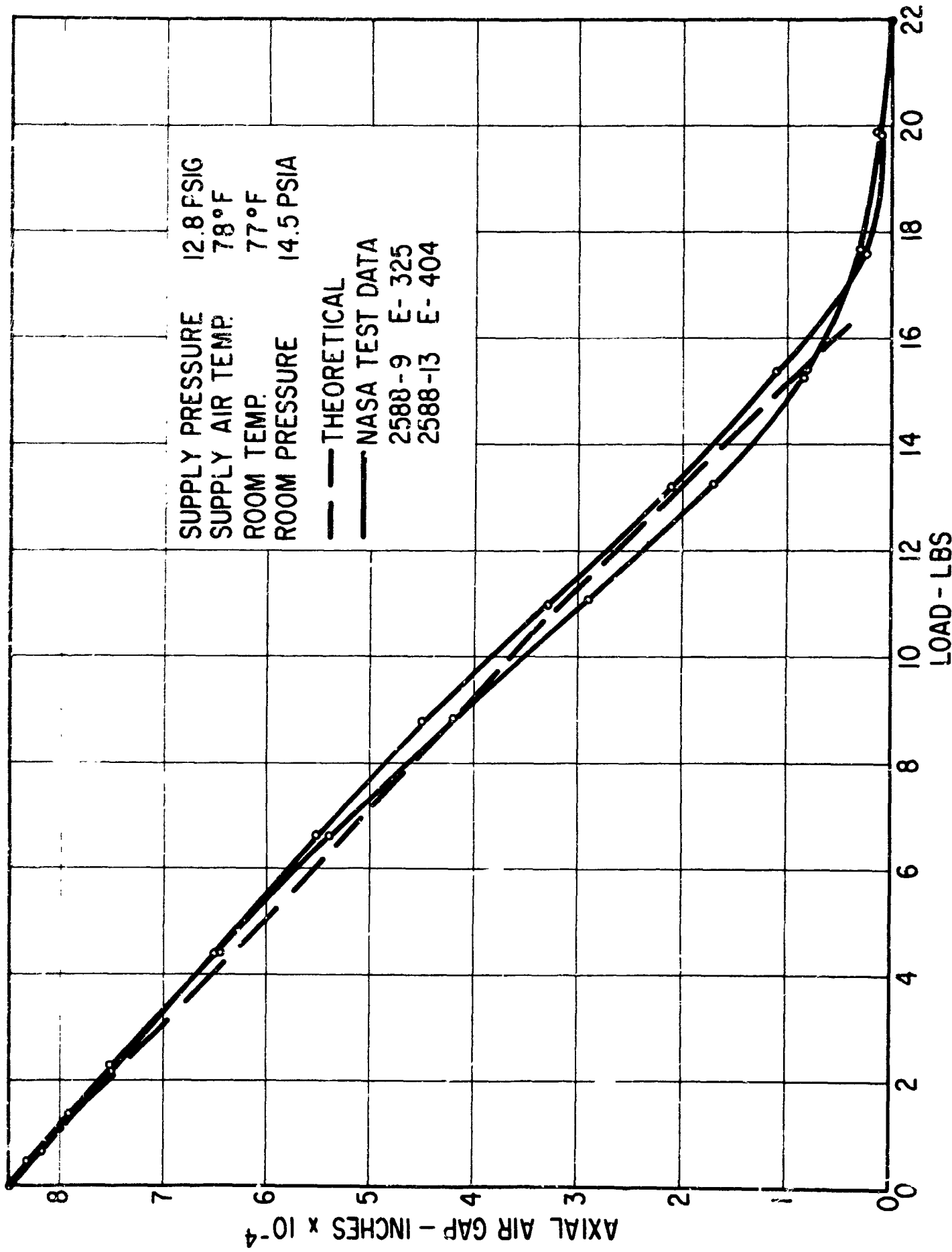


FIG 20 AXIAL MANNING - AIR GAP vs LOAD

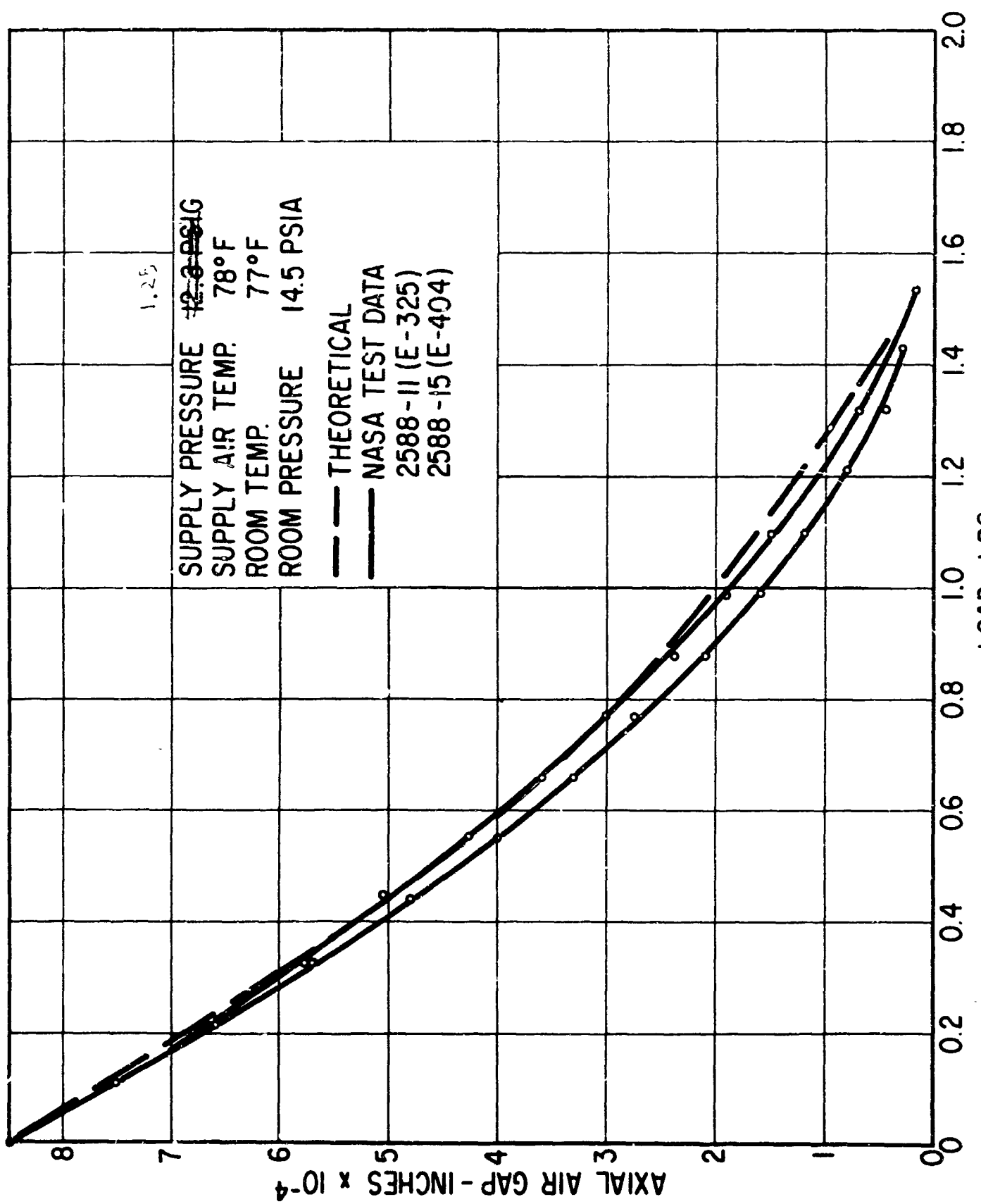


FIG. 21 AXIAL LOADING - AIR GAP vs LOAD

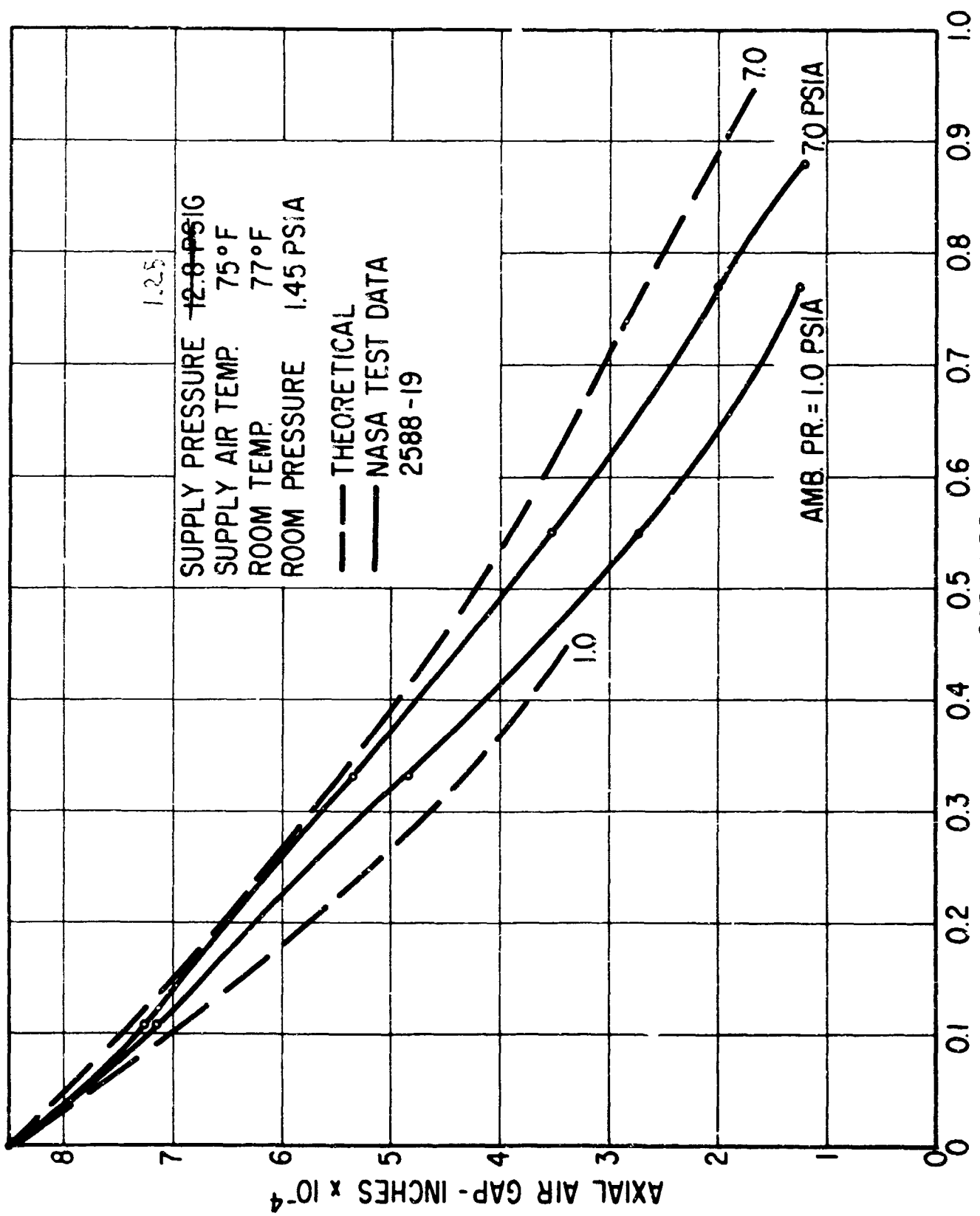


FIG.22 AXIAL LOADING-LOW AMBIENT PRESSURE
AIR GAP vs LOAD

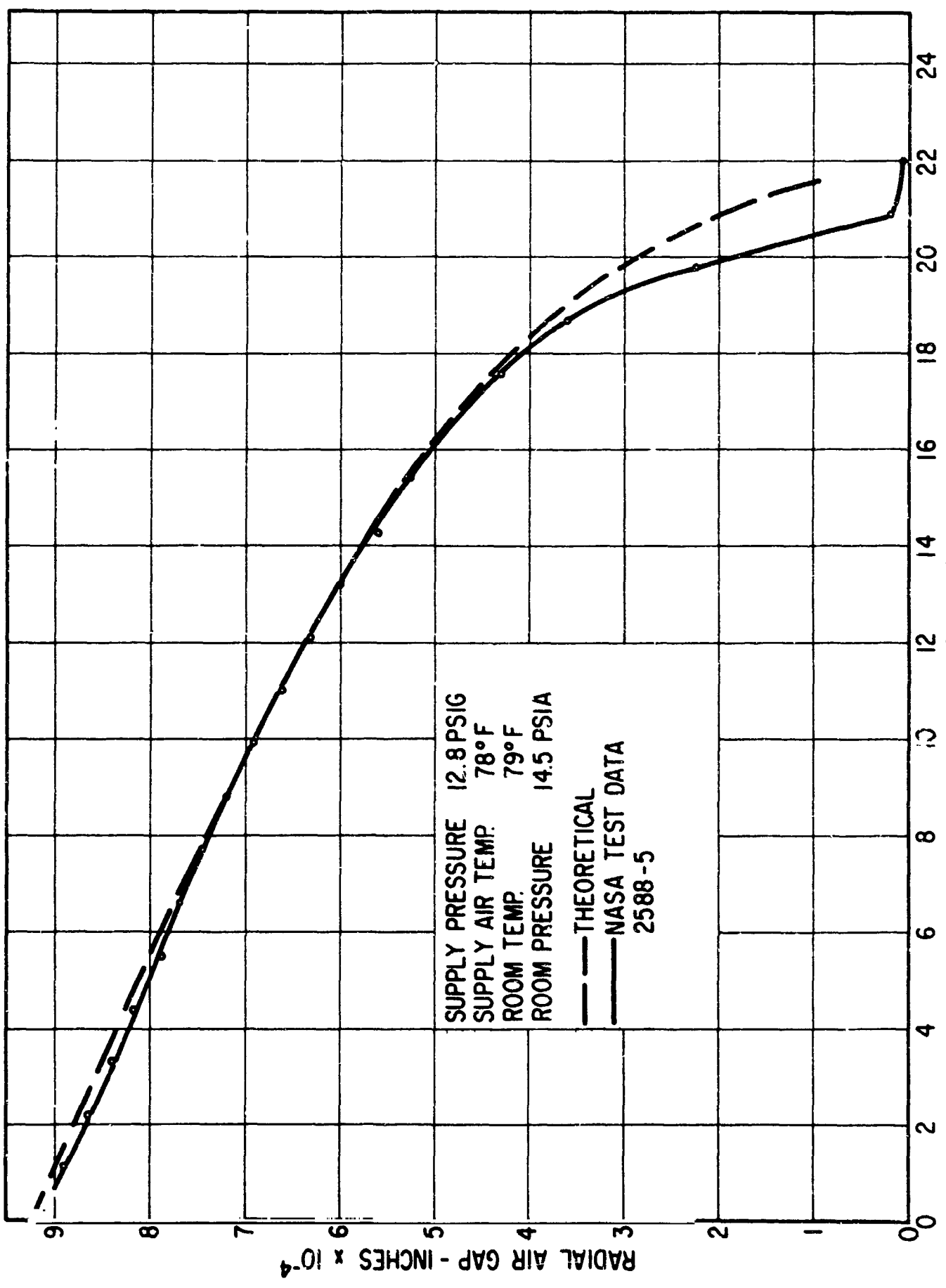


FIG.23 RADIAL LOADING - AIR GAP vs LOAD
SFFVF NO. 5256

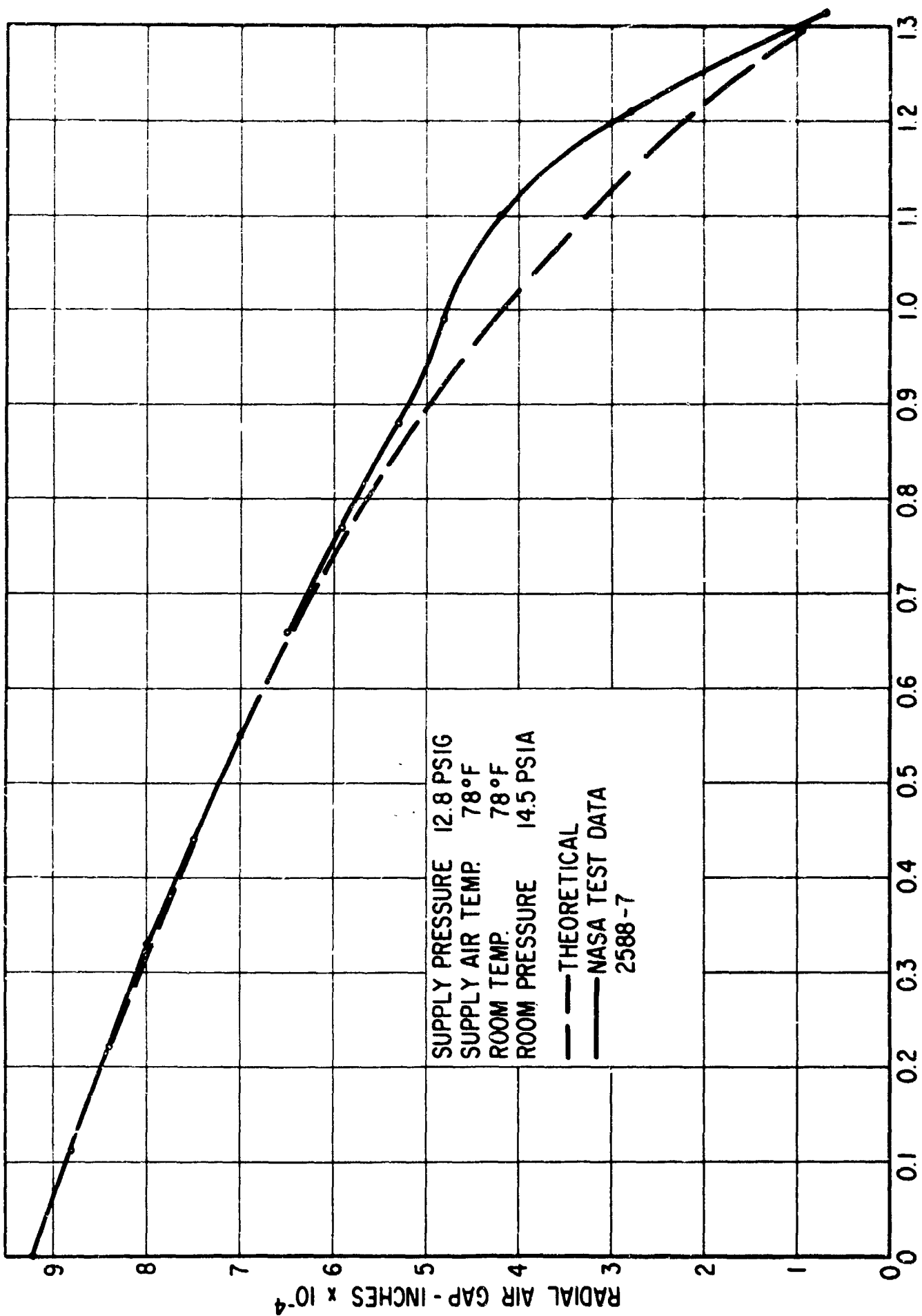


FIG.24 RADIAL LOADING - AIR GAP vs LOAD
 © EFFVF No 525

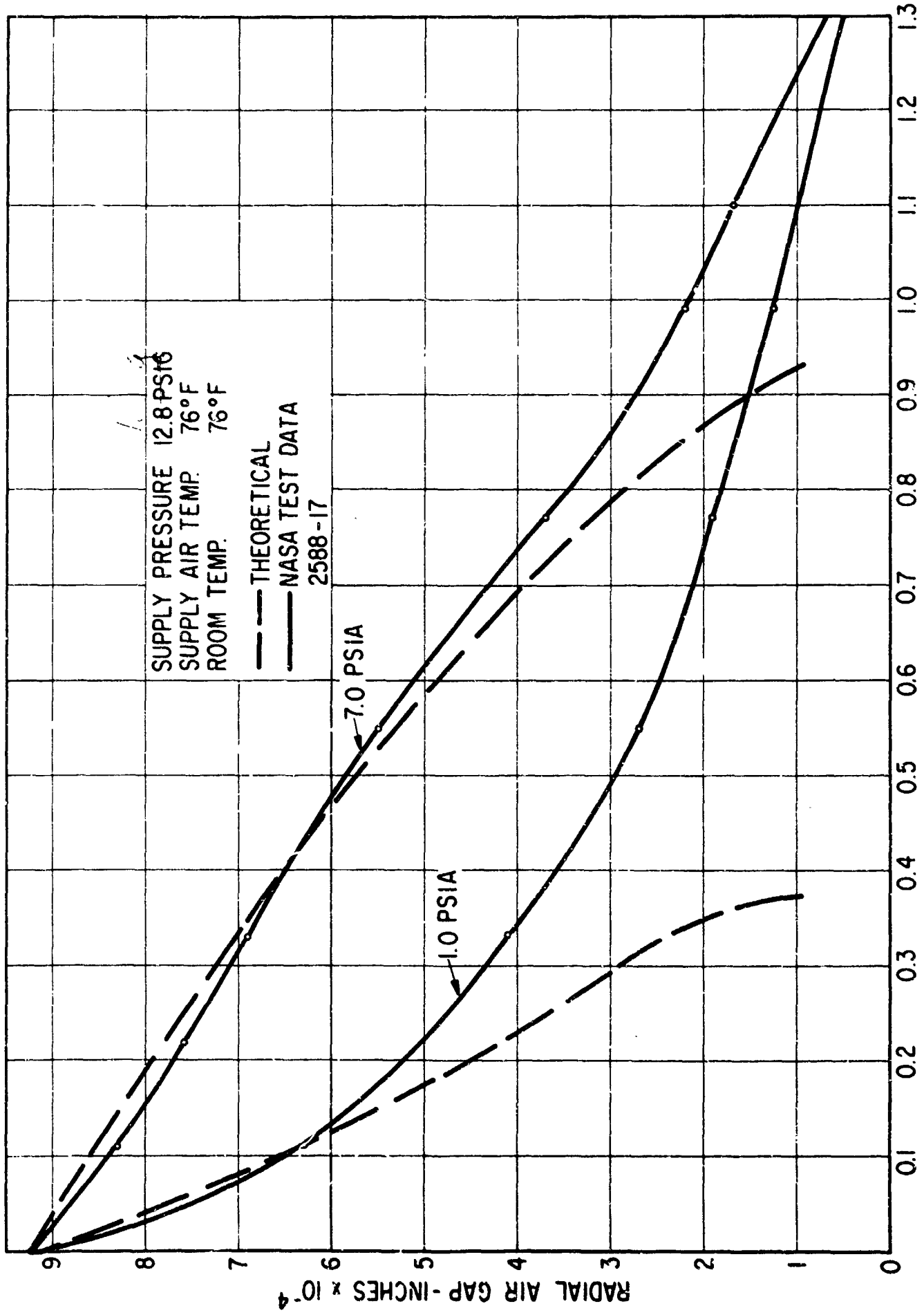


FIG.25 RADIAL LOADING - LOW AMBIENT PRESSURE
AIR GAP vs LOAD - SLEEVE NUMBER 5256

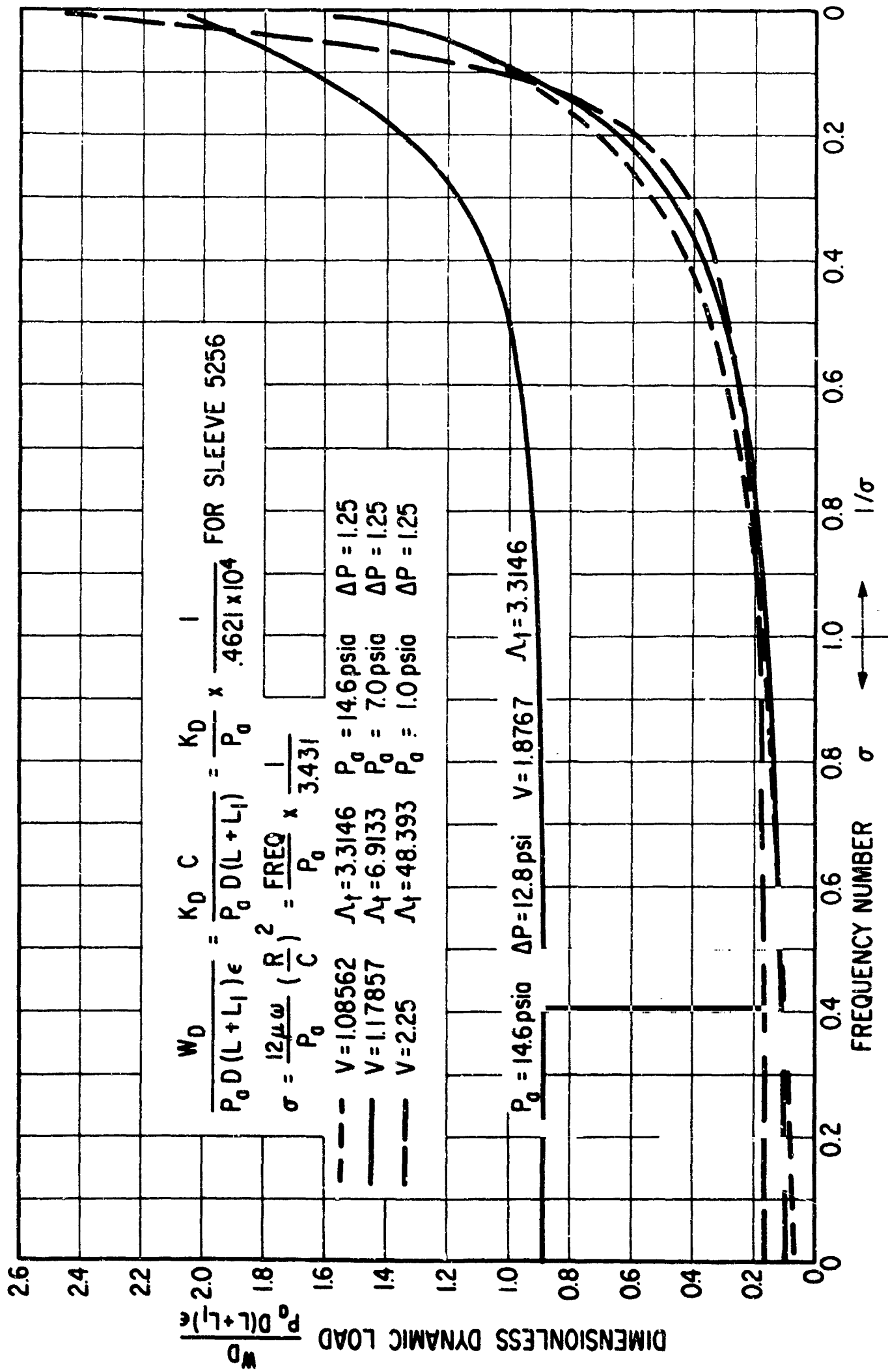
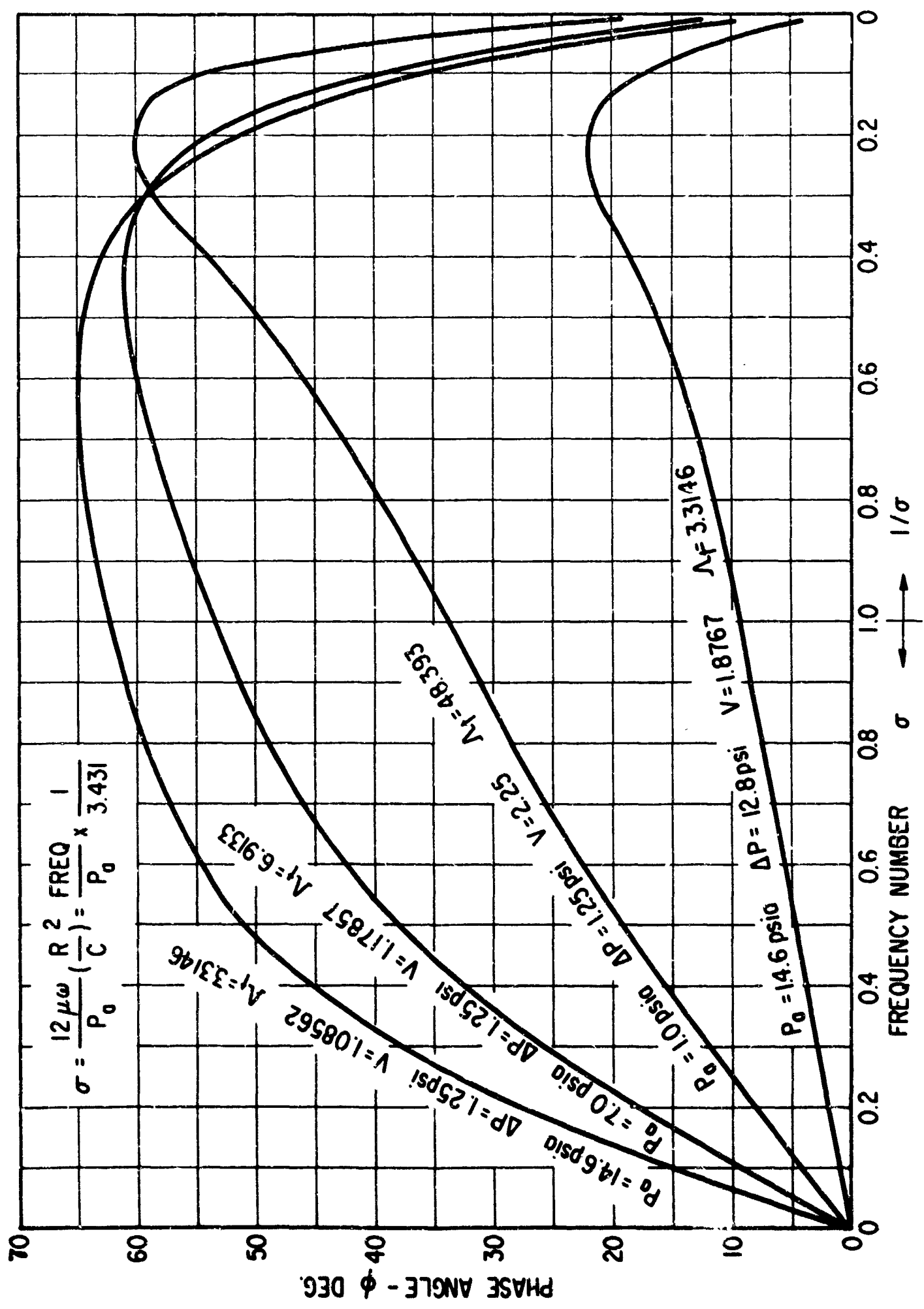


FIG. 26 JOURNAL BEARING - DYNAMIC LOAD vs FREQUENCY NUMBER

FIG. 27 JOURNAL BEARING-LOAD PHASE vs FREQUENCY NUMBER



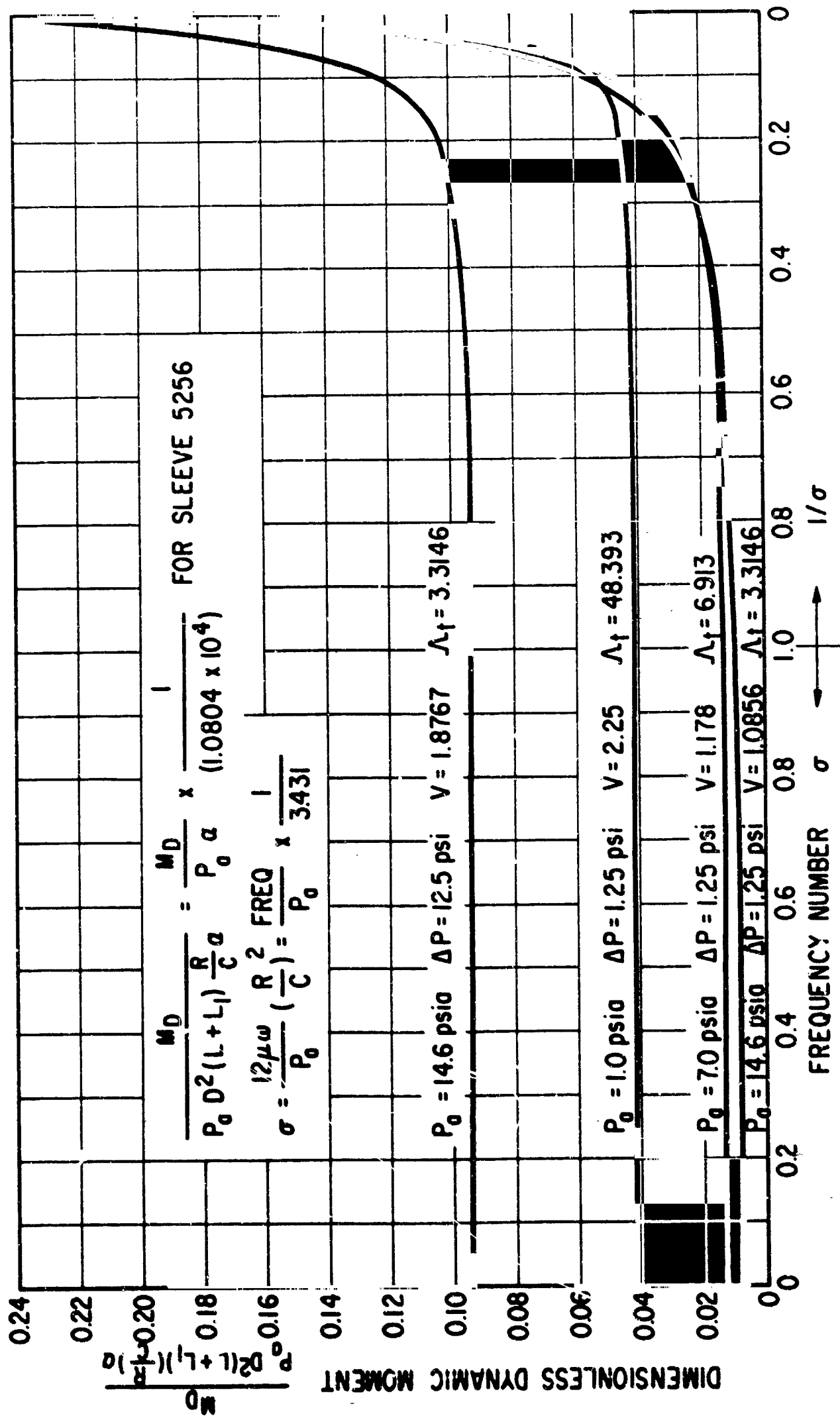
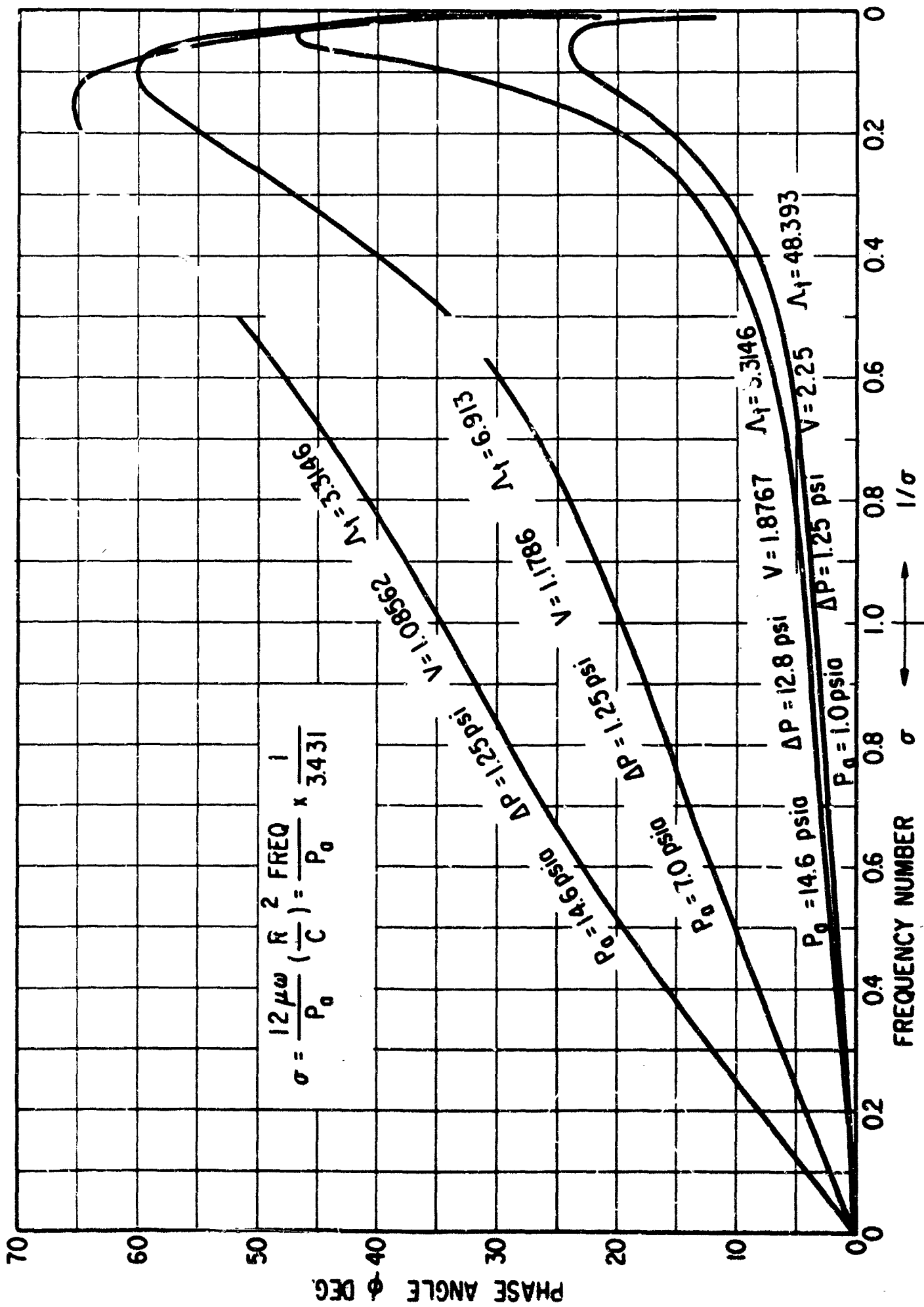


FIG. 28 JOURNAL BEARING - DYNAMIC MOMENT vs FREQUENCY NUMBER



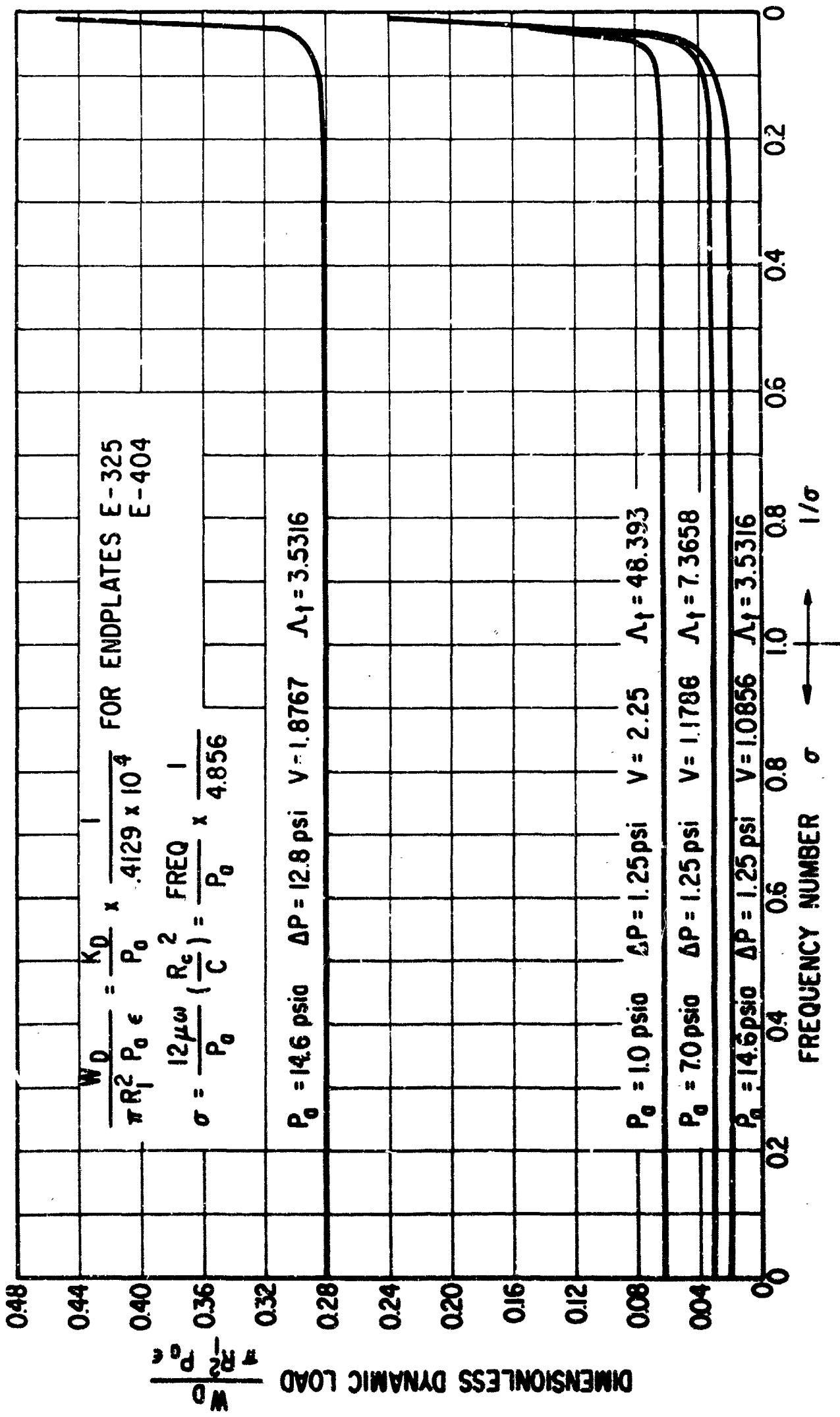


FIG. 30 THRUST BEARING - DYNAMIC LOAD vs FREQUENCY NUMBER

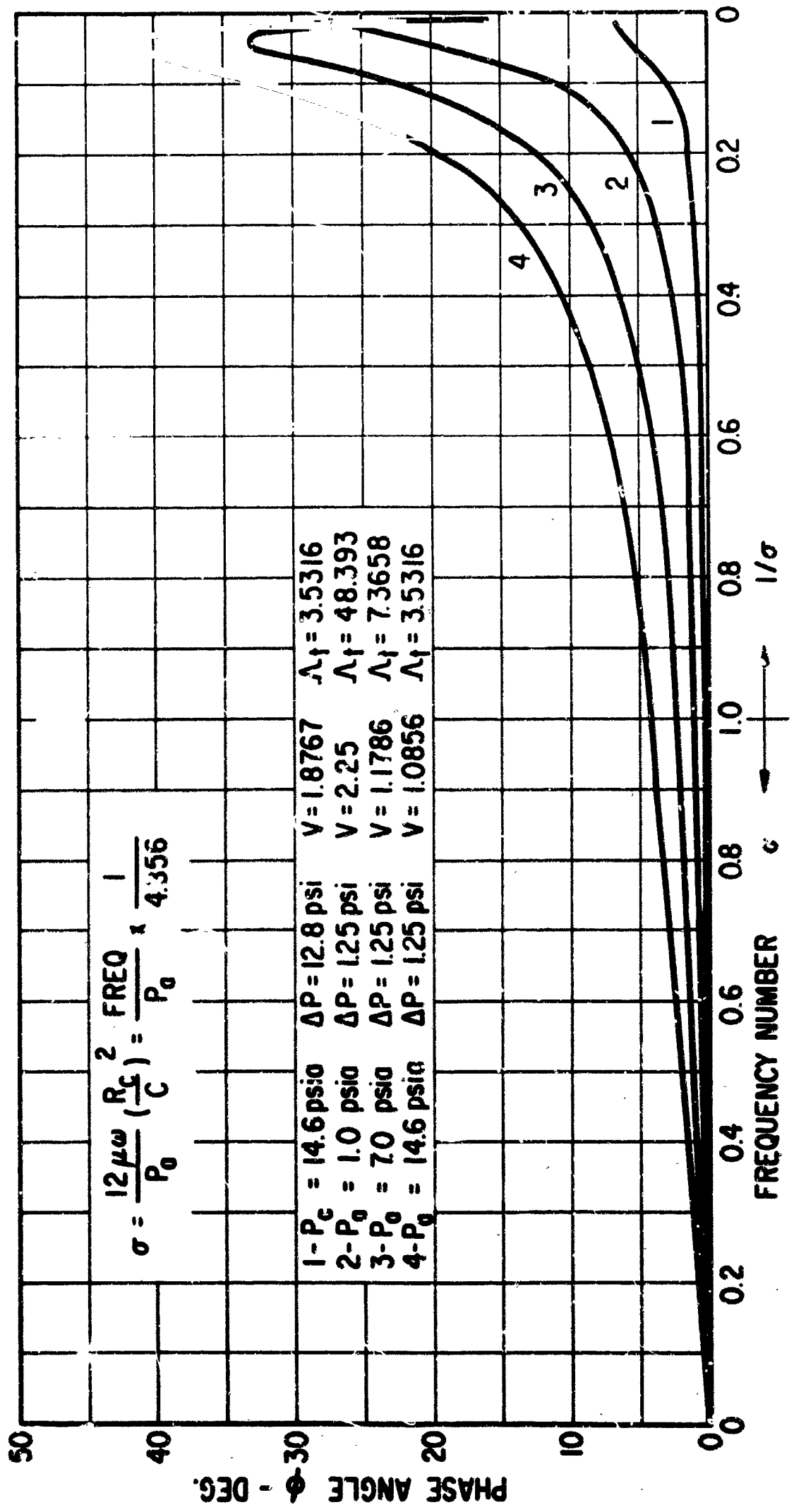


FIG. 31 THRUST BEARING - LOAD PHASE vs FREQUENCY NUMBER

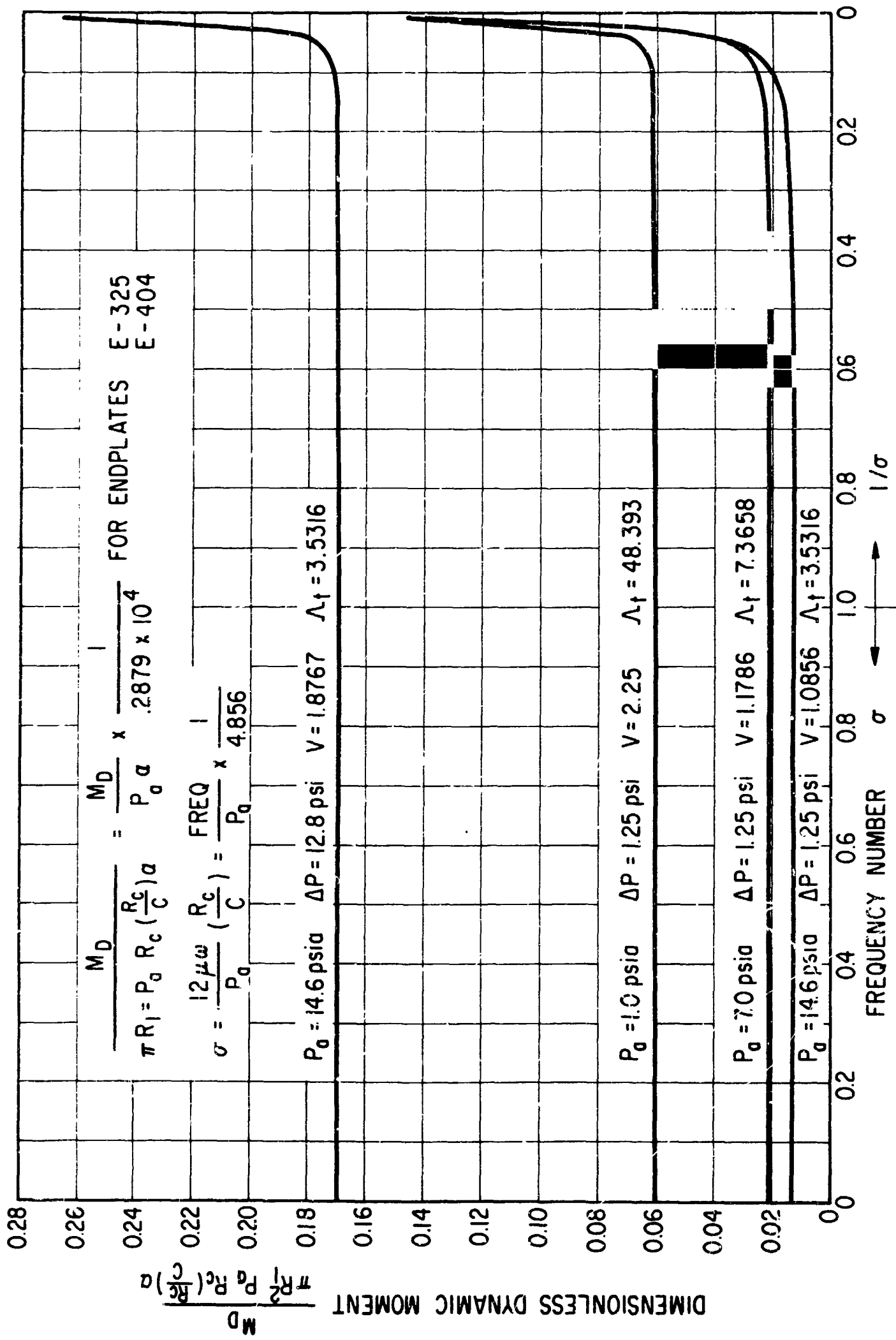


FIG. 32 THRUST BEARING - DYNAMIC MOMENT vs FREQUENCY NUMBER

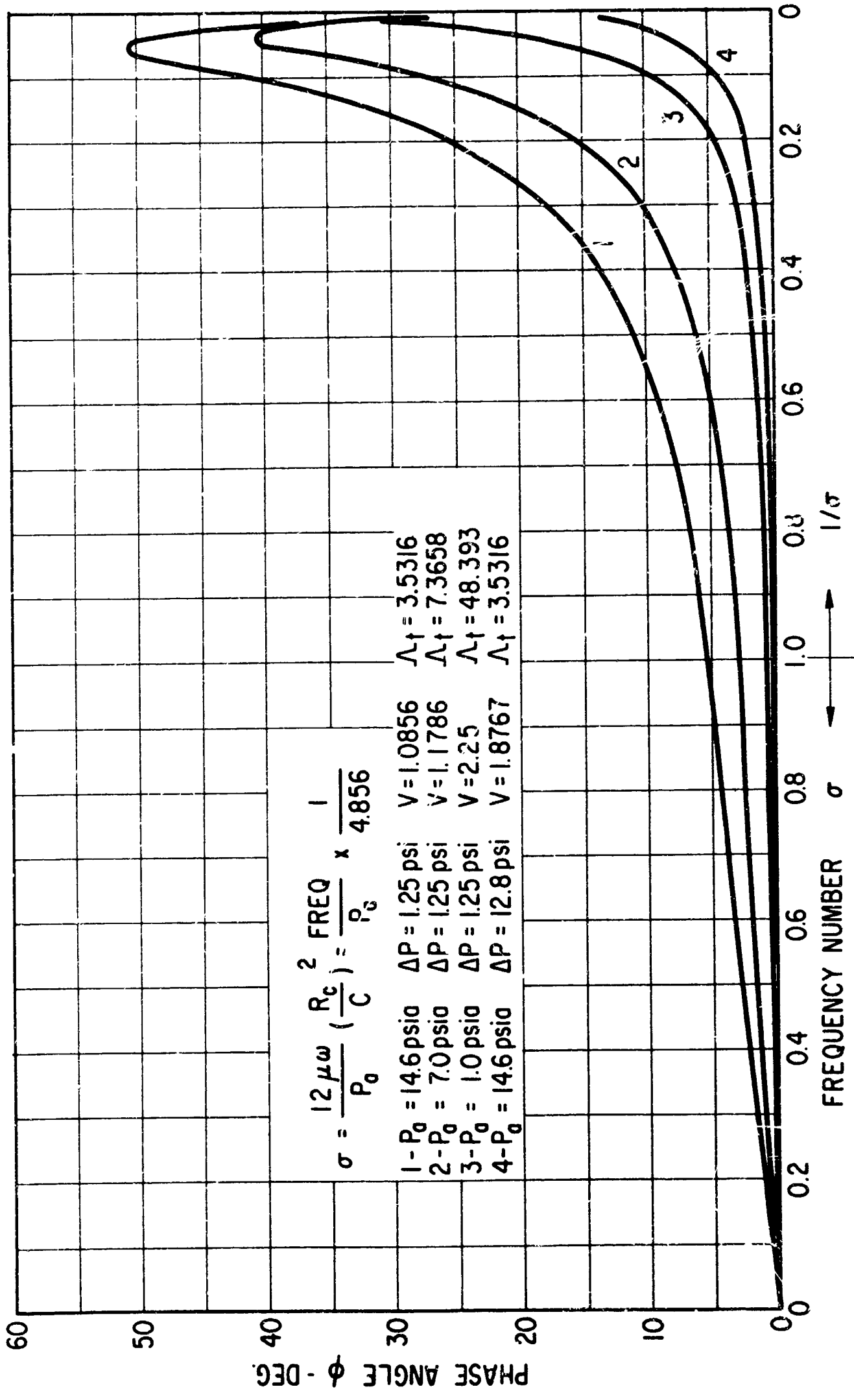


FIG. 33 THRUST BEARING - MOMENT PHASE vs FREQUENCY NUMBER

NOMENCLATURE

| | |
|------------|--|
| A | Orifice flow area - inch ² |
| a, B, C, D | Millipore flow coefficients |
| a | Orifice radius - inch |
| a, b | Dimensions of rectangular pad, representing thrust segment, figs. 8 and 9 - inch |
| C | Radial clearance in journal bearing, axial clearance in thrust bearing - inch |
| C | Source strength |
| D | Journal bearing diameter - inch |
| d | Source location, see fig. 9 - inch |
| d | Feeding hole diameter - inch |
| E, F, G | Functions for use in finite difference equations, see eqs. (H.23), (H.24), (H.30), (G.31), (G.37) |
| e | Journal bearing eccentricity - inch |
| f | Pressure function, short journal bearing, see eq. (F.7) |
| H | Pressure variable, representing $(P_o P_i)$, see eqs. (B.14), (G.7), (G.26), (H.6), (H.20) |
| H_i, H_o | Value of H at downstream orifice |
| H'_o | $\frac{dH}{ds}$ or $\frac{dH}{dr}$ at feeding plane |
| h | Bearing film thickness, dimensionless: $1 + \epsilon \cos\theta$, or in inch |
| k | Adiabatic gas exponent |
| L | Journal bearing length, from feeding plane to bearing end, see fig. 3 - inch |
| L | Journal bearing length between feeding planes, see fig. 3 - inch |
| M | Mass flow through one orifice - lbs.sec/in |
| M_T | Total bearing mass flow - lbs.sec/in |
| M_D | Dynamic bearing moment - lbs.inch |
| M'_D | Dimensionless dynamic moment, see eqs. (G.63) and (H.73) |
| m | Dimensionless mass flow through one orifice, see eq. (A.11) |

NOMENCLATURE (cont'd)

| | |
|----------------------|---|
| m' | $= \frac{dm}{d(\frac{P}{V})}$ |
| m_0 | Dimensionless orifice mass flow when $\epsilon=0$ |
| m'_0 | $= \left[\frac{dm}{d(\frac{P}{V})} \right]_{\epsilon=0}$ |
| m | Number of finite difference increments |
| N | Number of feeding holes in bearing |
| n | Running index |
| P | Gas film pressure, dimensionless: $\frac{P(\text{psia})}{P_a}$, or in psia |
| P_a | Ambient pressure at end of bearing - psia |
| P_s | Supply pressure - psia |
| P_i | Orifice downstream pressure, dimensionless: $\frac{P_i(\text{psia})}{P_a}$, or in psia |
| P_r | Dimensionless pressure in thrust bearing recess |
| P_0 | Dimensionless pressure when $\epsilon=0$ |
| P_1 | Dimensionless first order pressure coefficient, see eq. (B.2) |
| p, q, s, t, v, w | Functions for use in finite difference equations, see eqs. (G.40), (G.41), (H.37), (H.38) |
| Q_x, Q_z, Q_r, Q_0 | Mass flow per inch - lbs.sec/in ² |
| q | $= \Lambda_t V m_0$, dimensionless mass flow in journal bearing |
| q_T | $= \Lambda_T V m_0$, dimensionless mass flow in thrust bearing |
| R | Journal bearing radius - inch |
| R_1 | Outer radius of thrust bearing - inch |
| R_2 | Inner radius of thrust bearing - inch |
| R_c | Radius of feeding plane circle in thrust bearing - inch |
| RT | (Gas constant).(total temperature) - in ² /sec ² |
| r | Radial coordinate in thrust bearing, dimensionless: $\frac{r(\text{inch})}{R_c}$, or in inch |
| r' | $= \frac{r(\text{inch})}{R_2}$ dimensionless radial thrust bearing coordinate |
| T | Infinite series given by eq. (E.39) |
| t | Time - seconds |

NOMENCLATURE (cont'd)

| | |
|-----------------|--|
| U_1, U_2 | Bearing surface velocities, see figs. 1 and 2 - in/sec |
| U | Dimensionless pressure function, see eq. (E.20) |
| U, W | Circumferential and axial gas velocity in journal bearing - in/sec |
| U, V | Radial and tangential gas velocity in thrust bearing - in/sec |
| V | $= P_s/P_a$, pressure ratio |
| W | Load of journal and thrust bearing - lbs |
| W_2 | Load of journal bearing outside feeding planes - lbs |
| W_1 | Load of journal bearing between feeding planes - lbs |
| W_c | Load including effect of inherent compensation- lbs |
| W_d | Dynamic bearing load - lbs |
| W'_d | Dimensionless dynamic load, see eqs. (G.62) and (H.72) |
| x, y, z | Circumferential, radial and axial coordinates for journal bearing, see fig. 1 - inch |
| α | Orifice flow coefficient |
| α | Angular vibration amplitude - radius |
| α, β | $\alpha + i\beta = \sqrt{1 + \frac{i\omega}{P_{ci}}}$.. see eqs. (G.18) and (G.19) |
| β | $= \ln \eta / \ln \gamma$, geometrical thrust bearing parameter |
| γ | $= R_c/R_2$, dimensionless inner radius of thrust bearing |
| γ_n | Fourier coefficients for U , see eq. (E.21) |
| ϵ | $= e/c$, eccentricity ratio |
| ϵ | Dimensionless vibration amplitude |
| ξ, ξ' | $= z/R$, dimensionless axial coordinates for journal bearing, see fig. 3 |
| ξ | $= 2\pi \frac{x}{a}$, dimensionless x-coordinate for rectangular pad, appendix E |
| η | $= L/D$, dimensionless length between feeding planes in journal bearing |
| η | $= R_1/R_c$, dimensionless outer radius of thrust bearing |
| η | Adiabatic efficiency of orifice |

NOMENCLATURE (cont'd)

| | |
|------------------------|---|
| $\theta, \bar{\theta}$ | Circumferential coordinate in journal bearing, see fig. 1 - radians |
| Θ | Tangential coordinate in thrust bearing - radians |
| α | $= d/a$, dimensionless coordinate for orifice in rectangular pad, appendix E |
| μ | Gas viscosity - lbs.sec/in ² |
| v | Vena contracta coefficient of orifice |
| ξ | $= L/D$, dimensionless length outside feeding planes in journal bearing, see fig. 3 |
| ξ | $= b/a$, aspect ratio of rectangular pad, appendix E, see figs. 8 and 9 |
| ρ | Mass density - lbs.sec ² /in ⁴ |
| δ | $= \frac{12\mu\omega}{P_a} \left(\frac{R}{C}\right)^2$, frequency number |
| σ | $= a^2/dC$, inherent compensation factor |
| τ | $= \omega t$, dimensionless time |
| ϕ | Journal bearing attitude angle, see fig. 1 - radians |
| $\dot{\phi}$ | Angular velocity of journal center - rad/sec |
| ψ | $= 2\pi \frac{y}{a}$, dimensionless y-coordinate for rectangular pad, appendix E |
| ϕ_w | Phase angle for translatory vibration, see eq. (G.62) and (H.72) - radians |
| ϕ_m | Phase angle for rotational vibration, see eqs. (G.63) and (H.73) - radians |
| $\Psi(x)$ | $= \int_0^x e^{t^2} dt$, related error function |
| ω | Angular speed - rad/sec |
| ω | Frequency - rad/sec |
| Δs | Dimensionless axial increment in finite difference equation for journal bearing |
| Δr | Dimensionless radial increment in finite difference equation for thrust bearing |
| Λ | $= \frac{6\mu\omega}{P_a} \left(\frac{R}{C}\right)^2$, bearing number |
| Λ_t | $= \frac{6\mu N a^2 \sqrt{RT}}{P_a C^3}$, feeding parameter for journal bearing |
| Λ_T | $= \frac{12\mu N a^2 \sqrt{RT}}{P_a C^3 (1+\rho)}$, feeding parameter for thrust bearing |